Examining the role of a novel stromal cell protein CD362/Syndecan-2 in the breast tumour microenvironment.

A PhD Thesis Submitted to the School of Medicine, National University of Ireland, Galway, as partial fulfilment of the requirements for the degree of Doctor of Philosophy

Author

Paul Gerard Loftus B.Sc. M.Res.

The studies presented in this thesis were supported by Irish Research Council grants EBPPG/2014/109, EBPPG/2015/215 and FAMRI award 072101.

Academic Supervisors: Prof Tim O'Brien and Dr Laura Barkley

Employment Supervisor: Dr Stephen Elliman

Submitted May 2019

"NIHIL ENIM TANTAM VIM HABET AD ANIMI MAGNITUDINEM GIGNENDAM, QUAM POSSE SINGULA, QUAE IN VITA OCCURRUNT, VIA AC RATIONE EXPLORARE EAQUE SEMPER SIC INTUERI"

- MARCI ANTONINI IMPERATORIS

- COMMENTARIORUM QUOS IPSE SIBI SCRIPSIT,

- LIBER III.XI

"Nothing has such power to broaden the mind, as the ability to investigate, systematically and truly, all that comes under thy observation in life"

-Marcus Aurelius
-Meditations,
-Book 3.11

ACKNOWLEDGEMENTS

I would like to start by sincerely thanking my supervisors, **Dr Laura Barkley** and **Dr Stephen Elliman**, without whom this work would never have been possible. To Laura for her constant guidance, training and reassurances throughout the course of this project, you have always ensured the smooth progression of this work from result to result and for that I will be eternally grateful. To Steve for taking a chance on me back in 2013 and giving me a job in Orbsen Therapeutics, but also for believing that I could accomplish more and for encouraging me to fulfil my desire to do a PhD.

I would also like to thank my academic supervisor **Prof. Tim O'Brien**, for always being available despite his hectic schedule and for treating me with the upmost respect and encouragement throughout the course of this work.

I would like to thank all members of Orbsen Therapeutics, past and present for their support and friendship over the past six years. In particular **Luke Watson,** for the huge amount of time he contributed to this work, especially his surgical expertise, but also for being a true friend and gentleman. There aren't many people of his ilk, and I am honoured to call him my best man.

I would also like to thank the members of my GRC committee: **Dr Linda Howard**, for her guidance and support all the way back to my masters in 2011. **Dr Róisín Dwyer**, for her vast knowledge and expertise and allowing us to use her orthotopic model of breast cancer. **Prof. Matt Griffin**, for his support and keen intellect throughout this project, particularly with our immunological pathways and assays, but also for agreeing to chair my *viva voce.*

I am grateful to both my internal examiner **Prof. Michael O'Dwyer** and external examiner **Prof. Thomas Hughes** for taking the time to examine my thesis and for coming for my *viva voce.*

To the lads, **Dr Paul Lohan**, **Dr Dave Browe**, **Paddy Costello**, **Dr Ollie Treacy** and **Luke Watson** (again), thanks for listening and helping me through this PhD. Ye are an outstanding bunch of men that I am proud to call my friends and groomsmen.

To my family: **Denise Loftus**, Mom, thanks for literally everything, your limitless love and support has encouraged me to always strive to be a better person in the hope of one day emulating the amazing person that you are. There is no doubt that you have made me the man I am today. **Gerry Loftus**, Dad, thanks for being the best role model a son could have, you are a truly outstanding man. Your devotion and guidance (and a few boots off the couch) is among the main driving factors for my pursuit of a PhD. It may take my whole life, but I hope to someday be half the man you are. **Ailíse Loftus**, sister, thank you for your lifetime of encouragement and support. From reading bed time stories to me when I was a child to helping me with my homework as a teenager to having nerd life chats over wine as adults. You have always been there for me, and are a truly incredible human being. **Rebecca Loftus**, sister, you are a truly wonderful soul, your light-hearted nature has encouraged me to always have fun and smile, plus your tough love as a kid enabled the development of my thick skin (those nails were sharp). But most importantly thank you for igniting my passion for science, without you I would never have travelled this road, and for that I will be eternally grateful.

Finally, I would like to make a special thank you to my inamorata, colleague, mentor and fiancée **Dr Laura Deedigan,** without whom, none of this would have been possible. You have always encouraged me to be a better person and scientist. You equipped me with the tools and skills I have needed for this work and your unrelenting emotional and intellectual

support ensured that I never stopped. You are the best thing that has ever happened to me and there are no words which would accurately describe how grateful I am. I love you and hope to repay your support and kindness over the course of our lives together.

ABSTRACT

Tumour-associated stromal cells play a key role in initiating and sustaining tumour growth, metastasis, immune control and chemo-resistance. Thus, identifying stromal proteins that contribute to carcinogenesis may open new therapeutic paradigms.

We have identified Syndecan-2 (SDC2/CD362) as a novel antigen for identification of stromal cells (SC) from breast cancer tissue. SDC2 is a cell surface heparan sulfate proteoglycan that has been shown to be elevated in breast and other cancers. We demonstrate that $SDC2^+$ SC and $SDC2^+$ epithelial cells are present in murine and human breast tumours by flow cytometry and that levels of SDC2 are elevated in the sera of triple negative breast cancer patients. ShRNA knockdown of SDC2 in MDA-MB-231 triple negative breast cancer cells (BCC) inhibits TGFβ-induced markers of epithelial to mesenchymal transition (EMT) and BCC migration. Knocking down SDC2 in primary human tumour-derived SC also limits TGFβ signalling, inhibiting the ability of SC to suppress T cell proliferation. Our data indicates that modulation of SDC2 in human tumour-derived SC significantly alters tumour carcinogenesis in a xenograft orthotopic breast cancer model. Thus we hypothesise SDC2 is a functional protein within the tumour microenvironment (TME) promoting tumour growth, migration and immune-suppression; and therefore therapeutic targeting of SDC2 may yield a novel treatment for breast cancer. To that end, we generated novel SDC2 peptides that inhibit the clonogenic survival, migration and TGFβ-induced EMT of BCC *in vitro*. In addition, SDC2 peptides inhibit the immune suppressive properties of SC and this correlates with a decrease in expression of immune suppressive mediators CXCR4 and PD-L1. Importantly, SDC2 peptides display anti-tumourigenic properties *in vivo* as overexpression of a SDC2 peptide in SC within the TME reduces breast carcinogenesis in both xenograft and syngeneic mouse models.

TABLE OF CONTENTS

LIST OF FIGURES

LIST OF TABLES

LIST OF ABBREVIATIONS

αMEM	Alpha minimum essential medium
αSMA	Alpha smooth muscle actin
ACK	Ammonium-chloride-potassium
Ad	Adenovirus
AdCt	Adenovirus empty control
AdS2	Adenovirus for Syndecan-2 overexpression
AJCC	American Joint Committee on Cancer
ALL	Acute lymphoblastic leukaemia
ANOVA	Analysis of variance
APS	Ammonium persulphate
BCA	Bichinchoninic acid assay
BCC	Breast cancer cell
BMI	Body mass index
BM-MSC	Bone marrow derived mesenchymal stromal cell
BRCA1	Breast cancer 1
BRCA2	Breast cancer 2
Breg	Regulatory B cells
BSA	Bovine serum albumin
CAF	Cancer associated fibroblast
CAR	Chimeric antigen receptor
CDH1	E-cadherin
cDNA	Complementary deoxyribonucleic acid
CFSE	Carboxyfluorescein succinimidyl ester
CIM	Cell invasion and migration
CRI	Cancer related inflammation
CS	Chondroitin sulfate

CSF-1	Colony stimulating factor-1
CTGF	Connective tissue growth factor
CTLA4	Cytotoxic T-lymphocyte antigen 4
CO_2	Carbon dioxide
CXCR4	C-X-C chemokine receptor type 4
CXCL12	C-X-C motif chemokine 12
C57BL/6	C57 black 6
DC	Dendritic cell
DCIS	Ductal carcinoma in situ
dH_2O	Distilled water
DMEM	Dulbecco's minimum essential medium
DNA	Deoxyribonucleic acid
dNTP	Nucleoside triphosphate
ECL	Enhanced chemiluminescence
ECM	Extracellular matrix
EDTA	Ethylene diamine tetra-acetic acid
EGF	Epithelial growth factor
ELISA	Enzyme-linked immunosorbent assay
EMT	Epithelial to mesenchymal transition
EpCAM	Epithelial cell adhesion marker
ER	Estrogen receptor
ERBB2	Epidermal growth factor receptor 2
ERK1/2	Extracellular signal-regulated kinase
ESR1	Estrogen receptor α
FACS	Fluorescence activated cell sorting
FAK	Focal adhesion kinase
FAP	Fibroblast activation protein

FBS	Fetal bovine serum
FGF	Fibroblast growth factor
FGF-2	Fibroblast growth factor-2
FN1	Fibronectin
FOXA1	Forkhead box protein A1
FSP	Fibroblast secretory protein
F1	Syndecan-2 fragment 1
F2	Syndecan-2 fragment 2
g	gram
G	Standard acceleration due to gravity
GAPDH	Glyceraldehyde 3-phosphate dehydrogenase
GATA3	GATA binding protein 3
GFP	Green fluorescent protein
GP38	Podoplanin
GRB7	Growth factor receptor bound protein
GST	Glutathione S-transferase
HCl	Hydrochloric acid
H&E	Haematoxylin & Eosin
HEK	Human embryonic kidney
HER2	Human epidermal growth factor 2
HGF	Hepatocyte growth factor
HIF-1	Hypoxia-inducible factor 1
H_2O	Water
HRP	Horse radish peroxidase
HSPG	Heparan sulfate proteoglycan
ICAM1	Intracellular adhesion molecule 1
IDO	Indolamine 2,3 dioxygenase

IGFR1	Insulin-like growth factor-1 receptor
IgG	Immunoglobulin G
IP	Immunoprecipitation
ISCT	International Society for Cell Therapy
ITGB1	Integrin β1
L	Litre
LB	Lysogeny broth
LCIS	Lobular carcinoma in situ
µg	Microgram
µl	Microliter
µm	Micrometre
MACS	Magnetic activated cell sorting
MAPK	Mitogen-activated protein kinase
MDA-MB-231	M.D. Anderson-Metastatic Breast cancer-231
MDM2	E3 ubiquitin-protein ligase
MEF	Mouse embryonic fibroblasts
MFP	Mammary fat pad
mg	Milligram
MHC	Major histocompatibility complex
ml	Millilitre
mm	Millimetre
MMP1	Matrix metalloproteinase-1
MMTV	Mouse mammary tumour virus
mMSC	Mouse mesenchymal stromal cell
mSDC2-F2-Fc	Mouse Syndecan-2-fragment 2-Fc bound peptide
MOI	Multiplicity of infection
mRNA	Messenger RNA

MSC	Mesenchymal stromal cell
mTSC	Mouse tumour stromal cell
MW	Molecular weight
NaCl	Sodium chloride
NaN_3	Sodium azide
NaOH	Sodium hydroxide
NK	Natural killer
NOD:SCID	Non-obese diabetic: severe combined immune-deficiency
NOS_2	Nitrogen oxidase synthase
N-MSC	Normal tissue-derived MSC
NUIG	National university of Ireland, Galway
ORF	Open reading frame
PAI-1	Plasminogen activator inhibitor 1
PBS	Phosphate buffered saline
PBMC	Peripheral blood mononuclear cell
PCR	Polymerase chain reaction
PD-1	Programmed cell death protein 1
PDGF	Platelet derived growth factor
PDGFRα	Platelet-derived growth factor receptor alpha
PDGFRβ	Platelet-derived growth factor receptor beta
PD-L1	Programmed cell death protein ligand 1
PD-L2	Programmed cell death protein ligand 2
PGE2	Prostaglandin E2
pH	The Potential of Hydrogen
PR	Progesterone receptor
PyMT	Polyoma middle tumour-antigen
qPCR	Quantitative polymerase chain reaction

RNA	Ribonucleic acid
RPM	Revolutions per minute
RPMI	Roswell Park Memorial Institute
RTCA	Real time cell adhesion
RTK	Receptor tyrosine kinase
RT-PCR	Reverse transcription- polymerase chain reaction
SC	Stromal cell
SCA-1	Stem cells antigen-1
SDC2	Syndecan-2
SDC2-F1-Fc	Syndecan-2-fragment 1-Fc bound peptide
SDC2-F2-Fc	Syndecan-2-fragment 2-Fc bound peptide
SDS	Sodium dodecyl sulphate
SDS-PAGE	Sodium dodecyl sulphate-polyacrylamide gel electrophoresis
SERD	Selective estrogen down regulators
SERM	Selective estrogen receptor modulator
ShCt	Short hairpin non-targeting RNA control
ShRNA	Short hairpin RNA
ShS2	Short hairpin RNA for Syndecan-2
SNAI1	Snail family transcriptional repressor 1
Stim	Stimulation
TCR	T-cell receptor
TAM	Tumour-associated macrophage
TAN	Tumour-associated neutrophil
TBS	Tris buffered saline
TBP	TATA box binding protein
TEMED	N, N, N’, N’ –tetramethylethylenediamine
TGFβ	Transforming growth factor-β

TGFβR3	Transforming growth factor-β receptor 3
TIL	Tumour-infiltrating lymphocytes
TH1	CD4 T helper 1
TH2	CD4 T helper 2
TH17	CD4 T helper 17
TMB	3,3′,5,5′-Tetramethylbenzidine
TME	Tumour microenvironment
T-MSC	Tumour tissue-educated MSC
TN	Triple negative
TNBC	Triple negative breast cancer
TNFα	Tumour necrosis factor-α
TNM	Tumour size, lymph node status and metastatic burden
TP53INP1	Tumour protein 53-inducible nuclear protein 1
TRAIL	Tumour necrosis factor-related apoptosis-inducing ligand
Tris	Tris (hydroxymethyl) aminomethane
Treg	T regulatory cells
TSC	Tumour stromal cells
UCHG	University college hospital, Galway
UC-MSC	Umbilical cord derived mesenchymal stromal cell
UPR	Unfolded protein response
VCAM1	Vascular cell adhesion protein 1
VEGF	Vascular endothelial growth factor
Wnt	Wingless-integrated
ZEB1	Zinc finger E-box binding homeobox 1
°C	Degrees centigrade
4PL	Four parameter logistic regression

DECLARATION

I declare that all the work in this thesis was performed personally unless stated otherwise. No part of this work has been submitted for consideration as part of any other degree or award.

Paul Loftus

_____

CHAPTER 1

INTRODUCTION

1.1. BREAST CANCER

1.1.1. PREVALENCE AND INCIDENCE

Breast cancer is the most commonly diagnosed cancer in the world, it is estimated that there are 8.15 million people suffering from breast cancer at any given time [1]. It is the most frequent cause of female cancer related mortality in less developed regions and the second most in more developed areas with 324,000 and 198,000 deaths per year respectively [1-3].

Risk Factors

There are a number of risk factors which have been attributed to increases in breast cancer prevalence. Studies have shown relationships between reproductive risk factors and breast cancer. Two separate studies concluded that nulliparity and delayed childbearing were associated with ER+ breast cancer and that each successive birth reduces breast cancer risk [4, 5]. Alcohol has been shown to be a risk factor for numerous cancers and breast cancer is no exception, multiple epidemiologic studies have shown link between breast cancer and increased alcohol consumption [6, 7]. Numerous observational, randomised and controlled trials have highlighted a link between postmenopausal hormone use and breast cancer incidence [8-11]. After menopause the predominant source of endogenous estrogen is from the adipose tissue and therefore body mass index (BMI) and weight gain after menopause has been characterised as a breast cancer risk factor [12, 13]. Genetic factors also play a significant role in breast cancer onset, individuals with mutations on either breast cancer 1 or breast cancer 2 (BRCA1 & 2) genes have a substantially higher probability of breast cancer.

Where roughly 12% of women will develop breast cancer over their lifetime this increases to 72% in the case of BRCA1 mutations and 69% with BRCA2 mutations [14].

Pathology of breast cancer

Breast cancer is an uncontrolled growth of cells which can develop in one of several areas including the ducts, lobules or in non-glandular tissue. Due to increases in uptake of screening and increased awareness of symptoms in the general public, doctors can detect non-invasive pre-cancerous conditions before they spread. These include ductal carcinoma in situ (DCIS) which accounts for 85% of carcinomas in situ and lobular carcinoma in situ (LCIS) which accounts for the other 15% [15-17]. Despite these names nearly all breast cancers arise from the structure called the terminal duct lobular unit and the true distinction between the two is cytological and morphological [15]. DCIS as the name suggests is a cancerous growth in the ducts of mammary tissue and in the majority of cases early detection of DCIS has a high regression rate, however unchecked 25% of cases can form invasive breast cancer within 10 years. The other form, LCIS, is a cancerous growth in the milk-producing lobules of the breast and can be benign, but does increase risk of developing cancer later in life [15, 18]. If left unchecked both forms of in situ carcinomas may penetrate the lining of the ducts and lobules and invade surrounding connective and adipose tissues thereby becoming invasive. Invasive ductal carcinoma is the dominant form of breast cancer, resulting from DCIS; this is followed by invasive lobular carcinoma derived from LCIS [15]. (**Fig 1.1**).

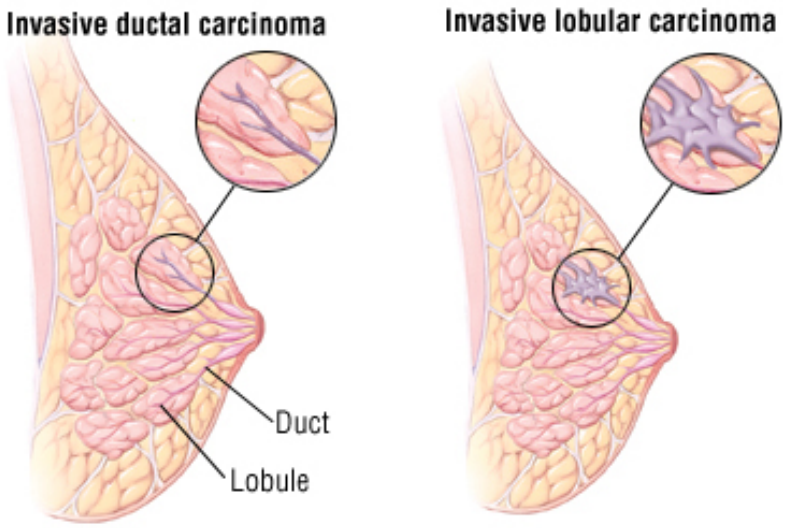

Figure 1.1. Pathology of mammary tissue, visualising invasive and ductal and lobular carcinomas [19].

There are also rarer forms of breast cancer such as medullary which accounts for 3-5% of breast cancers, mucinous 1-7% and tubular carcinomas 1-5% which tend to be slow growing, as well as Paget's disease 2% which originates in the milk ducts of the nipple [19-23]. The most aggressive and difficult to treat however is inflammatory carcinoma [24]. Inflammatory breast cancer can originate from both the lobule and the ducts and accounts for 2.5% of all breast cancers [25] and is characterised by local calor and rubor and high rates of metastases (approximately 30%) due to lymphatic involvement [26, 27].

1.1.2. BREAST CANCER SUBTYPES

Based on hormone receptor status of epithelial cells, breast cancer can be defined into 4 hierarchical subtypes. These include Luminal A, Luminal B, Human epidermal growth factor 2 (HER2), and basal-like or triple negative (TN) breast cancer [28, 29] (**Table 1.1**).

Table 1.1. Breast cancer subtype classification

Subtype	Estrogen Receptor	Progesterone Receptor	HER2
Luminal A	Positive	Positive or Negative	Negative
Luminal B	Positive	Positive or Negative	Positive or Negative
HER2	Negative	Negative	Positive
Basal/TN	Negative	Negative	Negative

Luminal Breast Cancer

Luminal A and B subtypes of breast cancer both express estrogen receptor (ER), can express progesterone receptor (PR) and display a similar phenotype to the resident luminal cells of the breast tissue inhibiting early detection somewhat [30]. Luminal A tumours are the most commonly occurring breast cancer subtype accounting for 50-60% of all breast cancers [30]. Compared to Luminal B, they possess higher expression of ER and associated genes such as estrogen receptor α (ESR1), GATA binding protein 3 (GATA3) and forkhead box protein A1 (FOXA1) and do not express HER2 [31]. Luminal B tumours on the other hand exhibit lower levels of ER-related genes, variable levels of HER2 and high levels of proliferation related genes such as, Ki-67, MKI67, BIRC5, and cyclin B1, and are therefore associated with a worse prognosis than their Luminal A counterparts [32-34] (**Fig. 1.2**).

Her2

Human epidermal growth factor 2 (HER2) was discovered as a proto-oncogene in 1985, and was later identified to be overexpressed in ~30% of breast cancers with a more aggressive phenotype and poorer disease free survival when compared to luminal cancers [35]. The HER2 overexpressing breast cancer subtype is defined by increased expression of epidermal

growth factor receptor 2 (ERBB2) at the RNA and protein level and by increased levels of co-amplified genes, such as growth factor receptor bound protein 7 (GRB7). HER2 tumours express low levels of ER and PR and are associated with a poor clinical outcome [36, 37] (**Fig. 1.2**).

Basal

The basal-like subtype was originally described in 1982 as a classification for breast cancers that expressed high molecular weight cytokeratins in their myoepithelial cells [38]. This subtype of breast cancer is characterised by negative expression of ER, PR and HER2, which is why they are often referred to as triple negative (TN), however basal breast cancer has been known to be less susceptible to chemotherapy than TN. Of all other subtypes this is the subtype associated with worst prognosis and poorest disease free survival as ER, PR and HER2 targeting therapies prove ineffective [29] (**Fig 1.2.**). The basal-like subtype has more recently been broken down further with the identification of a claudin-low TN breast cancer, which exhibits low levels of epithelial junction proteins claudin3, 4 and 7 as well as low levels of E-cadherin [39].

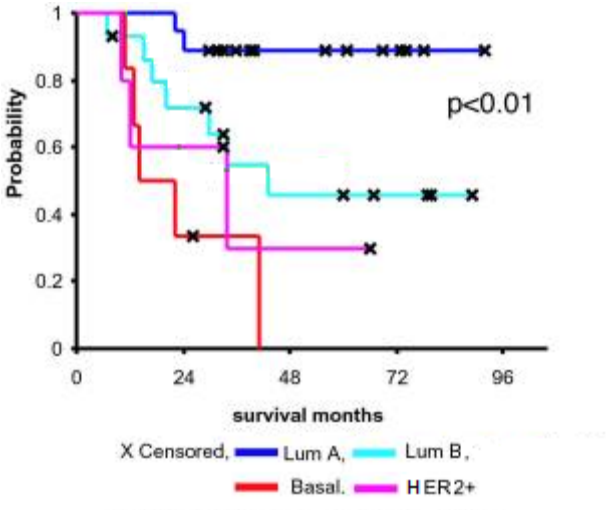

Figure 1.2. Overall survival analysis 49 breast cancer patients, uniformly treated in a prospective study, based on subtype**.** Adapted from [29].

1.1.3. CURRENT STANDARD OF CARE

Breast cancer treatment options depend on a number of factors including general health of the patient, age, family history and menopausal status. A number of other factors contribute to describe cancer stage, the staging system most often used is the American Joint Committee on Cancer (AJCC) TNM system [40]. This system factors in seven key pieces of information including, **T**umour size, lymph **N**ode status and **M**etastatic burden (**TNM**), but also hormone receptor status (estrogen receptor - ER, progesterone receptor – PR), human epidermal growth factor receptor 2 - HER2 status and cancer grade based on histological phenotype of cancerous cells. Based on this information breast cancer can be divided into 4 stages. Stage 1 breast cancer are generally small and have not spread to major lymph nodes, breast conserving surgery or mastectomy is the primary treatment, followed in some cases by radiation therapy to lower the chances of recurrence. If stage I cancer is hormone receptor positive a hormone therapy such as tamoxifen or aromatase inhibitors may be administered after surgery and in some cases adjuvant chemotherapy such as taxanes or anthracyclines depending on age of patient [41]. Stage II breast cancers are generally larger and have spread to lymph nodes thus in addition to stage I therapy systemic neoadjuvant hormone and chemo-therapies are utilised before surgery. Lymph nodes may also be removed by sentinel lymph node biopsy or axillary lymph node dissection. After surgery, adjuvant chemotherapy and radiotherapy is often utilised [42]. Stage III breast cancer is considered advanced cancer and is generally invasive with the detection of spreading to lymph nodes, inflammatory breast cancer falls within this category. All previous methods are utilised in a combinational therapy approach to reduce tumour burden. Breast cancers described as stage IV indicates that cancer has spread beyond the breast to other areas of the body including the brain, bones, lungs or liver, even with all previously described therapies, prognosis is poor (**Table 1.2.**).

Table 1.2. 5-year survival rates depending on stage of breast cancer [43].

Breast Cancer Stage	5-Year Survival Female	5-Year Survival Male
0	100%	100%
I	100%	100%
II	93%	91%
III	72%	72%
IV	22%	20%

Luminal Breast Cancer

The ER was the first molecule identified as a target for breast cancer therapy and tamoxifen became the first approved targeted therapy in 1977 [44]. Tamoxifen is a selective estrogen receptor modulator (SERM) which, when broken down in the liver produces metabolites which bind to the ER with high affinity, thereby blocking subsequent upregulation of proliferative genes, manifesting in reduced recurrence rates and mortality in luminal breast cancer [45]. Since 1977 numerous other ER targeting therapies have emerged including selective estrogen down regulators (SERDs) such as fulvestrant which displays antagonistic properties [46, 47] and aromatase inhibitors which prevent estrogen synthesis, for use in post-menopausal female breast cancer [48] (**Fig 1.3.**). More recently combinations of estrogen receptor therapies with mTOR/PI3K inhibitors such as everlolimus are being used for advanced ER/HER2 positive luminal B breast cancer [49].

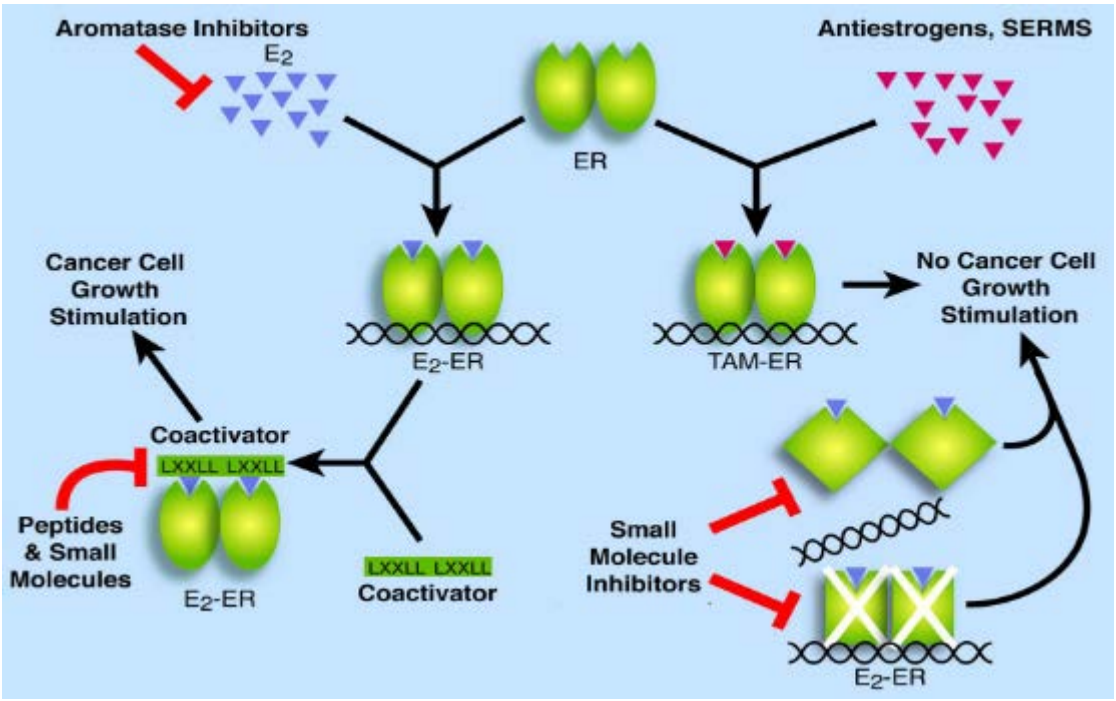

Figure 1.3. Therapeutic targeting of the estrogen receptor. ER signalling can be blocked by aromatase inhibition of precursors, anti-estrogens, or with peptides and small molecule inhibitors [50].

Her2

The discovery of HER2 in breast and ovarian cancer lead to the development of early targeted therapies in the form of monoclonal antibodies leading to the development of trastuzumab which became the first targeted anti kinase therapeutic agent based on genomic research [51, 52]. Trastuzumab prevents constitutive activation of HER2, induces internalisation and degradation of the protein, and stimulates the immune system to recognise HER2-overexpressing cells. Another clinically approved drug, the small molecule, Lapatinib binds to HER2 and HER1 and inhibits tumorigenic receptor signalling [53] (**Fig 1.4.**). Since then other targeted therapies have been clinically approved including pertuzumab, a second generation HER2 targeting antibody [54] and a kinase inhibitor lapatinib which binds both HER1 and HER2 causing internalisation and degradation [55]. Together these treatments represent the front line therapy for HER2 positive breast cancer. However, within the HER

overexpressing subtype, are tumours which become resistant to HER2 receptor targeting, through receptor dimerization with insulin-like growth factor-1 receptor (IGFR1) imparting drug resistance, indicating a need for further therapeutic targeting [56].

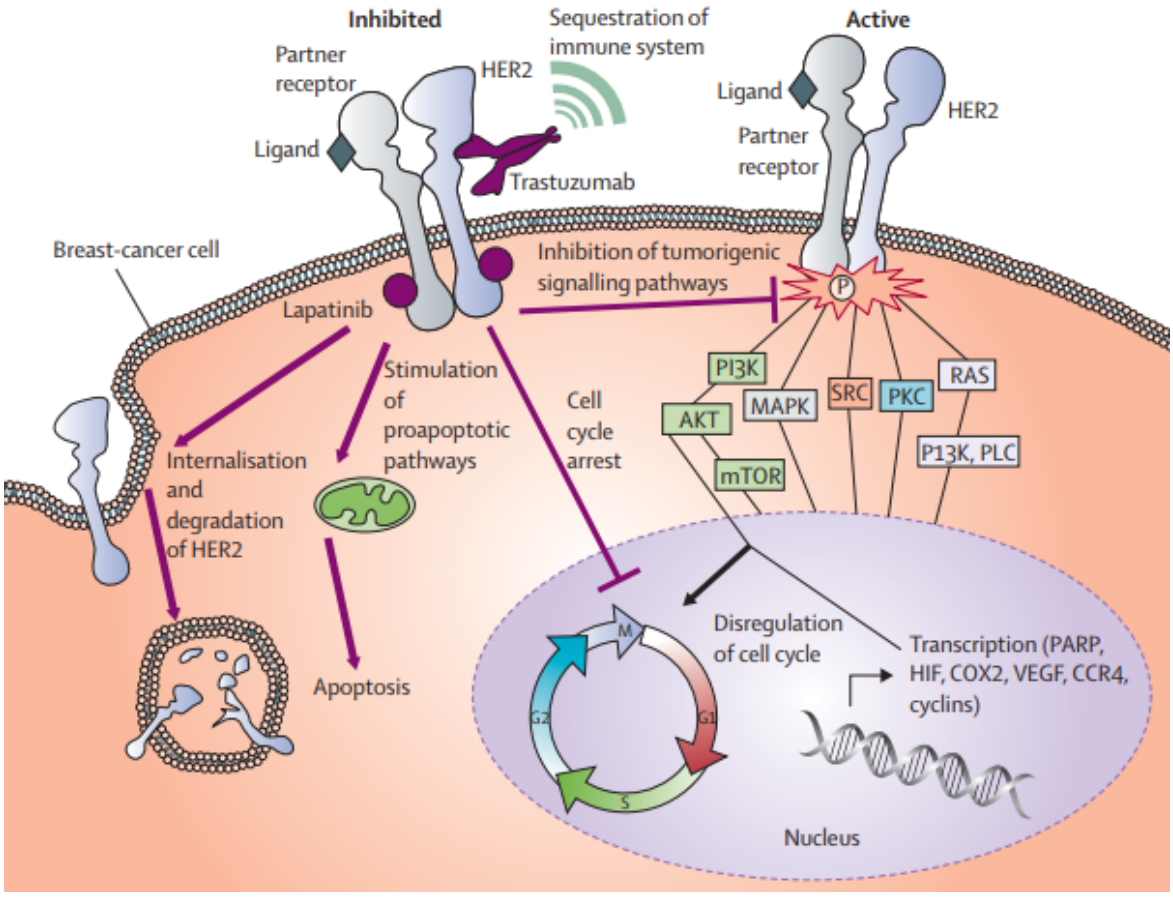

Figure 1.4. Mechanism of action of current therapies for HER2 overexpressing breast cancers. HER2 signalling can be blocked by trastuzumab inhibition of HER2 or small molecule inhibitor lapatinib inhibition of HER1/2 [57].

TNBC

Triple negative breast cancer is generally more susceptible to chemotherapy than other subtypes due to higher rates of proliferation [58], however due to lack of hormone receptors there are no effective targeted hormone therapies. Due to this, neoadjuvant chemotherapy along with adjuvant chemotherapy and radiotherapy are not always effective [59]. This is

confounded by the fact that, once metastasised, this subtype has a high tendency to involve organs such as liver, lung and brain manifesting in shortened median overall survival when compared to other subtypes [60, 61].

Current state of the art therapy is not always effective however, with 5 year recurrence rates among subtypes ranging from 0.8% (luminal A), 1.5% (luminal B), 8.4% (HER2), 7.1 % (TN) [59]. This would suggest that additional strategies to treat breast cancer are required in order to improve disease free survival rates. It is becoming increasingly clear that other cells within the breast tumour microenvironment (TME) contribute to the growth, spread, survival and recurrence of breast cancer [62]. With this knowledge, cancer research has shifted focus from chemotherapeutic or cytotoxic agents, to newer therapies tailored to activate or inhibit various pathways or constituents of the tumour microenvironment (TME) be they tumourigenic or non-tumourigenic cells [63, 64].

2.2 THE BREAST TUMOUR MICROENVIRONMENT

Previously described pathways and targeted therapies pertain to the epithelial compartment of breast tumours, however tumours are characterised by the recruitment and conditioning of other cell types to create a unique environment which supports tumour progression and metastases. This is termed the tumour microenvironment. The TME grows to become a complex network of cancer epithelial cells and stroma consisting of mesenchymal stromal cells (MSCs), cancer associated fibroblasts (CAFs), immune cells and endothelia, encased in a dense extracellular matrix (ECM) (**Fig 1.5.**). Cells recruited to the TME become integral cogs in maintaining growth, angiogenesis and metastases of tumours through secretion of growth factors, cytokines and inflammatory mediators [62].

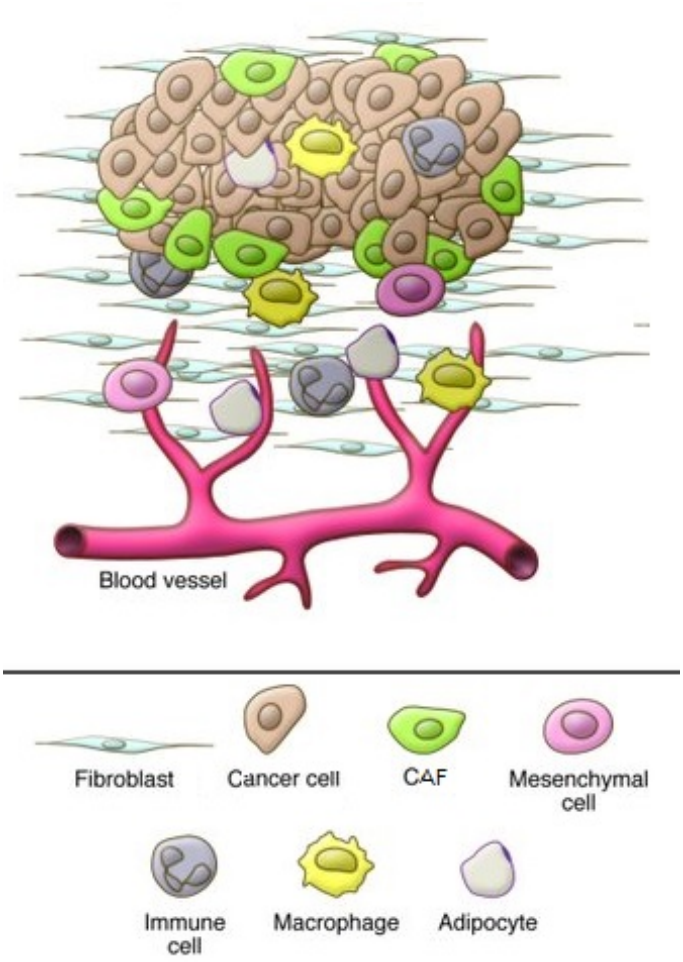

Figure 1.5. Constituents of the breast tumour microenvironment. Adapted from [65].

2.2.1 EPITHELIAL TO MESENCHYMAL TRANSITION

A well characterised phenotype in breast cancer epithelia is EMT, which is the process by which human epithelial mammary cells attain a mesenchymal phenotype [66]. EMT allows cells to migrate from the primary tumour site and metastasise to distal sites. The process of EMT is more prevalent in TN breast cancer, both basal-like and claudin-low, as tumours of this nature express higher levels of EMT proteins such as E-cadherin, SNAI1 and ZEB1 and p53 which can stabilise mutations [39, 67]. The mechanism which induces this phenotype involves an intricate network of signalling pathways including transforming growth factor-β (TGF-β/Smad), Tumour necrosis factor-α (TNF-α/NF-κB), Notch, Wingless-integrated

(Wnt/β-catenin) and receptor tyrosine kinase (RTK) and thus targeting these EMT pathways may be a viable strategy in targeting breast cancer [68].

TGFβ

Transforming growth factor-β has been defined as both a tumour promoter and suppressor depending on stage of cancer progression [69]. In the early stages of tumour progression TGF-β acts as a tumour suppressor by inducing growth arrest and apoptosis, however as the tumour progresses growth inhibition is diminished and the phenotype of EMT is retained or even accelerated [70]. Reductions in TGF-β signalling in tumour cells is accompanied by increased TGF-β ligand secretion which binds to its associated receptors TGFβRI and TGFβRII inducing activation of the Smad2/3 pathway [71] (**Fig 1.6.**). Overexpression of Smad2 and Smad3 has been shown to increase EMT in a mammary epithelial model [72] and conversely Smad3 knockout in primary tubular epithelial cells blocks TGF-β induced EMT and decreased motility, thereby decreasing metastatic potential [73]. TGF-β signalling can also occur via Smad-independent pathways such as the activation of JNK and p38 mitogen-activated protein kinase (MAPK) through TRAF6 [74] and small GTPases RhoA and RhoB [75, 76] (**Fig 1.6.**).

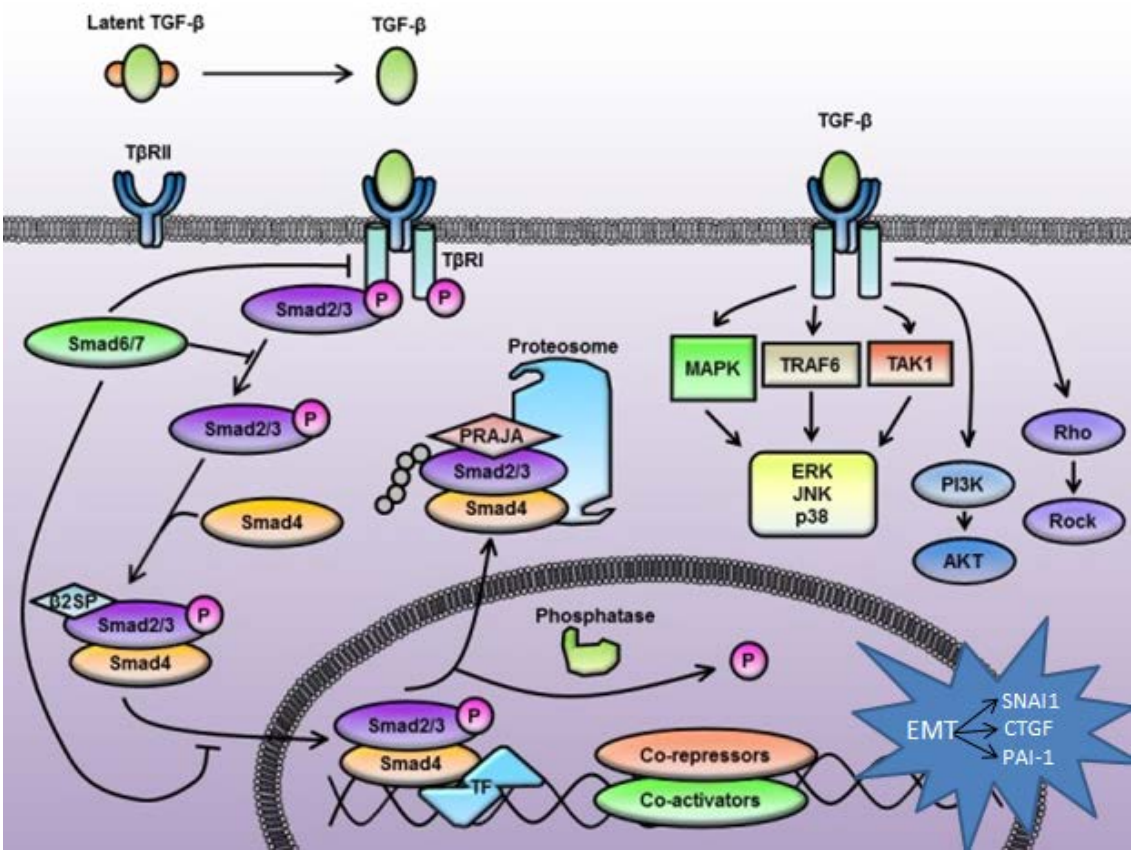

Figure 1.6. TGF-β signalling, through Smad-dependent and Smad-independent pathways activating EMT, adapted from [77].

The combination of TGF-β signalling through both Smad-dependent and independent pathways regulates the transcription of key EMT regulators SNAI1, Slug and Twist [78] as well as other EMT promoting genes such as PAI-1 and CTGF which induce myofibroblast differentiation and ECM production respectively [79, 80]. The combination of TGF-β with other EMT promoting proteins allows maintenance of the mesenchymal phenotype of tumour cells which have metastasised [81]. It has been shown in numerous studies that TGFβ receptor antagonists can reduce the EMT phenotype and decrease metastases [82-84]. However due to the duality in function of the TGFβ pathway in cancer, in some cases, the absence of TGFβ can exacerbate tumorigenesis [85, 86]. To date the most successful methods of TGFβ inhibition lays with clinically approved large-molecule inhibitors including

monoclonal antibodies such as fresolimumab (GC1008) [87], small molecule kinase inhibitors such as galunisertib (LY2157299) [88] and anti-sense oligonucleotides that inhibit protein translation such as AP12009, AP11014 and lucanix [89-91] these therapies have all shown varying degrees of success in cancer remission, usually as part of a combinational therapy with other chemotherapeutics (**Fig 1.7.**). However as with most therapies there are limitations in respect of specificity and toxicity and due to the involvement of TGFβ in numerous normal physiological functions, off target effects have been seen [92].

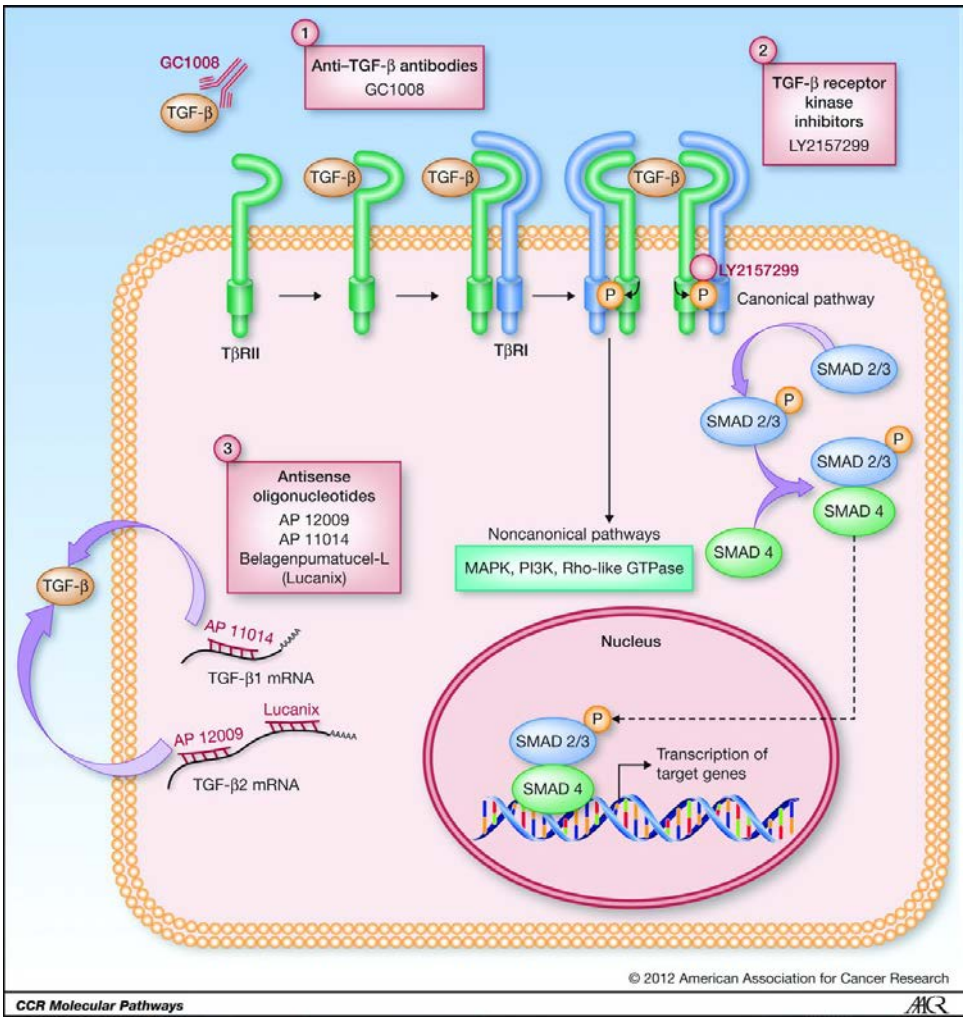

Figure 1.7. Mechanism of action of TGFβ signalling and current targeted therapies. TGFβ signalling can be inhibited through monoclonal antibody mediated inhibition of protein binding, or kinase inhibition of signalling pathways, as well as disruption of mRNA transcription [93].

TNFα

Tumour necrosis factor-α is a pivotal pro-inflammatory cytokine which also has been shown to induce EMT [94]. TNF-α signals through its two distinct cell surface receptors to initiate release of NF-κB which in turn has been shown to amplify production of TGFβ in head and neck cancers [95, 96]. Furthermore NF-κB has been shown to induce transcription of the key EMT markers Snail, Slug, Twist, ZEB1 and ZEB2 [97-99]. Targeting of TNFα has been the focus of research for a number of diseases and has led to the production of therapies which have shown efficacy in cancer treatment when used as part of a combination therapy, including the monoclonal antibody infliximab [100] and a small molecule etanercept [101]. Furthermore, studies have shown TNFα targeted therapies also effectively decrease TGFβ signalling, highlighting the close ties between TNFα/TGFβ signalling in EMT [102].

Notch Signalling

In the breast cancer setting, the Notch signalling pathway is involved in EMT amplification after initial activation by TGFβ or TNFα signals [103]. TGF-β has been shown to increase Notch signalling through Smad3 [104]. Elevated levels of Notch promote the hallmark suppression of E-cadherin through Slug upregulation, which further increases TGFβ production and activates Wnt signalling [104]. A Notch targeting monoclonal antibody demcizumab is currently undergoing phase II clinical trials for efficacy in lung cancer [105], as well as a small molecule inhibitor MK-0752 in phase I pancreatic cancer [106].

Wnt Signalling

The Wnt pathway plays a central role in cell proliferation and oncogenesis and within the mammary gland, canonical Wnt signalling has a dominant role in regulating cell interactions between epithelial and mesenchymal cells critical for morphogenesis [107]. Wnt signalling

manifests in the formation of a complex which regulates normal cell function but signalling can be disrupted in cancerous settings to enhance cell-cell adhesion and trigger EMT [108, 109]. Wnt can stabilise levels of SNAI1 to induce EMT and metastases [110]. As with other pro-oncogenic pathways a number of targeted therapies have shown promise such as monoclonal antibody vantictumab [111] and small molecules ipafricept and LGK974 [112, 113].

RTKs

In addition to the other EMT signalling pathways mentioned, numerous receptor tyrosine kinase pathways (RTKs) have been shown to play roles in EMT and metastases [114]. High levels of TGF-β within the TME along with constitutive RTK activation has been shown to be necessary and sufficient for induction of EMT [115-117]. Therapeutic targeting of RTKs in cancer has been extremely successful as one of the more notable RTK pathways lies in the EGFR family of which HER2 is a part. There has also been successful inhibition of EGFR tyrosine kinase using small molecule inhibitors such as Imatinib [118]. Furthermore the RTK VEGF and VEGFR can be targeted in the same manner and has been done successfully using the monoclonal antibody becacizumab [119] and small molecule inhibitor sunitinib [120].

Over the past ten years basic research into understanding the pathways and mechanisms involved in tumourigenesis has been translated to clinical approved therapies (**Table 1.3.)**. Significant strides have been made in targeting the main pathways involved in cancer EMT; however there are numerous other elements within the TME which still require investigation.

Table 1.3. Signalling pathway targeted therapies, clinically approved or in trial.

Pathway	Monoclonal	Small Molecule	Oligonucleotide
TGFβ	fresolimumab	galunisertib	AP12009, AP11014, Lucanix
TNFα	infliximab	etanercept	
Notch	demcizumab	MK-0752	
Wnt	vantictumab	ipafricept, LGK974	
RTK	becacizumab	sunitinib	

Epithelial cells are generally the most abundant constituent of the TME, and therefore the most targeted, but the targeting of these cells alone may not be sufficient for tumour regression. The heterogeneous mix of cells present within the TME may impart resistance to many therapies, be it poor infiltration of drugs through vasculature or evasion from immune detection and clearance [121]. Therefore strategies are being devised to target the individual constituents of the TME. The non-epithelial component of the TME is commonly referred to as the tumour stroma. It is well defined that the stroma plays a significant role in tumour progression [122]. At present a great deal of research is being focussed on highlighting the characteristics of specific cell components within the tumour stroma with the overarching aim of developing therapies which target these components in the treatment of cancer.

1.2.2 BREAST TUMOUR MESENCHYMAL STROMAL CELLS

Mesenchymal stromal cells are one of the initiating stromal cells within the TME and though they account for a small percentage, roughly 0.01%-1.1% in both prostate cancer and lymphomas, they significantly contribute to the formation of the tumour associated stroma [123-125]. In a normal physiological setting, MSCs reside in almost every tissue, with highest concentrations detected in the bone marrow and adipose tissue, here they can home to

sites of injury or inflammation through chemokine signalling such as the C-X-C chemokine receptor type 4/ C-X-C motif chemokine 12 (CXCR4/CXCL12) pathway [126, 127]. Defined by the International Society for Cell Therapy (ISCT) in 2006 as cells positive for CD105, CD73 & CD90 with negative expression of CD45, CD34, CD14, CD11b & MHCII [128]. MSCs have been characterised by their ability to differentiate into multiple lineages including muscle, cartilage, adipose, bone and connective tissues depending on source tissue [129] and also their ability to suppress T-cell and B-cell proliferation [130, 131]. In the breast TME there is recruitment and proliferation of MSCs through the same endocrine pathways as in the cases of injury or inflammation [132]. MSCs have been shown to home to inflammatory cytokines produced by cancer cells *in vitro* such as TNFα, IFNγ and IL-1β [133, 134], growth factors such as TGFβ, PDGF and HGF [133, 135] and chemokines such as CXCL12/CXCR4, matrix metalloproteinase-1 (MMP1) and vascular cell adhesion protein 1 (VCAM-1) [136-138]. Several papers suggest in the TME MSCs may differentiate into cancer associated fibroblast (CAFs) which then secrete higher levels of TGFβ, VEGF, IL-4 and IL-10 [139] and express higher levels alpha smooth muscle actin (αSMA), platelet-derived growth factor receptor beta (PDGFRβ), Desmin, fibroblast secretory protein (FSP) and fibroblast activation protein (FAP) differentiating them from their MSC precursors [140] however the origin of CAF is not clearly defined. In mouse models of breast and colon cancer high levels of VEGF in the TME have been shown to induce the differentiation of adipose derived MSC into cells which promote vascular growth [140-142] thereby promoting neovascularisation [143], manifesting in the aberrant leaky vasculature seen in many breast and stomach cancers which contributes to metastases [144, 145].

MSCs within tumours that do not differentiate into CAF have been shown to exist in two states referred to as normal tissue-derived MSC (N-MSC) and tumour tissue-educated MSC (T-MSC) [146]. N-MSC and T-MSC display very similar phenotypes in terms of cell surface

antigen profile [147, 148] however p53 expression has been observed to be low or absent in T-MSC [149]. It has also been shown that T-MSCs isolated from gastric and hepatocellular cancers exhibit significantly greater proliferative capacity and shorter doubling times due to presence of E3 ubiquitin-protein ligase (MDM2) and p21 not seen in N-MSCs [150] this manifests in higher levels of MSCs in tumour tissue than in normal tissues [147, 151]. T-MSCs have also been shown to have increased migratory potential over N-MSC and also a greater resistance to the chemotherapeutic cisplatin [150]. Due to the differing phenotype N-MSCs have been reported to exert some anti-tumorigenic effects, such as reducing tumour cell growth through inhibition of Wnt signalling [152, 153] and inducing apoptosis through upregulation of caspase 3 in blood, liver and breast cancers [153, 154]. N-MSCs have also been shown to induce apoptosis of vascular endothelial cells inhibiting vasculogeneis in cancers of the brain [155]. However while N-MSCs display some anti-tumorigenic effects they have also been shown to promote tumour migration through CXCR4 and VCAM [156, 157], promote EMT [158], and suppress the immune response through regulatory T-cell upregulation in cancers of the breast, bone and blood [159]. While there is evidence to suggest N-MSCs have partial anti-tumoural properties, T-MSCs have been shown to promote tumorigenesis. T-MSCs display a greater immune-suppressive capacity than N-MSC through increased expression of immunosuppressive factors PD-L1, TGFβ, IL-4 and IL-10, increasing levels of T-reg cells in breast and bone cancer [146, 160]. T-MSCs show a greater promotion of EMT through elevated secretion of CCL5 which activates EMT genes, ZEB1, Snai1 and CXCR4 [123], this is accompanied with increased proliferation of cancer cells [161], a summary of this is found in **Table 1.4.**

Table 1.4. Differences between N-MSC and T-MSC on various tumourigenic pathways

Phenotype	N-MSC	T-MSC
Tumour Cell Proliferation	↓	↑
Tumour Angiogenesis	↓	↑
Tumour EMT	↑	↑↑
Lymphocyte Inhibition	↑	↑↑

Recent research has focused on using MSCs as a drug delivery method in solid tumours due to their affinity to locate, engraft, proliferate and survive within the TME. One such strategy involved adenoviral overexpression of IFNβ in bone marrow derived MSC and showed tumour regression in a xenograft model of breast cancer [162], while others have used overexpression of IL-12 in bone marrow MSC to increase intra-tumoural apoptosis in a xenograft model of triple negative breast cancer [163]. A number of papers have shown therapeutic efficacy of adipose derived MSCs overexpressing tumour necrosis factor-related apoptosis-inducing ligand (TRAIL) in mouse models of cervical cancer and gliomas [164, 165]. MSCs are particularly suited to TRAIL delivery as they are inherently immune to TRAIL induced apoptosis [166] and this therapy is currently undergoing clinical trials in the treatment of lung cancer (NCT03298763). More recently MSCs are being nano-engineered to carry chemotherapeutics such as paclitaxel and doxorubicin, where they can home directly to tumours and deliver their payload over the course of several days, decreasing off target effects seen with conventional chemotherapy [167, 168]. A newly emerging therapy in the MSC field involves the use of extracellular vesicles or exosomes derived from MSCs in the treatment of disease. Exosomes are cell derived vesicles which are present in all tissues, they are the primary bioactive vesicles responsible for paracrine signalling in MSCs and can affect

the survival, proliferation, gene expression and migration of recipient cells [169]. In the cancer setting, MSCs are being engineered to overexpress anti-tumorigenic genes such as TRAIL, TNF or microRNAs and their subsequent extracellular vesicles possess anti-tumorigenic properties which have shown very promising results in reducing tumour burden in mouse models of breast cancer [170-172]. Exosomes represent a cell free therapy and thus could be advantageous as a commercial product. Direct targeting of MSCs in the TME is difficult due to lack of functional markers to differentiate them from CAFs and numerous studies have shown off- target affects such as cachexia and anaemia due targeting of normal MSCs elsewhere in the body [173].

1.2.3 CANCER ASSOCIATED FIBROBLASTS

Fibroblasts in healthy tissue are an important component at many levels. Primarily they are responsible for synthesis, deposition and remodelling of the ECM, while they also function as producers of a number of soluble paracrine growth factors which can regulate cell survival and proliferation such as fibroblast growth factor (FGF) and IL-1 [174]. In cancer, the stroma contains elevated levels of fibroblasts which are pathologically activated and termed cancer associated fibroblasts (CAFs) [175, 176]. They are derived from a number of precursors such as MSCs, epithelial cells through EMT and resident fibroblasts through TGFβ mediated reprogramming [177-179] (**Fig 1.7.)**.

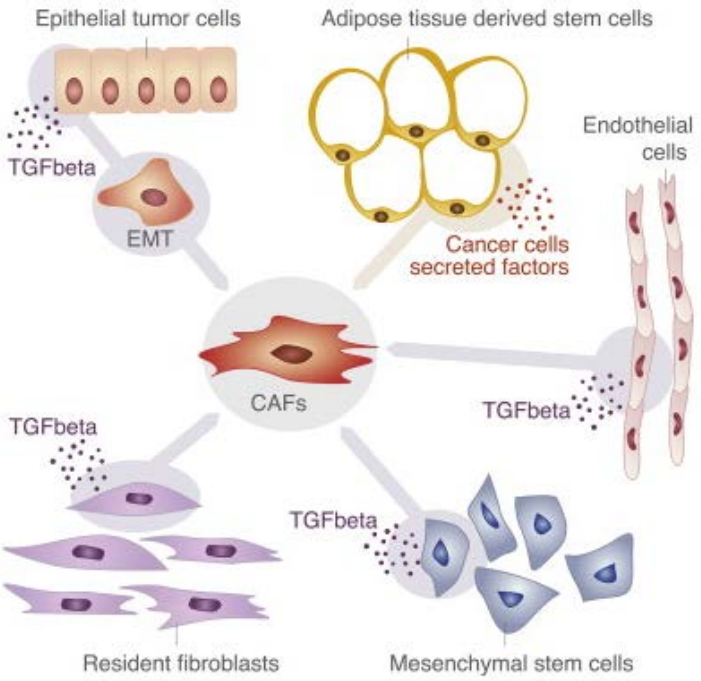

Figure 1.7. Reprogramming of cells to CAFs via TGFβ signalling. TGFβ stimulates EMT of epithelial cells, endothelial to mesenchymal transition in endothelial cells, MSC differentiation from bone marrow and adipose as well as fibroblast reprogramming [180]

CAFs have been observed to proliferate at roughly twice the speed of their normal fibroblast counterparts in pancreatic cancer due to down regulation of tumour protein 53-inducible nuclear protein 1 (TP53INP1) [181]. CAFs are characterised by their enhanced production of collagens and hyaluronic acid [182, 183], as a result they are commonly located in dense disorganised ECM of fibrillar collagen [184, 185]. Normal fibroblasts have been shown to suppress tumour formation in mouse models [186], however CAFs promote some of the more significant phenotypes associated with solid tumours. They are known to secrete a number of pro-tumorigenic growth factors such as hepatocyte growth factor (HGF) fibroblast growth factor (FGF), vascular endothelial growth factor (VEGF), epithelial growth factor (EGF), platelet derived growth factor (PDGF) and TGFβ all of which contribute towards EMT [177, 187]. Breast tumour derived CAFs also produce the chemokine CXCL12 [188] which is a chemoattractant for cells expressing its receptor CXCR4 which is present on MSCs and

endothelial progenitor cells thereby enhancing recruitment of MSCs to the TME and enhancing angiogenesis [188, 189]. CAFs have been shown to suppress the local immune response through TGFβ, intracellular adhesion molecule 1 (ICAM1) and programmed cell death protein ligand 1 and 2 (PD-L1, PD-L2) mediated suppression or death of T-cells [190-192]. These along with expression of the growth factors mentioned, manifests in proliferation, invasion, neo-angiogenesis, T-cell suppression and extracellular matrix remodelling within tumours. In pancreatic ductal adenocarcinoma, stroma can comprise up to 80% of the tumour, the majority cell type being CAFs [193], these tumours are more resistant to chemotherapy due to high intra-tumoural pressure and poor vasculature, chemotherapeutics simply cannot perfuse the tumour [194]. A recent study has characterised CAFs into 4 distinct subsets which accumulate differently in BC subtypes and have varying immune-modulatory properties, CAF-S1-4 [195]. This study found that in particular the CAF-S1 subset had a greater affinity for attracting and differentiating T-cells to regulatory T-cells thereby imparting stronger immune-suppression and possible resistance to immunotherapies. Furthermore CAF-S1 and CAF-S4 were preferentially detected in HER2 and TNBC and not in Luminal A or B thereby indicating their use as a further prognostic marker in identifying tumour subtype.

Because of their key role in tumour maintenance, growth and chemo-resistance, CAFs are primary targets in a number of mono and combination therapies. Pre-clinical studies targeting FAP+ CAFs through systemic ablation has shown tumour regression mediated by immune cell infiltration of the tumour [196]. Further studies have shown FAP+ CAFs secrete high levels of CXCL12 which prevents T-cell accumulation [197], additionally blocking of its receptor CXCR4 with the drug AMD3100 reverses this, allowing T-cell accumulation, and when combined with a PD-L1 inhibitor can yield the tumour regression [198]. Another study has targeted NG2+ and PDGFRβ+ cells in a mouse model of breast cancer [199], CAFs

express both of these markers however so too do pericytes which reside in the vascular system including that of tumours. This model showed that ablation of cells expressing these markers suppressed tumour growth but enhanced hypoxia associated EMT and metastases, highlighting the inherent limitations of cellular targeting.

Another approach involves treatment with chemotherapeutics nab-paclitaxel and gemcitabine for advanced pancreatic cancer, these drugs have been effective at reducing stromal burden, shown by marked reductions in CAF populations. This therapy effectively softens tumours allowing permeabilization for subsequent chemotherapeutics [200]. Another group has shown the efficacy of a combination of two further chemotherapeutics bortezomib and panobinostat in the reduction of CAF burden. The authors hypothesise that this combination acts by synergistic induction of apoptosis activated through unfolded protein response (UPR) which is caused by inhibition of protein degradation in ubiquitin-proteasome and aggresome system [201]. Another study demonstrates the action of pirfenidone (PFD) an anti-fibrotic agent and TGFβ antagonist, in combination with doxorubicin. They showed PFD suppressed the ability of CAFs to deposit collagen via TGFβ in TNBC tumours, effectively sensitising the tumours to further therapy. When this was combined with the chemotherapeutic doxorubicin they achieved reduction in tumour growth and metastases through increased perfusion [202].

Targeting CAFs within the tumour microenvironment represents a promising strategy for reducing tumour burden. However due to their inherent lack of unique distinguishing markers, directed therapy has wide reaching implications for off target effects. CAFs share striking similarities and function with MSCs and together they create an environment of immune-suppression and fibrosis imparting key features necessary for the maintenance of the TME. With this in mind work is being undertaken to target the individual pathways and

mechanisms by which MSC/CAF, herby referred to as tumour stromal cells (TSCs), aid tumourigenesis in an effort to breach the TME while limiting off target effects.

1.2.4 TUMOUR IMMUNE CELLS

T-lymphocytes

There are many different T cell populations which reside in the tumour microenvironment such as cytotoxic CD8 T cells and CD4 T helper 1, 2 and 17 cells (TH1, TH2,TH17), and the presence of these cells in cancers of the breast, kidney, ovary and lung may signify increased effectiveness of the use of immune cell targeting therapies [203]. The response of these lymphocytes, known as type 1 immune responses, function optimally against acute infections and are inhibited shortly after activation to limit tissue damage [204]. Downregulation of this response is controlled by immunosuppressive T regulatory cells (Tregs) and high percentages of Tregs within tumours has been described as tumour promoting [205]. High levels of Tregs in the TME is accompanied by further production of immunosuppressive cytokines IL-10 and TGFβ, and cell mediated contact inhibition through cytotoxic T-lymphocyte antigen 4 (CTLA4) and programmed cell death protein 1 (PD-1) [206]. Directly targeting the Treg population in cancer has shown a 52% response rate in advanced cutaneous melanoma through blockage of CTLA4 and PD-1. Ipilimumab is an anti-CTLA4 antibody which was approved in 2011 which shows efficacy through depletion of CTLA4+ Tregs through monocyte cytotoxicity [207]. Anti PD-1 antibodies such as pembrolizumab and nivolumab have been used in combination with Anti CTLA4 to increase CD8 T cell activation in response to Treg depletion and has shown efficacy in phase 3 clinical trials for lung cancer [208]. TSC have been shown to downregulate T-cell activation and skew differentiation towards Tregs through expression and or secretion of a number of immune-modulatory proteins such as PD-L1, PD-L2, CTLA-4, indolamine 2,3 dioxygenase (IDO), nitrogen

oxidase synthase (NOS_2) prostaglandin E2 (PGE_2) HGF, TGFβ and IL10 [130, 190, 195, 198, 209-211] (**Fig 1.8.**).

Therapies targeting the activation of the T cell response and adoptive cell transfer have been the focus of a great deal of research recently culminating with the advent of chimeric antigen receptor (CAR)-T cell therapy [212] whereby autologous T-cells are engineered *ex vivo* to express recombinant CAR directed against the signal transducer CD19 which attack malignant B-cells in cancers such as acute lymphoblastic leukaemia (ALL) and B-cell lymphoma [213, 214]. More recently the employment of CAR-T cells in solid tumours is being investigated through engineering multiple CARs directed to the constituents of the immunosuppressive environment in the TME such as CD278 CD27 and FAP however research is still in early development [215-218]. Another successful approach involves adoptive cell therapy using tumour-infiltrating lymphocytes (TIL) for metastatic melanoma. This approach involves isolation and expansion of TILs in culture stimulated with IL-2 and anti-CD3 antibody before re-administration to patient [219] and has yielded response rates of over 50% [220].

B-lymphocytes

Similarly to T lymphocytes, B cell infiltration into the TME is associated with increased effectiveness of targeted therapies in breast cancer [221]. However there also exists a tumour promoting B cell subpopulation which produces immunosuppressive IL10, known as regulatory B cells (Bregs) [222]. Bregs appear to favour lung metastases in a mouse model of breast cancer and inhibit clearance of tumour cells by anti-CD20 therapy [223, 224]. Bregs reside in the lymphoid tissue surrounding tumours and in tumour draining lymph nodes and elicit their effects on trafficking immune cells and myeloid cells [225, 226]. Several studies have identified programmed cell death ligand 1 (PD-L1) as a crucial mediator of Bregs [227]

and thus anti-PD-L1 therapy could have positive effects on Breg suppression and immune cell trafficking to the TME. Again it has been shown that MSC/CAFs promote Breg differentiation and B-cell suppression through expression of IDO [228, 229] (**Fig 1.8.**).

Natural killer cells

Innate cytotoxic lymphocytes, natural killer (NK) cells as their name suggests, spontaneously kill cells deemed dangerous to the host such as cancer cells or foreign cells. Granzyme B and perforin are the core molecules required for NK cell mediated tumour destruction [230]. While their presence in high numbers in tumours is generally associated with a positive prognosis [231], as with other lymphocytes they become suppressed by factors present and or expressed by MSC/CAFs within the TME such as TGFβ, PGE_2 and IDO, limiting their effects [203, 232] (**Fig 1.8.**). Additionally NK cells can be directly suppressed by Tregs, MDSCs or platelets within the TME [233, 234]. The ability of NK cells to target cancer has made them the focus of adoptive cell therapies and has shown promise for some blood cancers [235, 236]. More recently the development of CAR-NK cells is being investigated. CAR-NK cells present several advantages over CAR-T such as short life span eliminating need for clearance, inherent down-regulation of tumour-antigen expression would not affect NKs and the cytokine storm syndrome associated with CAR-T would not be as severe with CAR-NK [237, 238]. However clinical trials are still in early stages (NCT03056339, NCT02839954) and efficacy is yet to be determined.

Tumour-associated macrophages

Tumour-associated macrophages (TAMs) are abundant in most cancers and are associated with a poor prognosis [239]. TAMs have a critical role in driving cancer related inflammation (CRI) which is one of the hallmarks of cancer [240]. TAMs arise in tumours from circulating precursors such as monocytes and monocyte related MDSCs that subsequently undergo differentiation into TAMs [241] and presence of these cells is also directly linked to tumour metastases [242]. Colony stimulating factor-1 (CSF-1) is a chief chemoattractant expressed in tumours responsible for monocyte recruitment to the TME. It is also linked with macrophage survival and polarization, directing macrophages to an immunosuppressive M2 phenotype [243, 244]. Multiple other signals within the TME have been attributed to the skewing of macrophages from M1 to M2 phenotype including factors expressed by MSC/CAF such as TGFβ, IDO and IL-10 (**Fig 1.8.**), but also as a result of the hypoxia niche within solid tumours activating the HIF pathway [240, 245, 246]. Furthermore, direct co-culture of macrophage with CAF has been shown to induce M2 differentiation [247].

TAMs not only suppress the adaptive immunity but also encourage angiogenesis, and produce EGF which stimulates cancer growth and IL-1 which promotes metastases [243]. The well characterised role of CSF-1 in macrophage recruitment, proliferation and differentiation has made it the prime candidate for therapeutic targeting within the TME. A number of clinical trials are ongoing investigating pexidartinib a small molecule inhibitor of CSF-1R [248] and emactuzumab and anti-CSF-1R antibody [249] and have shown safety and varying levels of success, however their use alone may not be sufficient and combinational approaches are being investigated. One such combination at the forefront of clinical trials is a combination with anti-PD-L1 therapies, pembrolizumab or Atezolizumab (NCT02452424, NCT02323191) as PD-L1 is upregulated on the surface of TAMs among other components of

the immunosuppressive niche within the TME [250]. Combinations of anti-CSF-1R (LY3022855) anti-PD-L1 (durvalumab) and anti-CTLA-4 (tremelimumab) are also being investigated (NCT02718911) effectively targeting both TAMs and Tregs thereby allowing immune cell activation and tumour regression.

Tumour-associated neutrophils

Tumour-associated neutrophils (TANs) make up a significant proportion of leucocytes that infiltrate the TME and they have a dichotomous relationship with cancer. TANs can be subcategorised into N1 and N2 subsets analogous to M1 and M2 macrophage, N1 being tumour suppressing and N2 tumour promoting [251]. Cytokines present within solid tumours many of which are secreted by MSC/CAFs e.g. IL-35 and TGFβ, skew differentiation towards an N2 phenotype (**Fig 1.8.**) N2 neutrophils show a degree of cell plasticity and are able to switch back to N1 cells under favourable conditions [251, 252]. TANs have been linked with multiple metastasis promoting roles in cancer, primarily metastatic lung seeding [253, 254]. The main chemo attractants responsible for neutrophil trafficking to tumours are CXCR2 ligands such as CXCL1, CXCL2 and CXCL5 [255], and thus targeting these chemokines has become the focus of a number of clinical trials investigating the use of the small molecule inhibitor of CXCR2 reparixin in metastatic breast cancer (NCT01861054, NCT02370238).

Dendritic cells

Dendritic cells (DCs) have important roles in antigen processing and presentation to T-cells essentially linking the innate and adaptive immune responses [256]. However within the TME, the hypoxic, inflammatory environment impairs DC function, favouring macrophage differentiation due to high CSF-1 levels [257]. Additionally high intra-tumoural levels of MSC/CAF secreted, PGE_2, IDO and IL-10 interfere with DC maturation (**Fig 1.8.**), favouring

the immature DC which induces immune tolerance through T cell deletion and Treg expansion [258-260].

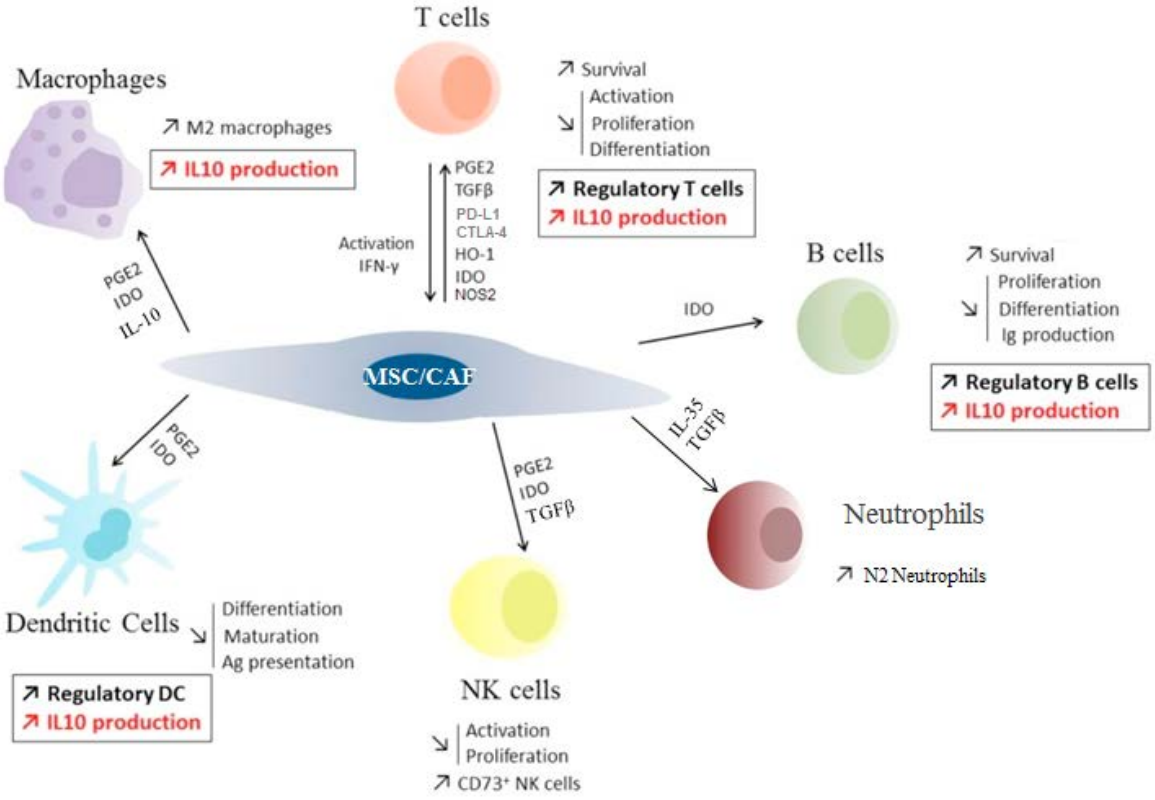

Figure 1.8. Mechanisms of MSC/CAF mediated immune-modulation of various immune cells. Factors secreted by MSC/CAFs induce the differentiation of regulatory immune cells such as Tregs, Bregs, suppressed NK cells, M2 macrophage, N2 neutrophils and prevent dendritic cell maturation. Adapted from [261].

It is clear from the literature that TSCs robustly modulate the immune response in the TME. TSCs elicit their immune-modulation through direct cell-cell interaction via PD-L1 and PD-L2, through secretion of enzymes and cytokines, such as IDO and IL-10 but most importantly through the persistent secretion of TGFβ [160, 198, 209, 211]. The presence of TSCs therefore encourages the differentiation of Tregs, Bregs, M2 macrophages and N2 neutrophils in addition to inhibiting activation of NK cells and maturation of DCs thereby disabling any immune response. The discovery of therapeutics which limit the action of TSCs within the

TME would therefore not only curtail tumour growth but also enable immune cell activation and immune mediated tumour destruction.

1.2.5 TUMOUR ENDOTHELIA

Angiogenesis is an essential step in tumour development and is heavily responsible for metastases. In a normal setting the process of angiogenesis is a controlled response to stimuli leading to neovascularisation which supports changing tissue requirements [262]. However in the developing TME, hypoxia, nutrient deprivation and the presence of MSC/CAFs triggers a cascade of pro-angiogenic cytokine secretion such as VEGF, TGFβ and platelet-derived growth factor (PDGF) which stimulates endothelial sprouting and proliferation [263, 264]. The induction of angiogenesis initially provides the developing tumour with more oxygen, but the constant release of cytokines leads to continuous vascular remodelling causing leaky and irregular blood flow [265]. This vasculature in turn recruits active platelets which secrete additional PDGF, in turn recruiting and activating further perivascular cells, MSCs and CAFs, creating a metaphorical "snowball effect" [266]. The clinically approved anti-angiogenic therapies bevacizumab and sorfenib are currently under investigation for cancer treatment and show varying degrees of success. Bevacizumab is a VEGF-A targeting antibody and sorfenib a tyrosine kinase inhibitor which targets VEGF and PDGF receptors [267]. However, success of anti-angiogenic therapies is heavily dependent on tumour subtype, luminal cancers but not basal display high levels of these receptors, imparting sensitivity to targeting [268].

1.2.6 TUMOUR EXTRACELLULAR MATRIX

The ECM is composed of approximately 300 proteins which regulate tissue homeostasis, inflammation and disease [269], the major constituents are fibrous proteins such as collagens, elastins, fibronectins and lamenins, and proteoglycans such as heparan sulfate, chondroitin

sulfate, keratan sulfate and hyaluronic acid [270]. Within the TME, ECM is responsible for tumour stiffness, topography, porosity and solubility, and unlike normal tissue, tumour ECM is continuously remodelled [271]. Fibroblasts and myofibroblasts are recruited to the TME under hypoxic conditions through the angiogenic pathway mentioned previously [266]. Here the presence of TGFβ stimulates differentiation into CAFs which rapidly synthesise ECM proteins which are then in turn remodelled by matrix metalloproteases (MMPs) [272]. Within the ECM, collagens represent 90% of all proteins [273] and increased collagen deposition has been recognised as a hallmark of cancer [274, 275]. Hypoxia is key in initiating this cascade and hypoxia-inducible factor 1 (HIF1) has been highlighted as a key mediator of fibrosis and ECM deposition [276, 277]. Specifically HIF1 has been shown to regulate collagen modifying enzymes intracellularly and extracellularly [278-280] and thus the HIF1 pathway would be a viable candidate for therapeutic targeting. Two HIF1 inhibitors which have shown promise pre-clinically and are undergoing phase 1 clinical trials, are the topoisomerase I inhibitor topotecan [281] and cardiac glycoside digoxin [282].

Heparan sulfate proteoglycans

Proteoglycans are present within all cellular and tissue compartments including tumours, either in ECM, on the cell surface or intracellularly [283]. Heparan sulfate proteoglycans (HSPGs) are complex molecules of one or more heparan sulfate chains bound covalently to a protein backbone [284] and can be found on the cell surface and in extracellular matrix [285]. Cell surface HSPGs bind cytokines, chemokines and growth factors, acting as co-receptors and protecting themselves from proteolysis [286]. Membrane bound HSPGs cooperate with a variety of cell adhesion receptors facilitating cell motility, cell-cell interaction and cell-ECM adhesion [287, 288]. The biological functions of HSPGs are therefore critically involved in

cancer, affecting growth, invasion and metastases through regulation of ECM modulating, pro-angiogenic and immune-suppressive biosynthetic enzymes [289].

Syndecans

The syndecans are a family of four transmembrane proteoglycans bearing heparan sulfate glycosaminoglycan chains [290]. The core protein contains a short intracellular domain, a highly conserved transmembrane domain and an ectodomain with varied coupling of HS and chondroitin sulfate (CS) chains which differentiates the four family members (**Fig 1.9.**) [291]. Syndecans are responsible for regulation of cell migration, adhesion, gene expression and organisation of cytoskeleton through binding of ECM proteins [292]. Since these are all pathways involved in cancer progression it is logical to deduce syndecans have a role in cancer development.

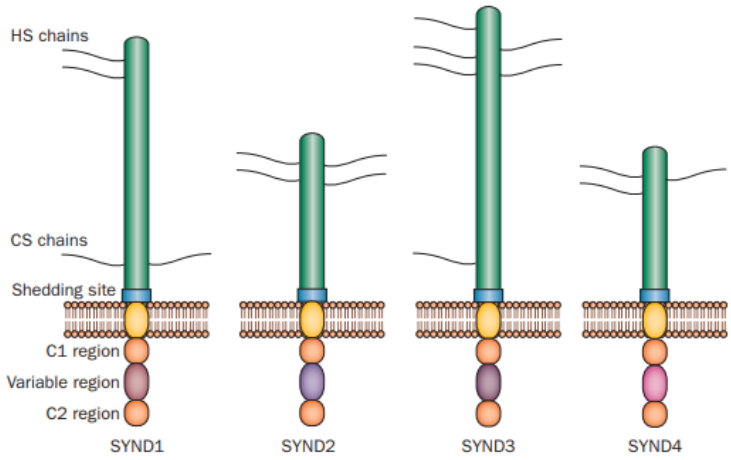

Figure 1.9. Schematic representation of SDC1-4 [293].

Syndecan-1 (SDC1) is the main syndecan expressed on epithelial cells of adult tissues, and has been found on developing cells of mesenchymal origin and differentiating lymphoid cells [294]. Importantly SDC1 has been shown to be critically involved in cancer differentiation specifically through involvement in EMT [295, 296]. E-cadherin shedding during EMT is

accompanied by SDC1 repression through SNAI1 [297], this coordinated loss has been documented in many epithelial cancers such as squamous cell, colorectal and prostate cancer [298-300]. Elevated levels of cell membrane SDC1 have been detected in breast cancers [301]. Interestingly SDC1 along with SDC4 have been shown to be induced in breast tumour stromal cells and their levels are correlated to a more aggressive cancer phenotype [302]. Furthermore expression of stromal SDC1 in the TME has been found to be a significant prognostic marker for relapse and poor outcomes [303]. While little has been published on the links between SDC4 in cancer and there have been no links made between SDC3 and cancer, there is a growing body of literature drawing connections between SDC2 and various cancers.

1.3 SYNDECAN-2

1.3.1 SYNDECAN-2 STRUCTURE

Syndecan-2 (SDC2) is abundantly expressed by mesenchymal cells, parenchymal cells and neurites [304-306]. The core protein consists of an ectodomain containing an N-terminal signal peptide, HS chains and a cleavage site, a single transmembrane domain and a C-terminal short cytoplasmic tail which contains a variable region specific to SDC2, responsible for binding to PDZ-containing cytoplasmic proteins such as syntenin [307, 308] (**Fig 1.10.**). The bound HS chains of SDC2 are composed of repeating di-saccharides, and their epigenetic modification through sulfation and epimerisation allows SDC2 to bind a variety of growth factors, membrane receptors and ECM proteins [309]. The transmembrane domain of SDC2 is needed for homodimerisation and oligomerisation leading to specific interactions with molecular partners such as fibronectin [310].

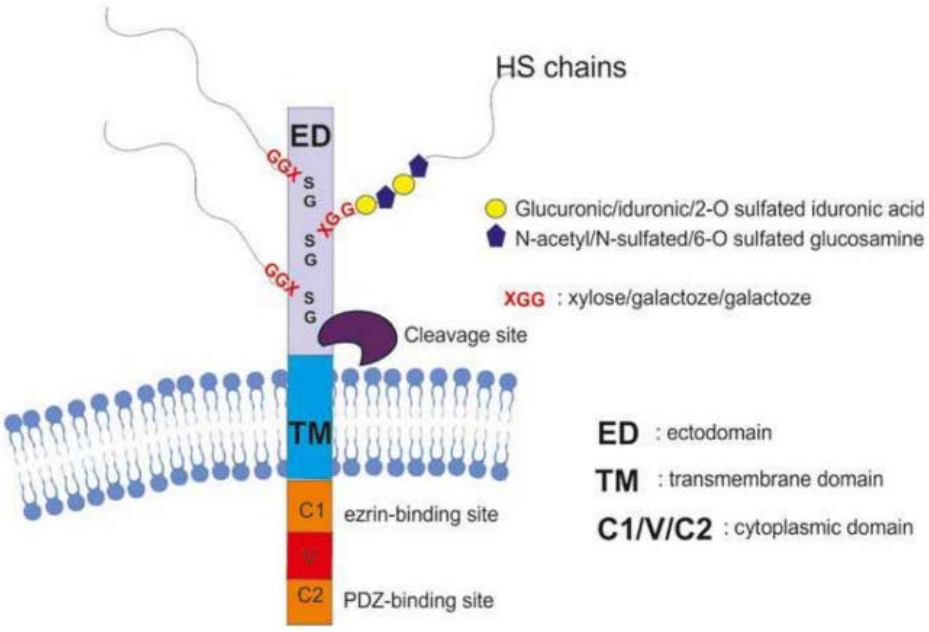

Figure 1.10. Schematic representation of SDC2 structure [311].

1.3.2 THE ROLE OF SYNDECAN-2

SDC2 has been found to regulate a number of cell functions, critical for tissue development and homeostasis including cell migration, adhesion, proliferation, differentiation and angiogenesis [307]. The majority of these roles are initiated through interaction with ECM proteins, integrins and with growth factors and their receptors. SDC2 has been highlighted as a co-receptor for growth factors such as fibroblast growth factor (FGF), epidermal growth factor (EGF) , vascular endothelial growth factor (VEGF) hepatocyte growth factor (HGF) and TGFβ [309, 312-314]. Importantly SDC2 interacts not only with TGFβ but also controls the expression of all three TGFβ receptors and promotes receptor localisation in the membrane [314]. SDC2 was demonstrated to mediate TGFβ signalling in unilateral nephrectomy and facilitate TGFβ1 dependent renal fibrosis [315]. In other indications SDC2 has been shown to downregulate TGFβ1 signalling imparting an anti-fibrotic role in lung fibrosis through TGFβRI internalisation [316]. Furthermore, inhibition of SDC2 with short interfering RNA has been shown to inhibit TGFβ signalling and adhesion in fibrosarcoma cells [317]. Conversely a study in periodontal fibroblasts and osteoblasts has highlighted a negative feedback relation by which TGFβ1 can upregulate SDC2 [318]. Furthermore the action of SDC2 shedding through cleavage by matrix metalloproteases (MMPs) regulates the action of growth factors involved in angiogenesis [319].

SDC2 plays an important role in actin reorganisation and regulation of membrane signalling networks through the binding of the ERM protein ezrin [320] which is necessary for apoptosis, cell-cell and cell-ECM communication which has ties to tumour growth and metastases [321]. Co-localisation of ezrin and SDC2 initiates RhoA GTPase and cdc42 Rho GTPase activation, forming actin rich cell micro spikes and filopodia in fibroblast-like cells [322, 323]. Actin rearrangement and filopodia formation can also be triggered by syntenin-1

another SDC2 binding partner, which has been highlighted as a step in the process of EMT in colon cancer cells [324]. In mesenchymal cells SDC2 interacts with integrin β1 (ITGB1) in the presence of Rho-GTP, Rho-kinase and CD148 to enable cell focal adhesion formation and spreading [322, 325]. Downregulation of SDC2 in endothelial cells has been shown to impair vasculogeneis through the same pathways inhibiting cell adhesion and spreading [326]. These key pathways indicate the importance of SDC2 in the formation of complex networks which has a critical impact on cell fate.

1.3.3 SYNDECAN-2 IN CANCER

There is a growing body of evidence to suggest SDC2 has a role in cancer progression. Increased SDC2 expression levels have been associated with metastatic ability of breast cancer and invasive index [327], it has also been described as a relapse and survival prediction factor of pancreatic cancer [328]. As previously described SDC2 participates in a number of signalling pathways almost all of which have indications in cancer and EMT [329] but also SDC2 itself can trigger EMT through induction of E-Cadherin shedding [330]. As previously mentioned SDC2 is primarily a mesenchymal marker [304-306] but due to its role in EMT, its expression has been detected in the stromal and epithelial compartment of various cancers.

1.3.4 SDC2 IN EPITHELIAL CANCER

The overexpression of epithelial derived SDC2 has been detected in breast and colon cancers and its presence has been correlated with a more aggressive phenotype through increased cell proliferation, adhesion and spreading [327, 331-333]. Overexpression of SDC2 in colon cancer lines HTC116 and HT-29 has been shown to increase adhesion and migration as well as *in vivo* growth, through interaction with fibronectin and upregulation of MMP-7 activity [334, 335]. Interestingly MMP-7 has been shown to directly cleave SDC2 from the cell

surface, and shed SDC2 has been shown to enhance tumourigenesis [290, 336]. Additionally SDC2 has been found to interact with caveolin-2, a regulator of endocytosis and intracellular signalling, to promote a more aggressive breast cancer phenotype [337]. Knockdown of SDC2 in a breast cancer cell line has been shown to attenuate tumour growth and metastases, by induction of apoptosis [338]. The expression of both cell surface SDC2 and shed SDC2 has been found to be a negative prognostic marker in breast and colon cancer and expression is correlated to other disease progression markers such as RKIP, FAK and PI3K [336-338].

1.3.5 SDC2 IN STROMAL CANCER

The role of stromal SDC2 in solid tumours is still quite unknown, in fibrosarcoma however, a tumour of mesenchymal origin SDC2 has been shown to be highly expressed [339]. Its presence has been associated with increased migration and invasion through activation of the tyrosine kinase, focal adhesion kinase (FAK) [339]. It has also been shown to phosphorylate extracellular signal-regulated kinase (ERK1/2) which is responsible for a number of pro-tumorigenic phenotypes such as tumour differentiation, proliferation and survival [340, 341]. As previously discussed SDC2 is a co-receptor for numerous growth factors, including TGFβ [314] as such SDC2 can facilitate the binding of TGFβ2 and subsequent expression of SMAD2 which has been shown to mediate fibrosarcoma cell adhesion [317]. The SDC2 mediated increase in TGFβ signalling also facilitates FAK and ITGB1 expression which further controls cell adhesion of fibrosarcoma cells [317]. Another mechanism of SDC2 previously discussed, the formation of filopodia [323] has pro-tumorigenic effects in fibrosarcoma through increased metastatic potential [339]. The complete role of SDC2 in the stromal compartment of tumours remains to be defined, but a review of the literature points to it as pro-oncogenic factor.

1.4 SPECIFIC AIMS OF THE PHD THESIS

In summary the literature suggests a key role for epithelial-derived SDC2 in cancer progression. Due to the role of SDC2 in many pro-oncogenic pathways such as EMT, adhesion, angiogenesis, and TGFβ signalling this would imply blocking SDC2 is a viable approach to inhibit carcinogenesis. However, SDC2 is also expressed in the stromal compartment of tumours and has the potential to effect tumour growth, metastasis and immunosuppression within the TME. Therefore the aim of this project is to modulate expression of syndecan-2 within epithelial or stromal cells of the breast tumour microenvironment and study its effects on breast tumour growth and metastasis.

Aim 1

Preliminary work has established that SDC2 protein and $SDC2^{+}$ stromal cells have pro-migratory and immunosuppressive properties respectively. Therefore we would like to investigate the pathways by which SDC2 elicits these two phenotypes. In the first instance we have decided to focus on the TGFβ pathway because of its well characterised role in cancer and interplay with SDC2. Using adenovirus SDC2 overexpression and SDC2 knockdown systems we will determine the effect of SDC2 modulation on TGFβ signalling in breast cancer and stromal cells. We will also determine the effect of SDC2 knockdown on the characteristics of triple negative breast cancer cell migration and stromal cell mediated immune-suppression.

Aim 2

Preliminary work has generated N-terminal deletion peptides of human SDC2 and demonstrated that specific SDC2-peptides have anti-migratory and anti-inflammatory

properties. We will establish if these SDC2-based-therapeutics effect TGFβ signalling, migration or immune-suppression in breast cancer and stromal cells.

1.5 HYPOTHESIS

Blockade of stromal or epithelial SDC2 will inhibit breast tumour growth and metastasis.

CHAPTER 2

MATERIALS & METHODS

2.1. CHEMICALS, REAGENTS & EQUIPMENT

2.1.1. ANTIBODIES

Table 2.1. List of flow cytometry antibodies

Target	Species	Flurochrome	Isotype	Dilution	Supplier
CD3	Human	Unconjugated	n/a	1/20,000	BD Biosciences, Cat#551916
CD4	Human	PE-Cy7	Mouse IgG1, κ	1/83	BD Biosciences, Cat#557852
CD4	Mouse	PerCP-Cy5.5	Rat IgG2a, κ	1/200	BD Biosciences, Cat#561115
CD8a	Mouse	Pe-Cy7	Rat IgG2a, κ	1/200	BD Biosciences, Cat#561097
CD11b	Human	PE-Cy7	Mouse IgG1, κ	1/20	BD Biosciences, Cat#557743
CD11b	Mouse	FITC	Rat IgG2b, κ	1/10	BD Biosciences, Cat#553310
CD11b	Mouse	APC-Cy7	Rat IgG2b, κ	1/50	BD Biosciences, Cat#553312

2.1.1. ANTIBODIES CONTINUED

Table 2.1. List of flow cytometry antibodies continued

Target	Species	Flurochrome	Isotype	Dilution	Supplier
CD11c	Mouse	PE	Hamster IgG1, λ	1/50	BD Biosciences, Cat#553802
CD14	Human	APC	Mouse IgG2a, κ	1/5	BD Biosciences, Cat#561383
CD15	Human	FITC	Mouse IgM, κ	1/5	BD Biosciences, Cat#555401
CD16/32	Mouse	Unconjugated	Rat IgG2a, λ	1/100	BioLegend, Cat#101301
CD25	Mouse	APC-Cy7	Rat IgG1, λ	1/200	BD Biosciences, Cat#557658
CD28	Human	Unconjugated	n/a	1/100	BD Biosciences, Cat#556620
CD29	Human	PE-Cy5	Mouse IgG1, κ	1/100	BioLegend, Cat#303005
CD34	Human	PE	Mouse IgG1, κ	1/5	BD Biosciences, Cat#550619
CD44	Mouse	APC	Rat IgG2b, κ	1/400	BD Biosciences, Cat#559250
CD45	Human	FITC	Mouse IgG1, κ	1/100	BD Biosciences, Cat#555482

2.1.1. ANTIBODIES CONTINUED

Table 2.1. List of flow cytometry antibodies continued

Target	Species	Flurochrome	Isotype	Dilution	Supplier
CD45	Mouse	BV450	Rat IgG2b, κ	1/500	BD Biosciences, Cat#560368
CD45	Mouse	APC-Cy7	Rat IgG2b, κ	1/200	BD Biosciences, Cat#557659
CD62L	Mouse	PE	Rat IgG2a, κ	1/200	ThermoFisher, Cat#12-0621-82
CD73	Human	PE	Mouse IgG1, κ	1/20	BD Biosciences, Cat#550257
CD80	Human	PE-Cy7	Mouse IgG1, κ	1/20	BD Biosciences, Cat#561135
CD80	Mouse	FITC	Hamster IgG2, κ	1/10	BD Biosciences, Cat#553768
CD86	Human	AF488	Mouse IgG2b, κ	1/20	Biolegend, Cat#305413
CD86	Mouse	PE-Cy7	Rat IgG2a, κ	1/20	BD Biosciences, Cat#560582
CD90	Human	PE	Mouse IgG1, κ	1/100	BD Biosciences, Cat#555596

2.1.1. ANTIBODIES CONTINUED

Table 2.1. List of flow cytometry antibodies continued

Target	Species	Flurochrome	Isotype	Dilution	Supplier
CD105	Human	PE	Mouse IgG1, κ	1/10	BioLegend, Cat#323205
CD105	Mouse	AF-488	Rat IgG2a, κ	1/20	BioLegend, Cat#120405
CD117	Human	PE	Mouse IgG1	1/10	BD Biosciences, Cat#555714
CD140a (PDGFRα)	Human	PE	Mouse IgG2a, κ	1/5	BD Biosciences, Cat#556002
CD184 (CXCR4)	Human	PE-Cy5	Mouse IgG2a, κ	1/50	ThermoFisher, Cat#15-999-42
CD184 (CXCR4)	Mouse	BV510	Rat IgG2a, κ	1/100	BD Biosciences, Cat#563468
CD274 (PD-L1)	Human	PE-Cy7	Mouse IgG1, κ	1/67	BD Biosciences, Cat#558017
CD274 (PD-L1	Mouse	PerCP-eFluor710	Rat IgG2a, λ	1/100	ThermoFisher, Cat#46-5982-82
CD326 (EpCAM)	Human	FITC	Mouse IgG2b, κ	1/50	BioLegend, Cat#369813

2.1.1. ANTIBODIES CONTINUED

Table 2.1. List of flow cytometry antibodies continued

Target	Species	Flurochrome	Isotype	Dilution	Supplier
CD326 (EpCAM)	Mouse	PE-Cy7	Rat IgG2a, κ	1/100	BioLegend, Cat#118207
CD362 (Sdc2)	Mouse/ Human	APC	Rat IgG2b	1/50	R&D Systems, Cat#FAB2965A
F4/80	Mouse	APC	Rat IgG2a, κ	1/100	BioLegend, Cat#123151
FAP	Human	Unconjugated	Sheep IgG	1/50	R&D Systems Cat#AF3715
GP38 (Podoplanin)	Human	PE	Rat IgG2a	1/100	ThermoFisher, Cat#12-9381-42
GP38 (Podoplanin)	Mouse	PE	Hamster IgG	1/100	ThermoFisher, Cat#12-5381-82
Ly6C	Mouse	PerCP-Cy5.5	Rat IgM, κ	1/50	BD Biosciences, Cat#560525
Ly6G	Mouse	Pe-Cy7	Rat IgG2a, κ	1/100	BD Biosciences, Cat#560601
MHCI	Human	PE-Cy7	Mouse IgG1, κ	1/20	BD Biosciences, Cat#560651

2.1.1. ANTIBODIES CONTINUED

Table 2.1. List of flow cytometry antibodies continued

Target	Species	Flurochrome	Isotype	Dilution	Supplier
MCHI	Mouse	PE	Mouse IgG2a, κ	1/20	BD Biosciences, Cat#553566
MHCII	Human	FITC	Mouse IgG2a, κ	1/200	BioLegend, Cat#343303
MHCII	Mouse	PE	Rat IgG2b, κ	1/100	BD Biosciences, Cat#557000
NG2	Human	PE	Mouse IgG1	1/10	R&D Systems, Cat#FAB2585P
SCA-1	Mouse	FITC	Rat IgG2a, κ	1/100	BD Biosciences, Cat#557405
Ter119 (Ly-76)	Mouse	BV450	Rat IgG2b, κ	1/250	BD Biosciences, Cat#560504

2.1.1. ANTIBODIES CONTINUED

Table 2.2. List of primary western blot antibodies

Antigen	Species	Isotype	Dilution	Supplier
Cre	Bacteriophage P1	Rabbit IgG	1/1000	Abcam, Cat#ab190177
Fibronectin	Human	Mouse IgG1	1/1000	R&D Systems, Cat#MAB1918-SP
IgG FC	Mouse	Goat IgG1	1/1000	ThermoFisher, Cat#A16086
Sdc2	Human	Rat IgG	1/500	R&D Systems, Cat#MAB2965-SP
PD-L1/B7-H1	Human	Goat IgG	1/1000	R&D Systems, Cat#AF156-SP
pSmad2	Human	Rabbit IgG	1/1000	New England Biolabs, Cat#3108T

Table 2.3. List of secondary western blot antibodies

Antigen	Species	Dilution	Supplier
Anti-Rabbit IgG	Goat	1/1000	Santa Cruz, Cat#sc-2004
Anti-Mouse IgG	Goat	1/1000	Santa Cruz, Cat#sc-2005
Anti-Rat IgG	Goat	1/1000	Abcam, Cat#ab97057
Anti-Goat IgG	Donkey	1/1000	Santa Cruz, Cat#sc-2354

2.1.2. BUFFERS & SOLUTIONS

Table 2.4. List of buffers and solutions

Name	Recipe
Acid Alcohol Solution	1% (v/v) Concentrated HCl in 70% Ethanol.
Ammonia Water Solution	0.2% (v/v) Concentrated NaOH in dH_2O.
Crystal Violet Stain	20% (v/v) Methanol, 0.5% (w/v) Crystal Violet in dH_2O.
Blocking Buffer	5% (w/v) Semi-Skimmed Dry Milk in TBS-Tween.
FACS Buffer	1% (v/v) FBS, 0.1% (w/v) NaN_3 in PBS.
Growth Factor Reconstitution Buffer	0.1% BSA in PBS.
Human Tumour Digestion Buffer	0.1% (w/v) Collagenase III, in DMEM.
Mouse Bone Marrow Digestion Buffer	2.5mg/ml Collagenase I, 4mg/ml Dispase II Protease, 0.2mg/ml DNase in DMEM.
Mouse Tumour Digestion Buffer	1.5mg/ml Collagenase I, 30U/ml Hyaluronidase in DMEM.
Phosphate-Buffered Saline (PBS)	5 X Tablets in 1L dH_2O.
Protein Lysis Buffer	50mM Tris buffer pH 7.4, 300mM NaCl, 1mM EDTA, 1% (v/v) Triton-X-100, Complete protease & phosphatase inhibitors (Roche, Basel, Switzerland) 1/50ml, in dH_2O

2.1.2. BUFFERS & SOLUTIONS CONTINUED

Table 2.4. List of buffers and solutions continued

Name	Recipe
4x Reducing Protein Loading Buffer	8mM Tris-HCl pH6.8, 10% (v/v) glycerol, 2% (w/v) SDS, 4% (v/v) β-Mercaptoethanol, 0.2% (w/v) Bromophenol blue, 0.1% Sodium azide in dH_2O.
12% Resolving Gel	25% (v/v) 1.5M Tris-HCl pH 8.8, 12% (w/v) Acrylamide, 0.001% (w/v) SDS, 0.0005% (w/v) APS, 0.0005% (v/v) TEMED in dH_2O.
10X Running Buffer	0.25M Tris-HCl, 1.9M Glycine; 1% (v/v) SDS in 1L dH_2O
50X TAE Buffer	2M Tris-Base, 0.5M EDTA, 57.1ml Glacial Acetic Acid adjust to 1L with dH_2O.
4% Stacking gel	25% (v/v) 0.5M Tris-HCl pH 6.8, 4% (w/v) Acrylamide, 0.001% (w/v) SDS, 0.0005% (w/v) APS, 0.001% (v/v) TEMED in dH_2O.
1X Transfer Buffer	10% (v/v) 10X Transfer Buffer, 20% (v/v) 100% Methanol in dH_2O.
10X Transfer Buffer	0.25M Tris, 1.9M Glycine, 1% (v/w) SDS to 1L in dH_2O.
10X Tris-Buffered saline (TBS)	0.25M Tris-HCl pH 8.0, 1.5M NaCl, in dH_2O.
Tris-HCl 0.5M pH 6.8	125mM Tris, 400ml dH_2O, adjust to pH 6.8 with HCl; adjust to 500ml with dH2O.

2.1.3. BUFFERS & SOLUTIONS CONTINUED

Table 2.4. List of buffers and solutions continued

Name	Recipe
Tris-HCl 1.5M pH 8.8	375mM Tris, 400ml dH_2O, adjust to pH 8.8 with HCl; adjust to 500ml with dH2O.
TBS-Tween	100ml 10X TBS, 1% (v/v) Tween 20, to 1L with dH_2O.

2.1.3. CELL LINES

Table 2.5. List of cell lines and culture conditions

Cell	Cell Origin	Source	Culture Medium	Conditions	Plating Density
E0771	Murine Breast Cancer Cell Line		10% FBS, 100U/ml Penicillin, 100µg/ml Streptomycin in DMEM	5% CO_2 37°C	Thaw: 15,000/cm^2 Subculture: 5,000/cm^2
Human MSC	Human Bone Marrow Mesenchymal Stromal Cell	Orbsen Therapeutics Ltd. (Galway, Ireland)	10% FBS, 100U/ml Penicillin, 100µg/ml Streptomycin, 1ng/ml FGF-2 in α-MEM	5% CO_2 2% O_2 37°C	Thaw: 5,700/cm^2 Subculture: 2,800/cm^2

2.1.3. CELL LINES CONTINUED

Table 2.5. List of cell lines and culture conditions continued

Cell	Cell Origin	Source	Culture Medium	Conditions	Plating Density
Human PBMC	Human Peripheral Blood Mononuclear Cells	Harvested fresh from whole blood.	10% FBS, 2mM L-Glutamine, 0.1M Non-Essential Amino Acids, 1mM Sodium Pyruvate, 55µM β-mercaptoethanol in RPMI	5% CO_2 37°C	Fresh: $6.25x10^6/cm^2$
Human USC	Human Umbilical Stromal Cells	Orbsen Therapeutics Ltd. (Galway, Ireland)	10% FBS, 100U/ml Penicillin, 100µg/ml Streptomycin, 1ng/ml FGF-2 in α-MEM	5% CO_2 2% O_2 37°C	Thaw: $5,700/cm^2$ Subculture: $2,800/cm^2$
Human TSC	Human Tumour Derived Stromal Cells	Isolated from tissue samples from UCHG (Galway, Ireland)	10% FBS, 100U/ml Penicillin, 100µg/ml Streptomycin, 1ng/ml FGF-2 in α-MEM	5% CO_2 2% O_2 37°C	Thaw: $5,700/cm^2$ Subculture: $2,800/cm^2$

2.1.3. CELL LINES CONTINUED

Table 2.5. List of cell lines and culture conditions continued

Cell	Cell Origin	Source	Culture Medium	Conditions	Plating Density
MDA-MB-231	Human Triple Negative Breast Cancer Cell Line	American Type Culture Collections (Rockville, MD)	10% FBS, 100U/ml Penicillin, 100µg/ml Streptomycin in DMEM	5% CO_2 37°C	Thaw: 15,000/cm^2 Subculture: 5,000/cm^2
Murine MSC	Murine Bone Marrow Derived Stromal Cells	Orbsen Therapeutics Ltd. (Galway, Ireland)	10% FBS, 10% ES, 100U/ml Penicillin, 100µg/ml Streptomycin in α-MEM	5% CO_2 5% O_2 37°C	Thaw: 15,000/cm^2 Subculture: 7,000/cm^2
Murine TSC	Murine Tumour Derived Stromal Cells	Isolated from PyMT mammary breast tumours.	10% FBS, 10% ES, 100U/ml Penicillin, 100µg/ml Streptomycin in α-MEM	5% CO_2 5% O_2 37°C	Thaw: 15,000/cm^2 Subculture: 7,000/cm^2

2.1.4. CONSUMABLES

Table 2.6. List of consumables

Product	Supplier
Amersham™ Protran™ 0.2µm Nitrocellulose	GE Healthcare, Cat#10600001
T-25 Cell Culture Flask	ThermoFisher, Cat#136196
T-75 Cell Culture Flask	ThermoFisher, Cat#178905
T-175 Cell Culture Flask	ThermoFisher, Cat#178883
1.8ml Cryovials	ThermoFisher, Cat#V7884-450EA
10cm Dish	Sarstedt, Cat#83.3902
MicroAmp™ Fast Optical 96-Well Reaction Plate	ThermoFisher, Cat#4346907
MicroAmp® Optical Adhesive Film	ThermoFisher, Cat#4311971
LS+ Positive Selection Column	Miltenyi, Cat#130-042-401
Parafilm	Sigma-Aldrich, Cat#P6543-1EA
5ml Pipette	Sarstedt, Cat#86.1253.001
10ml Pipette	Sarstedt, Cat#86.1254.001
25ml Pipette	Sarstedt, Cat#86.1685.001
50ml Pipette	Sarstedt, Cat#86.1256.001
RNase-free Microfuge Tubes (1.5 mL)	ThermoFisher, Cat#AM12400
RTCA CIM Plate 16	Cambridge Bioscience, Cat#5665817001
1.5ml Screw Cap Tubes	Sarstedt, Cat#72.692
Superfrost Plus Adhesion Slides	ThermoFisher, Cat#J1800AMNT
Vetbond Tissue Adhesive	Medray, Cat#IM1469SB

2.1.6. CONSUMABLES CONTINUED

Table 2.6. List of consumables continued

Product	Supplier
Via1-Cassette	Chemometec, Cat# 941-0012
6-Well Cell Culture Plate	Sarstedt, Cat#83.3920.001
12-Well Cell Culture Plate	Sarstedt, Cat#83.3921
24-Well Cell Culture Plate	Sarstedt, Cat#83.3922.005
96-Well Round Bottom Cell Culture Plate	Sarstedt, Cat#82.1582.001
96-Well V-Bottom Cell Culture Plate	Sarstedt, Cat#83.3926

2.1.6. MOUSE MODELS

Table 2.7. List of mouse models

Name	Background	Supplier
B6-SDC2<tm1PG>/N (Sdc2)	C57BL/6N	Polygene, Switzerland
MMTV-PyVT,-mCherry,-Ova (PyMT:ChOVA)	C57BL/6	Krummel Lab, US
B6N.FVB-Tmem163Tg(ACTB-cre)2Mrt/CjDswJ (βActin-Cre)	C57BL/6NJ	Jackson Laboratory, Cat#019099
NOD.CB17-Prkdcscid/J (NOD SCID)	NOD/ShiLtSz	Jackson Laboratory, Cat#001303

2.1.6. PCR PRIMERS AND RNA PROBES

Table 2.8. PCR primers (Eurofins Genomics)

Name	Sequence
Active GFP Forward	GCA AGC TGA CCC TGA AGT TC
Active GFP Reverse	TCC TTG AAG TCG ATG CCC TT
Inactive GFP Forward	TCC TTG AAG TCG ATG CCC TT
Inactive GFP Reverse	GCA AGC TGA CCC TGA AGT TC
PyMT Gene Forward	GGA AGC AAG TAC TTC ACA AGG G
PyMT Gene Reverse	GGA AAG TCA CTA GGA GCA GGG
SDC2 Gene Forward	TGG CTG GAC AGG AGA ATG
SDC2 Gene Reverse	CCT CAA TGG AGC TATT GTC
SDC2 Fragment Forward Primer	CCG GAA TTC ATG CGG CGC GCG TGG ATCC
SDC2 Fragment 1 Reverse	CAC TTC CAA AGA TAC TGT TG
SDC2 Fragment 2 Reverse	GTG CTG CTC CAA AAG TGG AA

Table 2.9. RNA probes (ThermoFisher)

Gene	Species	Exon Boundary	Assay Location	Amplicon Length	Code
CDH1	Human	6-7	956	80	Hs01023895_m1
CTGF	Human	4-5	959	60	Hs00170014_m1
CXCR4	Human	1-1	973	153	Hs00607978_s1
CXCR4	Mouse	2	1144	148	Mm01996749_s1

2.1.6. PCR PRIMERS AND RNA PROBES CONTINUED

Table 2.9. RNA probes (ThermoFisher) continued

Gene	Species	Exon Boundary	Assay Location	Amplicon Length	Code
FN1	Human	8-9	1480	81	Hs01549976_m1
GAPDH	Mouse	7-7	1042	70	Mm03302249_g1
PAI-1	Human	2-3	431	82	Hs00167155_m1
PD-L1	Human	3-4	503	77	Hs00204257_m1
PD-L1	Mouse	3-4	483	77	Mm00452054_m1
SDC2	Human	1-2	676	103	Hs00299807_m1
SDC2	Human	4-5	1058	142	Hs0181433_m1
SDC2	Mouse	3-4	833	113	Mm04207492_m1
SMAD-7	Human	3-4	1031	105	Hs00998193_m1
SMAD-7	Mouse	1-2	2204	144	Mm00484742_m1
SNAI1	Human	1-2	166	66	Hs00195591_m1
TGFβR3	Human	15-16	2845	60	Hs00234257_m1
TBP	Human	2-3	578	91	HS00427620_m1
ZEB1	Human	5-6	1026	101	Hs01566408_m1

2.1.7. REAGENTS

Table 2.10. List of reagents

Reagent	Supplier
α-MEM	ThermoFisher, Cat#32561
ACK Lysing Buffer	ThermoFisher, Cat#A1049201
Acrylamide-Bis-Acrylamide 30% ratio 29:1	Sigma-Aldrich/Merck, Cat#A3574
Adenovirus – Sdc2	Welgene
Adenovirus – Control	Welgene
Adenovirus – Short Hairpin Sdc2	Welgene
Adenovirus – Short Hairpin Control	Welgene
Agarose	Sigma-Aldrich/Merck, Cat#A9539
Ammonium Hydroxide 1M	Sigma-Aldrich/Merck, Cat#09859
Ammoniumpersulfate (APS) 10% (w/v)	Sigma-Aldrich/Merck, Cat#A3678
β-Mercaptoethanol	Sigma-Aldrich/Merck, Cat#M6250
BCA Protein Assay Reagent (bicinchoninic acid)	ThermoFisher, Cat#23225
BglII Restriction Enzyme	New England Biolabs, Cat#R0144
Bromophenol Blue	Sigma-Aldrich/Merck, Cat#B5525
BSA (Bovine Serum Albumin)	Sigma-Aldrich/Merck, Cat#A2058
CellTrace™ CFSE Cell Proliferation Kit	ThermoFisher, Cat#C34571
Collagenase Type I	Sigma-Aldrich/Merck, Cat#SCR103
Collagenase Type III	Worthington Biochemical, Cat#LS004186

2.1.7. REAGENTS CONTINUED

Table 2.10. List of reagents continued

Reagent	Supplier
Prestained Protein Standard,(11–245 kDa)	New England Biolabs, Cat#P7712
Complete Protease Inhibitor Cocktail Tablets	Sigma-Aldrich/Merck, Cat#4693159001
CryoStor™ CS10	Sigma-Aldrich/Merck, Cat#C2874
Crystal Violet	Sigma-Aldrich/Merck, Cat#C0775
DirectPCR Lysis Reagent	Viagen, Cat#401-E
Dispase II Protease	Sigma-Aldrich/Merck, Cat#D4693
DMEM with Sodium Pyruvate	ThermoFisher, Cat#11995073
DNase	Sigma-Aldrich/Merck, Cat#4536282001
dNTP mix 10mM	ThermoFisher, Cat#18427013
Eosin Y Solution with Phloxine	Sigma-Aldrich/Merck, Cat#HT110332
ECL Western Blotting Substrate	ThermoFisher, Cat#32106
EcoRI Restriction Enzyme	New England Biolabs, Cat#R0101
Equine Serum	Sigma-Aldrich/Merck, Cat#H1270
Ethanol	Sigma-Aldrich/Merck, Cat#51976
Ethylenediaminetetraacetic Acid (EDTA)	Sigma-Aldrich/Merck, Cat#EDS
Fetal Bovine Serum (FBS)	Sigma-Aldrich/Merck, Cat#F2442
Fibroblast Growth Factor-2 (Human)	Peprotech, Cat#100-18B
Ficol®-Paque Premium	Sigma-Aldrich/Merck, Cat#GE17-1440-02
FuGENE® HD Transfection Reagent	Promega, Cat#E2311

2.1.7. REAGENTS CONTINUED

Table 2.10. List of reagents continued

Reagent	Supplier
Glycerol	Sigma-Aldrich/Merck, Cat#G5516
Glycine	Sigma-Aldrich/Merck, Cat#G8898
Hematoxylin, Harris modified	Sigma-Aldrich/Merck, Cat#HHS16
High-Capacity cDNA Reverse Transcription Kit	ThermoFisher, Cat#4368814
Hyaluronidase	Sigma-Aldrich/Merck, Cat#H2126
Hydrochloric Acid	Sigma-Aldrich/Merck, Cat#H1758
1kb Plus DNA Ladder	ThermoFisher, Cat#10787018
LB Agar	Sigma-Aldrich/Merck, Cat#L3027
LB Broth Powder	Sigma-Aldrich/Merck, Cat#L3022
L-Glutamine	Sigma-Aldrich/Merck, Cat#G5792
Marvel Dried Skimmed Milk Powder	Chivers
Methanol	Sigma-Aldrich/Merck, Cat#34860
Mouse Cell Depletion Kit	Miltenyi, Cat#130-104-694
10% Neutral Buffered Formalin	Sigma-Aldrich/Merck, Cat#HT501128
Nuclease-Free Water	ThermoFisher, Cat#AM9916
Non-essential Amino Acids	Sigma-Aldrich/Merck, Cat#M7145
One Shot™ TOP10 Chem Competent *E. coli*	ThermoFisher, Cat#C404010
Opti-MEM reduced serum	ThermoFisher, Cat#31985062

2.1.7. REAGENTS CONTINUED

Table 2.10. List of reagents continued

Reagent	Supplier
Orange DNA loading dye 6x	ThermoFisher, Cat#R0631
pFUSE-hIgG1-Fc1 expression plasmid	Invivogen, Cat#pfuse-hg1fc1
Penicillin/Streptomycin Solution (100X)	ThermoFisher, Cat#15140122
Phosphate-Buffered Saline	ThermoFisher, Cat#10010023
Phosphate-Buffered Saline Tablets	Sigma-Aldrich/Merck, Cat#79382
Platinum PFX DNA Polymerase Kit	ThermoFisher, Cat#11708039
Ponceau-S Solution	Sigma-Aldrich/Merck, Cat#P7170
2-Propanol	Sigma-Aldrich/Merck, Cat#I9516
Proteinase K	Bioline, Cat#BIO-37037
PureLink™ Plasmid Maxiprep Kit	ThermoFisher, Cat#K210006
RNeasy Kit	Qiagen, Cat#74106
RPMI 1640	ThermoFisher, Cat#11875
Smad2/3 Control Extracts	New England Biolabs, Cat#12052S
Sodium Azide	Sigma-Aldrich/Merck, Cat#S2002
Sodium Dodecyl Sulphate Solution 20% in H_2O	Sigma-Aldrich/Merck, Cat#05030
Sodium Hydroxide	Sigma-Aldrich/Merck, Cat#S8045
Sodium Pyruvate	Sigma-Aldrich/Merck, Cat#P5280
SYBR safe DNA Gel Stain 10,000X	ThermoFisher, Cat#S33102
Syndecan-2 ELISA Kit	Cusabio, Cat#CSB-EL020889HU

2.1.7. REAGENTS CONTINUED

Table 2.10. List of reagents continued

Reagent	Supplier
SYTOX™ Blue Dead Cell Stain	ThermoFisher, Cat#S34857
T4 DNA Ligase	New England Biolabs, Cat#M0202S
TaqMan™ Gene Expression Master Mix	ThermoFisher, Cat#4369016
1,2-Bis-(dimethylamine)-Ethane (TEMED)	Sigma-Aldrich/Merck, Cat#B42985
Transforming Growth Factor β1 (Human)	R&D Systems, Cat#240-B-010
Transforming Growth Factor β2 (Human)	R&D Systems, Cat#302-B-010
Transforming Growth Factor β3 (Human)	R&D Systems, Cat#243-B3-010
Tris-HCl	Sigma-Aldrich/Merck, Cat#10812846001
Trizma®Base	Sigma-Aldrich/Merck, Cat#T1503
Trypsin EDTA Solution 0.25%	ThermoFisher, Cat#2520056
Tween®20	Sigma-Aldrich/Merck, Cat#P9416
Zeocin	ThermoFisher, Cat#R25001

2.2. METHODS

2.2.1. MOLECULAR BIOLOGY METHODS

2.2.1.1. DNA ISOLATION AND POLYMERASE CHAIN REACTION (PCR)

Tissue or cells were digested using DirectPCR™ lysis reagent at a ratio of 100µl per sample with 0.3mg/ml proteinase K. Samples were incubated at 55°C for 3.45hours at 700rpm in an incubator shaker. After this incubation samples were heated to 85° for 30 minutes to inactivate the proteinase K. Tissue samples were centrifuged at 2000G for 10 seconds at room temperature to pellet hair and debris. Soluble lysate was transferred to a fresh tube for PCR.

PCR was performed using Platinum PFX polymerase according to manufacturer's instructions. A PCR master-mix was made according to **Table 2.11.** using primers from table 2.7. Five microlitres of sample DNA was combined with 45µl of master-mix and samples were transferred to a thermo-cycler and run according to **Table 2.12**.

Table 2.11. Platinum PFX Master-mix

Component	Volume for 1 Reaction
10X PFX Amplification Buffer	5µl
10mM dNTP Mixture	1.5µl
50mM $MgSO_4$	1µl
0.75µM Primers	1.5µl each
DNA Polymerase	0.4µl
Distilled H_2O	34.1µl

Table 2.12. PCR Settings

Temperature	Time	Cycles
94°C	3 minutes	1
94°C 55°C 68°C	15 seconds 30 seconds 1 minute	35
68°C	12 minutes	1
4°C	∞	n/a

2.2.1.2. AGAROSE GEL ELECTROPHORESIS

A 2% agarose gel is prepared by boiling 2% agarose in 1xTAE buffer (**Table 2.4.**). The agarose is allowed to cool before adding 1x SYBR Safe DNA gel stain. The gel is poured into a casting block and a comb is added for samples. While the gel is solidifying samples are mixed with 6x orange DNA loading dye. The gel is submerged in 1x TAE in a gel running chamber, samples are loaded along with a DNA ladder and the gel is run at 100V for 1.5 hours. After this point the gel is transferred to a Syngene G:BOX UV imager for detection.

2.2.1.3. PROTEIN EXTRACTION AND BCA ASSAY

Cells were lysed while still adhered in 6 well plates, 50-200ul of protein lysis buffer (**Table 2.4**.) was added to cells depending on confluency and plates were kept on ice for 20 minutes to allow complete lysis. After the incubation the cell lysate was centrifuged at 16,000G for 20 minutes at 4°C and the soluble supernatant transferred to a new tube.

A protein determination assay was performed with a Pierce BCA protein assay kit (Thermo Scientific) as per the manufacturer's instructions. Briefly, A and B reagents were combined

in a 50:1 ratio. Protein standards were made using bovine serum albumin in a range from 0-20µg/µl. Samples and standards were added to individual wells of a 96 well plate, in duplicate, after which 200µl of assay reagent was added. The assay plate was incubated for 2hours at 37°C and the OD was detected with a plate reader at 562nm.

2.2.1.4. WESTERN BLOT

A 12% resolving gel was prepared according to (**Table 2.4**.), and was then poured into a 1.5mm gel casting mould. Isopropanol was carefully layered on top to ensure a smooth interface. After polymerisation, a 4% stacking gel was prepared according to (**Table 2.4**.). The isopropanol was poured off and the stacking gel was layered on top of the resolving gel and a comb secured. Protein samples were diluted to enable maximum loading of protein, mixed with 4x reducing protein loading buffer (**Table 2.4**.) and boiled at 95°C for 5minutes. Samples were loaded on the gel along with a prestained protein ladder (New England Biolabs). The loaded gel was then electrophoresed in SDS running buffer (**Table 2.4**.) at 120-125V constant ~30mA for 1.5 hours. After electrophoresis, the gel was removed from the casting plates, the stacking gel was removed and the resolving gel was equilibrated in transfer buffer (**Table 2.4**.). A nitrocellulose transfer membrane (GE Healthcare) was equilibrated by washing in 100% ethanol for 5mins followed by 3 rinses in distilled water and finally 2 washes in transfer buffer. A blotting cassette was prepared with a sponge and 5 Whatman filters on the anode, followed by the nitrocellulose membrane, the gel and 5 more filters with a sponge. The gel construct was immersed in transfer buffer and the proteins were transferred at 60V, 150mA, 9W for 1 hour in a Trans-Blot® Semi-Dry Transfer Cell system (Bio-Rad). The membrane was removed after and incubated for 2hours at room temperature in blocking buffer (**Table 2.4**.). The desired antibody was prepared in blocking buffer, and was incubated with the membrane on a roller at 4°C overnight. The following day the membrane was

washed 3 times for 10minutes each in TBS-T. The secondary antibody was then applied to the membrane in blocking buffer, and placed on a roller for 1hour at room temperature. After this time, the membrane was washed a further 3 times again for ten minutes each in TBS-T (**Table 2.4**.). The membrane was then equilibrated by briefly washed in TBS. The ECL western blotting substrate (Pierce) was prepared by mixing solution A and B in a 1:1 ratio; this was pipetted directly onto the membrane, followed by immediate imaging on an AlphaInnotech FluorChem Chemiluminescent Imaging System.

2.2.1.5. ENZYME-LINKED IMMUNOSORBENT ASSAY (ELISA)

SDC2 ELISA was performed on serum samples from UCHG according to manufacturer's instructions. Briefly serum was diluted 1:1 in sample diluent, and 100µl was added to each sample well and each protein standard well from 0-1500pg/ml. Sequentially, biotin-antibody, HRP-avidin and TMB substrate was added to the samples according to the protocol. Subsequently, optical density was read at 450nm and 500nm using a Victor^{3}™ plate reader (PerkinElmer). Protein concentration was determined by generating a four parameter logistic (4PL) curve-fit from the protein standards.

2.2.1.6. RT-QPCR ANALYSIS

Total RNA was isolated using the RNeasy mini kit (Qiagen) as per manufacturer's instructions. Briefly, 6 well plates containing adherent cells are washed 3 times in PBS before adding 350µl RLT Lysis buffer (Qiagen). Lysis buffer is incubated for 30seconds at room temperature, after which it is transferred 1.5ml Eppendorf tubes. 350µl of 70% ethanol is added then added and mixed by pipette, before transferring to Rneasy columns. Qiagen protocol is strictly adhered to from point culminating in 30ul of ultra-pure H_2O containing RNA of interest. RNA samples are quantified using a ND-1000 spectrophotometer. RNA is then transcribed into cDNA using a high capacity cDNA reverse transcription kit (Applied

Biosystems) following manufacturers guidelines up to a maximum of 10ul of sample or 2000ng of RNA.

RNA analyses were performed using TaqMan® Gene Expression Assays (Applied Biosystems). 10ng of cDNA was resuspended in 9ul of ultra-pure H_2O which 1ul of target probe was added with 10ul of TaqMan® Gene Expression Master Mix (Applied Biosystems). Measurement was done using an ABI7500 Real Time PCR machine (Applied Biosystems). Relative quantification was performed using TATA-box binding Protein (TBP) as endogenous control for human due to stability of expression in cancer and cancer stem cells [342, 343] and glyceraldehyde 3-phosphate dehydrogenase (GAPDH) for mouse based on literature relating to stability in mouse models [344].

2.2.1.7. SDC2 FRAGMENT GENERATION

To generate Fc-tagged Sdc2 fragment 1 (Sdc2-F1-Fc) and Fc-tagged Sdc2 fragment 2 (Sdc2-F2-Fc) cDNAs spanning the length of amino acid 1-79 (F1) and amino acid 1-87 (F2) were engineered using PCR. Forward and reverse primers were obtained from Eurofins and a Myc-DDK tagged open reading frame (ORF) clone of human SDC2 was obtained from OriGENE and used as template DNA. PCR was performed using a Platinum PFX PCR kit (Invitrogen) as per manufacturer's instructions (**Table 2.11, 2.12**).PCR fragments were digested with EcoR1 and BglII and were sub-cloned into EcoR1 and BglII sites within the multiple cloning site of the pFUSE-hIgG1-Fc1 expression plasmid (Invivogen, **Fig 2.1.**) in frame with the Fc tag. All cloning was verified by sequencing (EuroFins).

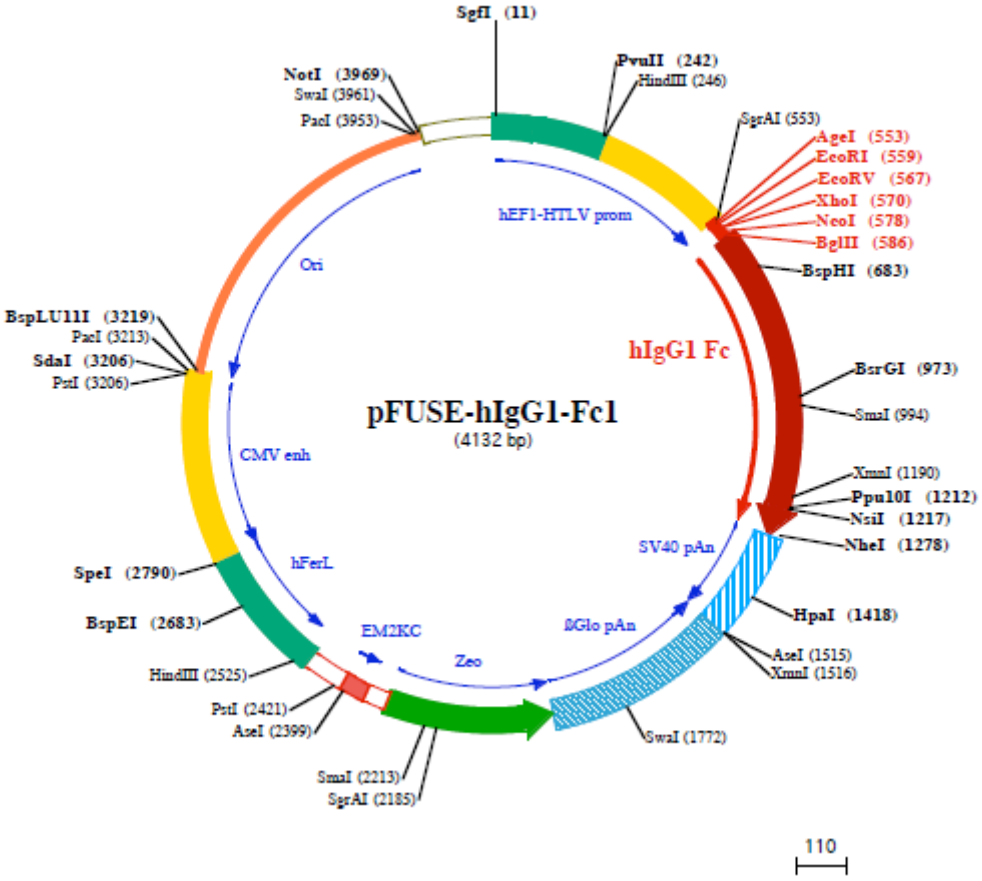

Figure 2.1. pFUSE-hIgG1-Fc1 expression plasmid. Schematic of FC expression plasmid used, EcoR1 and BglII cloning sites were selected.

2.2.1.8. TRANSFORMATION OF COMPETENT CELLS

One Shot™ TOP10 Chem Competent *E. coli* were thawed on ice from -80°C and 10µl of ligation mixture (**Table 2.13.**) was added to 50ul of bacteria. Bacteria and DNA were incubated on ice for 30 minutes after which point they were heat shocked at 42°C for 45 seconds. Samples were then returned to ice for 2 minutes and 250 µl LB broth was added, this mix was then incubated in a shaker for 1 hour at 37°C and 300rpm. Finally broth was spread on agar plates containing Zeocin antibiotic at 50µg/ml and incubated at 37°C overnight. The following day successful colonies were selected with a sterile pipette tip for mini-prep/maxi-prep.

Table 2.13. Ligation mixture.

Component	Volume for 1 reaction (10µl)
SDC2 Fragment DNA	1µl
Vector DNA	2ul
10X Ligase Buffer	1µl
T4 DNA Ligase	0.5µl
H_2O	5.5µl

2.2.1.9. PLASMID DNA PREPARATION

Colonies selected from the transformation (**Sect 2.2.1.8.**) were used to inoculate 5mls of LB broth containing Zeocin at 50µg/ml in a 15ml tube. Cultures were incubated in an orbital shaker overnight at 37°C at 200rpm. The following day 1ml of the bacterial culture is sampled to confirm presence of template DNA. DNA was extracted using an Isolate II DNA isolation kit (Bioline) as per manufacturer's instructions. After which point the DNA was digested using EcoR1 and BglII and was run on an agarose gel (**Sect 2.2.1.2.)**. Positive cultures were then selected for maxi-prep. The remaining 4ml of this starter culture was used to inoculate 200 ml of LB broth containing 50µg/ml Zeocin in a conical flask and then transferred to an incubator shaker overnight at 37°C and 200rpm. The following day bacteria are pelleted at 400G for 5 minutes at 4°C and DNA was prepared using a PureLink™ plasmid maxiprep kit as per manufacturer's instructions. DNA yield was then quantified using a Nanodrop ND-1000 at 260nm.

2.2.2 CELL BIOLOGY METHODS

All work using human tissue samples in this section were conducted under licences C.A.170530, C.A. 429, C.A. 45/05 and C.A.02/08 approved by the National University of Ireland, Galway research ethics committee.

2.2.2.1. CELL CULTURE

All cells were cultured in medium and conditions according to table 2.5. Cells were visually assessed daily using an upright microscope to confirm correct morphology and detect approach to confluency. Upon confluency cells were enzymatically removed from their plates using 0.25% trypsin/EDTA at 37°C for 2-5 minutes. Upon detachment, an equal volume of FBS-containing media was used to neutralise the trypsin. The cell suspension was then transferred to a sterile tube for cellular counting using a haemocytometer. Ten microlitres of the cell suspension was placed under the coverslip and 4 of 9 squares were counted and averaged to give total cell number per ml. Cells were then centrifuged at 400G for 5minutes at 4°C, washed in PBS, centrifuged again and resuspended in an appropriate volume of buffer, for the next intended step: cells to be cryopreserved were resuspended in CryoStor™ CS10 at $2x10^6$ cells per ml and frozen in aliquots of $1x10^6$ cells at -80°C, cells for subculture were resuspended in appropriate medium and re-plated according to densities in **table 2.5**, cells can be resuspended in protein lysis buffer for western blotting or directly lysed with RLT lysis buffer (Qiagen) for RNA analysis.

2.2.2.2. COLONY FORMATION ASSAY

Transduced or transfected cells were trypsinized, counted, and replated at a density of 500 cells/10-cm dish. 10 days later, colonies resulting from the surviving cells were washed twice

with PBS, fixed in 95% methanol for 5 minutes, stained with crystal violet solution (**Table 2.4.**) for 3minutes and rinsed under warm tap water. Colonies were then counted by eye.

2.2.2.3. ADENOVIRAL TRANSDUCTION

Cultured stromal or epithelial cells for transduction were plated in 6 well plates at $2x10^5$ cells per well and allowed to adhere in their preferred culture conditions for 12 hours. Following this rest adenovirus is added to wells at an MOI of 375 for knockdown short hairpin adenoviruses and an MOI of 125 for overexpression adenoviruses. Cells are returned to an incubator for 48 hours, after which RNA and protein is harvested from one well to assess transduction and others can proceed to further assays.

2.2.2.4. FUGENE HD TRANSFECTION

As before cultured cells for transfection are plated in 6 well plates at $2x10^5$ cells per well and allowed to adhere in their preferred culture conditions for 12 hours. A master mix containing 500ng of target DNA, 3ul of FuGENE HD in 100ul OptiMEM is prepared per well. 100ul of this is added per test well and returned to incubate for 48hours, after which RNA and protein is harvested from one well to assess transfection and others can proceed to further assays.

2.2.2.5. MIGRATION ASSAY

Migration was tracked using an xCELLigence real time cell analysis instrument; assays were set up following manufacturer's instructions. In brief, 160ul of test media is added to the bottom half of a RTCA DP CIM-Plate 16, ensuring there are no air bubbles. The top half of the plate is then fixed to the bottom and 50ul of serum free media is added to the wells to allow a background measurement. Cells are prepared and washed three times in serum free medium, cells are resuspended at $4x10^5$ cells/ml, 100ul of this cell suspension is added to the top wells which already contain 50µl of serum free media as described above. The plate is

incubated at 37°C and 5% CO_2 for 30 minutes to allow the cells to settle and equilibrate. Finally, CIM-Plates are inserted into the xCELLigence plate and the cell migration is measured every 15 minutes over a 48 hour period. Total migration is calculated over 48hours and normalised to control wells which contain no chemoattractant.

2.2.2.6. PHENOTYPIC ANALYSIS OF STROMAL CELLS

For staining, cells were washed with FACS buffer (**Table 2.4**.) antibodies were diluted in 50µl FACS buffer and added to $1x10^5$ cells for 30 minutes at 4°C in the dark. After incubation, cells were washed twice with FACS buffer and centrifuged at 400G for 3 minutes at 4°C to remove unbound Ab. Cells were then resuspended in 200µl FACS buffer and analysed using a FACS Canto II (BD Biosciences). Sytox Blue viability stain was added immediately prior to acquisition. All analysis was done using FlowJo™. The antibodies used were: GP38, Sdc2, NG2, CD105, MHCII, CD29, CD86, PDGFRα, CD14, CD34, CD15, MHCI, CD73, CD90, CD45, CD11b, CD80 and CD117 for human cells and CD11b, CD31, CD45, CD80, CD86, CD105, Sdc2, EpCAM, MHCI, MHCII, GP38, SCA-1and Ter119 for mouse cells, all in table 2.1.

2.2.2.7. T-CELL PROLIFERATION ASSAY

Whole blood samples (25-35ml) were collected from healthy donors on the day of assay by a qualified professional. Blood was mixed 1:1 with PBS and peripheral blood mononuclear cells (PBMCs) were isolated using Ficol®-Paque gradient centrifugation at 700G for 25minutes at 4°C with no brake. During this step stromal cells were added to wells of a 96 well plate at either $1x10^5$, $4x10^4$, or $1x10^4$ cells per well to give final ratios of 1:10, 1:50 and 1:200. The lymphocyte layer was removed from the Ficol gradient by pipette and cell suspensions were washed in PBS twice with centrifugation steps of 400G for 5minutes at 4°C. Cells were counted using a haemocytometer, and stained using CellTrace™ CFSE Cell

Proliferation Kit, (Invitrogen) at a 1 in 500 dilution for 6 minutes at 37°C protected from light. Reaction was stopped by adding an excess of ice cold T-cell media. $2x10^5$ CFSE labelled T cells were added per well of a 96 well plate. To stimulate T cell proliferation mouse anti-human CD3 0.05µg/ml (BD Biosciences) and mouse anti-human CD28 10µg/ml (BD Biosciences) were added to wells. Appropriate controls were plated into wells not containing stromal cells, including: un-stained and unstimulated, stained and unstimulated and finally stained and stimulated. Cells were incubated for 4 days to allow proliferation. After this cells were harvested by pipette into a new v-bottom 96 well plate and stained using PE-Cy7 mouse anti-human CD4 (BD Biosciences) for 30 minutes at 4°C in the dark. After incubation, cells were washed twice with FACS buffer and centrifuged at 400G for 3 minutes at 4°C to remove unbound Ab. Cells were then resuspended in 200µl FACS buffer and analysed using a MACSQuant (Miltenyi Biotech).Sytox Blue viability stain was automatically added immediately prior to acquisition. All analysis was carried out using FlowJo™ according to the gating strategy below; proliferation greater than 3 generations of CD4+ T-cells was graphed (**Fig 2.2.**).

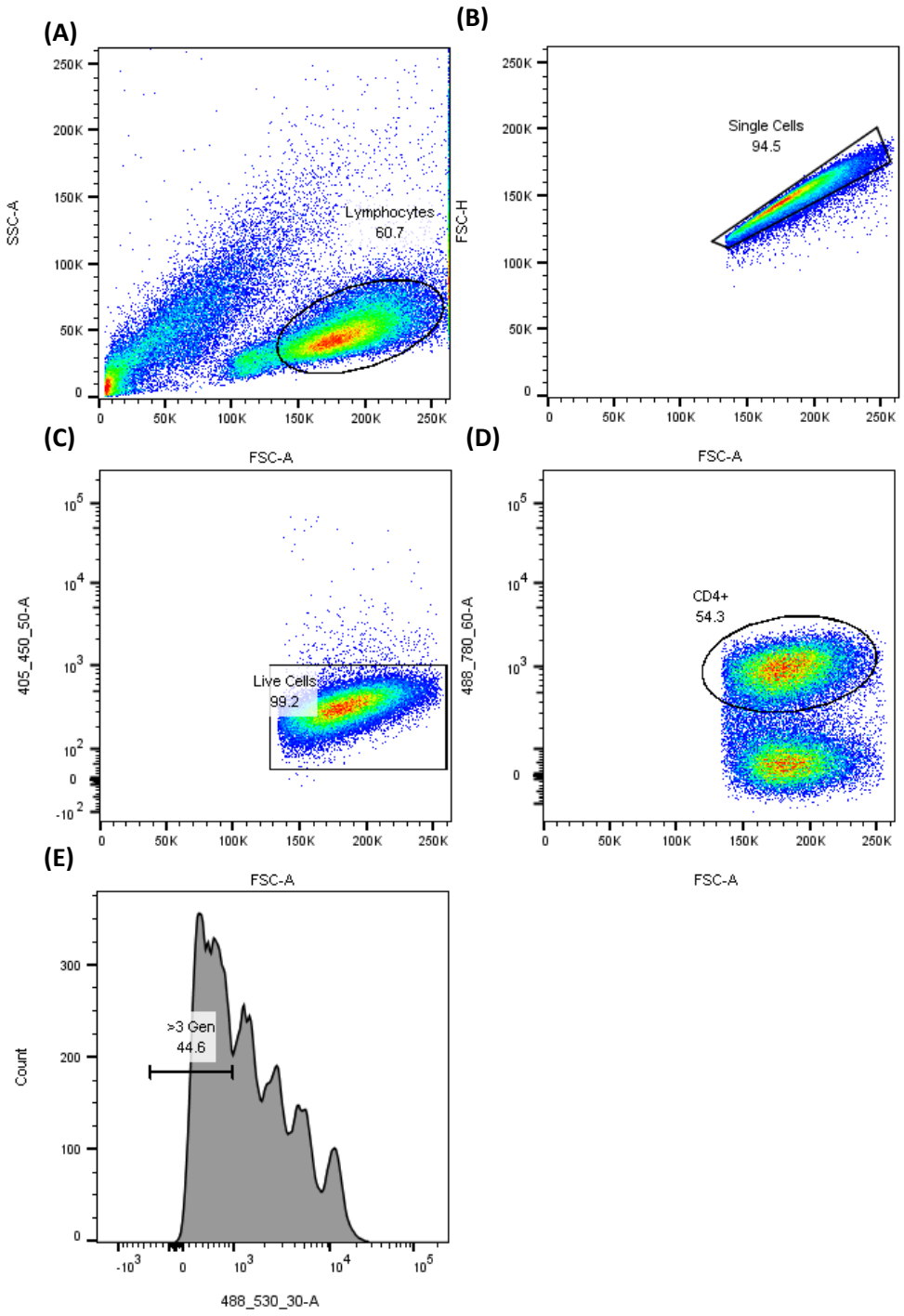

Figure 2.2. CD4 T-cell gating strategy ((A) Lymphocytes were gated on cell size to exclude debris. (B) Single cells were gated based on cell height vs granularity (C) Sytox negative, live cells were gated. (D) PE-Cy7 CD4+ cells were selected. (E) Proliferation greater than 3 generations of CFSE labelled cells were measured.

2.2.2.8. TGFB TIME COURSE EXPERIMENTS

Cells were plated in 6 well plates at a density of $2.2x10^4$ cells/cm^2**.** 12 hours later cells were transduced or transfected as described in (**Sect 2.2.2.3. and 2.2.2.5.)** and left to incubate for 48 hours. After this point the cells were exposed to serum free medium for 12 hours. Finally TGFβ3 (R&D) was added at a concentration of 20ng/ml for stromal cells or 5ng/ml for MDA-MB-231 cells. Cells were harvested at time points of 0, 2, 4 and 6 hours, by first washing twice with PBS followed by addition of 350 µl RLT lysis buffer (Qiagen).

2.2.3. IN VIVO METHODS

All procedures in this section were conducted under licences AE19125/P042 & AE19125/P049, approved by the Animals Care Research Ethics Committee of the National University of Ireland, Galway and conducted under licence from the Health Products Regulatory Authority, Ireland.

2.2.3.1. EAR PUNCH IDENTIFICATION OF MICE

In order to identify and determine the genotype of mice, ear punches were performed at 4 weeks of age according to **Fig 2.3**. Ear tissue was collected in sterile tubes, sterilising instruments with subsequent washes of sodium hypochlorite, 70% ethanol and water between mice to prevent cross contamination of specimens. Ear tissue is subsequently lysed and PCR determines genotype (**Sect 2.2.1.1.**).

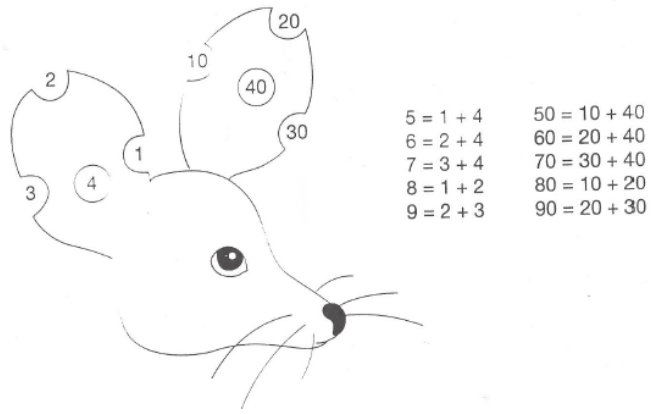

Figure 2.3. Ear punch identification chart.

2.2.3.2. TUMOUR GENERATION PROTOCOL

Mice of between 8-10 weeks of age were anaesthetised by 5% isofluorane inhalation for induction and 2% isofluorane for maintenance, and a small incision with a surgical scissors was made just medial of the midline and lateral of the fourth nipple (**Fig 2.4. A**). Cells at a concentration of $2x10^6$ cells for immune-compromised or $1x10^6$ cells for immune-competent

were injected in 100ul of sterile PBS by pushing the needle proximally and parallel to the skin into the mammary fat pad (MFP) before slowly injecting (**Fig 2.4. B**). The needle was removed and the wound closed over with a forceps (**Fig 2.4. C**). The incision was closed using Vetbond tissue adhesive (Medray) and allowed to dry (**Fig 2.4. D**). Mice were place in a recovery chamber at 37°C for ten minutes to regain consciousness, before relocation to cages. Tumour growth was monitored by calliper measurement 3-5 times per week. The long (L) and short (S) dimensions were taken and the approximate tumour volume calculated using the formula $(LxS^2)/2$.

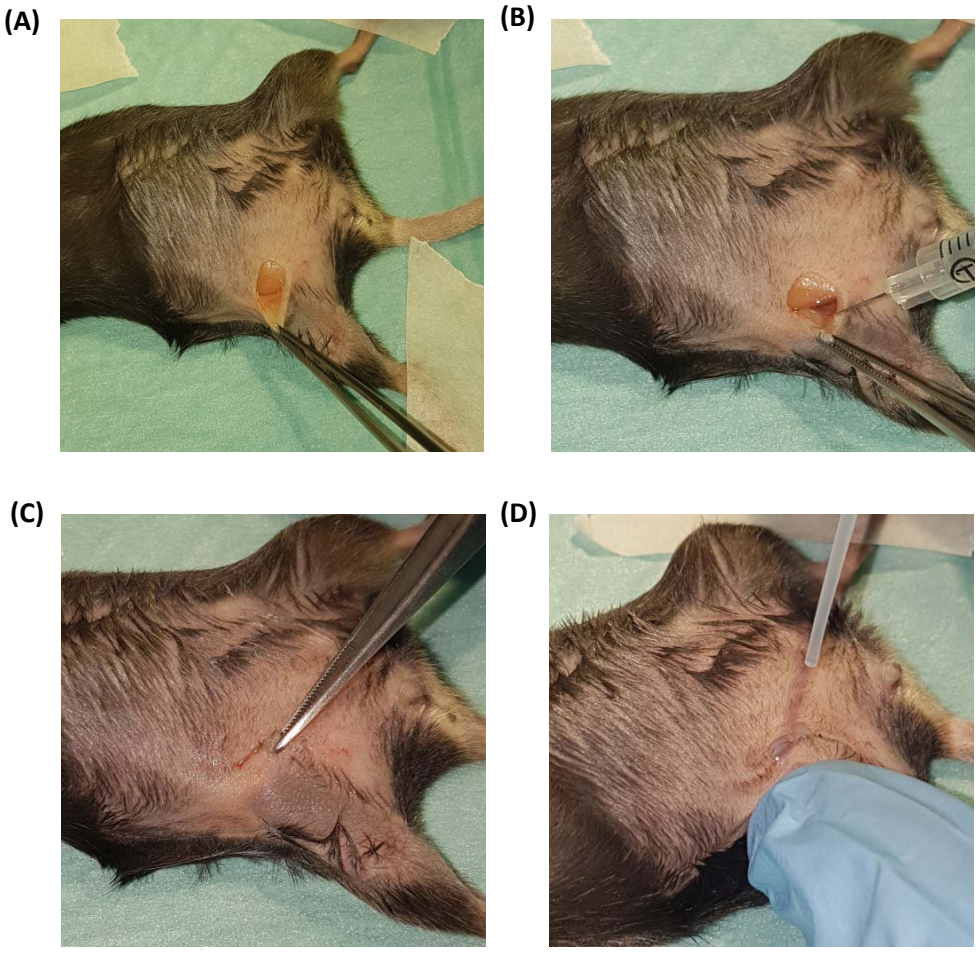

Figure 2.4. Mammary fat pat injection of cells. (A) Incision is made lateral to the 4th MFP. (B) Skin is retracted and cells are injected slowly into MFP. (C) Skin is stretched back over MFP with forceps. (D) Wound is glued shut using surgical glue.

2.2.3.3. MOUSE TISSUE HARVEST

Mice were euthanised by CO_2 asphyxiation followed by cervical dislocation and cardiac bleed. An incision was made to expose the breast tumour. Tumour was excised with a scalpel and stored in PBS. Next the diaphragm was pierced and rib cage removed, exposing the heart and lungs. An incision was made up the throat to expose the trachea, the clavicle was cut with a scissors and a cannula was inserted down the trachea into the lungs. A suture was tied around the cannula loosely; 1ml of 10% neutral buffered formalin was then injected into the lungs to inflate the tissue. Upon maximal inflation the cannula was removed, the suture tied off and the lungs were removed and immersed in 10% neutral buffered formalin.

2.2.3.4. HISTOLOGY AND SCORING OF LUNGS

Lungs were isolated (**Sect 2.2.3.3.**) and fixed in 10% neutral buffered formalin for 24 hours followed by 24hours of 100% ethanol and 24hours of 70% ethanol. Lungs were then processed using an Excelsior AS tissue processor overnight, involving incubations in formalin followed by dehydration through a series of alcohol and xylene baths with final immersion in paraffin wax. Processed tissues were removed the following day and embedded in paraffin wax cassettes. Sections of wax blocks were taken using a Leica-RM2235 microtome, a 5µm section was taken every 50µm throughout the lung sample and mounted on Superfrost Plus™ glass slides. Sections were incubated at 60°C overnight to melt off excess wax. Sections were then H&E Stained according to **Table 2.14**. Finally cover slides were attached using a drop of histomount xylene based mounting solution. Images were taken using an upright bright field microscope at 4x magnification. Lungs were graded according to the following scale: Grade 1 - no metastases, Grade 2 – small metastases, Grade 3 – 1 large or few small metastases, Grade 4 – many large and small metastases **Fig 2.5**. The highest grade detected within the lungs determined final score attributed to that animal.

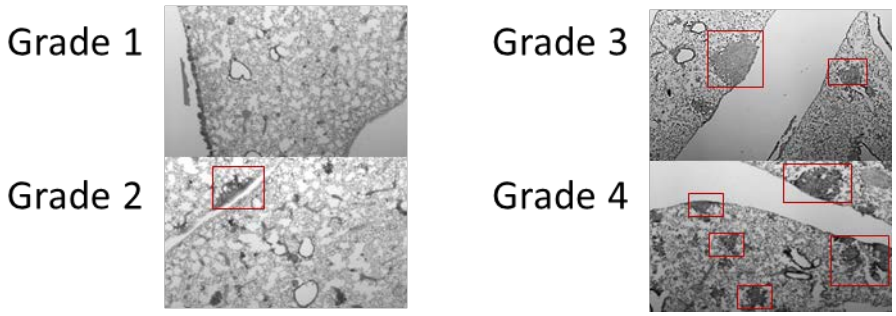

Figure 2.5. Histological scoring of lungs. Grade 1 - no metastases, Grade 2 – small metastases, Grade 3 – 1 large or few small metastases, Grade 4 – many large and small metastases.

Table 2.14. H&E staining protocol.

Reagent	**Incubation**
Xylene	2 Changes, 10 minutes each
100% Ethanol	2 Changes, 5 minutes each
95% Ethanol	2 minutes
70% Ethanol	2 minutes
Distilled H_2O	10 seconds
Harris Hematoxylin	8 minutes
Running Tap Water	5 minutes
1% Acid Alcohol	30 seconds
Running Tap Water	1 minute
2% Ammonia Water	45 seconds
Running Tap Water	5 minutes
Eosin-Phloxine Solution	45 seconds
95% Ethanol	5 minutes
100% Ethanol	2 Changes, 5 minutes each
Xylene	2 Changes, 5 minutes each

2.2.3.5. ISOLATION CELL SUSPENSIONS FROM MOUSE TUMOURS

Tumours were explanted roughly chopped using scalpel before being incubated for 30minutes at 37°C in mouse tumour digestion buffer (**Table 2.4.**). After 30mins supernatant was removed and put in cold mTSC media (**Table 2.5.**), fresh digestion buffer was added to cells for another 30 minutes at 37°C, this step was repeated once more. After the final digest all remaining cells were added combined and centrifuged at 400G for 5mins at 4°C. The pellet was resuspended in 0.25% trypsin for 5 minutes before neutralisation using mTSC media. The cells were again pelleted as above and resuspended in ACK lysis buffer for 1 minute to reduce red blood cell numbers. This step was neutralised with mTSC media. Cells were finally resuspended in mTSC media and passed through a 100-micron cell strainer to obtain a single cell suspension. Cells were counted using a NucleoCounter® NC-200 automated cell counter and plated at a density of $1x10^5$ cells/cm^2, or alternately resuspended in FACs buffer for flow cytometric analysis.

2.2.3.6. PyMT BREAST TUMOUR ANALYSIS

To block antibody-Fc receptor binding single cell suspensions of $1x10^5$ cells were first incubated with anti-mouse CD16/32 blocking antibody for 15 minutes at 4°C in the dark. For FAP staining, cells were incubated with sheep anti-FAP antibody for 30 minutes at 4°C in the dark, before washing and re-blocking with CD16/32 as before. Cells were then incubated with biotin at 1/1000 dilution for 30 minutes at 4°C in the dark. Cells were washed twice with FACS buffer and centrifuged at 400G for 3 minutes at 4°C cells were then incubated with PE conjugated streptavidin at a 1/400 dilution for 30 minutes at 4°C in the dark. Cells were then washed again as above and incubated for 30minutes with a cocktail of mouse Ter119, CD45, CD31, Syndecan-2 and EpCAM antibodies at the dilutions specified in **Table 2.1**. Cells were

analysed using a FACS Canto II (BD Biosciences). Sytox Blue viability stain was added immediately prior to acquisition. All analysis was done using FlowJo™ software.

2.2.3.7. XENOGRAFT BREAST TUMOUR ANALYSIS .

Single cell suspensions from xenograft tumours first underwent MACS using a mouse cell depletion kit (Miltenyi Biotech). Briefly $4x10^6$ cells were incubated with mouse cell depletion cocktail for 15 minutes at 4°C; cells were then passed through an LS column in a magnetic field. Flow through of human enriched cells were counted, washed and incubated with the following cocktail for 30 minutes EpCAM, GP38, Syndecan-2, PD-L1 and CXCR4 (**Table 2.1.**). In parallel to this pre-MACS bulk cells were washed and stained with the following cocktail of mouse-specific antibodies for 30 minutes: Ter119, CD45, CD31, Syndecan-2, EpCAM and GP38 (**Table 2.1.**). Viability was assessed using Sytox blue staining. Data was collected using a MACSQuant™ Analyser 10 flow cytometer (Miltenyi) and analysed using FlowJo software.

2.2.3.8. EO771 BREAST TUMOUR ANALYSIS

Single cell suspensions were obtained from E0771 tumours (**Sect 2.2.3.5.**), cells were washed and stained with the following cocktail of mouse-specific antibodies, panel 1: Ter119, CD45, CD31, Syndecan-2, EpCAM, GP38, CXCR4 and PD-L1, panel 2: CD62, CD4, CD8, CD44 and CD25, panel 3: CD11c, Ly6C, Ly6G, F4/80, CD11b (**Table 2.1.**). Cells were incubated with appropriate antibody cocktail for 30 minutes at 4°C in the dark. After incubation, cells were washed twice with FACS buffer and centrifuged at 400G for 3 minutes at 4°C to remove unbound Ab. Cells were then resuspended in 200µl FACS buffer and analysed using a MACSQuant™ Analyser 10 flow cytometer (Miltenyi Biotech). Sytox Blue viability stain was automatically added immediately prior to acquisition. All analysis was carried out using FlowJo™ software.

2.2.3.9. ISOLATION OF HUMAN TUMOUR-ASSOCIATED STROMAL CELLS

After ethical approval and written informed consent, fresh specimens of human breast tumours were harvested from patients undergoing surgery at University College Hospital Galway. Tissues were washed, minced finely with scalpels, and digested overnight in human tumour digestion buffer (**Table 2.4.**) at 37^{o}C and 5% CO_2**.** Collagenase-dissociated mammary cells were pelleted at 400G for 5 minutes at 37°C and cell pellets were resuspended in 2 ml of pre-warmed Trypsin-EDTA by gentle pipetting and left to incubate at 37^{o}C for 2 minutes**.** Trypsin was inactivated with PBS supplemented with 2% FBS. Cells were pelleted as before, resuspended in FACS buffer and filtered through a 100 μm cell strainer. Cells were pelleted and resuspended in FACS buffer or stromal cell growth medium and viable cells counted using a haemocytometer. 100,000 cells were incubated for 30 minutes at 4°C in the dark with CD45 or SDC2 antibodies alone or in combination. Viability was assessed using Sytox blue staining. Data was collected using a BD FACS Canto II flow cytometer (BD Bioscience) and analysed using FlowJo software. Alternatively cells were plated in stromal cell growth media and expanded (**Sect 2.2.2.1**).

2.2.3.10. ISOLATION OF MURINE BONE-MARROW-DERIVED MESENCHYMAL STROMAL CELLS

Mice were euthanized by CO_2 asphyxiation, the femur, tibia, humerus, ulna and radius were removed. All flesh was stripped from the bones using scalpels. Bones were crushed in a mortar and pestle with 3 changes of 500µl DMEM pooling all into a 15ml tube. Digestion solution was added to the settled bone marrow (BM) clumps and mixed gently. The digestion was left at 37°C for 15mins. The supernatant was removed and added to 5mls of complete mMSC media to stop digestion. A further 250µl of digestion solution was added to the clumps and the process was repeated twice as described above. Finally cells were centrifuged

at 400G for 5minutes at 4°C. Cells were then either plated at $5x10^4$ cells/cm^2 or resuspended in FACS buffer for flow cytometric analysis.

CHAPTER 3

RESULTS & DISCUSSION

PART I

Investigating the role of SDC2 in the breast tumour microenvironment

3.1 BACKGROUND

Clinicians have likened solid tumours to rocks, due to a dense, fibrotic mass called the stroma which surrounds the cancer cells in the tumour microenvironment [62]. Such stroma, consisting of MSCs, CAFs, immune cells, endothelia and ECM accompanies most solid tumours, but its extent and compactness are exceptional in breast cancer [345]. Since breast cancer can be exceptionally deadly due to its high metastatic potential, researchers have wondered whether the stroma is at least partly responsible. Some recent studies now make that case and argue for the idea that the stroma is blocking drug penetration and contributing to tumour survival, and that drugs that punch holes in the stromal barrier can be effective [196-198]. Several combination therapies are now in clinical trials to test this stromal depletion hypothesis, based on the premise that the tumour stroma microenvironment and MSC therein function to promote cancer growth and invasion while simultaneously limiting the delivery of chemotherapy [346].

As mentioned before mesenchymal stromal cells in the tumour microenvironment secrete a number of cytokines and chemokines which impact on cancer progression and survival [123]. These cells play pivotal roles in the TGFβ, SDF-1 and PDL-1 pathways in cancer, and have therefore become the focus of a great deal of research [126, 130]. However targeting these SCs is difficult due to lack of functional marker proteins that identify homogeneous cells

within the heterogeneous cancer stroma in vivo. Whilst ablation of FAP+ stromal cells reduces tumour size, this also causes anaemia and cachexia due to targeting of healthy MSC and stroma in the marrow and muscle respectively [173].

Unpublished data from Orbsen Therapeutics indicates syndecan-2 (SDC2)/CD362 is a novel cell surface marker for identification of MSC from mouse and human tissues, including bone marrow, fat, muscle, lymph nodes, and tumour stroma. $SDC2^{+}$MSC suppress $CD4^{+}$ T lymphocyte proliferation *in vitro*. SDC2 protein can reduce $CD4^{+}$ T lymphocyte activation. Histology reveals increased levels SDC2 protein in human breast carcinoma samples.

We propose SDC2 is a functional marker within the breast TME and that blocking SDC2 secreted by MSC may be safe and effective. SDC2 expression seems to be limited to very few cancer types such as pancreas, colon and prostate and only one functional study has related SDC2 function to breast cancer development [309, 338]. Therefore the aim of chapter 3 is to investigate the role of SDC2 in the breast tumour microenvironment. Specifically we will adenovirally modulate SDC2 in both epithelial and stromal compartments of breast cancer to test the resulting effects on breast carcinogenesis. This chapter should answer the question as to whether SDC2 is a valuable therapeutic target within the breast TME

3.2. RESULTS

3.2.1. SDC2 IS PRESENT IN BREAST CANCER TISSUE AND SERUM FROM PATIENTS

As discussed previously the detection of elevated levels of SDC2 in the sera is an indicator of a poor prognosis in colon cancer but also that SDC2 expression levels have been associated with metastatic ability of cancer and invasive index [290, 327]. To identify if this correlation exists in breast cancer, we performed an ELISA (**Sect. 2.2.1.5.**) on 80 serum samples of various breast cancer subtypes, from the breast cancer biobank in University College Hospital Galway (UCHG). Patients were not age or gender matched, and some had undergone neo-adjuvant chemotherapy. Control samples were taken from patients without breast cancer. Samples were assayed blind, results were decoded at a later date and it was concluded that indeed SDC2 is significantly elevated in the serum of patients with triple negative breast cancer with a mean value of 4693±305.4pg/ml compared to 2959±422.4pg/ml for non-tumour control, 2715±429.5pg/ml and 2822±428.7pg/ml for luminal A and B respectively and 3168±325.4pg/ml for HER2 overexpressing tumours (**Fig. 3.1. A**). We know from the literature that SDC2 expression is elevated in breast cancer epithelia however we also know from work by Orbsen Therapeutics that SDC2 is expressed on the surface of MSCs. Therefore we hypothesised that the increase in SDC2 protein detected in TNBC could also be of stromal origin. To investigate this we preformed flow cytometry on three enzymatically digested breast cancer tissue samples. Analysis revealed the presence of cell surface SDC2 in both CD45 negative (2.22±1.29%) and positive (3.43±1.54%) populations indicating the role for SDC2 in both compartments (**Fig. 3.1. B**).

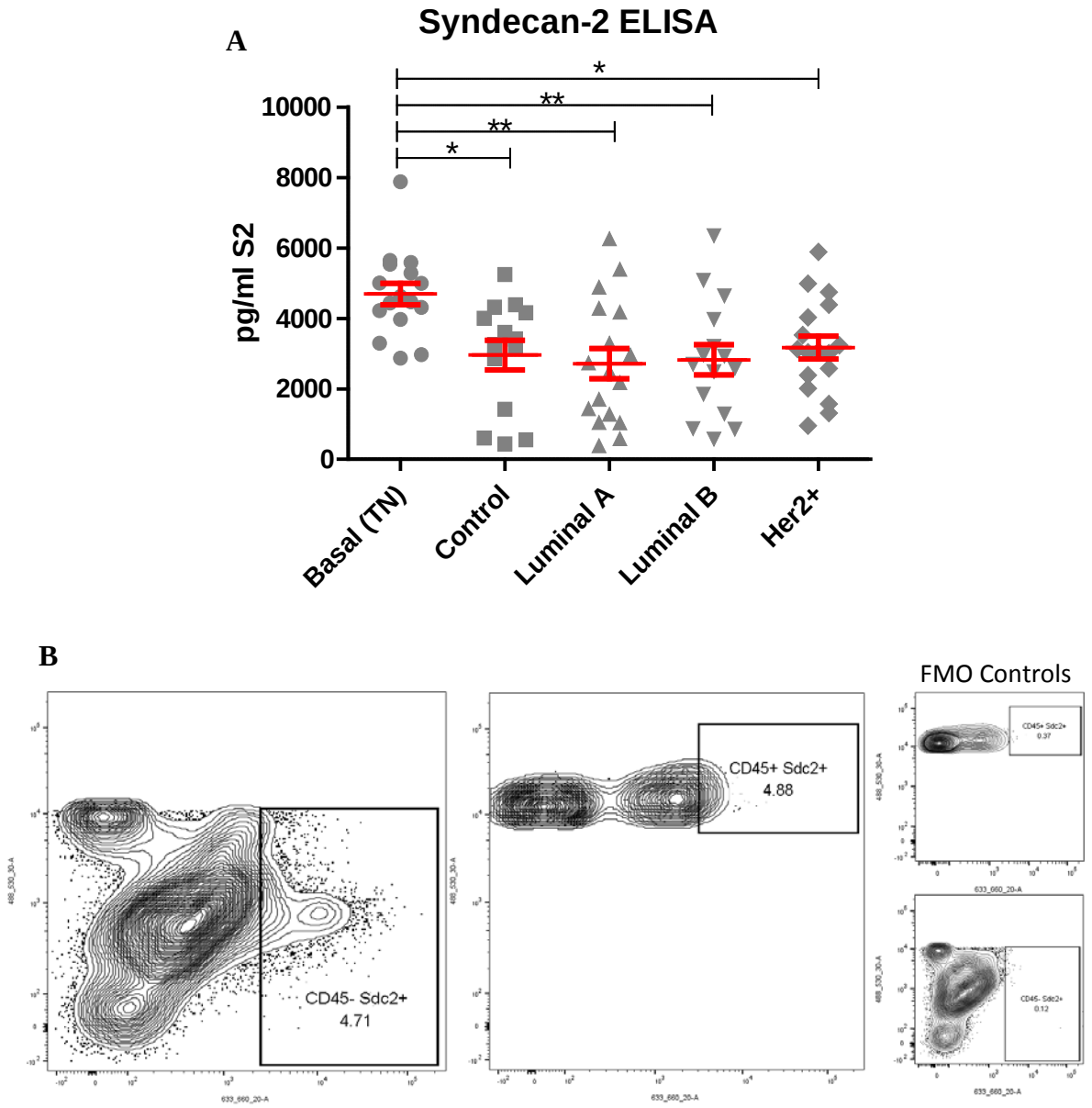

Figure 3.1. SDC2 is present in breast cancer tissue and serum from patients. (**A**) An ELISA kit for SDC2 was used to detect SDC2 levels in serum samples from patients of the breast cancer clinic in UCHG, samples were run in triplicate and mean protein levels were interpolated from a four parameter logistic regression (4PL) standard curve, analysis is by 1-way ANOVA using Tukey's multiple comparison post-test (* $p \leq 0.05$, ** $p \leq 0.01$). (**B**) Flow cytometry of single cell suspension from a breast cancer sample shows CD45- SDC2+ and CD45+ SDC2+ populations, fluorescence minus one (FMO) stains show no non-specific staining.

3.2.2. SDC2 CONTROLS THE MIGRATORY POTENTIAL OF TRIPLE NEGATIVE BREAST CANCER CELLS.

We began our work to highlight the role of SDC2 in breast cancer epithelia using the triple negative breast cancer cell line MDA-MB-231. We selected this line due to our preliminary findings suggesting elevated levels of SDC2 in TNBC. The literature suggests SDC2 plays key roles in migration and adhesion [307] we therefore began to investigate this characteristic in TNBC. To begin the migrative ability of the cell line MDA-MB-231 was assayed towards a number of factors using an xCELLigence cell migration system (**Sect. 2.2.2.5.**). Serum free media (-serum) and serum containing media (+serum) were used as negative and positive controls for migration, stromal cell conditioned media and stromal cell conditioned media containing recombinant full length SDC2 were assayed. It was found that MDA-MB-231 breast cancer cells (BCCs) migrate more efficiently towards stromal cell conditioned media and pre-incubation with recombinant SDC2 significantly increased this capacity (**Fig. 3.2. A**). This would suggest that SDC2 is a potent chemoattractant for TNBCs. Therefore to follow on from this finding, the effect of SDC2 knockdown in relation to migrative capacity was assayed. MDA-MB-231 BCCs were transduced with adenoviral short hairpin RNA for SDC2 (ShS2) or control non target short hairpin adenovirus (ShCt) (**Sect. 2.2.2.1.**) The ability of ShS2 and ShCt transduced MDA-MB-231 cells to migrate to serum free media (-Serum) and serum containing media (+Serum) was assessed. The results show a significant impairment of migratory ability in cells transduced with ShS2 (**Fig. 3.2. B**). Further RNA analysis by RT-qPCR of MDA-MB-231 BCCs revealed that with knockdown of SDC2 caused a significant decrease in the pro-migratory gene CXCR4 (0.3448±0.0971) and adherence related EMT related genes fibronectin and ZEB1 (0.3367±0.1346, 0.3184±0.06283) [188, 310, 347] (**Fig. 3.2. C**).

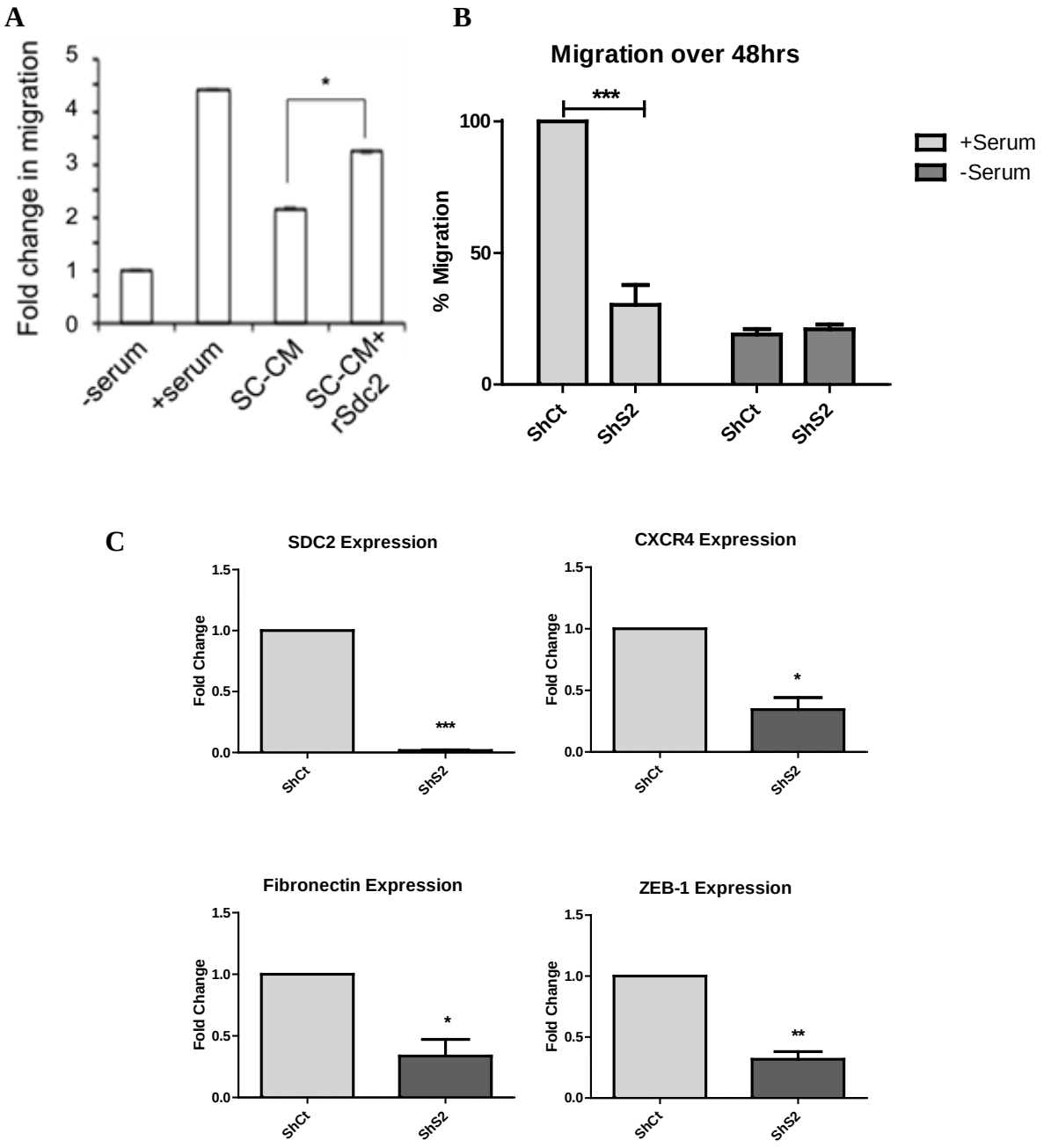

Figure 3.2. SDC2 enhances triple negative breast cancer cell migration. (**A**) SC-CM enhances the migration of MDA-MB-231 breast cancer cells (BCC), and addition of recombinant Sdc2 enhances migration towards SC-CM analysis using unpaired t-test (* $p \leq 0.05$). (**B**) Knockdown of Sdc2 significantly inhibits the ability of BCC to migrate towards serum containing media, analysis by 2-way ANOVA using Bonferroni post-test (*** $p \leq 0.001$, n=4). (**C**) RNA from MDA-MB-231 cells shown complete knockdown of SDC2 RNA along with significant reductions in CXCR4, Fibronectin and ZEB1, analysis by 2-way ANOVA (* $p \leq 0.05$, ** $p \leq 0.01$, *** $p \leq 0.001$, n=3).

3.2.3. SDC2 knockdown attenuates the effects of TGFβ stimulation in breast cancer cells.

Our data above suggests SDC2 affects CXCR4, Fibronectin and ZEB1 expression; all of which are regulated by TGFβ signalling [348-350]. Indeed, SDC2 has been shown to interact with the TGFβ pathway and this can exert both tumour suppressive and pro-oncogenic properties depending on the stage of cancer [314, 317]. There is abundant evidence from the literature to implicate TGFβ in cancer progression and the epithelial to mesenchymal transition [70, 78, 81]. Therefore targeting this pathway has become the focus of much research, specifically blocking of the TGFβ pathway [87, 88, 351]. Here we wanted to assess the effect of SDC2 knockdown on TGFβ signalling in triple negative breast cancer cells, using our short hairpin RNA adenovirus (**Sect. 2.2.2.1.**) with administration of a TGFβ time course (**Sect. 2.2.2.8.**)..

Successful knockdown of SDC2 was determined by RT-qPCR (**Fig 3.3. A**) and western blot analysis (**Fig 3.3. B**) Western blot analysis also demonstrates a reduction in TGFβ mediated upregulation of fibronectin which has been shown to induce EMT [352]as well as a being a molecular partner of SDC2 [310] (**Fig. 3.3. B**). TGFβ signalling was induced in ShCt transduced cells as shown by upregulation in Smad-7 (8.466±0.632) CTGF (1.39±0.112), PAI-1 (4.386±1.779) and SNAI1 (5.908±0.859). Interestingly, TGFβ-induced upregulation of these specific genes are attenuated in ShS2 transduced MDA-MB-231 cells compared to ShCt transduced cells. Specifically, TGFβ-induced upregulation of SMAD7 (2.622±1.272) and CTGF (0.508±0.064) is significantly reduced in ShS2 transduced cells (**Fig. 3.3. C**). A trend towards a reduction in (plasminogen activation inhibitor-1) PAI-1 (1.433±0.670) and SNAI1 (3.253±0.915) expression was also seen (**Fig. 3.3. D**). In summary this data suggest SDC2 plays a significant role in aiding the process of EMT in triple negative breast cancer cells.

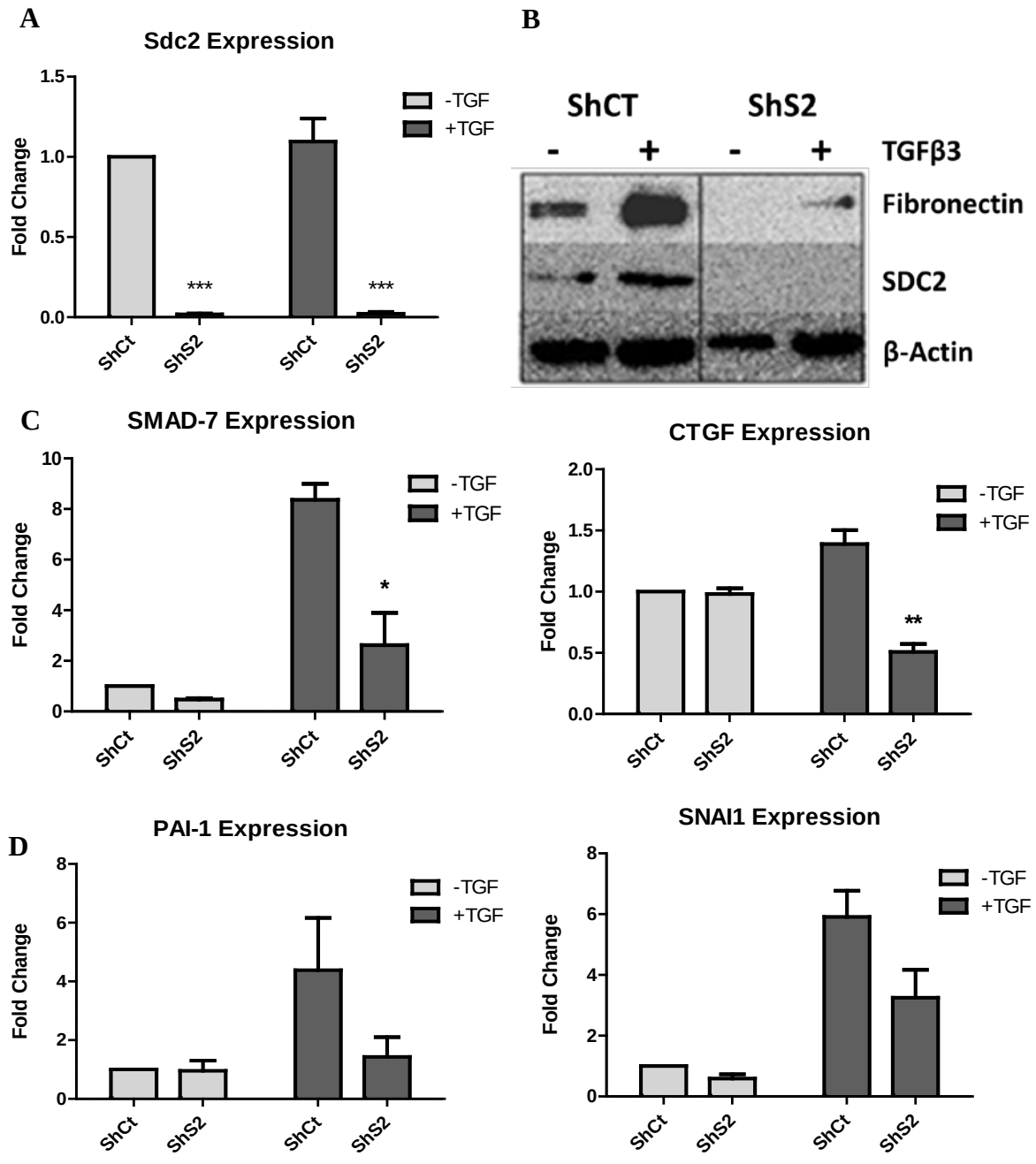

Figure 3.3 SDC2 knockdown impairs TGFβ signalling and EMT induction in breast cancer cells. (**A**) SDC2 knockdown of RNA is strongly significant, along with inhibition TGFβ induced increases in SDC2, analysis by 2-way ANOVA (*** $p \leq 0.001$ n=3). (**B**) SDC2 protein is lost with knockdown as well as its molecular partner fibronectin (**C**) TGFβ signalling is significantly reduced as evident in negative regulator SMAD7 and the EMT marker CTGF, analysis by 2-way ANOVA (* $p \leq 0.05$ ** $p \leq 0.01$ n=3). (**D**) A trend towards reduction in EMT markers PAI-1 and SNAI1 (n=3).

3.2.4. Isolation and characterisation of tumour derived MSCs and comparison to normal MSCs.

Up until now evidence suggests a pro-tumourigenic role for Sdc2 within epithelial BCC, however we also know SDC2 is expressed on the cell surface of MSCs [353] which are an important component of the breast TME. Our data above suggests there are a population of $SDC2^{+}$ $CD45^{-}$ population of cells within human breast tumours which could represent $SDC2^{+}$ stromal cells. Therefore to explore this idea further we wanted to determine if $SDC2^{+}$ MSCs are present within human breast cancer tissue. To do this we developed a process to isolate breast tumour derived mesenchymal stromal cells (TSC) for our studies. After ethical approval and informed patient consent, fresh specimens of human breast tumours were harvested from patients undergoing surgery at University College Hospital Galway, enzymatically digested and cultured under conditions to enable MSC growth (**Sect. 2.2.3.9.**). The mesenchymal phenotype of isolated cells was evaluated (**Sect. 2.2.2.6.**) according to presence or absence of defined cell surface molecules set out by the ISCT [128], Positivity for CD105, CD73 & CD90 with negative expression of CD45, CD34, CD14, CD11b & MHCII (**Fig. 3.4.**). TSC donors 1, 3 and 4 displayed dual intensity expression of CD105 and TSC1 also had a dual intensity expression of CD90. This would indicate the presence of a subpopulation of non-MSC contaminating cells; as a result these donors were excluded from further experiments. Stromal cells isolated from primary tumours also displayed greater expression of SDC2 than stromal cells from umbilical cord (**Fig. 3.5. A**). Growth characteristics were then assessed over 12 passages, in parallel to UC-MSC and BM-MSC. Tumour derived SC proliferated consistently faster than UC and BM derived SC (**Fig. 3.5. B**). Finally the ability of TSCs to suppress CD3 & CD28 mediated stimulation of CD4 T-cells was assessed and compared to UC-MSCs using a co-culture experiment with PMBCs (**Sect. 2.2.2.7.**). Results indicate that TSCs display similar levels of suppression to UC-MSCs at ratios of 1:10 and 1:50; however

at a ratio of 1:200 TSCs suppress T-cell proliferation more effectively (54.27±1.955 UC-MSC, 41.92±0.838 TSC) (**Fig. 3.5. C**).

In summary tumour-derived stromal cells were successfully isolated from primary breast cancer tissue, and displayed correct presence of ISCT markers demonstrating that they are of mesenchymal lineage. When compared to UC-MSCs, TSCs show greater expression of SDC2, increased proliferative capacity as well as increased immunosuppressive properties.

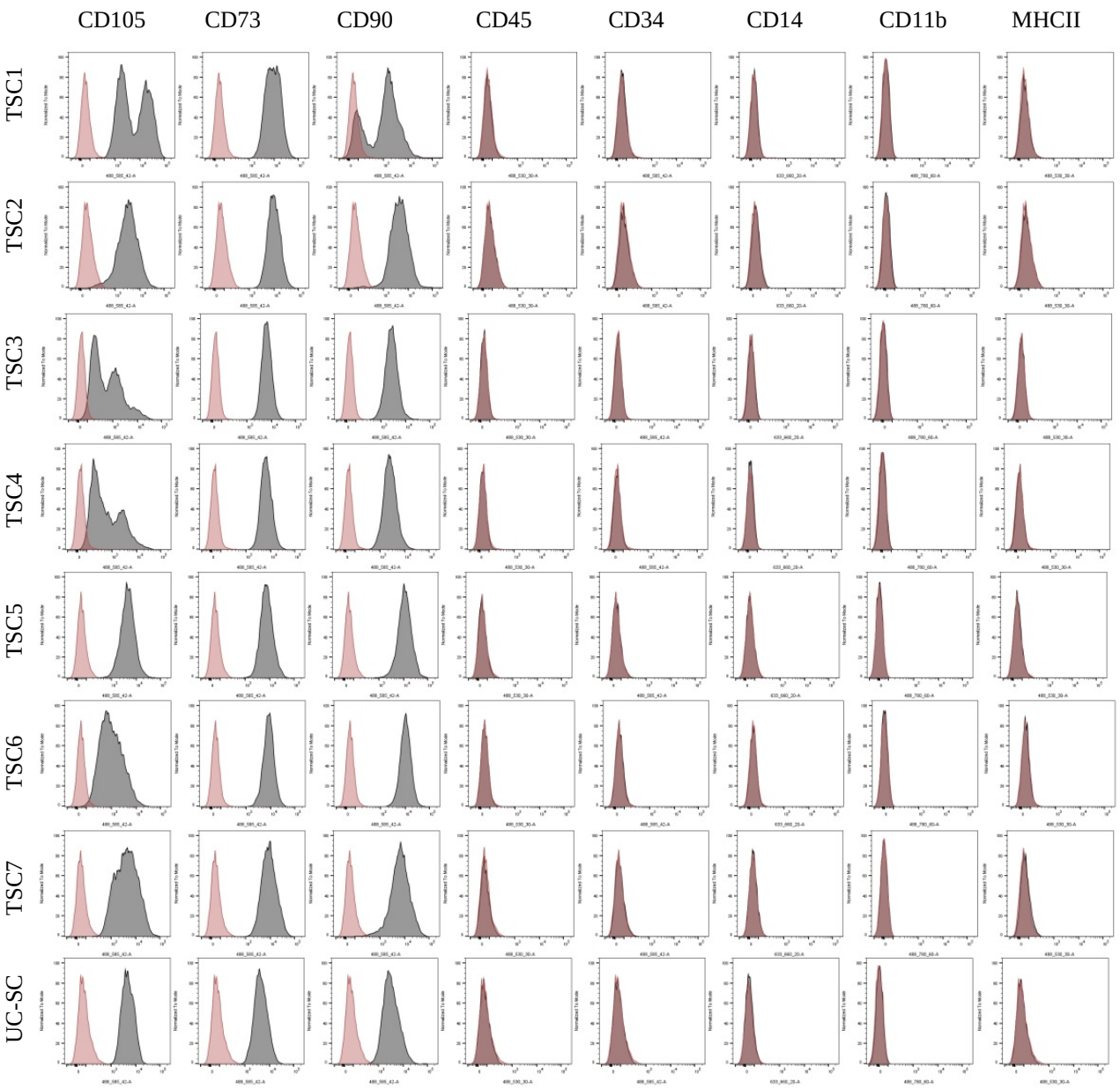

Figure 3.4. Cell surface phenotype tumour derived stromal cells. TSCs display presence or absence of defined ISCT markers of MSCs, donors 1, 3 and 4 display dual expression levels of CD105 and CD90.

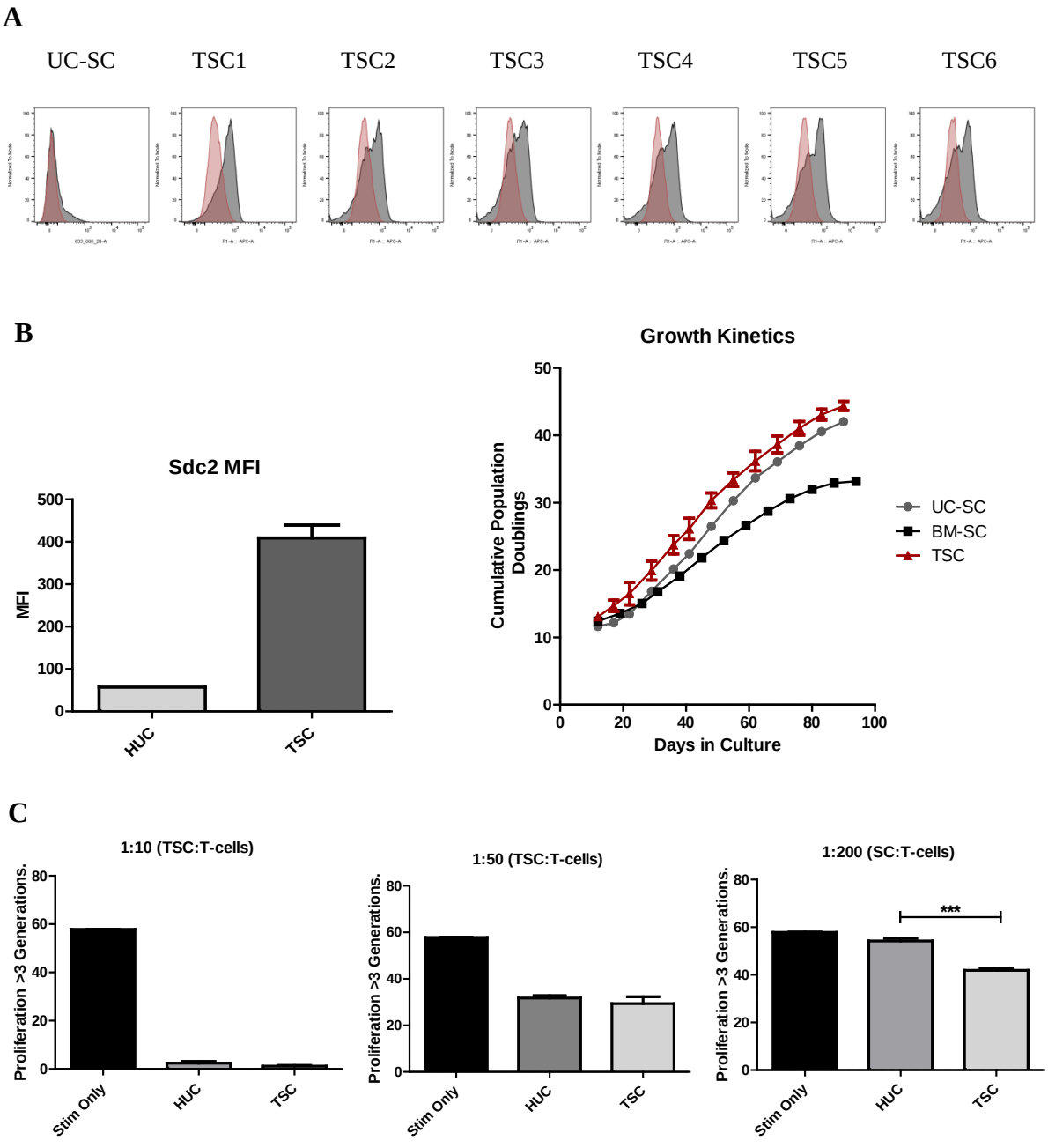

Figure 3.5. Stromal cells isolated from primary tumours display greater proliferative and immune-suppressive capacity. (**A**) TSCs express higher levels of SDC2 (**B**) Growth kinetics of TSC outperform UC and BM derived SC. (**C**) TSC display similar suppression of CD4 T cell proliferation at 1:10 and 1:50 but outperform at 1:200, 1-way ANOVA using Tukey's multiple comparison post-test (***$p \leq 0.001$ n=3).

3.2.5. SDC2 knockdown attenuates the effects of TGFβ stimulation in UC-MSCs and induces a pre-apoptotic phenotype.

In order to assess if SDC2 plays a similar role in TGFβ signalling in MSCs we used the same adenovirus as before for knockdown of SDC2. In this instance we used human umbilical stromal cells (UC-SC) from Orbsen Therapeutics and transduced as before (**Sect. 2.2.2.1.)** with our titrated TGFβ time course (**Sect. 2.2.2.8**.). We observed again interference in the TGFβ signalling pathway through significantly decreased levels of SMAD7 after stimulation (5.383±1.266 ShCt and 1.927±0.638 ShS2) and a trend towards reduction in the EMT marker PAI-1 (1.206±0.160 ShCt and 0.667±0.093 ShS2) (**Fig. 3.6. A**). This was result was confirmed to have significant SDC2 knockdown (0.051±0.026) (**Fig. 3.6. B**). However we observed a phenotype of reduced proliferation and significantly impaired colony forming ability (1/3.6 ShCt, 1/150 ShS2) (**Fig. 3.6. C**).

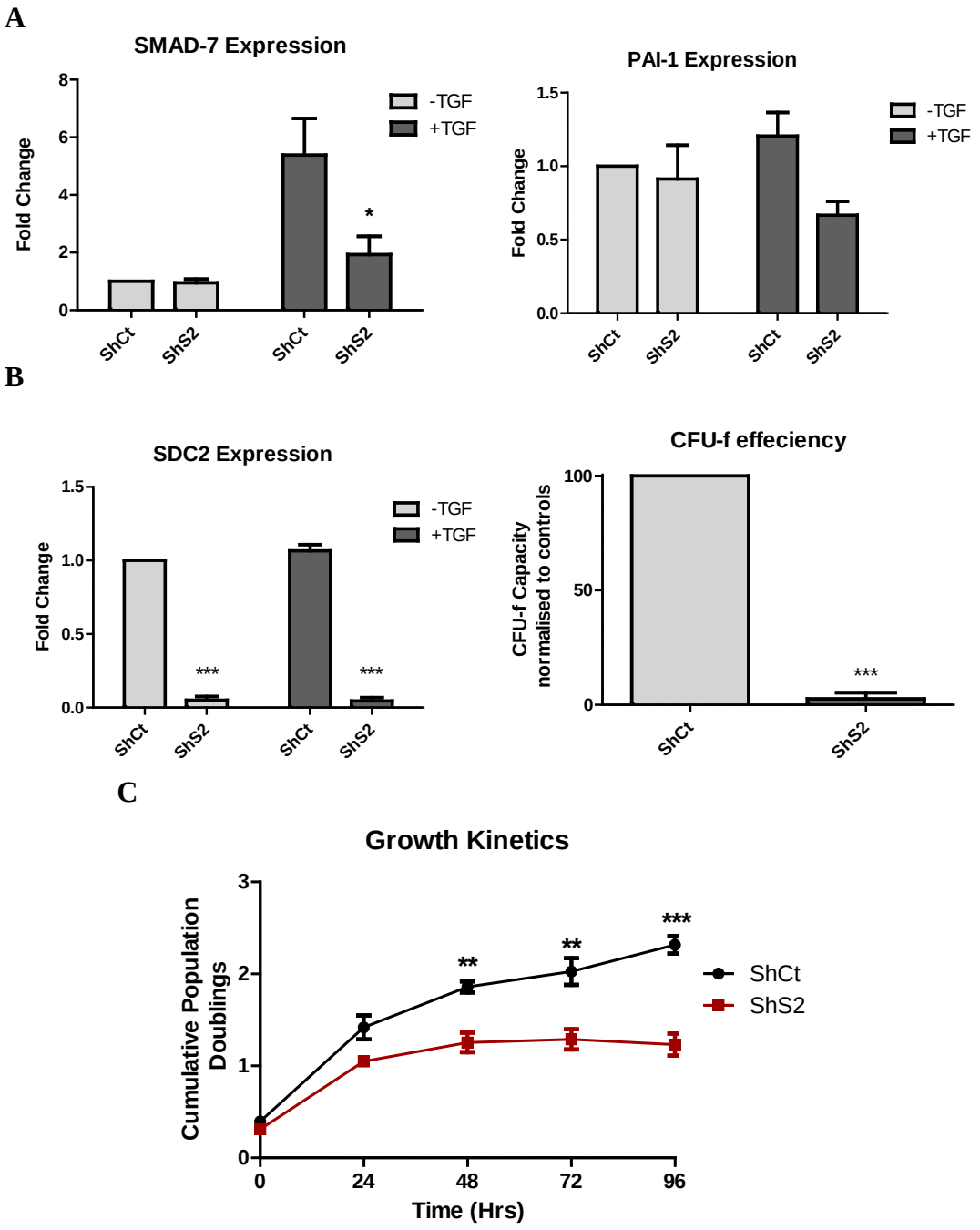

Figure 3.6. SDC2 knockdown attenuates the effects of TGFβ stimulation in MSCs but impairs clonogenic and proliferative ability (**A**) SDC2 knockdown in UC-SC attenuates effects of TGFβ signalling as seen with a significant decrease in SMAD7 signalling and trend towards a reduction in PAI-1 analysis by 2-way ANOVA (* p≤0.05). (**B**) SDC2 RNA is significantly downregulated by adenovirus analysis by 2-way ANOVA (*** p≤0.001). (**C**) Colony forming ability of UC-SC after knockdown is significantly impaired, analysis by unpaired t-test (*** p≤0.001, n=3), and proliferation ceases 48hours after knockdown, 2-way ANOVA (***p≤0.01, *** p≤0.001, n=2).

3.2.6. SDC2 knockdown in tumour derived stromal cells impairs TGFβ signalling without impairing phenotype.

To investigate the interaction between SDC2 and TGFβ in TSCs, we knocked down SDC2 as before (**Sect 2.2.2.2.**) and administered a TGFβ time course (**Sect 2.2.2.8.**). In tumour derived stromal cells transduced with ShS2 TGFβ signalling was again inhibited as detected through decreases in SMAD7 RNA (5.315±0.7960 ShCt, 2.361±0.470 ShS2); however differences in EMT markers were not as stark, perhaps due to TME conditioning. We detected trends towards a reduction in PAI-1 (1.044±0.286 ShCt, 0.599±0.078 ShS2) and CTGF (3.359±1.177 ShCt, 1.832±0.168 ShS2) as seen in MDA-MB-231s and UC-SC (**Fig. 3.7. A**). Importantly SDC2 was strongly knocked down (0.038±0.007) with no significant impact on colony forming ability, there was even a non-significant increase in proliferation rates detected (**Fig. 3.7. B**).

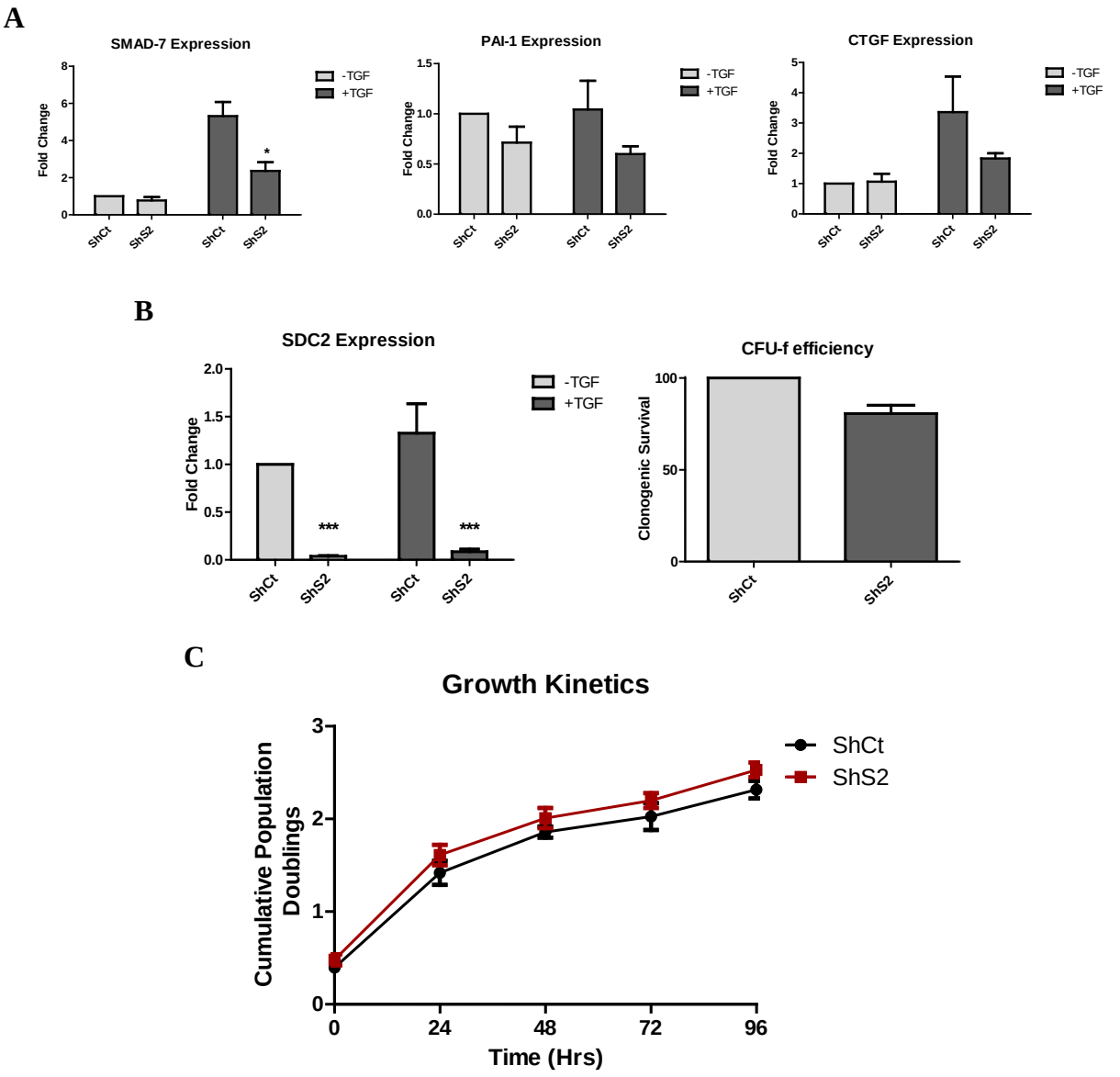

Figure 3.7. Knockdown of SDC2 in tumour derived stromal cells impairs TGFβ signalling without affecting clonogenic or proliferative ability. (**A**) SDC2 knockdown in TSC significantly impairs TGFβ signalling as detected through SMAD7 analysis by 2-way ANOVA (*p≤0.05 n=3), there was a trend towards a reduction in EMT markers PAI-1 and CTGF (n=3). (**B**) SDC2 RNA was significantly knocked down analysis by 2-way ANOVA (***p≤0.001 n=3), there was no impact to colony forming ability or growth rates (n=3, n=2).

3.2.7. SDC2 increases both migrative ability and immune-suppressive capacity of tumour derived stromal cells.

Stromal cells are well defined by their ability to migrate to sites of inflammation and cause local immune-suppression [126, 130]. We have shown in previous experiments that SDC2 aids the migrative capacity and TGFβ signalling of breast cancer cells, and we know from the literature that TGFβ is immunosuppressive [203, 240], therefore we wanted to test the effects of SDC2 knockdown on migrative and immune-suppressive capacities of these stromal cells. In order achieve this, we knocked down SDC2 as before (**Sect. 2.2.2.1.**) and seeded into wells of an xCELLigence real time cell analysis instrument (**Sect. 2.2.2.5.**) and monitored ability to migrate to +/- serum controls over 48 hours. It was found that SDC2 knockdown significantly impairs migrative capacity of TSC towards serum containing media (66.545±12.612%). Further RNA analysis showed SDC2 knockdown was significant (0.018±0.006), and importantly CXCR4 RNA was significantly downregulated (0.299±0.094), a pathway critical in MSC homing [188] (**Fig. 3.8. A & C**).

We next assessed the effects of SDC2 modulation on the ability to suppress CD3 & CD28 mediated stimulation of CD4 T-cells. This was assessed using a co-culture experiment of TSCs with PMBCs as before (**Sect. 2.2.2.7.**), however for this experiment we also assessed SDC2 overexpression using an adenoviral vector (AdS2) versus a non-targeting control (AdCt) (**Sect. 2.2.2.1.**). The results showed a clear picture that SDC2 affects SC mediated immune suppression of CD4 T-cells. We detected a significant decrease in CD4 proliferation in TSC overexpressing SDC2 (24.34±2.145 AdCt, 12.23±3.066 AdS2) and the opposite when SDC2 was knocked down (14.41±2.982 ShCt, 26.22±2.593 ShS2) (**Fig. 3.8. B**). SDC2 overexpression and knockdown was quantified by RT-PCR, (158.8±10.42 AdS2, 0.018±0.006 ShS2), (**Fig. 3.8. C**).

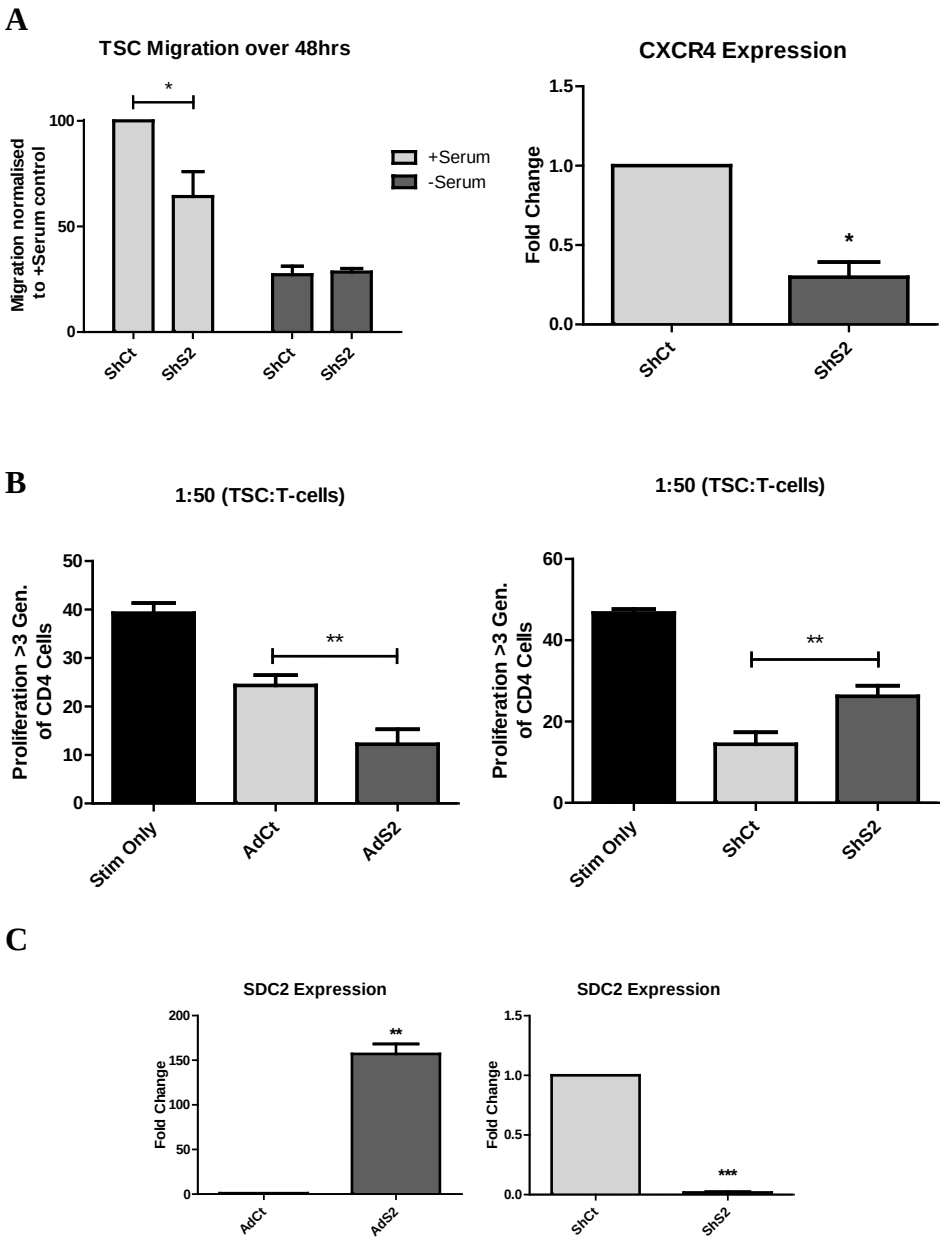

Figure 3.8 SDC2 knockdown impairs the migrative and immune-suppressive capacity of tumour derived stromal cells (**A**) TSCs with a knockdown of SDC2 show impaired migrative ability towards serum containing media over controls, 2-way ANOVA (*p≤0.05 n=3), CXCR4 RNA expression was also significantly reduced over controls, 2-way ANOVA (*p≤0.05, n=3). (**B**) CD4 T-cell proliferation was significantly reduced in cells overexpressing SDC2 and conversely increased when SDC2 was knocked down, 1-way ANOVA with Tukey's multiple comparison post-test (**p≤0.01, n=3). (**C**) SDC2 RNA was significantly increased with adenoviral SDC2 and decreased with adenoviral Sh-SDC2, 2-way ANOVA (**p≤0.01, ***p≤0.001, n=3)

3.2.8. Optimisation of a xenograft model of orthotopic breast cancer.

Our *in vitro* data describes a pro-migratory, immune-suppressive role for SDC2 in breast cancer stroma and thus we decided to test if these results translate *in vivo*. In order to perform this; we established an orthotopic breast cancer model in Orbsen therapeutics with the guidance of Dr Róisín Dwyer of the Lambe institute, UCHG (**Sect. 2.2.3.2.**). Our initial investigation was to assess the number of MDA-MB-231 cells required for consistent tumour growth. Cell numbers of $2x10^6$, $1x10^6$ and $5x10^5$ were administered to NOD:SCID immunocompromised mice based on previously published literature [354, 355], with 4 mice per group. Tumour growth was measured three times per weeks; animals were euthanised before a maximum tumour size of $2.5cm^3$ was reached. The results showed a consistent increase in tumour growth in the $2x10^6$ with cell administration group, 100% of mice developed tumours. Comparably cell doses of $1x10^6$ and $5x10^5$ displayed slower growth kinetics and percentage tumour establishment with 75% and 25% respectively. The $2x10^6$ group was selected based on this data for future experiments (**Fig. 3.9. A**).

We next sought to determine the optimal stromal cell number for co-administration with MDA-MB-231 cells to achieve tumour growth. We selected ratios of 1:3, 1:10 and 1:100, TSC: BCC based on previously published literature [356, 357] along with a $2x10^6$ BCC only control group, and again we selected 4 mice per group. The ratios selected are generally below normal ratios seen in many papers, which administer more MSC than BCC; we however selected numbers more phenotypic of spontaneous tumours. Tumour growth was again measured three times per weeks up until a terminal size of $2.5mm^3$. The results from this study indicated a slight increase in growth rates in the 1:10 ratio over MDA alone, with 100% tumour establishment. Comparably ratios of 1:3 and 1:100 showed delayed growth kinetics but also had 100% tumour establishment. The increase in growth kinetics indicated

the presence of stromal benefit and thus the cell ratio of 1:10 TSC:BCC was selected for future SDC2 modulation experiments (**Fig. 3.9. B**).

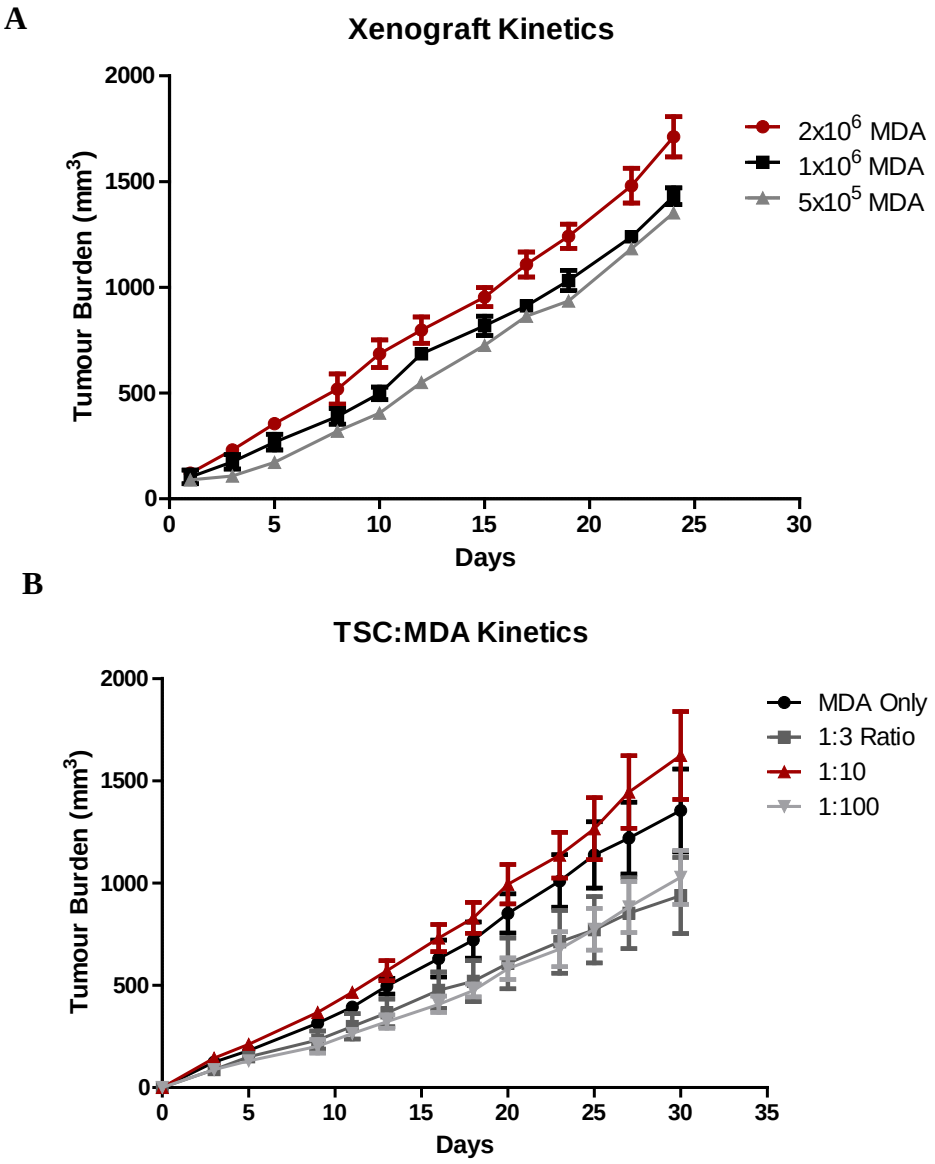

Figure 3.9. Optimisation of a xenograft model of orthotopic breast cancer. (**A**) Xenograft kinetics show $2x10^6$ MDA-MB-231 cells display superior growth kinetics and consistency. (**B**) The 1:10 ratio of TSC:MDA shows superior growth rates to ratios of 1:3 and 1:100.

3.2.9. Stromal Sdc2 Overexpression Enhances tumour growth.

In order to assess the effects of stromal SDC2 overexpression on breast tumour carcinogenesis, TSCs were transduced with adenoviral SDC2 (AdS2) or adenoviral control (AdCt) (**Sect. 2.2.2.1.**) and qPCR analysis confirmed that Sdc2 expression increased 149 fold in AdS2 cells compared to AdCt cells. Transduced TSCs were mixed 1:10 with MDA-MB-231 cells and injected in MFP of 10 NOD:SCID mice (**Sect. 2.2.3.2.**). Tumour growth was measured three times per weeks up until a terminal size of 2.5mm^3. When results were tabulated it was shown that SDC2 overexpression significantly enhances tumour growth kinetics as assessed by raw tumour measurements, at the endpoint of the study tumours with stromal SDC2 overexpression were significantly larger than controls (1873.32±90.595 vs 1246.825±109.186) tumours with stromal SDC2 overexpression also displayed more consistent establishment 100% vs 80% (**Fig.3.9. A**).

Tumours were explanted (**Sect. 2.2.3.3**.) and enzymatically digested (**Sect. 2.2.3.5.**) a proportion of the sample was put through a mouse cell depletion MACs column in order to separate human cells from mouse cells. Both whole tumour and human only samples were stained with a human or mouse panel for flow cytometry (**Sect. 2.2.3.7.**). Analysis of surface expression of the whole tumour sample, showed a significant increase in recruited mouse epithelial EpCAM+ cells, and trends towards an increase in infiltrating CD31+ endothelial vasculature in tumours with stromal SDC2 overexpression (**Fig. 3.10. B**). There was also a non-significant elevation of SDC2 detected at the endpoint of the study indicating the effects of SDC2 overexpression persisted up to 30 days (**Fig. 3.10. B**). This finding was corroborated at RNA level as analysis of human only cells indicated significant increases in SDC2. Further RNA analysis of human only cells revealed significant elevations in TGFβ regulator SMAD7 and EMT marker PAI-1 in tumours with stromal SDC2 overexpression. This was

accompanied by a significant increase in CXCR4 indicating a more active migratory pathway (**Fig. 3.10. C**).

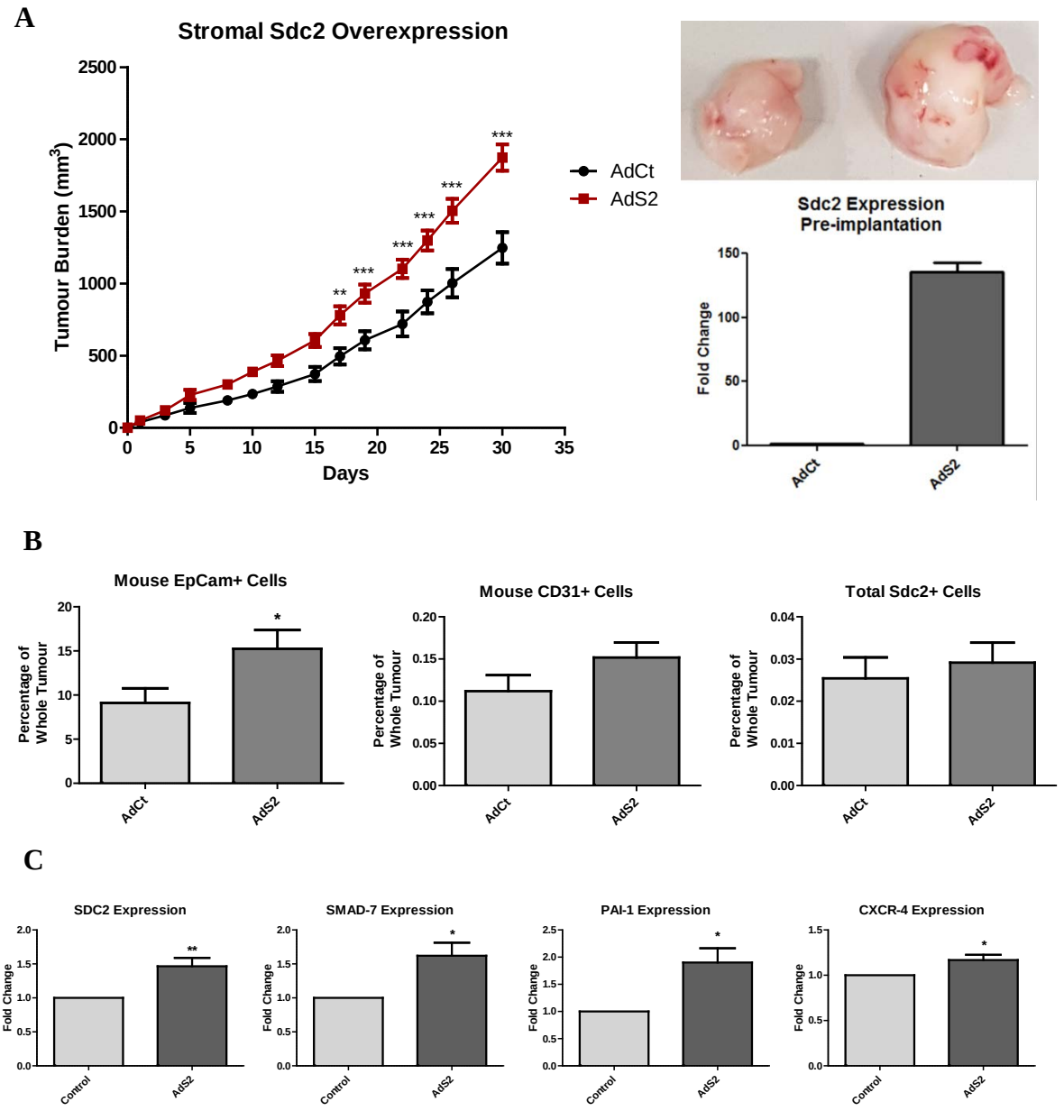

Figure 3.10. Stromal SDC2 overexpression enhances tumour growth (**A**) Overexpression of SDC2 significantly increased growth kinetics of tumours, 2-way ANOVA with Bonferroni post-tests (**p≤0.01, ***p≤0.001, n=8, n=10). (**B**) Analysis of cell surface markers indicates a significant increase in mouse contributed epithelia with trends of increase endothelia and SDC2, unpaired t-test (*p≤0.05, n=8, n=10). (**C**) RNA analysis of human only cells indicates significant increases in SDC2, SMAD7 and PAI-1 and CXCR4, 2-way ANOVA (*p≤0.05, **p≤0.01, n=8, n=10).

3.2.10. Stromal SDC2 overexpression enhances metastases to the lung.

On the day of harvest lungs of the mice were explanted (**Sect. 2.2.3.3.**). They were then processed, H&E stained and scored (**Sect. 2.2.3.4.**) (**Fig. 3.11. A**). Analysis revealed a significant increase in the number of metastatic lesions in the lungs of mice with AdS2 treated stroma compared to AdCt (**Fig. 3.11. B**).

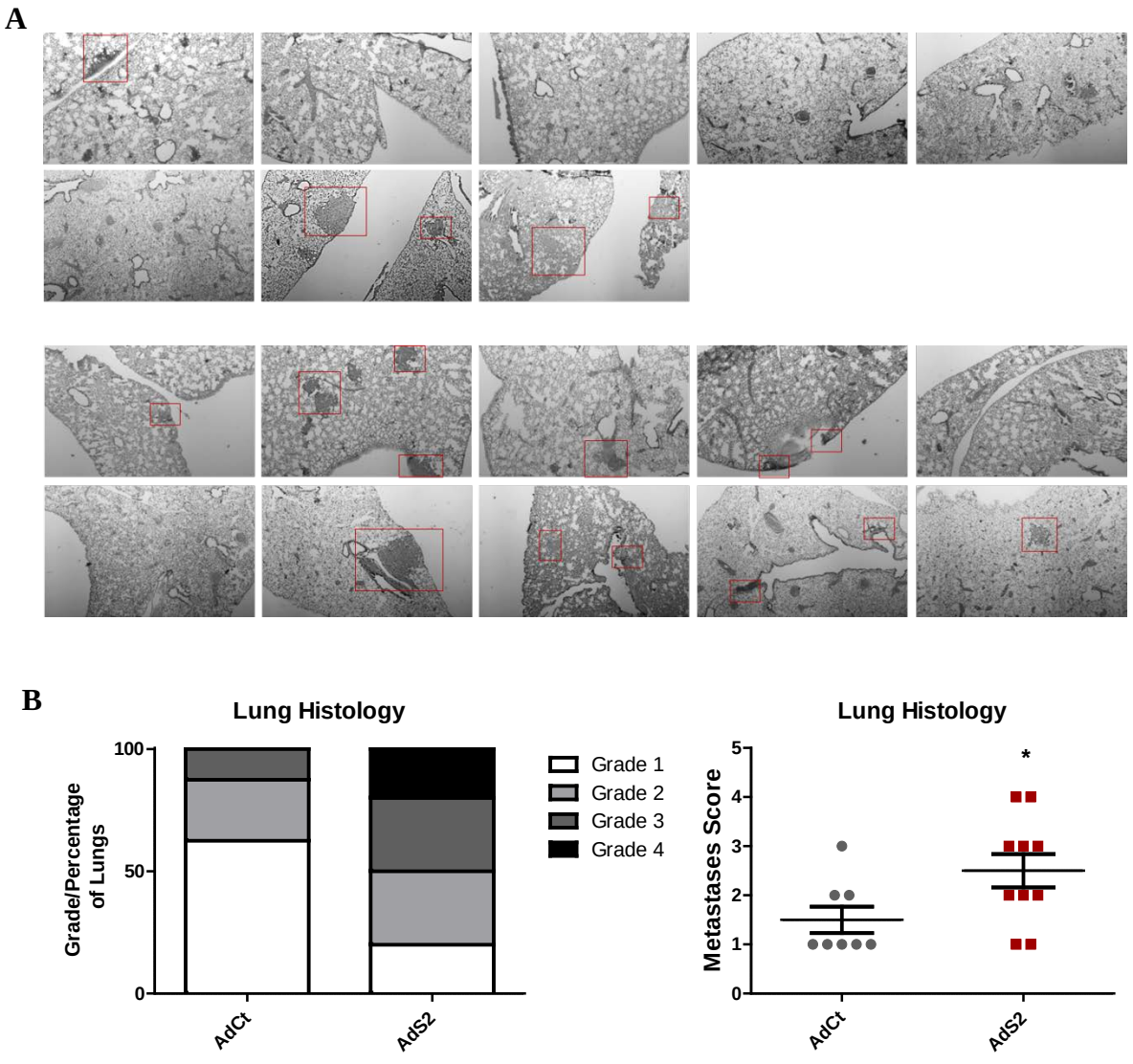

Figure 3.11. Stromal SDC2 overexpression enhances metastases to the lung. (**A**) Representative images of lung histology based on worst score 3 of 8 mice in the Ad control group and 8 of 10 mice in AdS2 formed metastases. (**B**) Grading of lung histology reveals a significant increase in metastases in AdS2 group, unpaired t-test (*p≤0.05, n=8, n=10).

3.2.11. Stromal Sdc2 knockdown impairs tumour growth.

In parallel to the overexpression studies TSCs were transduced with adenoviral short-hairpin SDC2 (ShS2) or adenoviral short-hairpin control (ShCt) (**Sect. 2.2.2.1.**), to assess the effects of stromal SDC2 knockdown on breast tumour carcinogenesis. Cells were mixed 1:10 with MDA-MB-231 cells and injected in MFP of 10 NOD:SCID (**Sect. 2.2.3.2.**). Tumour growth was measured as before, three times per weeks up until a terminal size of 2.5mm^3. When results were analysed it was shown that knockdown of stromal SDC2 significantly impairs tumour growth kinetics at later time points as assessed by raw tumour measurements. By the endpoint of the study tumours with stromal SDC2 knockdown were significantly smaller than controls (1176.889±82.44 vs 1511.86±82.471) tumours with stromal SDC2 knockdown also displayed slightly less establishment 90% vs 100% (**Fig. 3.12. A**).

As before, tumours were explanted, digested, separated and stained (**Sect. 2.2.3.3., 2.2.3.5., 2.2.3.7.**). Analysis of surface expression of the whole tumour fraction showed a trend towards a reduction in recruited mouse epithelial EpCAM+ cells, and infiltrating CD31+ endothelial vasculature in tumours with stromal knockdown SDC2 the inverse to what was seen with stromal overexpression. Surface SDC2 also showed a significant reduction in the ShS2 group at the endpoint of the study (**Fig. 3.12. B**). Again this finding translated to the RNA as was detected in the human only fraction, which showed a trend towards a reduction in SDC2 in the ShS2 group, suggesting SDC2 remained slightly repressed within the tumour for the duration of the study. We also detected a significant decrease in SMAD7 accompanied by a trend towards repression of TGFβR3 in the ShS2 treated group. Interestingly CXCR4 RNA was also significantly decreased in the ShS2 group mimicking our *in vitro* findings. (**Fig. 3.12. C**).

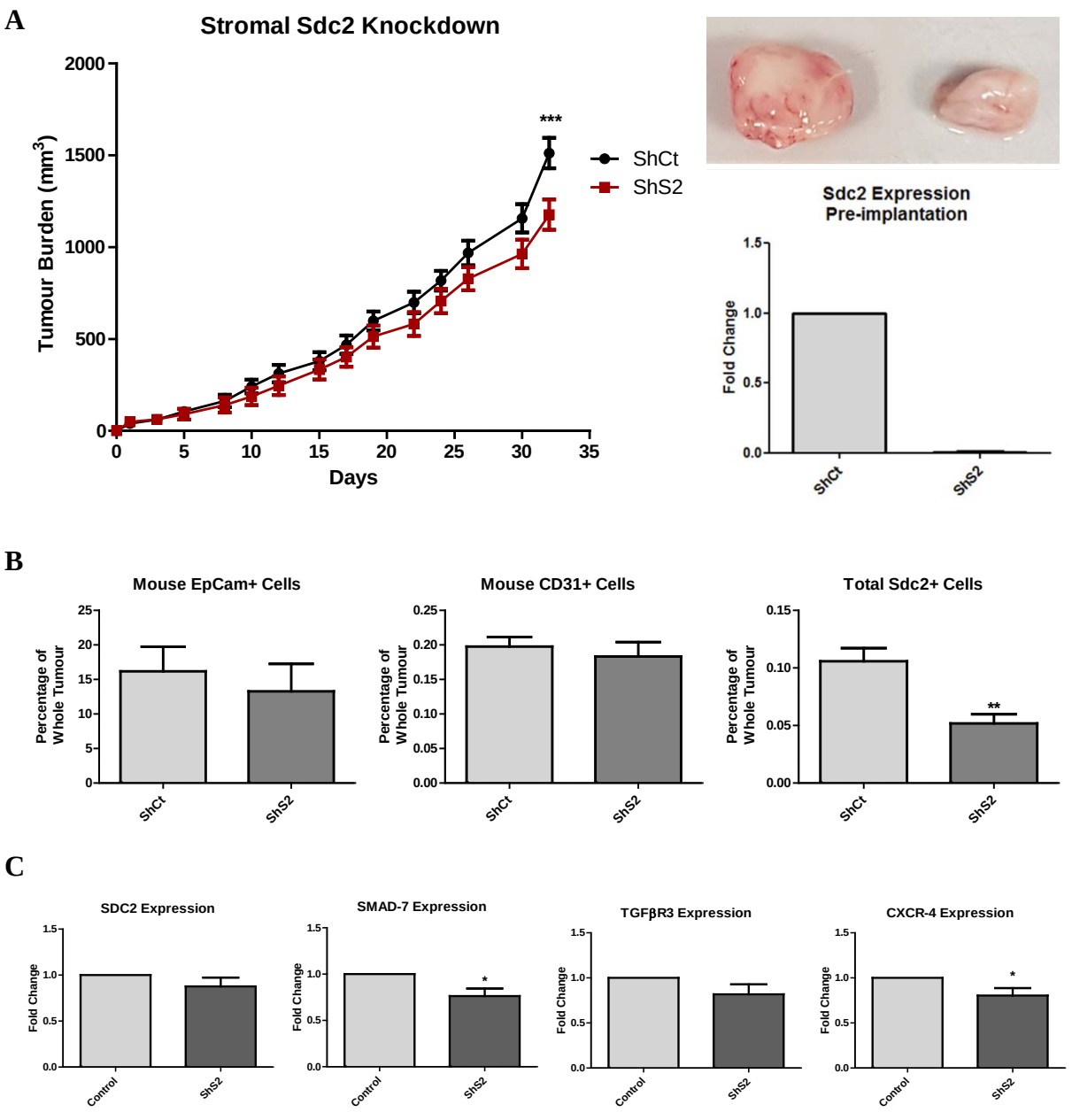

Figure 3.12. Stromal Sdc2 knockdown impairs tumour growth. (**A**) Knockdown of SDC2 significantly impaired growth kinetics at later stages, 2-way ANOVA with Bonferroni post-tests (***p≤0.001, n=10, n=9). (**B**) Analysis of cell surface markers indicates non-significant decreases in mouse contributed epithelia and endothelia and with a significant reduction in surface SDC2, unpaired t-test (*p≤0.05, n=10, n=9). (**C**) RNA analysis of human only cells indicates a trend of less SDC2 and TGFβR3 RNA with a significant decreases in SMAD7 and CXCR4 RNA, 2-way ANOVA (*p≤0.05, n=10, n=9).

3.2.12. Stromal SDC2 knockdown decreases frequency of lung metastases.

As before lungs were explanted (**Sect. 2.2.3.3.**), processed, H&E stained and scored (**Sect. 2.2.3.4.**) (**Fig. 3.13. A**). Analysis revealed a no significant difference in number of metastatic lesions and thus the overall metastases score. However a higher proportion of control animals had detectable metastatic lesion in tumours with stromal SDC2 knockdown, 40% versus 22%. (**Fig. 3.13. B**).

A

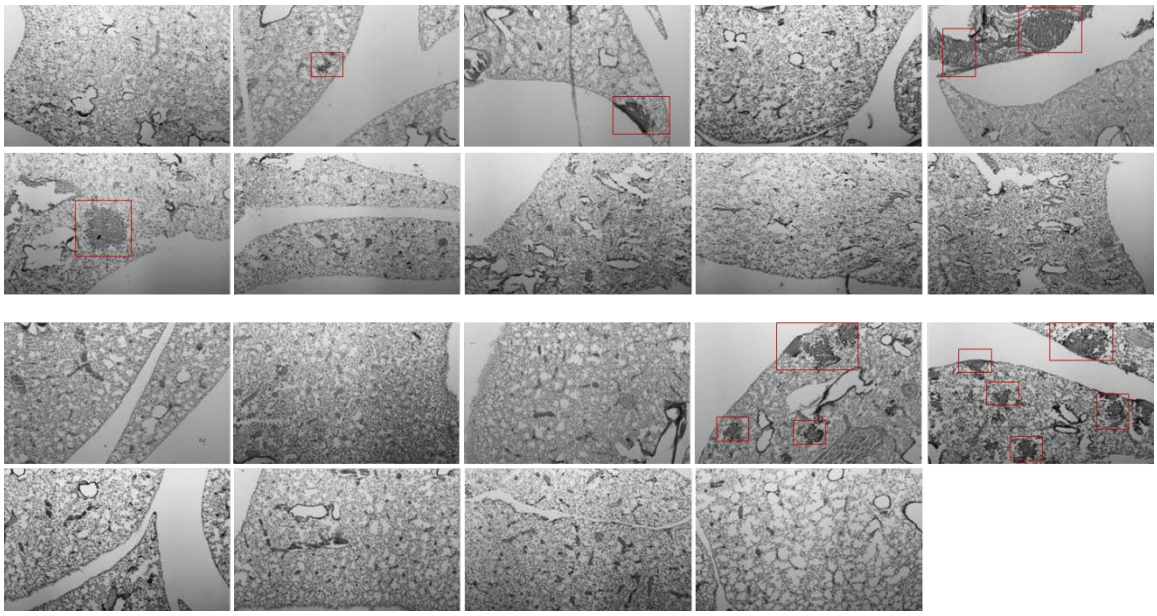

B

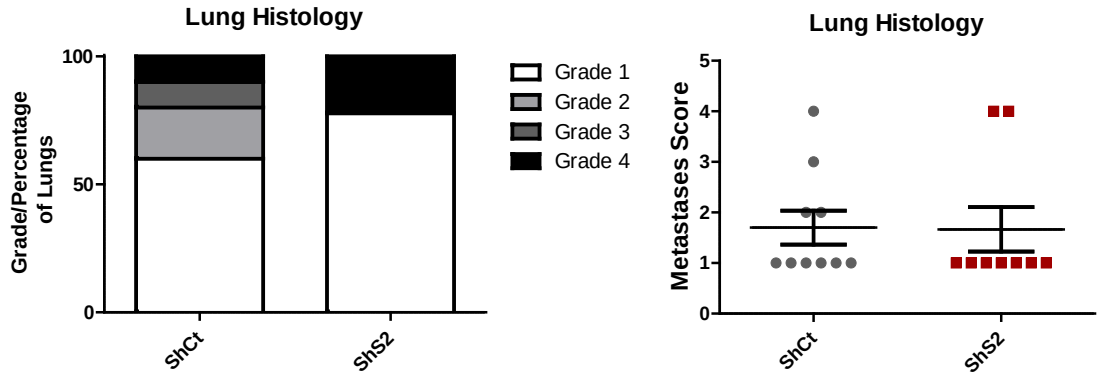

Figure 3.13. Stromal SDC2 knockdown decreases frequency of lung metastases. (**A**) Representative images of lung histology based on worst score 4 of 10 mice in the Sh control group and 2 of 9 mice in ShS2 formed metastases. (**B**) Grading of lung histology reveals no significant differences in metastases (n=10, n=9).

3.3. DISCUSSION

In this study we investigated the characteristics and phenotype of modulation of Syndecan-2 in breast cancer epithelial cells as well as normal and tumour stromal cells. SDC2, a HSPG, is upregulated in the epithelial compartment of a number of cancers such as breast and colon cancer [327, 331-333]. It has been demonstrated that SDC2 has a pro-tumourigenic role in breast and pancreatic cancers controlling cell survival, migration and adhesion [327, 328]. Data from Orbsen Therapeutics indicated SDC2 as a novel stromal marker which could isolate a pure population of stromal cells from multiple tissues and species. Our lab connected the dots and drew a link between SDC2 and breast cancers, due to the role stroma plays in this particular cancer. Our initial studies indicated the presence of elevated levels of SDC2 in breast cancer tissue and the presence of higher levels of shed SDC2 in the serum of patients with triple negative breast cancer (**Fig. 3.1.**). Triple negative breast cancer remains the most elusive and deadly forms of breast cancer, and represents an unmet clinical need for treatment. Our data indicated SDC2 as a possible prognostic marker for triple negative breast cancer therefore we wanted to establish if stromal-derived SDC2 had a pro-tumourigenic role within the breast TME.

In order to unravel this initial experiments investigated the addition of exogenous recombinant SDC2 to MDA-MB-231s and we noted that a preconditioning step bolstered their migrative potential (**Fig. 3.2. A**). Our work became focused on SDC2 knockdown in these cells and effects on their characteristics and phenotype. We relied on assessment of changes in RNA expression as readouts of experimental effects due to consistency of results after TGFβ stimulation. It is worth noting that changes in protein expression would have been a valuable tool in corroborating these results, howevere we experienced ongoing western blot and water quality issues throughout this work which left us to rely on RNA expression. We

used previously developed adenoviruses to overexpress and knockdown SDC2. In the first instance we knocked down SDC2 in breast cancer TNBC epithelial cells and showed a significant impairment of migrative capacity over 3 separate experiments (**Fig. 3.2. B**), further RNA analysis revealed repression of the CXCR4 gene associated with CXCR4/CXCL12 cell homing. CXCR4 has been well studied and published that CXCR4 antagonists are effective in controlling tumour growth [198]. A number of publications have suggested a link between SDC4 and CXCR4 co-localisation as well data indicating heparan sulfates as binding partners of CXCL12 [358, 359]. Literature also suggests CXCR4 signalling induces MMP production which causes Syndecan shedding and that heparan sulfate proteoglycans protect CXCL12 from proteolytic destruction [360, 361]. This indicates the possible presence of a positive feedback loop between CXCR4 and SDC2 expression. Along with this we detected decreases in fibronectin expression which is a molecular partner of SDC2 involved in adhesion [310] and ZEB1 which promotes EMT and angiogenesis through VEGF [347]. Interestingly it has been shown that fibronectin regulates EMT through switching TGFβ signalling from canonical (tumour suppressive) to non-canonical (tumour promoting) through a PEAK1/ZEB1 signalling axis [362, 363] (**Fig. 3.2. C**). Our data suggests SDC2 as a possible regulator of this process as we know from the literature that SDC2 interacts with and controls expression of all three TGFβ receptors [314].

To further delineate the mechanism by which SDC2 effects BCC migration we focussed on the TGFβ pathway. The link between SDC2 and TGFβ signalling had been shown by a number of groups [314-316]. We set out to define this connection in our triple negative breast cancer cell line using our previously titrated adenovirus. Initially we had strived to detect upregulation in TGFβ signalling by measuring increases in phosphorylated SMAD2/3 protein, however due to issues with detection we opted for RNA upregulation of inhibitory SMAD7. TGFβ3 was selected due to numerous publications linking it to SDC2 [314, 317].

Recombinant TGFβ3 at a ratio of 5ng/ml was found to give robust and consistent induction of SMAD7 after 2 hours. When we knocked down SDC2 in three separate experiments we saw significant reductions in SMAD7 signalling and an important EMT marker CTGF (**Fig. 3.3. A**). In breast cancer epithelial CTGF facilitates tumour growth and metastasis via promotion of collagen I fibre deposition and orientation at the primary tumour stroma [364]. This result indicates that repression of SDC2, a heparan sulfate proteoglycan ECM molecule, negatively impacts coordination of collage I, the primary constituent of the tumour ECM [270]. We also detected non-significant decreases in PAI-1 a gene which has been published as a promoter of EMT in triple negative breast cancer [365] and SNAI1 one of the hallmark EMT genes [78] (**Fig 3.3. B**). These results indicate that SDC2 impacts TGFβ signalling and the process of EMT in BCCs and is in line with previously published literature [317].

At this stage we were confident our SDC2 knockdown adenovirus was efficient and was giving us similar phenotypes to previously published data therefore we were keen to use this along with a SDC2 overexpression adenovirus in order to manipulate SDC2 in tumour stromal cells. The purpose of these studies was to ascertain how SDC2 affected tumour stromal cell function. Therefore we developed a process to isolate TSCs from breast cancer patients. We began collecting breast tumour samples from UCHG. We optimised an enzymatic digestion, stromal isolation and hypoxic culture protocol and began culturing tumour derived stromal cells. We performed a number of assays to characterise these cells to confirm they are stromal cells and not fibroblasts. Donors were screened by cell surface molecule expression based on the conditions set out by the ISCT [128] (**Fig 3.4.**). TSC donors 1, 3 and 4 displayed slightly irregular phenotypes so were not used for further assays. We also determined that TSC displayed higher surface levels of SDC2 than their normal counter parts (**Fig. 3.5. A**). Proliferation was then assessed over 12 passages in culture, TSCs consistently outperformed stromal cells from other tissues (**Fig. 3.5. B**) and finally we

showed TSC had a heightened immune-suppressive function over UC-SC. We theorise that the increased ability of these tumour derived stromal cells is due to TME conditioning.

We began our work on stromal SDC2 knockdown using umbilical stromal cells from Orbsen Therapeutics using previously defined knockdown methods before subjecting to our battery of assays. We detected significant inhibition of TGFβ signalling through decreases in SMAD7 (**Fig. 3.6. A**) It became apparent however, that knockdown of SDC2 in these cells was not tolerated as well as in MDA-MB-231. Proliferation declined and cells lost colony forming ability upon subculture (**Fig. 3.6. C**). Work in parallel at Orbsen Therapeutics has detected a similar phenotype in both BM-MSC and UC-MSC; the findings suggest SDC2 knockdown induces cell death through activation of p38 mitogen-activated protein kinases and subsequent activation of p53 and upregulation of p21. The results of this work are in preparation for a co-authored publication.

We next proceeded to knockdown SDC2 in our tumour derived stromal cells (TSC) with adenoviral Sh-SDC2; our findings indicated a significant repression in TGFβ signalling through decreases in SMAD7. We did not detect significant decreases in PAI-1 and CTGF however indicating a lesser effect of SDC2 knockdown despite RNA expression comparable to MDA-MB-231s (**Fig 3.7. A**). We performed CFU-f and proliferation experiments to assess the effects of SDC2 knockdown in these cells, we detected no change to growth or colony forming ability indicating the cell death pathway is not active (**Fig. 3.7. B&C**). Due to ability of these stromal cells to re-adhere after knockdown we proceeded to test their migratory potential. It was concluded that SDC2 knockdown significantly impairs migrative capacity and RNA analysis of these cells indicated a repression of CXCR4, a phenotype we have previously seen in MDA-MB-231s (**Fig 3.8. A**). Finally we tested the effects of modulation of SDC2 on immune-suppressive function; we included the use of an adenoviral

overexpression vector for SDC2 which became available in Orbsen Therapeutics. Our data indicated that SDC2 was necessary and sufficient for immune-suppression based on a significant finding in 3 biological replicates we hypothesised this effect was partly due the effect described by Rovira-Clave et al of SDC2 causing TCR shedding [366](**Fig. 3.8. B**). Therefore in summary our data indicates that as well as SDC2 controlling the tumourigenic properties of breast cancer epithelial cells, SDC2 also has a pro-tumourigenic role within breast tumour stromal cells.

Our *in vitro* findings indicated a significant role for SDC2 in breast cancer both in epithelia and stroma. So we devised a strategy to test these data *in vivo*, we began by optimisation of a xenograft model of breast cancer in immune-compromised NOD:SCID mice. Based on the literature we selected a number of doses of breast cancer cells to consistently establish tumours in our model. Our dose optimisation studies enabled us to select a dose/cell number of $2x10^6$ MDA-MB-231 cells mixed with TSC at a ratio of 1:10 TSC:MDA (**Fig. 3.9.**).

After this data was gathered we began so assess the effect of SDC2 modulation on breast carcinogenesis. We had originally envisioned modulating SDC2 in the epithelial MDA-MB-231 cells however, all adenoviral constructs impaired tumour forming ability and no tumours were formed. When we modulated SDC2 in the TSCs however we did not significantly impair tumour forming ability of MDA-MB-231, we did however see differences in growth kinetics depending on SDC2 status and we could detect human stromal cells persisting in the tumours to the endpoint (**Fig. 3.14**). We concluded that SDC2 significantly affect breast tumour carcinogenesis (**Fig. 3.10. A, Fig. 3.12. A**). Overexpression of SDC2 significantly increased tumour growth rates and imparted greater recruitment of mouse derived epithelial cells perhaps through greater ECM production (**Fig. 3.10. B**). We also detected heightened TGFβ signalling through increases in SMAD7 RNA as well as higher levels of the TGFβ

regulated EMT gene PAI-1 (**Fig. 3.10. C**). Histological analysis of explanted and stained lung sections revealed a significant increase in metastases both in prevalence (38% vs 80%) and grade (**Fig. 3.11.**). However histological scoring was limited by sample size, only one third of the lung was analysed and we did not account for cumulative number or size of metastases, scoring was done by worst metastases slide detected. Our RNA analysis of the tumours indicated a significant increase in the pro-migratory gene CXCR4, this finding correlated with the increase in metastases seen (**Fig. 3.10. C**). In this same model in the case of SDC2 knockdown we saw the opposite effect; growth kinetics indicated a significant reduction in growth kinetics over the course of the study (**Fig. 3.12.**). TGFβ signalling was also significantly impaired through SMAD7 however we did not detect significant differences in mouse cell recruitment or EMT marker induction (**Fig 3.12. B & C**). Interestingly we did see a significant reduction in CXCR4 RNA expression, which correlated with *in vitro* findings and also with a decrease in number of mice with lung metastases (**Fig. 3.12. C, Fig. 3.13.**). We did not however detect any significant differences in metastatic grade.

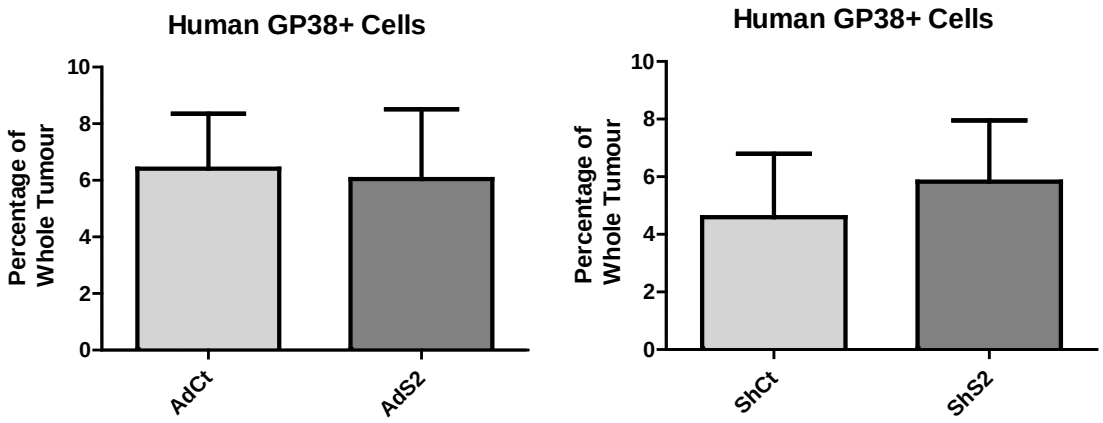

Figure 3.14. Presence of human stromal cells in xenograft models at endpoint of study. Explanted, digested and purified human cell fraction of tumours revealed presence of stromal cells identified by GP38 expression on the cell surface. (6.41±1.947% **AdCt**, 6.045±2.464% **AdS2**, 4.597±2.197% **ShCt**, 5.828±2.129% **ShS2**).

3.4. CONCLUSIONS

Together our findings indicate a significant role of SDC2 in breast cancer carcinogenesis. We have shown that SDC2 is present in breast cancer tissue and is a possible prognostic marker of triple negative breast cancer as detectable in serum samples. We have shown that SDC2 plays pivotal roles in breast cancer cell migration and EMT through regulation of CXCR4, fibronectin and ZEB1. We have also shown that stromal cells isolated from primary breast tumours have higher SDC2 expression and display a more proliferative and immune-suppressive phenotype than stromal cells from normal tissues. We have also shown that SDC2 is critical for the migratory and immunosuppressive properties of these tumour derived stromal cells. Finally we have proven that SDC2 significantly impacts carcinogenesis in our xenograft model of breast cancer. We have shown stromal SDC2 modulation affects growth kinetics, metastases, TGFβ signalling and EMT. Our data definitively highlights SDC2 as a potential therapeutic target in breast cancer.

CHAPTER 4

RESULTS & DISCUSSION

PART II

Therapeutic targeting of SDC2

4.1. BACKGROUND

Our data to this point suggest that therapeutic targeting of SDC2 within the tumour microenvironment may inhibit TGFβ signalling, immunosuppression and metastases. Therefore developing a strategy to block SDC2 became our priority.

Over the past twenty years there have been major advances in the understanding of the molecular mechanism of cancer. As a result research has shifted from investigating chemotherapeutics that display off target effects and has focussed on screening for therapeutic targets for direct inhibition [367]. Blocking antibodies have been the cutting edge of therapeutic targeting of specific pathways in recent years. This strategy has yielded a number of FDA approved therapies including anti-PD-1 antibodies pembrolizumab and nivolumab [208] or anti-TGFβ antibody fresolimumab [87]. More recent clinical trials are investigating the use of specific small molecule chemical inhibitors of tumorigenic pathways such as TGFβ kinase inhibitor SB-505124 [351], TNFα inhibitor etanercept [101] or WNT signalling inhibitor ipafricept [112]. However in recent years, peptide based therapeutics have emerged as effective alternatives to both systems [368]. Peptide based therapeutics possess several favourable characteristic such as higher potency and specificity which enables greater effects in smaller doses when compared to small molecule pharmacologics [369]. An inherent disadvantage to small peptide biologics is their short half-life and rapid biodegradation [370,

371]. However the innate properties of peptides allow ease of synthesis as well as modification and many peptide therapeutics overcome this obstacle by coupling the peptide to the FC domain of IgG1 such as FGF-FC therapies which have shown success in multiple cancers [372]. The broad success of peptide biologics can be seen across the field, currently there are 60 clinically approved peptide therapeutics and another 150 in active development [373], in 2017 the global peptide therapeutics market was valued at approximately $23 billion and it is expected to increase to $43 billion by the end of 2024 [374].

Importantly in 2009 a group demonstrated that a SDC1 core protein derived peptide inhibitor, named synstatin (SSTN), can disrupt integrin $\alpha_v\beta_3$ and $\alpha_v\beta_5$ interactions. They went on to show systemic delivery of SSTN blocks angiogenesis in an orthotopic mouse model of breast cancer manifesting in impaired tumour growth [375]. The interaction between syndecans and angiogenesis is not limited to SDC1 however data from the Whiteford group in 2013 and 2014 showed GST-fusion tagging of the entire mature SDC2 and SDC3 ectodomains has anti-angiogenic properties [376, 377]. Furthermore, administration of GST tagged SDC2 peptide containing only the SDC2 adhesion regulatory domain inhibited angiogenesis in human and rodent tumour models through CD148 mediated inactivation of integrin β1 [376].

As such the Barkley lab began development of deletion mutants of SDC2 containing different functional elements, in a FLAG expression vector. Twelve peptide constructs were generated for investigation (**Fig 4.1.**) of these; peptides 1 and 2 were highlighted as having potential therapeutic properties. Our specific aim in Chapter 4 is to identify the effects of these peptides in the pathways set out in Chapter 3 and to answer the question: can SDC2-peptide biologics block TGFβ signalling, reduce metastases or enable immune cell activation/infiltration in breast cancer.

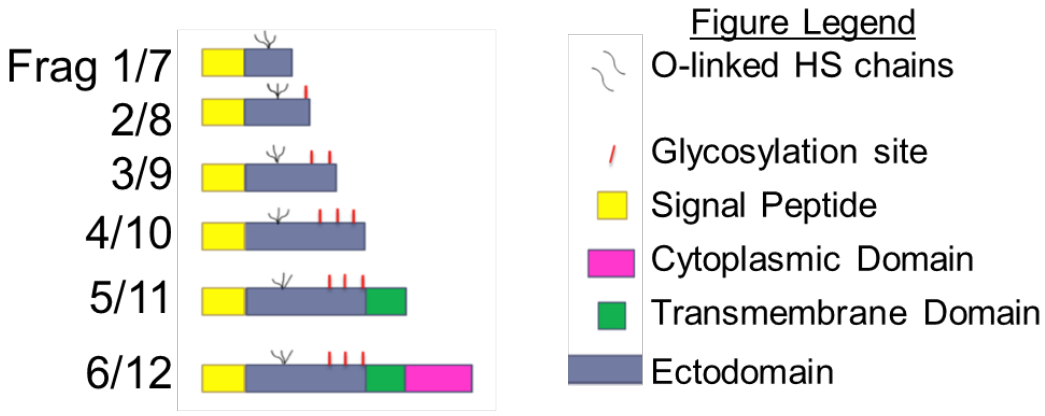

Figure 4.1. Generation of deletion mutants containing different functional domains of Sdc2. Fragments 1-6 contain the signal peptide, whereas fragments 7-8 do not. Fragment 1 contains amino acids 1-79 and fragment 2 contains amino acids 1-87. Fragment 6 represents full length SDC2.

4.2. RESULTS

4.2.1. SDC2 peptides impair triple negative breast cancer cell migration and clonogenicity.

To begin our work validating the therapeutic potential of SDC2 peptides 1 and 2, hereafter called SDC2-F1 & SDC2-F2 we needed to stabilise peptide expression. Previous iterations of SDC2 peptides were generated in FLAG expression vectors, however smaller peptides were found to be less stable. We selected an Fc expression vector, to impart a structural stabilisation to allow robust expression for testing in future experiments (**Sect. 2.2.1.7.**) (**Fig 4.2. B)**. DNA was produced by transformation of competent cells and subsequent maxi-prep (**Sect. 2.2.1.8. & 2.2.1.9.**) to produce SDC2-F1-Fc and SDC2-F2-Fc. Because of our previous data indicating SDC2 knockdown impairs TNBC migration our first series of assays was to assess the effects of SDC2-F1-Fc and SDC2-F2-Fc on triple negative breast cancer cell migration and clonogenicity. MDA-MB-231 cells were pre-incubated with F1-Fc, F2-Fc or no treatment and were seeded into an xCELLigence cell migration system (**Sect. 2.2.2.5.**). The ability of MDA-MB-231 cells to migrate towards stromal cell conditioned media was assessed. It was found that pre-incubation of MDA-MD-231 cells with SDC2-F1-Fc and F2-Fc significantly impaired migration towards stromal cell conditioned media (81.67±0.333% F1, 72.00±5.508% F2) (**Fig.4.2. A**). To assess effects on clonogenicity MDA-MB-231 cells were transfected with SDC2-F1-Fc, F2-Fc and an empty vector-Fc (EV-Fc) control (**Sect. 2.2.2.4**). Expression was detected by western blot (**Sect 2.2.1.4.**) for IgG:FC (**Fig. 4.2. B**). Transfected cells were sub-cultured to determine the ability of cells to form colonies (**Sect. 2.2.2.3.**). It was found that overexpression of SDC2-F1-Fc & F2-Fc significantly impaired clonogenicity of MDA-MB-231 cells (70.00±3.055% F1, 62.33±3.844% F2) (**Fig. 4.2. C**).

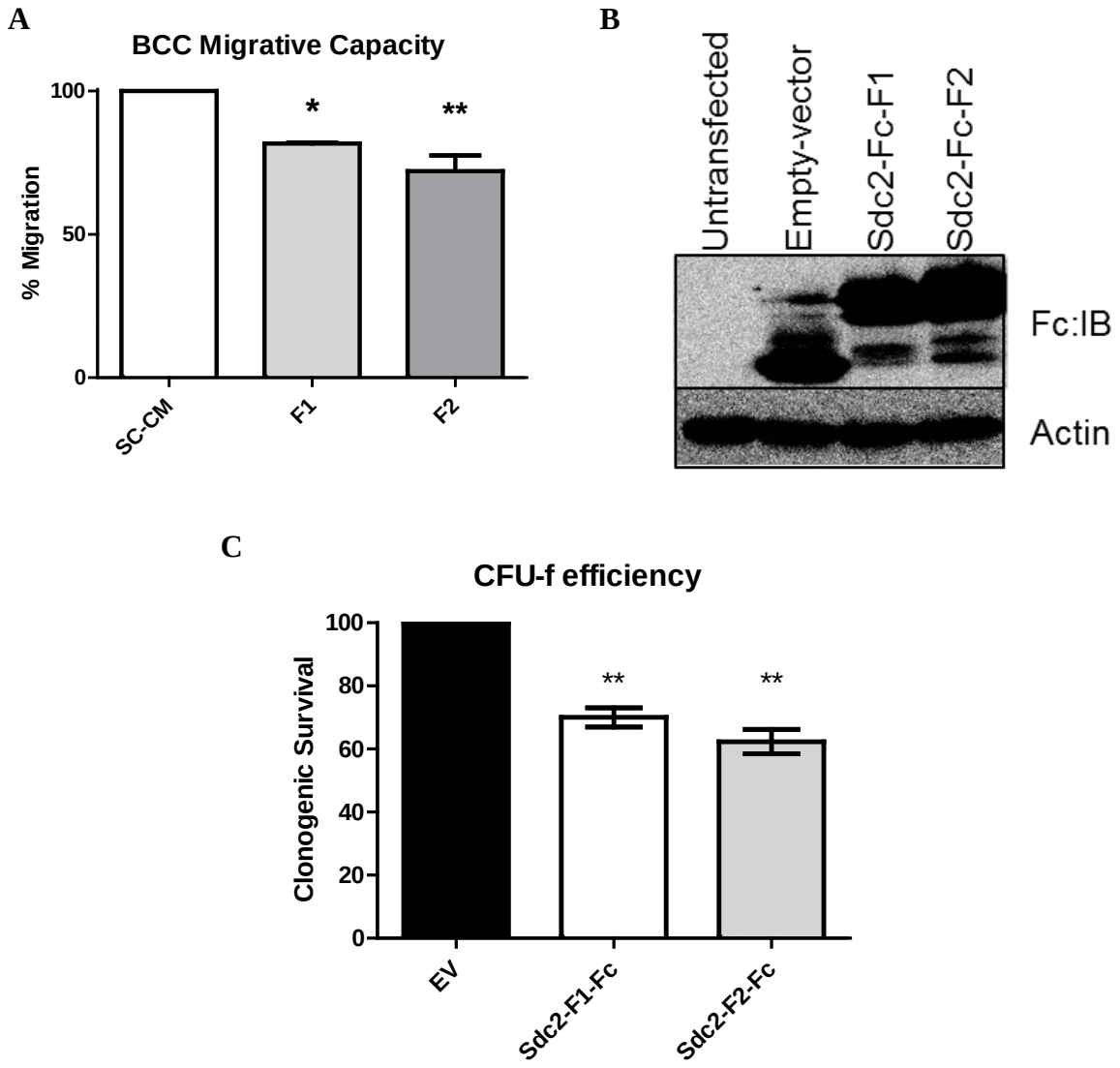

Figure 4.2. SDC2-F1-Fc and SDC2-F2-Fc impair migration and clonogenicity of triple negative breast cancer cells. (A) Pre-conditioning of MDA-MB-231 cells with SDC2-F1-Fc and F2-Fc, significantly impairs migrative capacity, 1-way ANOVA with Tukey's multiple comparison post-test (*p≤0.05, **p≤0.01, n=3). (B) Representative image of fragment protein overexpression as detected by western blot. (C) Overexpression of F1-Fc and F2-Fc impairs colony forming ability of MDA-MB-231 cells over EV control, 1-way ANOVA with Tukey's multiple comparison post-test (**p≤0.01, n=3).

4.2.2. SDC2 peptides impair TGFβ induction of EMT in triple negative breast cancer cells.

Our previous studies indicate knocking down SDC2 impaired TGFβ signalling in MDA-MB-231 cells, therefore we wanted to establish if overexpression of SDC2 peptides had an effect on the TGFβ pathway in a similar. Thus, MDA-MB-231 cells were transfected with EV, F1 or F2 (**Sect. 2.2.2.4.**) and treated with TGFβ similar to previous experiments (**Sect. 2.2.2.8.**). A significant reduction in CTGF induction in response to TGFβ was observed in MDA-MB-231s overexpressing SDC2-F1-Fc and F2-Fc (3.55±0.58 EV, 1.933±0.318 F1, 1.760±0.389 F2) (**Fig. 4.3. A**), this coincided with significant reductions in PAI-1 (21.0±3 EV, 11.033±3.484 F2) and SNAI1 (52.0±12.014 EV, 37.333±8.95 F2) signalling when cells were transfected with SDC2-F2-Fc (**Fig 4.3. B**). A trend towards a reduction in SMAD7 expression (19.773±5.312 EV, 10.667±4.391 F1, 6.833±1.241 F2) and detected a robust upregulation of SDC2 peptide RNA expression (68.16±14.29 F1, 155.4±34.58 F2) (**Fig 4.3. C**).

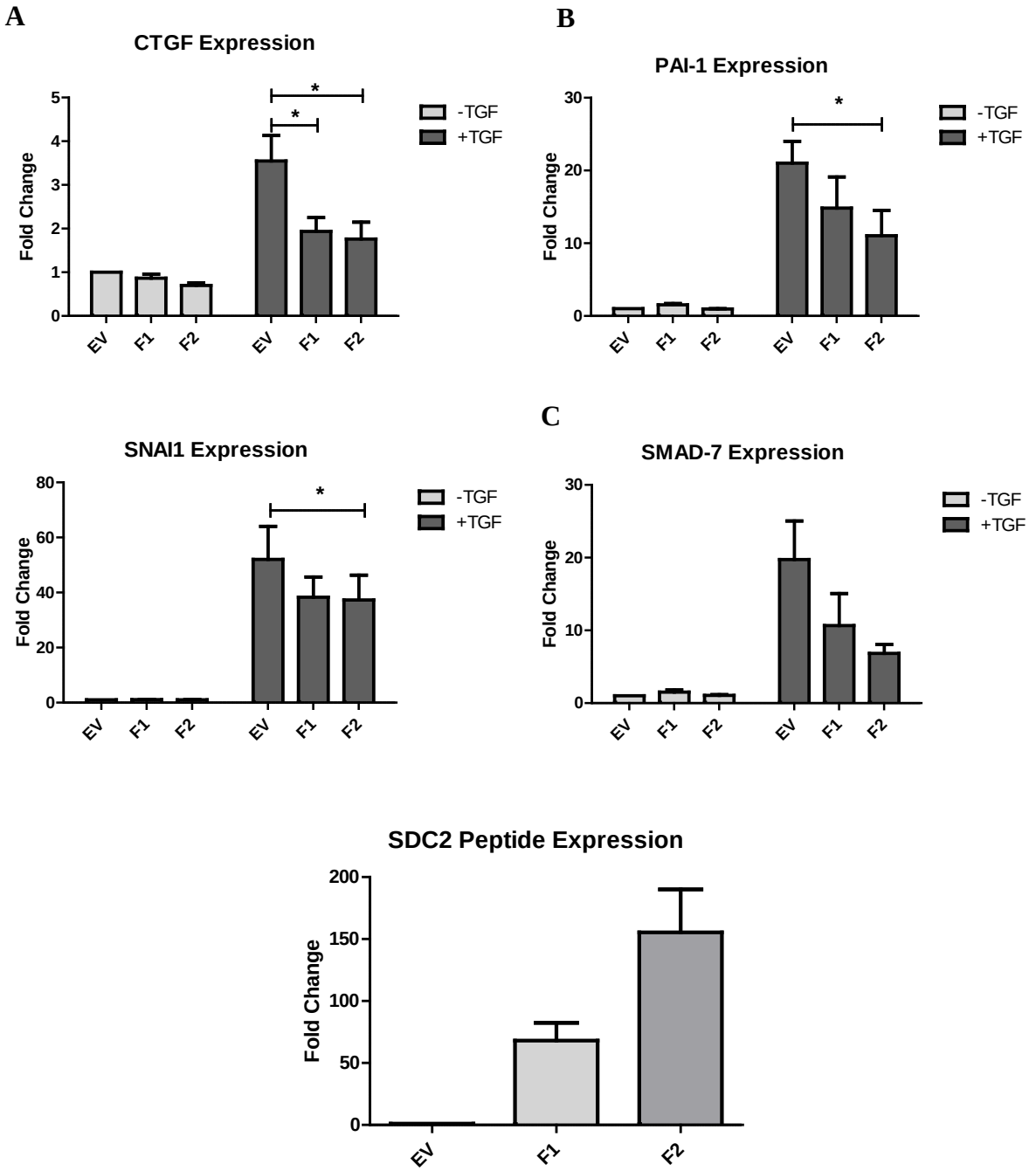

Figure 4.3. Overexpression of SDC2 peptides in MDA-MB-231 cells impairs TGFβ mediated induction of EMT. (A) Both SDC2-F1-Fc and F2-Fc significantly reduced TGFβ induction of CTGF, 1-way ANOVA with Tukey's multiple comparison post-test (*p≤0.05, n=3). (B) SDC2-F2-Fc significantly impairs PAI-1 and SNAI1 induction, 1-way ANOVA with Tukey's multiple comparison post-test (*p≤0.05, n=3). (C) There is a trend towards a reduction in TGFβ signalling and robust upregulation of SDC2 peptide RNA when normalised to endogenous SDC2 levels in EV (n=3).

4.2.3. SDC2 peptides inhibit the migratory and immune-suppressive properties of tumour stromal cells via CXCR4 and PD-L1.

Our initial peptide studies indicate SDC2-F1-Fc and F2-Fc impair TGFβ signalling in MDA-MB-231 cells in a similar manner to adenoviral SDC2 knockdown, we therefore wanted to establish if overexpression of SDC2 peptides in tumour stromal cells would have similar results to our adenoviral work. To begin, SDC2-F1-Fc and F2-Fc were overexpressed in TSC using FuGENE as before (**Sect. 2.2.2.4.**) and the effects on TGFβ signalling were assessed using our optimised time-course protocol (**Sect. 2.2.2.8.**). SDC2 peptide overexpression was consistent in TSCs as detected by RNA expression (376±81.46 F1, 331.3±63.2 F2) (**Fig 4.4. A**). Overexpression of SDC2-F1-FC or F2-Fc in TSCs had no effect on the TGFβ induced upregulation of SMAD7, interestingly however TGFβ mediated induction of the pro-metastatic marker, CXCR4 was significantly inhibited (10.113±0.785 EV, 2.747±0.907 F1, 1.395±0.515 F2) (**Fig 4.4. B**). This result represented a significant finding as therapeutics which target CXCR4 are currently in clinical trials [378]. We selected SDC2-F2-Fc for closer study due to more robust impairment of CXCR4 upregulation, for inclusion in an xCELLigence system migration assay to assess if this impairment translates to reduced migratory potential. The assay was set up as per previous experiments, with peptide transfection and then migration assay using + or – serum as nutrient gradient controls (**Sect 2.2.2.4., 2.2.2.5.**). Results showed that fragment 2 significantly impaired the migrative ability of TSCs towards serum containing media (76.545±5.556) (**Fig 4.4. C**). Previous work showed that adenoviral knockdown of SDC2 impaired the ability of TSCs to suppress $CD4^+$ T-cells therefore we sought to test the effects of SDC2 peptides on this process. To do this, TSCs overexpressing peptides 1 and 2 were assayed in a T-cell proliferation assay to assess effects on suppressive capacity of TSCs. The experiment was set up as described previously (**Sect 2.2.2.4., 2.2.2.7.**) and it was found that fragment 1 could slightly but significantly

reduce suppressive ability, whereas the effects of fragment 2 were not significant, however a trend was detected (6.383±0.556 EV, 11.9±1.44 F1, 8.88±0.317 F2) (**Fig. 4.4. D**). It was hypothesised that SDC2 peptides may impair PD-L1 signalling thereby reducing suppressive capacity, as PD-L1 has been shown to be TGFβ regulated. In order to test this theory, protein lysates were probed with anti-PD-L1 antibody (**Sect. 2.2.1.3., 2.2.1.4.**). A stark reduction in PD-L1 protein was detected in TSCs overexpressing SDC2-F2-Fc (**Fig 4.5. E**).

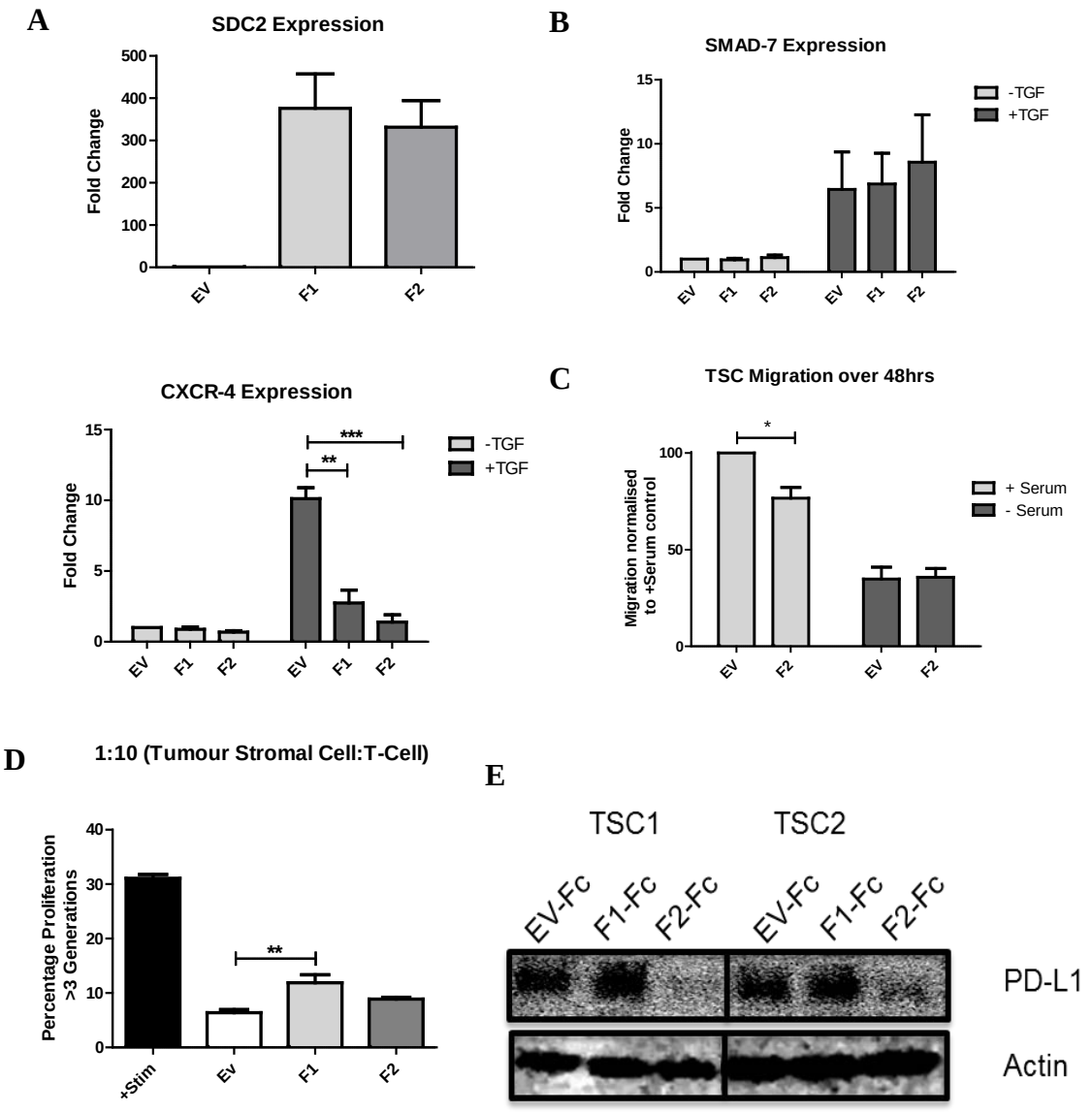

Figure 4.4. SDC2 peptides impair the migratory and immune-suppressive properties of TSC via CXCR4 and PD-L1. (A) Fragment overexpression was robust and consistent in TSCs (n=3). (B) TGFβ signalling was not affected as detected through consistent SMAD7 induction however CXCR4 expression was significantly impaired after TGFβ stimulation, 1-way ANOVA with Tukey's multiple comparison post-test (**p≤0.01, ***p≤0.001, n=3). (C) SDC2-F2-Fc significantly impairs TSC migration towards serum, 2-way ANOVA (***p≤0.001, n=3). (D) SDC2-F1-Fc significantly impairs $CD4^+$ T-cell suppression of TSCs 1-way ANOVA with Tukey's multiple comparison post-test (**p≤0.01, n=2). (E) PD-L1 protein was robustly diminished in TSCs overexpressing F2 (n=2).

4.2.4. SDC2 peptides inhibit CXCR4 and the immune-suppressive properties of normal stromal cells.

As SDC2 peptides appear to affect the tumourigenic properties of TSC, we wanted to determine if they affected normal SC biology. To assess if SDC2 peptide therapy would be specific to TSCs or might it also affect normal SCs elsewhere in the body. To begin, we performed a series of experiments investigating the effects of SDC2 peptide overexpression in umbilical derived stromal cells. SDC2 peptides 1 and 2 were overexpressed using FuGENE as previously described (**Sect. 2.2.2.4.**) and the effects on TGFβ signalling were assessed using our optimised time-course protocol (**Sect. 2.2.2.8.**). SDC2 peptides were highly expressed as detected by RNA analysis; expression rates varied donor to donor leading to inconsistent TGFβ signalling data as seen in high SEM values (2954.949±609.538 F1, 6308.733±2363.144 F2) (**Fig. 4.5. A**). Again we did not detect any changes in TGFβ signalling in these cells through RNA analysis of SMAD7 upregulation **(Fig 4.5. B)**. RNA analysis did however indicate a strongly significant downregulation of endogenous CXCR4 gene expression with both peptides in three biological replicates (0.2±.054 F1, 0.188±0.045 F2) (**Fig. 4.5. C**). This may indicate repression of the endogenous homing capacity of normal stromal cells to sites of inflammation or tumour. A trend towards an increase in CTGF was noted in peptide treated groups (4.243±1.58 F1, 5.142±2.535 F2) indicating MSC differentiation towards a fibroblastic lineage [379] (**Fig. 4.5. D**).With the knowledge of heighted CTGF expression being described as a hallmark fibroblastic differentiation we hypothesised that cells would be less immunosuppressive. To assess this we overexpressed F1 & F2 in UC-MSCs (Sect. 2.2.2.4) for co-culture experimentation with PBMCs to detect changes in immunosuppressive properties (**Sect. 2.2.2.7.**). The results showed fragment transduction significantly reduced the capabilities of HUC cells to suppress $CD4^+$ T-cells (21.42±3.95 EV, 32.72±2.215 F1, 31.18±0.5945 F2) (**Fig. 4.5. E**).

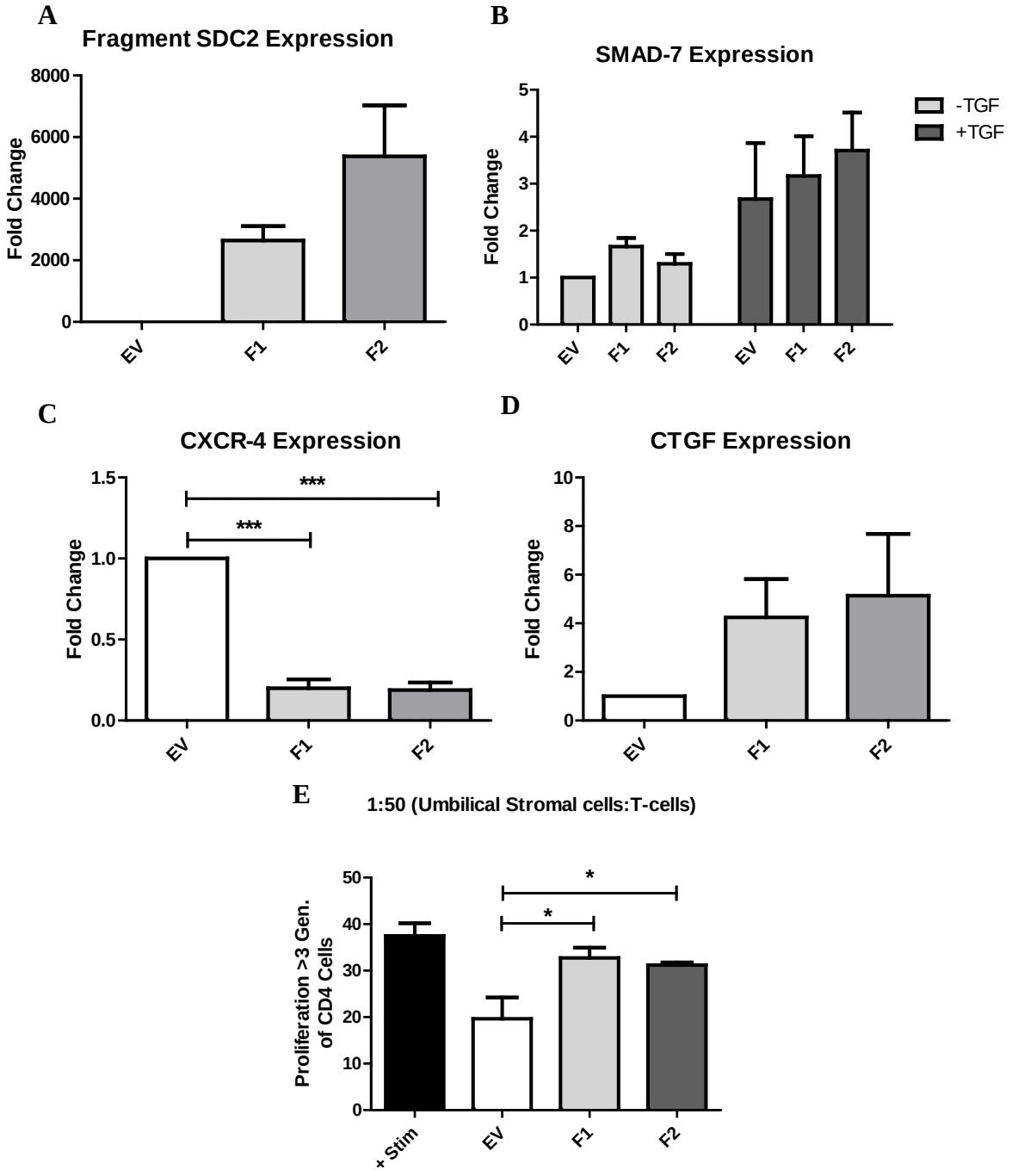

Figure 4.5. Overexpression of SDC2 peptides in normal stromal cells inhibits endogenous CXCR4 and diminishes immune-suppressive capacity. (A) SDC2 peptide RNA was highly expressed but expression rates varied between donors (n=3). (B) The TGFβ pathway is not affected by SDC2 fragment overexpression.(C) Overexpression of SDC2-F1-Fc & F2-Fc significantly represses CXCR4 expression, 1-way ANOVA with Tukey's multiple comparison post-test (***$p \leq 0.001$, n=3). (D) There was a trend towards an increase in the fibroblastic marker CTGF (n=3). (E) Peptide overexpression in UC-MSCs significantly inhibited $CD4^+$ T-cell suppression, 1-way ANOVA with Tukey's multiple comparison post-test (*$p \leq 0.05$, n=3).

4.2.5. Stromal overexpression of SDC2-F2-Fc inhibits tumour growth.

These findings suggest SDC2 peptides affect TGFβ signalling in BCC, and the migratory and immune-suppressive properties of TSCs therefore we wanted to establish if overexpression of Sdc2 peptides in TSCs within the TME effected tumour growth and metastasis *in vivo*. Our preliminary work with peptides 1 and 2 suggested overexpression of SDC2-F2-Fc in TSC gave more significant reductions in CXCR4 and PD-L1 signalling. As such we became keen to investigate if these effects translate to an *in vivo* setting. To test this we assessed the effect of stromal SDC2-F2-Fc versus EV in our previously optimised NOD:SCID xenograft model of breast cancer. We began as previously described with fragment transfection of TSC with FuGENE (**Sect. 2.2.2.4.**). We then mixed TSCs with MDA-MB-231 cells at a pre-determined ratio of 1:10 and injected cells orthotopically into the 4th MFP with 5 animals per group (**Sect. 2.2.3.2.**). Tumour growth was measured as before, three times per weeks up until a terminal size of 2.5mm^3. Growth kinetics from this study indicated that stromal overexpression of F2 caused a significant reduction in tumour growth kinetics at later stages (2126±194.6 EV, 1435.5±52.19 F2) and SDC2-F2-Fc RNA expression quantified in TSCs pre-implantation was within ranges seen for *in vitro* experiments (416.4fold) (**Fig. 4.6. A**). Tumour establishment levels were 100% for the EV group (5/5) and 80% for F2 (4/5).

As with previous xenograft studies, at the endpoint of the study tumours were explanted, digested, separated and stained with mouse and human panels for flow cytometry to enable assessment of implanted human TSCs and MDA-MB-231s against mouse cells recruited to the tumour (**Sect. 2.2.3.3., 2.2.3.5., 2.2.3.7.**). Surface analysis suggested a non-significant trend towards a reduction in mouse contributed endothelial cells in tumours with stromal F2 overexpression based on mouse specific CD31 expression (0.0988±0.0135% EV, 0.0777±0.0071% F2). Interestingly in the F2 group, we detected trends towards a reduction in

human specific CXCR4 (1.358±.0117% EV, 0.9385±0.2393% F2) and PD-L1 surface expression (26.33±5.201% EV, 14.14±2.46% F2) corroborating our *in vitro* findings (**Fig. 4.6. B**).

Subsequent RNA analysis of tumours revealed stromal F2 overexpression caused significant reductions in SMAD7 (0.756±0.041), CXCR4 (0.688±0.0798) and SDC2 (0.747±0.0582) expression indicating impairment of TGFβ signalling, chemokine mediated homing ability and repression of endogenous SDC2 possibly through outcompeting or blocking. We also detected a trend towards a reduction on PD-L1 gene expression which correlates with our *in vitro* data (0.813±0.131) (**Fig. 4.6. C**).

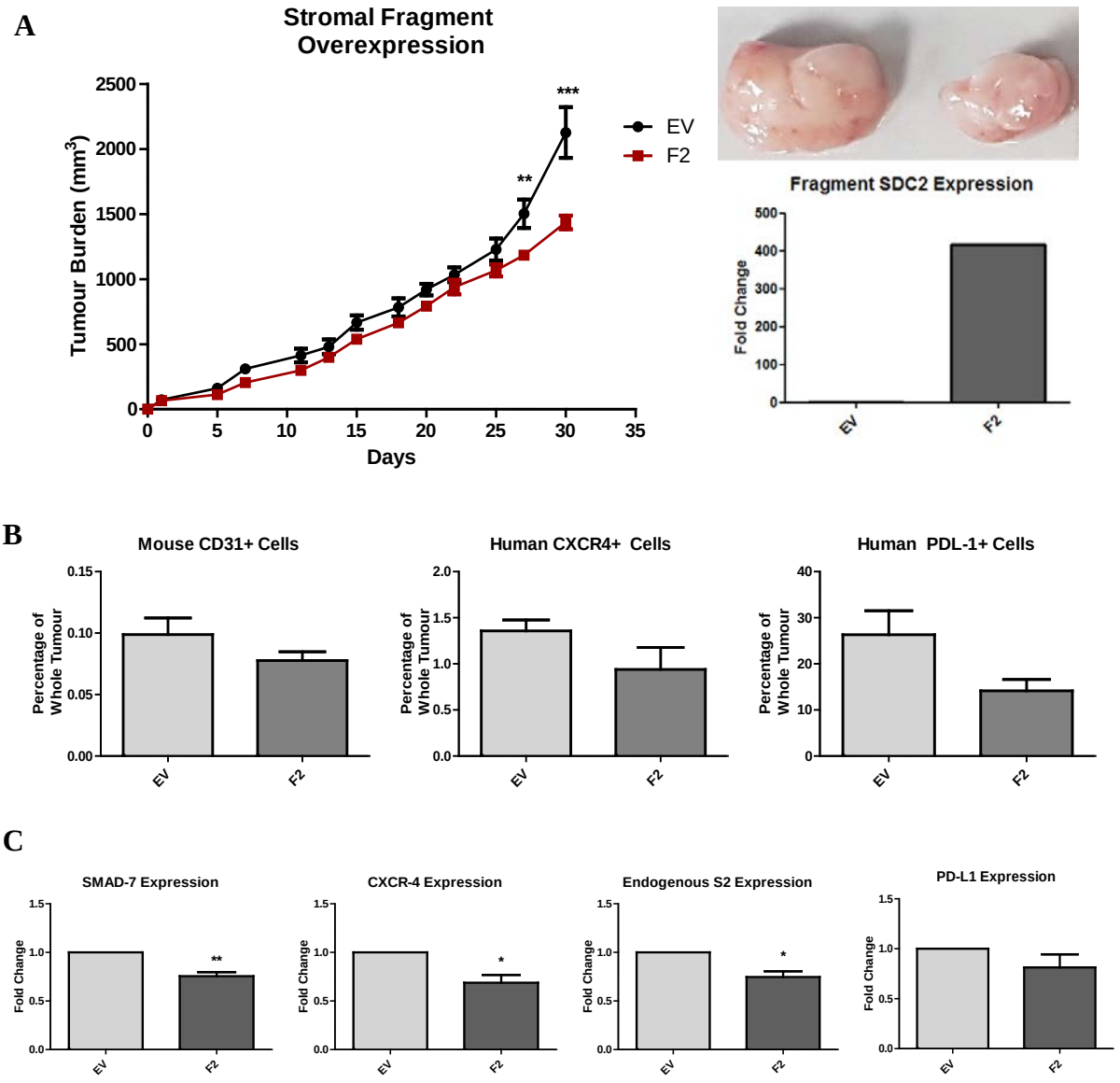

Fig 4.6. Overexpression of SDC2-F2-Fc in TSC inhibits xenograft tumour growth. (A) Overexpression of SDC2-F2-Fc in TSCs significantly impaired growth kinetics at later stages, 2-way ANOVA with Bonferroni post-tests (**p≤0.01, ***p≤0.001, n=5, n=4). (**B**) Analysis of cell surface markers indicates non-significant decreases in mouse contributed endothelia and human CXCR4^{+} and PD-L1^{+} cells, unpaired t-test (n=5, n=4). (**C**) RNA analysis of human only cells indicates significant decreases in SMAD7, CXCR4 and SDC2 RNA, with a non-significant decrease in PD-L1, 2-way ANOVA (*p≤0.05, **p≤0.01, n=5, n=4).

4.2.6. Stromal overexpression of SDC2 fragment 2 decreases frequency of lung metastases.

As with previous studies, lungs were explanted (**Sect. 2.2.3.3**.), processed, H&E stained and scored (**Sect. 2.2.3.4**.) (**Fig. 4.7. A**). Analysis revealed a non-significant difference in overall number of metastatic lesions due to low sample size, however a higher proportion of control animals had detectable metastases 80% versus 25% in knockdown tumours. (**Fig. 4.7. B**).

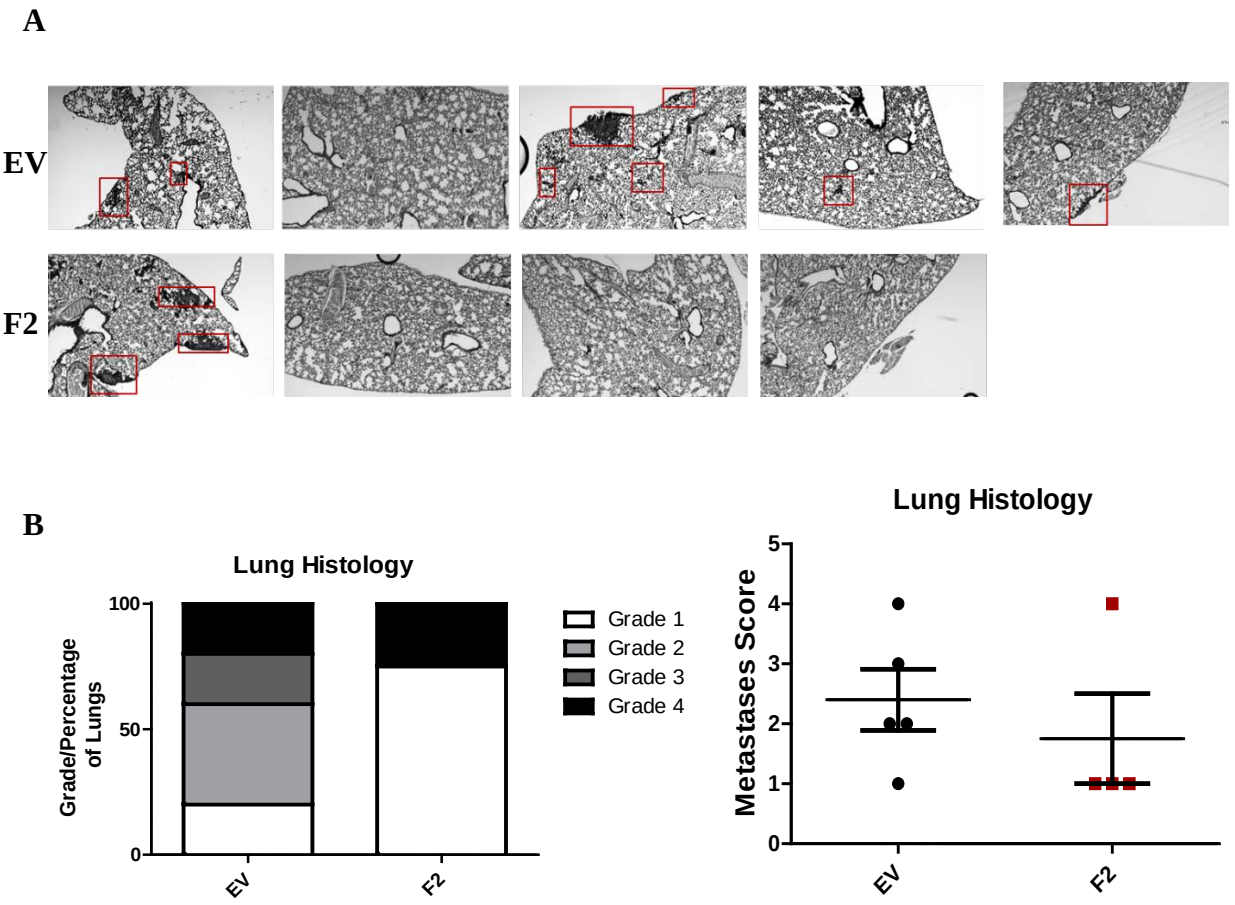

Figure 4.7. Frequency of metastatic lung lesions is decreased with stromal overexpression of SDC2-F2-Fc. (A) Representative images of lung histology based on worst score 4 of 5 mice in the EV control group and 1 of 4 mice in F2 group formed metastases. (**B**) Grading of lung histology reveals no significant differences in metastases (n=5, n=4).

4.2.7. Isolation and characterisation of PyMT mouse tumour derived stromal cells.

From our in vitro data it would suggest that Sdc2 peptides inhibit the immunosuppressive properties of stromal cells therefore to unravel if Sdc2 peptides possess immune suppressive properties in vivo we needed to use an immune competent breast cancer model. In order to accurately recapitulate this we utilised E0771 cells, a TNBC cell line isolated from C57BL/6 mice to prevent histocompatibility mismatch. Additionally we needed to isolate TSCs from a C57BL/6 model. For this we used the mouse model MMTV-PyVT,-mCherry,-Ova henceforth referred to as PyMT which is on a C57BL/6 background. This mouse model contains the mouse mammary tumour virus (MMTV) and thereby consistently develops palpable breast tumours between 18-24 weeks of age that reach terminal size roughly 15 days after onset (**fig. 4.8. A**).

Tumours were explanted and digested as with other models (**Sect. 2.2.3.3., 2.2.3.5.)** cells were stained for flow cytometry to assess constituents of tumours (**Sect 2.2.3.6.)**. Surface analysis of tumours revealed presence of SDC2 in stromal (FAP^+) and epithelial compartments ($EpCAM^+$) akin to our findings in human breast tumours (**Fig. 4.8. B**).

A fraction of the cells after digest were plated in culture to assess growth kinetics and phenotype. Previous work had been done using isolated mouse bone marrow derived MSCs (**Sect. 2.2.3.10.**) enabling comparison to a pool of normal mouse MSCs. Analysis of growth kinetics clearly indicated greater growth and potential of mouse TSCs when compared to bone marrow derived MSCs as well as maintained morphology a similar finding to human TSCs vs normal MSCs (**Fig 4.7. C).** Phenotype of TSC was then assessed using our mouse panel to ensure no contaminating epithelial (EpCAM), erythroid (Ter119), hematopoietic (CD45) or endothelial (CD31) cell lineages were present and the TSCs are in fact of stromal origin ($GP38^+$ $SCA\text{-}1^+$ $MCHII^-$) (**Fig 4.8. D**).

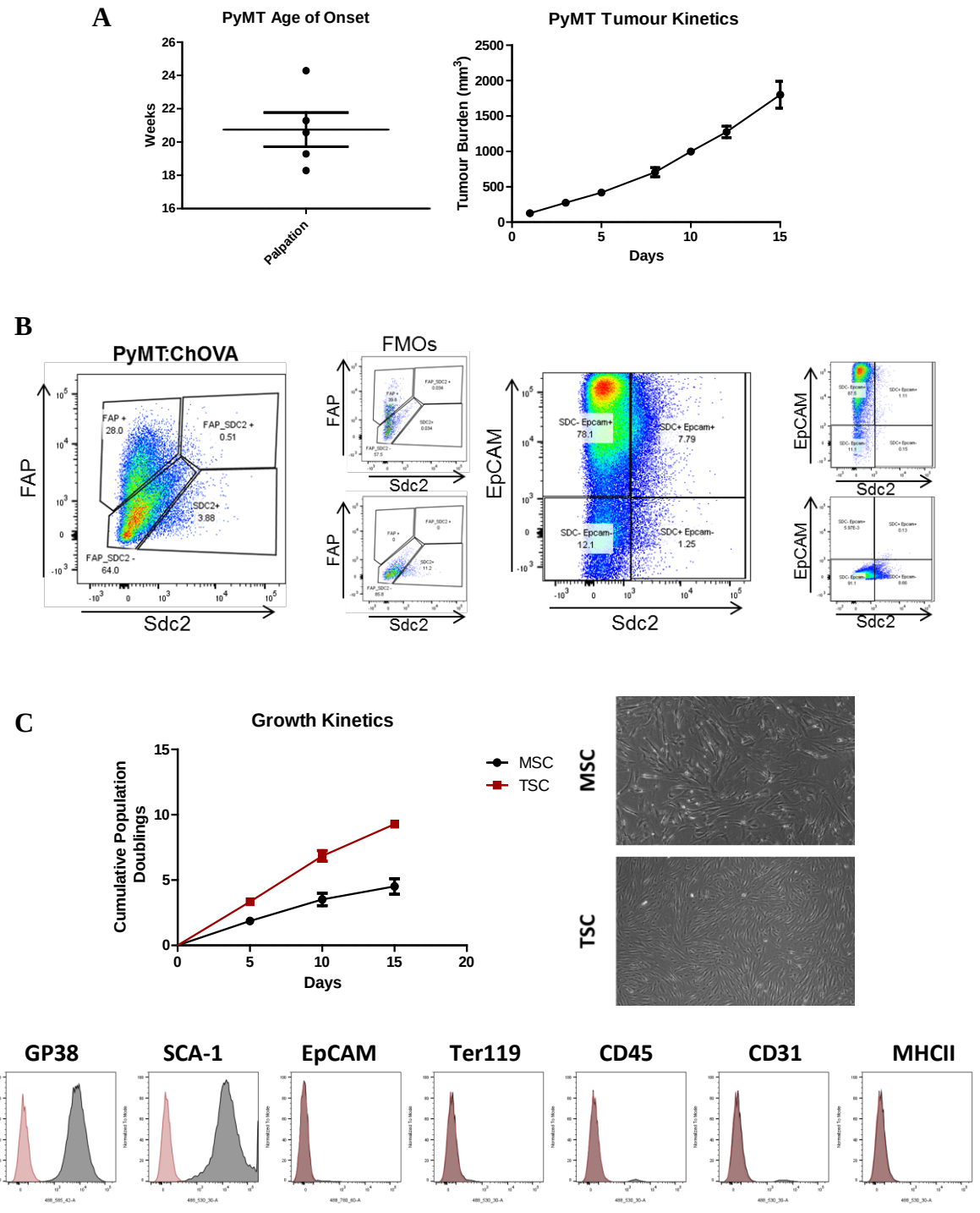

Figure 4.8. Isolation and characterisation of mouse TSCs from PyMT tumours. (**A**) PyMT tumour kinetics show consistent growth rates between 18-24 weeks. (**B**) Analysis of tumours shows presence of SDC2 in epithelial and stromal compartments. (**C**) Mouse tumour derived stromal cells display higher growth rates and maintained morphology in culture. (**D**) Phenotyping panel indicates presence of stromal markers GP38 and SCA-1 with absence of EpCAM, Ter119, CD45, CD31 and MHC-II.

4.2.8. Stromal overexpression of SDC2 fragment 2 significantly inhibits tumour growth in an immune competent model of breast cancer.

In parallel to the work in this thesis a master's student in our lab Luke Watson had begun development of a mouse variant of SDC2 fragment 2. Cloning was done from mouse full length SDC2 into a mouse FC vector. His work also established growth kinetics and dosing for an orthotopic model of mouse breast cancer using the mouse triple negative breast cancer cell E0771. As such, for the final part of this body of work we sought to determine the effect of SDC2-F2-Fc in mouse tumour derived stromal cells in an immune competent model, using E0771s as tumour initiators.

Our data suggests human SDC2-F2-Fc affects PD-L1 signalling as well as impairing the immune-suppressive capacity of stromal cells, thus we wanted to investigate whether this would translate to reductions in tumour growth in a mouse with a functioning immune system. In order to test this, we overexpressed mSDC2-F2-Fc in mouse derived TSCs (**Sect. 2.2.2.4.**), these were then mixed in a 1:10 ratio with $1x10^6$ E0771 cells a murine triple negative breast cancer cell line. This cell number had been previously optimised in the lab by Luke Watson. Cells were injected orthotopically into the 4^{th} MFP with 4 mice per group (**Sect. 2.2.3.2.**). Tumour kinetics indicated a significant reduction in tumour growth in mice with stromal overexpression of F2 at later stages of growth, as such at the endpoint of the experiment mSDC2-F2-Fc overexpressing tumours were significantly smaller than control tumours (2145.623±140.78 EV, 1422.75±110.73 F2). Western blot analysis indicates overexpression of mouse EV and F2 pre-implantation as detected by anti-mouse IgG-FC (**Fig. 4.9. A**).

At the endpoint of the study tumours were explanted, digested, and stained (**Sect. 2.2.3.3., 2.2.3.5., 2.2.3.8.).** The first stain panel was used to delineate cells of stromal (GP38),

epithelial (EpCAM), erythroid (Ter119), hematopoietic (CD45) or endothelial (CD31) origin and identify expression of SDC2, PD-L1 and CXCR4. The next panel identified populations of CD4 and CD8 T-cells and the final panel identified: monocytes (Ly6G- CD11b+ CD11c- Ly6Chi F4/80mid-low), macrophages (Ly6G- CD11b+ CD11c- Ly6Clo, F4/80+), dendritic cells (Ly6G- CD11b- CD11c+) and neutrophils (CD11b+ Ly6G+). Cell surface analysis of digested tumours indicated a significant increase in epithelial cells (7.355±0.674% EV, 11.04±1.337% F2) and stromal cells (6.173±0.325% EV, 7.385±0.361% F2) in tumours treated with fragment 2, this finding was contrary to previous studies, however due to the short time span of the study it could be deduced a higher proportion of the cells explanted were also the cells implanted E0771s being $EpCAM^{+}$ and TSCs $GP38^{+}$ (**Fig. 4.9. B**). All other surface markers assessed were at comparable levels for both treatments, however a trend was detected in presence of suppressed and activated $CD8^{+}$ T-cells. It was found that EV treated tumours tended to have slightly elevated levels of suppressed $CD8^{+}$ T-cells (0.1325±0.0197% EV, 0.1025±0.0206% F2) ; whereas F2 treated tumours had slightly elevated levels of activated $CD8^{+}$ T-cells (0.06±0.0058% EV, 0.265±0.0977% F2) (**Fig 4.9. C**). This activation of T-cells might possibly explain the differences in growth rates seen.

RNA was obtained from tumours to determine if TGFβ related genes such as SMAD7, CXCR4, PD-L1 were altered in mSDC2-F2-Fc expressing tumours (**Sect 2.2.1.7.**). We did not detect any impairment of TGFβ related upregulation of SMAD7 (0.998±0.0568); we did however detect significant reductions in genes of interest CXCR4 (0.7729±0.0282) and PD-L1 (0.6942±0.0594) which suggest a reduced immunosuppressive environment and supports our finding of $CD8^{+}$ T-cell activation (**Fig. 4.9. D).**

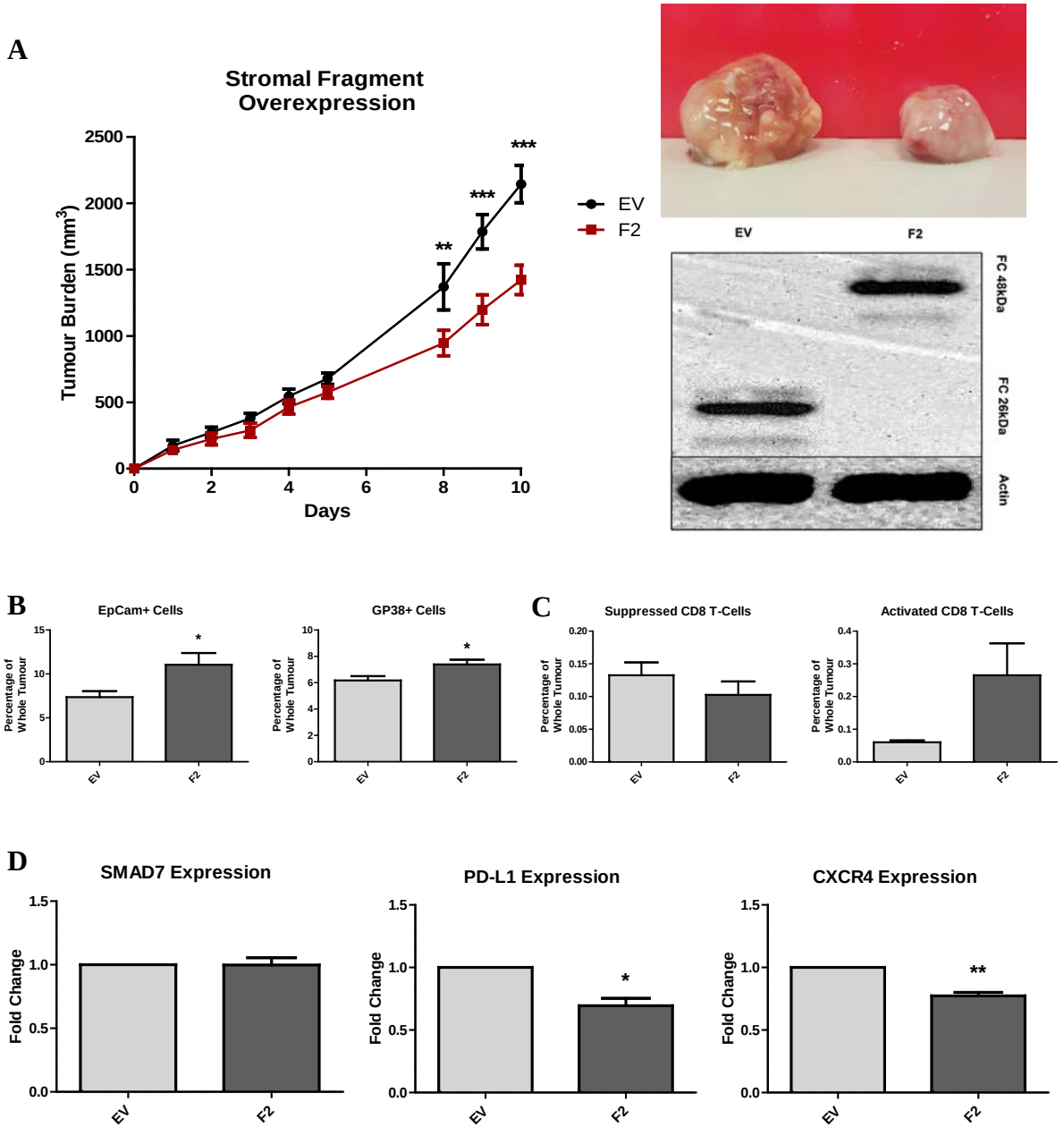

Figure 4.9. Tumour growth is inhibited by stromal overexpression of mSDC2-F2-Fc in an immune competent model of breast cancer. (**A**) Tumour growth kinetics show significantly reduced tumour growth in F2 treated tumours, with western blot showing expression of F2 pre-implantation, 2-way ANOVA with Bonferroni post-tests (**p≤0.01, ***p≤0.001, n=4). (**B**) Analysis of cell surface markers indicates non-significant increases in epithelial and stromal content in F2 treated tumours, unpaired t-test (*p≤0.05, n=4). (**C**) There is a trend seen in presence of suppressed and activated CD8+ T-cells between treatments (n=4). (**D**) RNA analysis of tumours indicates significant decreases in CXCR4 and PD-L1 RNA, 2-way ANOVA (*p≤0.05, **p≤0.01, n=4).

4.2.9. Stromal expression of SDC2 fragment 2 does not significantly affect metastases in an immune competent model.

As with previous studies, lungs were explanted (**Sect. 2.2.3.3**.), processed, H&E stained and scored (**Sect. 2.2.3.4**.) (**Fig. 4.10. A**). Analysis revealed a no significant difference in overall metastases score, however F2 treated tumours produced slightly lower grade metastases. (**Fig. 4.10. B**).

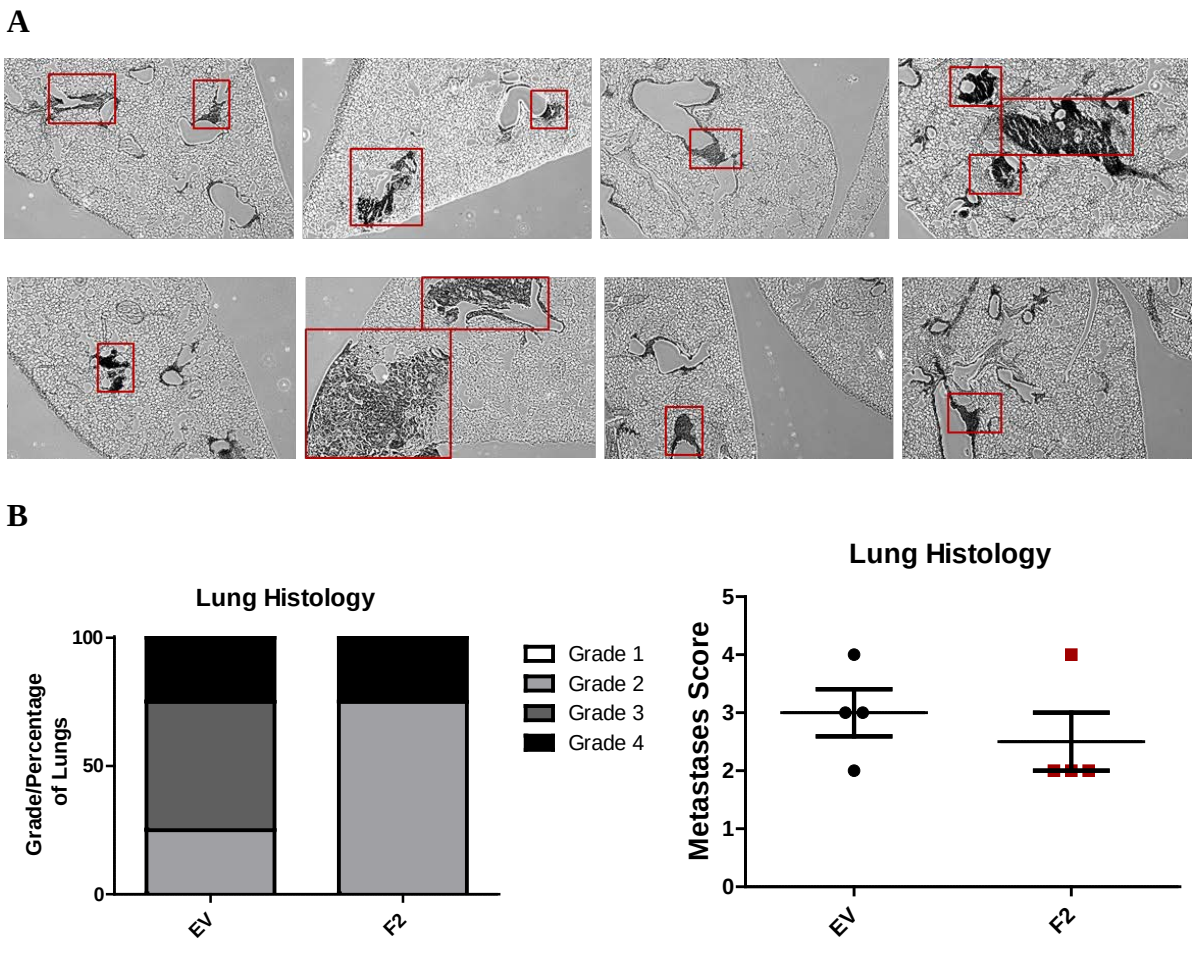

Figure 4.10. Metastases is not affected by stromal overexpression of SDC2 fragment 2 in an immune competent model. (A) Representative images of lung histology based on worst score all mice formed metastases. (**B**) Grading of lung histology reveals no significant differences in metastases (n=4).

4.3. DISCUSSION

In chapter 3 we highlighted some of the pathways by which SDC2 exhibits its tumourigenic properties. In this series of experiments we set out to test if SDC2 peptide therapeutics could act as inhibitors in these pathways. Preliminary work allowed identification of 2 candidate peptides for further study.

Initially we tested the anti-tumourigenic properties of SDC2 peptides in BCC and our data indicates SDC2-F1-Fc and SDC2-F2-Fc inhibit BCC migration, survival and TGFβ signalling. This result was determined through significant impairment of breast cancer cell migration and colony forming ability in BCC preconditioned with or overexpressing SDC2 peptides respectively (**Fig 4.2. A & C**). Furthermore both peptides significantly inhibited TGFβ mediated induction of the EMT gene CTGF [364] (**Fig. 4.3. B**), while significant reductions in EMT genes PAI-1 and SNAI1 were seen in BCC overexpressing SDC2-F2-Fc only [78, 365] (**Fig. 4.3. B**). Further work by the Dr Laura Barkley confirmed an interaction between SDC2 and TGFβR3 as shown by Chen *et al* [314] but has also shown that SDC2 fragments impaired this SDC2-TGFβR3 interaction. Thus confirming our hypothesis that SDC2 peptides could be blocking the TGFβ pathway by preventing full length SDC2 binding to TGFβR3.

Previous literature suggests administration of GST tagged full length SDC2 or the SDC2 adhesion regulatory domain alone can reduce angiogenesis [376]. Here we have shown that novel peptides containing the signal peptide and part of the ectodomain can illicit greater effects on BCC function, while being smaller in size and therefore easier to synthesise. This data indicated to us that inhibition of SDC2 with SDC2-F1-Fc and SDC2-F2-Fc peptides is a

viable strategy to recapitulate the effects seen with SDC2 knockdown on breast cancer carcinogenesis.

Whilst the anti-tumourigenic properties of SDC2 peptides have been reported before, a key goal of my research was to determine the effect of manipulating SDC2 within the stromal compartment of tumours. To explore this we began using human umbilical cord derived stromal cells overexpressing SDC2-F1-Fc and SDC2-F2-Fc and we saw little impact on TGFβ signalling, however, we detected strongly significant inhibition of CXCR4 gene expression, a gene we know to be involved in MSC homing and metastases [198] (**Fig 4.5. C**). Furthermore we detected a trend towards upregulation of CTGF in cells overexpressing fragments (**Fig 4.5. C**) indicating a more fibroblastic and immunogenic phenotype of these cells [379]. This theory was tested by PBMC co-culture assay and it was found that SDC2 peptides significantly reduce the immune-suppressive properties of these cells (**Fig 4.4. D**). However these stromal cells did not accurately recapitulate stromal cells found within the TME and therefore we developed a process to isolate patient-derived tumour stromal cells from breast tissue, and identified these to be stromal cells though surface marker profile and phenotype (**Fig 3.4. & 3.5.**). We began overexpressing SDC2-F1-Fc and SDC2-F2-Fc and subjecting these cells to our series of assays. Again we noted no significant differences in TGFβ signalling through SMAD7 gene expression, we did however detect significant impairment of TGFβ induction of CXCR4 (**Fig 4.4. B**). This result was novel as in previous data; knockdown of SDC2 in TSCs inhibited CXCR4 expression regardless of TGFβ stimulation (**Fig 3.8. B**) whereas this result implies peptide inhibition of upregulation in response to stimulus. We followed this finding up by assessment of migratory potential of TSCs overexpressing SDC2-F2-Fc only, due to a more significant reduction in CXCR4; it was found that indeed migrative ability was impaired (**Fig 4.4. C**). Finally the effects on $CD4^+$ T-cell suppression were assessed as with previous assays, it was found that SDC2-F1-

Fc displayed a slight but significant impairment of suppressive phenotype with SDC2-F2-Fc falling out of significance (**Fig 4.4. D**). It was at this point we hypothesised this impairment may be due to reductions in other immunomodulatory genes rather than just TGFβ as previously thought. Work was carried out by a Dr Laura Barkley to test the effects of SDC2 peptides on CTLA-4, PD-L1, PD-L2 and PGE2 and she showed an interaction with PD-L1 a marker well characterised for its role in carcinogenesis [206]. When we focused on this marker we found specifically SDC2-F2-Fc caused a reduction in PD-L1 protein levels in TSCs (**Fig 4.4. E**). The data from this series of experiments displayed evidence that SDC2 fragment 2 displays anti-migratory and anti-immune-suppressive functions through targeting both CXCR4 and PD-L1. There exists FDA approved therapies which successfully target these pathways for the treatment of cancer in the form of CXCR4 inhibitor AMD3100 and PD-L1 targeting antibodies such as atezolizumab and durvalumab [378, 380, 381]. To date no group has shown the effects of SDC2 based peptide therapeutics on stromal cells, our data suggests SDC2-F2-Fc may inhibit both the CXCR4 and PD-L1 pathways in stromal cells to elicit its effects, as such were confident to proceed to an *in vivo* model.

Using our xenograft model of breast cancer from chapter 3 began to assess the impact of overexpression of SDC2-F2-FC in the stromal compartment of these tumours. The results from the study showed similarities to the effects seen in Fig. 3.12, SDC2-F2-Fc significantly impaired growth rates at later stages of growth (**Fig 4.6. A**). We found trends towards reductions in mouse derived endothelia as well as human CXCR4 and PD-L1 surface expression (**Fig 4.6. B**). Interestingly we detected significant reductions in SMAD7 signalling in tumours overexpressing stromal F2 (**Fig 4.6. B**), our previous data showed SMAD7 signalling was not impaired in TSCs but there were trends towards reductions in MDA-MB-231s. This finding suggests secretion of SDC2 fragment 2 from stromal cells was enough to inhibit TGFβ signalling in MDA-MB-231s. A number of publication highlight the duality of

TGFβ signalling in cancer, it is suggested that it functions as a tumour suppressor in early tumourigenesis and a promoter at later stage [382, 383]. Perhaps the divergence in tumour growth at later stages that we detect in both SDC2 knockdown and fragment models is due in part to reduced TGFβ signalling at a point which this phenotypic switch occurs. This study also detected a significant reduction in CXCR4 gene expression (**Fig 4.6. B**) reinforcing our hypothesis that F2 blocks this migratory pathway. Previous work by Whiteford et al, administering GST tagged full length SDC2 displayed only decreases in angiogenesis in a HEK293T xenograft tumour model [376], here we have shown a similar decrease in endothelial cell infiltration, but also reductions in TGFβ signalling, and CXCR4 and PD-L1 expression in an orthotopic xenograft model of breast cancer.

When we analysed the lungs of mice from this study we did not see significant reductions in overall grade of metastases, we did however have a greater number of metastases free animals in F2 overexpressing tumours with 75% metastases free compared to 20% in EV control tumours **(Fig 4.7.)**. Literature suggests that blocking or inhibition of TGFβ, CXCR4 and PD-L1 with peptides inhibits cancer metastases in various cancer models [384-391]. Our data suggest SDC2-F2-Fc may indeed impair metastatic ability of breast cancer through these pathways; either repression of the CXCR4/CXCL12 homing pathway, inhibiting TSC migration; repression of PD-L1 inhibiting TSC immune-suppression and therefore survival; impairment of the TGFβ signalling in BCC affecting EMT. Regardless, the finding that SDC2 peptide therapeutics may inhibit metastases is a novel one in the field.

The final goal of this work was to test if our findings would hold true in a fully immune-competent model, using SDC2-F2-Fc due to its effects on PD-L1. This study represents the first time SDC2 has been therapeutically targeted in an immune-competent model of breast cancer in the field. We overexpressed mouse SDC2-F2-Fc in mouse TSCs, isolated from

PyMT breast tumours (**Fig 4.8.**). These were co-injected into the MFP of C57BL/6 with the mouse triple negative breast cancer line E0771. This final study was based heavily on preliminary data generated by Luke Watson from mouse SDC2-F2-Fc generation and sequencing, to E0771 tumour kinetics in C57BL/6 mice.

The growth kinetics from this study, as expected, far exceeded previous xenograft models, with tumours reaching terminal size in one third of the time 10 days vs 30 days. Despite the shortened window of study, we still detected a significant divergence in kinetics at later stages of tumourigenesis in SDC2-F2-Fc overexpressing tumours (**Fig 4.9. A**). We detected significant increases in proportion of EpCAM and GP38 expressing cells in F2 tumours, which we deduced to be due to the presence of a higher percentage of injected E0771 ($EpCAM^+$) and TSC ($GP38^+$) cells with less recruitment of other lineage cells possibly through reduced TGFβ signalling (**Fig 4.9. B**).

The use of an immune competent mouse allowed use of an immune staining panel and although analysis did not detect conclusive differences in lymphocyte levels, we detected a trend towards an increase of activated $CD8^+$ T-cells in F2 overexpressing tumours, paired with a trend towards decreased levels of suppressed $CD8^+$ T-cells (**Fig 4.9. C**). RNA analysis detected significantly reduced levels of PD-L1 gene expression (**Fig 4.9. D**) this result may be correlated with the increased levels of activated $CD8^+$ T-cells, perhaps somewhat explaining reductions in tumour growth.

Our investigation of RNA profile of these tumours highlighted a significantly reduced expression of the CXCR4 gene in F2 overexpressing tumours (**Fig. 4.9. D**). This result was in line with previous data in human cells; however analysis of lung histology revealed presence of metastases in every mouse (**Fig 4.10.**). There was a slight reduction in metastases severity in SDC2-F2-Fc treated tumours but it was not significant, implying repression of CXCR4

alone is not sufficient to reduce metastases in an immune competent model highlighting perhaps a need for a combinatorial therapeutic approach.

4.4. CONCLUSIONS

Taken together our findings suggest that therapeutic targeting of SDC2 with peptides to be effective at inhibiting TGFβ, CXCR4 and PD-L1 signalling in breast cancer. We have shown SDC2 peptides are capable of impairing triple negative breast cancer cell migration, clonogenicity and TGFβ induced EMT. We have shown that in stromal cells SDC2 peptides inhibit migration via CXCR4 and immune-suppression via PD-L1. This data has been thoroughly tested in xenograft and immune competent models manifesting in reduced tumour growth and altered metastatic properties. Our data suggests SDC2-F2-Fc as a prime candidate for combinational therapy, alone it is not sufficient for tumour regression but it sensitises key tumourigenic pathways. We hypothesise that combined with other therapies, be they cytotoxic or targeted, may be an effective strategy in reducing tumour burden in triple negative breast cancer.

CHAPTER 5

CONCLUDING REMARKS

& FUTURE PERSPECTIVES

5.1. CONCLUSIONS

The original aim set out in our Irish Research Council (IRC) PhD scholarship application was to identify the role of SDC2 in breast tumour carcinogenesis and test if SDC2 modulation within the breast tumour microenvironment affects breast tumour carcinogenesis. The working hypothesis was that stromal or epithelial blockade of SDC2 would inhibit tumour growth and metastases.

Our work has shown the role of SDC2 to be that of a significant contributor key tumourigenic pathways within the breast TME. We have highlighted that SDC2 may be a possible biomarker of triple negative breast cancer from patient serum sampling and that SDC2 is upregulated in cells isolated from both human and mouse breast cancers. Our data has shown that SDC2 knockdown in breast cancer epithelial cells inhibits TGFβ signalling, decreases migrative capacity and colony survival, this was then reflected in our peptide therapeutic strategy with SDC-F2-Fc. Literature suggests that blocking of TGFβ signalling with therapeutic inhibitors corresponds with decreases in breast cancer cell migration, survival, and EMT [392-394], thus validating our findings.

We have also shown evidence for the role of SDC2 in TGFβ signalling a well characterised pathway in the induction of the epithelial to mesenchymal transition of breast cancer. As well as decreased TGFβ signalling our data indicates SDC2 knockdown causes a decrease in endogenous fibronectin (FN1) and ZEB1 expression. It has been published that TGFβ

stimulation induces formation of a complex between PEAK1/ZEB1 in the presence of FN1, activating EMT. FN1 is a known molecular partner of SDC2, whereby SDC2 stabilises FN1 expression. Thus we hypothesis a role of SDC2 in this process, which may explain how SDC2 knockdown impairs TGFβ upregulation of both FN1 and ZEB1 [310, 347, 362, 363].

Together our data suggest that blocking of SDC2 within the epithelial compartment of breast cancer will result in reduction in tumour growth, metastases and EMT through impairment of TGFβ signalling.

Data from Orbsen Therapeutics highlighted SDC2 as a novel stromal marker which enables isolation of potent stromal cells from multiple tissues and species. Stromal cells in cancer usually comprise a very small percentage of the overall tumour mass but play pivotal roles in almost all carcinogenic pathways. They are known to secrete a number of key cytokines and chemokines which enable cancer proliferation, growth, survival, metastases and immune-suppression. Some of the most tumorigenic pathways in which stromal cells play a role are; activation of EMT, though secretion of TGFβ; T-cell suppression though PD-L1 expression and metastases though CXCR4/CXCL12 (**Fig. 5.1.**).

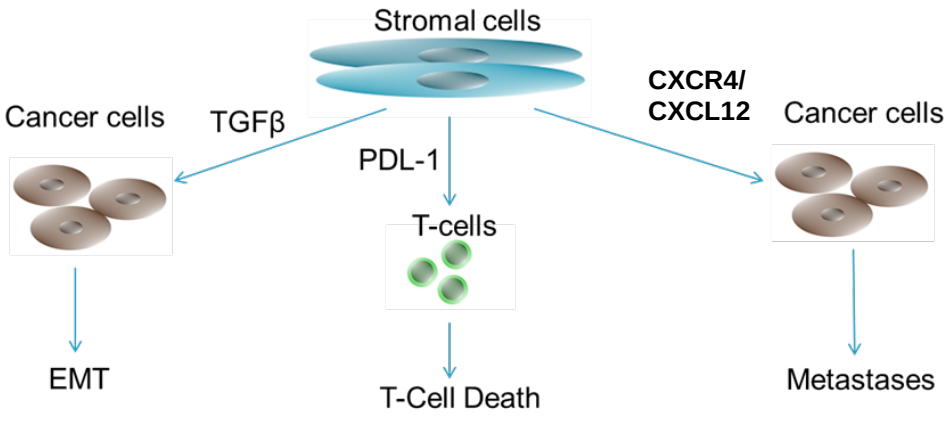

Figure 5.1. Stromal cells in cancer. Stromal cells secrete TGFβ which enhances EMT in cancer cells, PD-L1 expression inhibits T-cell mediated destruction of tumorous cells**,** CXCR4 expression enables translocation of cells towards sites of inflammation recruiting other cells to the tumour and encouraging metastases.

The literature suggests a role of SDC2 within the breast cancer epithelial compartment which our data set has reaffirmed. However there is very little published on the role of SDC2 in the stromal compartment of any cancer let alone breast cancer. Data from Orbsen Therapeutics suggest SDC2 is part of the anti-inflammatory cascade as it is upregulated on stromal cells in response to inflammatory cytokines and corticosteroids, therby increasing their capacity to suppress $CD4^+$ T-cells. Due to these findings and our preliminary data set, we focused our research on the roles of stromal specific SDC2 in breast carcinogenesis. Our SDC2 knockdown and peptide based inhibition studies have unravelled that stromal-derived SDC2 has unique pro-tumourigenic properties through two distinct mechanisms CXCR4/CXCL12 signalling, and T-cell suppression, however the mechanism by which adenoviral modulation and peptide targeting affects these pathways differ.

Our *in vitro* data show that SDC2 expression is upregulated in tumour derived stromal cells when compared to normal stroma and that it coincides with increased expression of the pro-migratory gene CXCR4. We have therefore hypothesised SDC2 and CXCR4 exist in a positive feedback loop. The literature suggests SDC2 co-localises with CXCR4 on the cell surface and its signalling, through its ligand CXCL12, increases MMP production, that in turn cleaves the ectodomain of SDC2 enabling SDC2 shedding. Shed heparin sulfate proteoglycans have been shown to not only stabilise CXCL12 but also mediate presentation to its receptor CXCR4 [358-361]. This hypothesis explains our findings as SDC2 knockdown decreases both endogenous CXCR4 levels and impairs the migratory capacity of stromal cells.

Furthermore we have shown that SDC2 overexpression increases the capacity of TSCs to suppress T-cells and conversely SDC2 knockdown diminished this capacity. This result is in line with the data produced by Dr Laura Deedigan at Orbsen Therapeutics, stimulating SDC2

with cytokines and corticosteroids. We hypothesise this result is due to the action of shed SDC2 on T-cell signalling. Literature suggests SDC2 induces T-cell receptor shedding in T-cells thereby suppressing their activation [366]. It would be interesting to test wether stimulation of normal MSC with BCC or TSCconditioned media would be sufficient to induce high levels of SDC2 and thereby increasing capacity to suppress $CD4^+$ T-cells.

We had originally envisaged creating a ubiquitous SDC2 knockout mouse to cross breed with the spontaneous tumour forming PyMT mouse to assess the effects of total SDC2 knockout on carcinogenesis. However it became apparent the closer we got to attaining a full SDC2 knockout mice that heterozygous knockdown of SDC2 imparted decreased fertility rates and litter size and that a full knockout was most likely embryonically lethal due the inability to attain pups of this genotype, but also the published roles of SDC2 in embryogenesis of zebrafish and xenopus [395-398]. This shifted our focus towards optimising our xenograft models.

The effects of TGFβ and CXCR4 inhibition held true *in vivo*, in our xenograft model of breast cancer, we detected impaired tumour growth when stroma lacked SDC2 expression and conversely stromal overexpression dependent enhancement of growth. We showed a correlation between CXCR4 and SDC2 expression and metastases. Likewise, SDC2 dependent changes in TGFβ signalling were observed. This confirmation of our hypotheses brought us to the conclusion that SDC2 is pro-oncogenic and a therapeutic target in the breast TME. A summary of our proposed mechanism of action can be seen in **Fig. 5.2**.

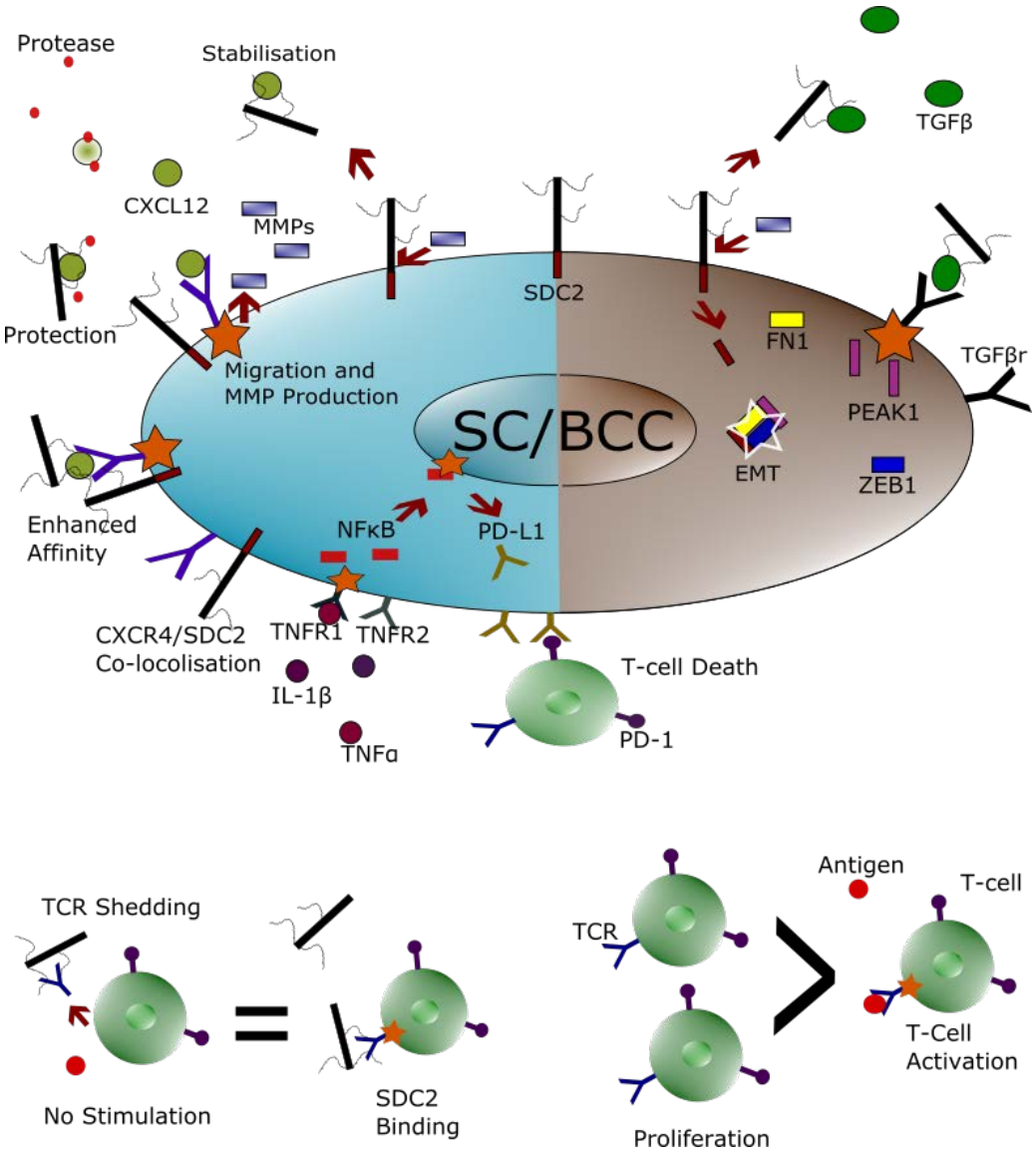

Figure 5.2. Hypothesised action of SDC2 modulation in stromal and breast cancer cells. Figure depicts the action of SDC2 enhancing TGFβ signalling and EMT through FN1/PEAK1/ZEB1 complex formation, enhancing CXCR4 signalling through co-localisation and increased affinity binding and finally immune-suppression through TCR receptor shedding.

We then showed that these pathways can be viably targeted with a SDC2 based therapeutic peptides *in vitro*, showing reduced migration, survival and TGFβ signalling of epithelial cells in a similar manner to SDC2 knockdown. We hypothesise this phenotype is manifested by competitive inhibition of full length SDC2 binding of TGFβ by SDC2 peptides (**Fig 4.11.**). Furthermore SDC2 peptides inhibit migration of stromal cells via CXCR4 similarly to SDC2

knockdown. This result indicates peptide inhibition of the proposed CXCR4/CXCL12/SDC2 feedback loop, perhaps allowing CXCL12 degradation, decreased binding affinity and thus CXCR4 gene repression.

A novel phenotype recognised with SDC2-F2-Fc was inhibition of endogenous PD-L1 protein. PD-L1 is upregulated in stromal cells in response to inflammatory stimuli and our preliminary data suggest SDC2-F1-Fc and SDC2-F2-Fc supress induction of NFκB when cells are stimulated with IL-1β and TNFα (**Fig 5.3**). We therefore hypothesise that SDC2 peptides competitively bind to and inhibit IL-1 β and TNFα, thereby reducing inflammatory activation and PD-L1 upregulation in stromal cells.

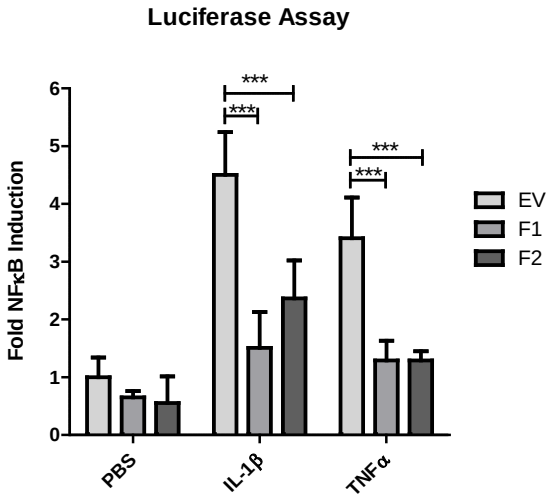

Figure 5.3. SDC2 fragments inhibit inflammatory mediated upregulation of NFκB. Both SDC2-F1-Fc and SDC2-F2-Fc significantly inhibit IL-1β and TNFα mediated upregulation of NFκB, 2-way ANOVA Bonferroni's multiple comparison post-test. Data courtesy of Dr Laura Barkley.

Finally we detected reductions in CXCR4 signalling in both of our *in vivo* models, with correlations to decreased metastatic ability. This was accompanied by reductions in SMAD7 gene expression in xenograft, and reductions in PD-L1 expression in our immune competent model, which correlated with a trend towards an increase in total activated T-cells. This data

confirms our hypothesis of SDC2-F2-Fc affecting CXCR4, TGFβ and PD-L1 signalling in breast cancer stroma. A summary of our hypothesised pathways are depicted in **Fig 5.4**.

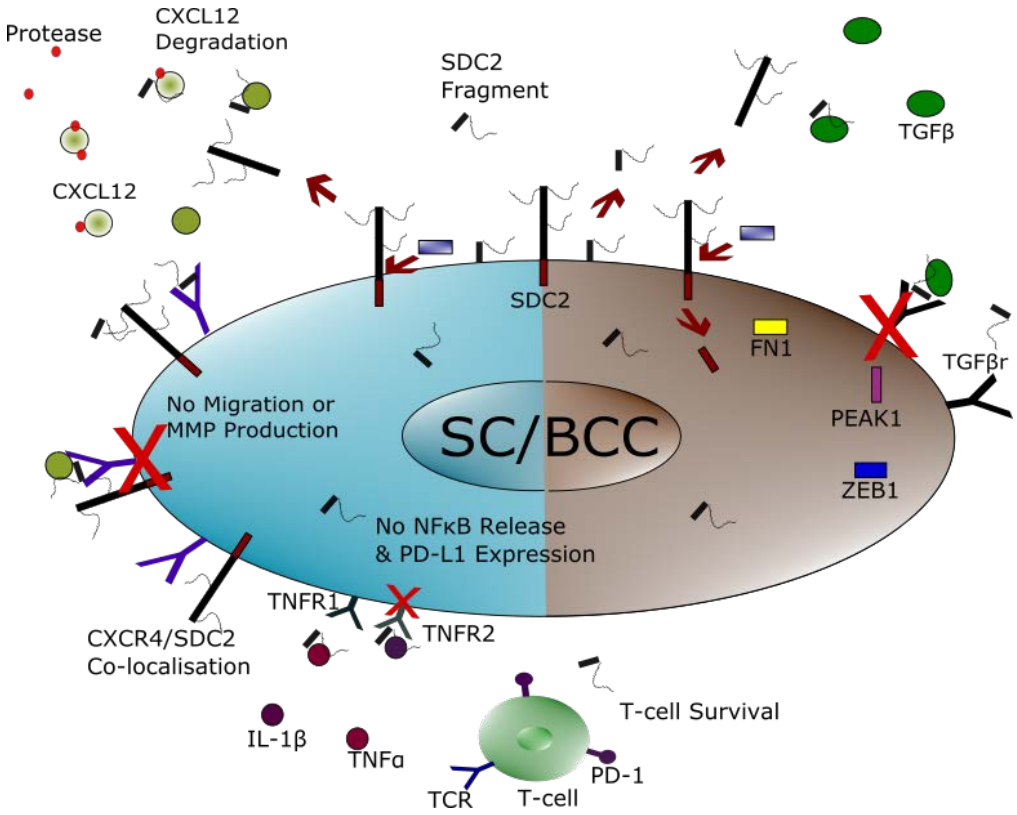

Figure 5.4. Hypothesised actions of SDC2 fragments in stromal and breast cancer cells. Figure depicts the action of SDC2 fragments inhibiting TGFβ signalling and therefore EMT induction, inhibiting CXCR4 signalling through competitively binding CXCL12 and CXCR4 and finally decreased PD-L1 production through interference in inflammatory stimulation.

Together our data clearly indicate a pro-oncogenic role of SDC2 in the TME of breast cancer. It can therefore be deduced that SDC2 modulation within the breast tumour microenvironment indeed affects breast tumour carcinogenesis. Finally that stromal or epithelial blockade of SDC2 inhibits tumour growth and metastases confirming our hypothesis.

5.2. FUTURE PERSPECTIVES

Here we have demonstrated in two models of breast cancer that inhibiting SDC2 function can inhibit tumour growth and metastases. We envisage therapeutic use of SDC2-F2-Fc to be part of a combinatorial therapy, many state of the art peptide inhibitors are being used in this manner such as the CXCR4 peptide inhibitor LY2510924 used in conjunction with idarubicin, and cytarabine [399]. The first step would be to perform a dose finding study of IP injected SDC2-F2-Fc peptide in our syngeneic orthotopic model, which would enable comparable growth kinetics. In order to accomplish this we would need to commercially synthesise at least 60mg of peptide, this would enable treatment of tumours upon palpation, twice a week with both 10 and 15mg/kg for 8 animals per group. Our data suggest that SDC2-F2-Fc peptide allows recruitment of activated T-cells and so we would suggest that SDC2-F2-Fc be administered in combination with CTLA-4 inhibitors which would increase its effectiveness. This series of experiments should produce substantial data and enable decisions on the future of this therapeutic approach.

Another line of enquiry could investigate the efficacy of SDC2 peptides F3-F12 in the treatment of breast cancer. Some preliminary work suggested peptide 8 inhibited the ability of stromal cells to block T-cell proliferation in a manner slightly exceeding SDC2-F2-Fc. SDC2-F8-Fc (19-87aa) is SDC2-F2-Fc (1-87aa) without the signal peptide of SDC2 therefore making it a smaller molecule, it remains to be determined if this would impart increased affinity to signal pathway interference.

Another strategy which could be employed is co-administration of F1 and F2; we know that F1 had a slightly greater impact on TSCs ability to suppress T-cell proliferation, perhaps a broad spectrum of SDC2 peptide sizes would prove to show more significant effects.

Finally Orbsen Therapeutics has shown that SDC2 is a novel marker for identification of a population of stromal cells which show high activity and potency and which are conserved across tissues and species. We have shown this marker to be upregulated in cancer stroma, there are few publications on the role of SDC2 in the stroma of cancers yet we have shown both its presence and its potency in this body of work. Therefore it could be deduced that other stroma heavy tumours such as prostate, pancreatic and colon cancers may also show upregulated SDC2 levels and therefore, SDC2 peptide inhibition may have positive effects in these tumours in the same manner to other rare stromal targets such as NG2 and FAP.

CHAPTER 6

BIBLIOGRAPHY

1. *Global, regional, and national incidence, prevalence, and years lived with disability for 328 diseases and injuries for 195 countries, 1990-2016: a systematic analysis for the Global Burden of Disease Study 2016.* Lancet, 2017. **390**(10100): p. 1211-1259.
2. Ferlay, J., et al., *Cancer incidence and mortality worldwide: sources, methods and major patterns in GLOBOCAN 2012.* Int J Cancer, 2015. **136**(5): p. E359-86.
3. Jemal, A., et al., *Global patterns of cancer incidence and mortality rates and trends.* Cancer Epidemiol Biomarkers Prev, 2010. **19**(8): p. 1893-907.
4. Althuis, M.D., et al., *Etiology of hormone receptor-defined breast cancer: a systematic review of the literature.* Cancer Epidemiol Biomarkers Prev, 2004. **13**(10): p. 1558-68.
5. Ma, H., et al., *Reproductive factors and breast cancer risk according to joint estrogen and progesterone receptor status: a meta-analysis of epidemiological studies.* Breast Cancer Res, 2006. **8**(4): p. R43.
6. Smith-Warner, S.A., et al., *Alcohol and breast cancer in women: a pooled analysis of cohort studies.* JAMA, 1998. **279**(7): p. 535-40.
7. Hamajima, N., et al., *Alcohol, tobacco and breast cancer--collaborative reanalysis of individual data from 53 epidemiological studies, including 58,515 women with breast cancer and 95,067 women without the disease.* Br J Cancer, 2002. **87**(11): p. 1234-45.
8. Lower, E.E., et al., *The effect of estrogen usage on the subsequent hormone receptor status of primary breast cancer.* Breast Cancer Res Treat, 1999. **58**(3): p. 205-11.
9. Gajdos, C., P.I. Tartter, and A. Babinszki, *Breast cancer diagnosed during hormone replacement therapy.* Obstet Gynecol, 2000. **95**(4): p. 513-8.
10. Li, C.I., et al., *Relationship between long durations and different regimens of hormone therapy and risk of breast cancer.* JAMA, 2003. **289**(24): p. 3254-63.
11. Hou, N., et al., *Hormone replacement therapy and breast cancer: heterogeneous risks by race, weight, and breast density.* J Natl Cancer Inst, 2013. **105**(18): p. 1365-72.
12. Eliassen, A.H., et al., *Adult weight change and risk of postmenopausal breast cancer.* JAMA, 2006. **296**(2): p. 193-201.
13. Key, T.J., et al., *Body mass index, serum sex hormones, and breast cancer risk in postmenopausal women.* J Natl Cancer Inst, 2003. **95**(16): p. 1218-26.
14. Kuchenbaecker, K.B., et al., *Risks of Breast, Ovarian, and Contralateral Breast Cancer for BRCA1 and BRCA2 Mutation Carriers.* JAMA, 2017. **317**(23): p. 2402-2416.
15. Tazaki, E., et al., *Histopathologcial and clonal study of combined lobular and ductal carcinoma of the breast.* Pathol Int, 2013. **63**(6): p. 297-304.
16. Wellings, S.R., H.M. Jensen, and R.G. Marcum, *An atlas of subgross pathology of the human breast with special reference to possible precancerous lesions.* J Natl Cancer Inst, 1975. **55**(2): p. 231-73.
17. Society, A.C., *Cancer facts & figures.* 2011.
18. Wagner, P.L., et al., *Clonal relationship between closely approximated low-grade ductal and lobular lesions in the breast: a molecular study of 10 cases.* Am J Clin Pathol, 2009. **132**(6): p. 871-6.
19. Harvard Health Publishing. *Breast Cancer*. 2014, ; Available from: https://www.health.harvard.edu/womens-health/breast-cancer.
20. Karakas, C., *Paget's disease of the breast.* J Carcinog, 2011. **10**: p. 31.
21. Breastcancer.org, *IDC Type: Medullary Carcinoma of the Breast.* 2017.

22. Dumitru, A., et al., *Mucinous Breast Cancer: a Review Study of 5 Year Experience from a Hospital-Based Series of Cases.* Maedica (Buchar), 2015. **10**(1): p. 14-8.
23. Sullivan, T., et al., *Tubular carcinoma of the breast: a retrospective analysis and review of the literature.* Breast Cancer Res Treat, 2005. **93**(3): p. 199-205.
24. van Uden, D.J., et al., *Inflammatory breast cancer: an overview.* Crit Rev Oncol Hematol, 2015. **93**(2): p. 116-26.
25. Hance, K.W., et al., *Trends in inflammatory breast carcinoma incidence and survival: the surveillance, epidemiology, and end results program at the National Cancer Institute.* J Natl Cancer Inst, 2005. **97**(13): p. 966-75.
26. Smoot, R.L., et al., *A single-center experience with inflammatory breast cancer, 1985-2003.* Arch Surg, 2006. **141**(6): p. 567-72; discussion 572-3.
27. Yang, W.T., et al., *Inflammatory breast cancer: PET/CT, MRI, mammography, and sonography findings.* Breast Cancer Res Treat, 2008. **109**(3): p. 417-26.
28. Perou, C.M., et al., *Molecular portraits of human breast tumours.* Nature, 2000. **406**(6797): p. 747-52.
29. Sorlie, T., et al., *Gene expression patterns of breast carcinomas distinguish tumor subclasses with clinical implications.* Proc Natl Acad Sci U S A, 2001. **98**(19): p. 10869-74.
30. Yersal, O. and S. Barutca, *Biological subtypes of breast cancer: Prognostic and therapeutic implications.* World J Clin Oncol, 2014. **5**(3): p. 412-24.
31. Sorlie, T., et al., *Repeated observation of breast tumor subtypes in independent gene expression data sets.* Proc Natl Acad Sci U S A, 2003. **100**(14): p. 8418-23.
32. Sorlie, T., *Molecular portraits of breast cancer: tumour subtypes as distinct disease entities.* Eur J Cancer, 2004. **40**(18): p. 2667-75.
33. Hashmi, A.A., et al., *Prognostic parameters of luminal A and luminal B intrinsic breast cancer subtypes of Pakistani patients.* World J Surg Oncol, 2018. **16**(1): p. 1.
34. Creighton, C.J., *The molecular profile of luminal B breast cancer.* Biologics, 2012. **6**: p. 289-97.
35. Slamon, D.J., et al., *Human breast cancer: correlation of relapse and survival with amplification of the HER-2/neu oncogene.* Science, 1987. **235**(4785): p. 177-82.
36. Kaptain, S., L.K. Tan, and B. Chen, *Her-2/neu and breast cancer.* Diagn Mol Pathol, 2001. **10**(3): p. 139-52.
37. Lal, P., L.K. Tan, and B. Chen, *Correlation of HER-2 status with estrogen and progesterone receptors and histologic features in 3,655 invasive breast carcinomas.* Am J Clin Pathol, 2005. **123**(4): p. 541-6.
38. Moll, R., et al., *The catalog of human cytokeratins: patterns of expression in normal epithelia, tumors and cultured cells.* Cell, 1982. **31**(1): p. 11-24.
39. Prat, A., et al., *Phenotypic and molecular characterization of the claudin-low intrinsic subtype of breast cancer.* Breast Cancer Res, 2010. **12**(5): p. R68.
40. Amin, M.B., et al., *The Eighth Edition AJCC Cancer Staging Manual: Continuing to build a bridge from a population-based to a more "personalized" approach to cancer staging.* CA Cancer J Clin, 2017. **67**(2): p. 93-99.
41. Peart, O., *Breast intervention and breast cancer treatment options.* Radiol Technol, 2015. **86**(5): p. 535M-558M; quiz 559-62.
42. Fowble, B.L., et al., *Role of postmastectomy radiation after neoadjuvant chemotherapy in stage II-III breast cancer.* Int J Radiat Oncol Biol Phys, 2012. **83**(2): p. 494-503.
43. Breastcancer.org, *What does prognosis mean?* 2017.
44. Henningsen, B., *Clinical experiences with tamoxifen for estrogen receptor blocking therapy in metastatic breast cancer.* Prog Clin Biol Res, 1977. **12**: p. 479-82.
45. *Aromatase inhibitors versus tamoxifen in early breast cancer: patient-level meta-analysis of the randomised trials.* Lancet, 2015. **386**(10001): p. 1341-1352.

46. Wakeling, A.E., M. Dukes, and J. Bowler, *A potent specific pure antiestrogen with clinical potential.* Cancer Res, 1991. **51**(15): p. 3867-73.
47. An, K.C., *Selective Estrogen Receptor Modulators.* Asian Spine J, 2016. **10**(4): p. 787-91.
48. Miller, W.R., *Aromatase inhibitors: mechanism of action and role in the treatment of breast cancer.* Semin Oncol, 2003. **30**(4 Suppl 14): p. 3-11.
49. Baselga, J., et al., *Everolimus in postmenopausal hormone-receptor-positive advanced breast cancer.* N Engl J Med, 2012. **366**(6): p. 520-9.
50. Shapiro, D., *How does estrogen induce proliferation of cancer cells?* 2017.
51. Hudziak, R.M., et al., *p185HER2 monoclonal antibody has antiproliferative effects in vitro and sensitizes human breast tumor cells to tumor necrosis factor.* Mol Cell Biol, 1989. **9**(3): p. 1165-72.
52. Fendly, B.M., et al., *Characterization of murine monoclonal antibodies reactive to either the human epidermal growth factor receptor or HER2/neu gene product.* Cancer Res, 1990. **50**(5): p. 1550-8.
53. Nielsen, D.L., M. Andersson, and C. Kamby, *HER2-targeted therapy in breast cancer. Monoclonal antibodies and tyrosine kinase inhibitors.* Cancer Treat Rev, 2009. **35**(2): p. 121-36.
54. Baselga, J., et al., *Pertuzumab plus trastuzumab plus docetaxel for metastatic breast cancer.* N Engl J Med, 2012. **366**(2): p. 109-19.
55. Nolting, M., T. Schneider-Merck, and M. Trepel, *Lapatinib.* Recent Results Cancer Res, 2014. **201**: p. 125-43.
56. Nahta, R., et al., *Insulin-like growth factor-I receptor/human epidermal growth factor receptor 2 heterodimerization contributes to trastuzumab resistance of breast cancer cells.* Cancer Res, 2005. **65**(23): p. 11118-28.
57. Jones, K.L. and A.U. Buzdar, *Evolving novel anti-HER2 strategies.* Lancet Oncol, 2009. **10**(12): p. 1179-87.
58. Malorni, L., et al., *Clinical and biologic features of triple-negative breast cancers in a large cohort of patients with long-term follow-up.* Breast Cancer Res Treat, 2012. **136**(3): p. 795-804.
59. Nguyen, P.L., et al., *Breast cancer subtype approximated by estrogen receptor, progesterone receptor, and HER-2 is associated with local and distant recurrence after breast-conserving therapy.* J Clin Oncol, 2008. **26**(14): p. 2373-8.
60. Bianchini, G., et al., *Triple-negative breast cancer: challenges and opportunities of a heterogeneous disease.* Nat Rev Clin Oncol, 2016. **13**(11): p. 674-690.
61. Lin, N.U., et al., *Sites of distant recurrence and clinical outcomes in patients with metastatic triple-negative breast cancer: high incidence of central nervous system metastases.* Cancer, 2008. **113**(10): p. 2638-45.
62. Balkwill, F.R., M. Capasso, and T. Hagemann, *The tumor microenvironment at a glance.* J Cell Sci, 2012. **125**(Pt 23): p. 5591-6.
63. Renfro, L.A., M.W. An, and S.J. Mandrekar, *Precision oncology: A new era of cancer clinical trials.* Cancer Lett, 2017. **387**: p. 121-126.
64. Mandrekar, S.J. and D.J. Sargent, *Clinical trial designs for predictive biomarker validation: theoretical considerations and practical challenges.* J Clin Oncol, 2009. **27**(24): p. 4027-34.
65. Korkaya, H., S. Liu, and M.S. Wicha, *Breast cancer stem cells, cytokine networks, and the tumor microenvironment.* J Clin Invest, 2011. **121**(10): p. 3804-9.
66. Morel, A.P., et al., *Generation of breast cancer stem cells through epithelial-mesenchymal transition.* PLoS One, 2008. **3**(8): p. e2888.
67. Neve, R.M., et al., *A collection of breast cancer cell lines for the study of functionally distinct cancer subtypes.* Cancer Cell, 2006. **10**(6): p. 515-27.
68. Jiang, Z., et al., *RB1 and p53 at the crossroad of EMT and triple-negative breast cancer.* Cell Cycle, 2011. **10**(10): p. 1563-70.

69. Derynck, R., R.J. Akhurst, and A. Balmain, *TGF-beta signaling in tumor suppression and cancer progression.* Nat Genet, 2001. **29**(2): p. 117-29.
70. Heldin, C.H., M. Landstrom, and A. Moustakas, *Mechanism of TGF-beta signaling to growth arrest, apoptosis, and epithelial-mesenchymal transition.* Curr Opin Cell Biol, 2009. **21**(2): p. 166-76.
71. de Caestecker, M.P., E. Piek, and A.B. Roberts, *Role of transforming growth factor-beta signaling in cancer.* J Natl Cancer Inst, 2000. **92**(17): p. 1388-402.
72. Valcourt, U., et al., *TGF-beta and the Smad signaling pathway support transcriptomic reprogramming during epithelial-mesenchymal cell transition.* Mol Biol Cell, 2005. **16**(4): p. 1987-2002.
73. Zavadil, J., et al., *Integration of TGF-beta/Smad and Jagged1/Notch signalling in epithelial-to-mesenchymal transition.* EMBO J, 2004. **23**(5): p. 1155-65.
74. Yamashita, M., et al., *TRAF6 mediates Smad-independent activation of JNK and p38 by TGF-beta.* Mol Cell, 2008. **31**(6): p. 918-24.
75. Bhowmick, N.A., et al., *Transforming growth factor-beta1 mediates epithelial to mesenchymal transdifferentiation through a RhoA-dependent mechanism.* Mol Biol Cell, 2001. **12**(1): p. 27-36.
76. Engel, M.E., P.K. Datta, and H.L. Moses, *RhoB is stabilized by transforming growth factor beta and antagonizes transcriptional activation.* J Biol Chem, 1998. **273**(16): p. 9921-6.
77. Sheen, Y.Y., et al., *Targeting the Transforming Growth Factor-beta Signaling in Cancer Therapy.* Biomol Ther (Seoul), 2013. **21**(5): p. 323-31.
78. Gavert, N. and A. Ben-Ze'ev, *Epithelial-mesenchymal transition and the invasive potential of tumors.* Trends Mol Med, 2008. **14**(5): p. 199-209.
79. Omori, K., et al., *Inhibition of Plasminogen Activator Inhibitor-1 Attenuates Transforming Growth Factor-beta-Dependent Epithelial Mesenchymal Transition and Differentiation of Fibroblasts to Myofibroblasts.* PLoS One, 2016. **11**(2): p. e0148969.
80. Kasai, H., et al., *TGF-beta1 induces human alveolar epithelial to mesenchymal cell transition (EMT).* Respir Res, 2005. **6**: p. 56.
81. Wang, Y. and B.P. Zhou, *Epithelial-mesenchymal transition in breast cancer progression and metastasis.* Chin J Cancer, 2011. **30**(9): p. 603-11.
82. Gorelik, L. and R.A. Flavell, *Immune-mediated eradication of tumors through the blockade of transforming growth factor-beta signaling in T cells.* Nat Med, 2001. **7**(10): p. 1118-22.
83. Yin, J.J., et al., *TGF-beta signaling blockade inhibits PTHrP secretion by breast cancer cells and bone metastases development.* J Clin Invest, 1999. **103**(2): p. 197-206.
84. Arteaga, C.L., et al., *Anti-transforming growth factor (TGF)-beta antibodies inhibit breast cancer cell tumorigenicity and increase mouse spleen natural killer cell activity. Implications for a possible role of tumor cell/host TGF-beta interactions in human breast cancer progression.* J Clin Invest, 1993. **92**(6): p. 2569-76.
85. Xie, W., et al., *Alterations of Smad signaling in human breast carcinoma are associated with poor outcome: a tissue microarray study.* Cancer Res, 2002. **62**(2): p. 497-505.
86. Huntley, S.P., et al., *Attenuated type II TGF-beta receptor signalling in human malignant oral keratinocytes induces a less differentiated and more aggressive phenotype that is associated with metastatic dissemination.* Int J Cancer, 2004. **110**(2): p. 170-6.
87. Morris, J.C., et al., *Phase I study of GC1008 (fresolimumab): a human anti-transforming growth factor-beta (TGFbeta) monoclonal antibody in patients with advanced malignant melanoma or renal cell carcinoma.* PLoS One, 2014. **9**(3): p. e90353.
88. Yingling, J.M., et al., *Preclinical assessment of galunisertib (LY2157299 monohydrate), a first-in-class transforming growth factor-beta receptor type I inhibitor.* Oncotarget, 2018. **9**(6): p. 6659-6677.
89. Hau, P., et al., *Inhibition of TGF-beta2 with AP 12009 in recurrent malignant gliomas: from preclinical to phase I/II studies.* Oligonucleotides, 2007. **17**(2): p. 201-12.

90. Nagaraj, N.S. and P.K. Datta, *Targeting the transforming growth factor-beta signaling pathway in human cancer.* Expert Opin Investig Drugs, 2010. **19**(1): p. 77-91.
91. Nemunaitis, J., et al., *Phase II study of belagenpumatucel-L, a transforming growth factor beta-2 antisense gene-modified allogeneic tumor cell vaccine in non-small-cell lung cancer.* J Clin Oncol, 2006. **24**(29): p. 4721-30.
92. Connolly, E.C., J. Freimuth, and R.J. Akhurst, *Complexities of TGF-beta targeted cancer therapy.* Int J Biol Sci, 2012. **8**(7): p. 964-78.
93. Smith, A.L., T.P. Robin, and H.L. Ford, *Molecular pathways: targeting the TGF-beta pathway for cancer therapy.* Clin Cancer Res, 2012. **18**(17): p. 4514-21.
94. Yu, L., et al., *Tumor necrosis factor alpha induces epithelial-mesenchymal transition and promotes metastasis via NF-kappaB signaling pathway-mediated TWIST expression in hypopharyngeal cancer.* Oncol Rep, 2014. **31**(1): p. 321-7.
95. Aggarwal, B.B., *Signalling pathways of the TNF superfamily: a double-edged sword.* Nat Rev Immunol, 2003. **3**(9): p. 745-56.
96. Freudlsperger, C., et al., *TGF-beta and NF-kappaB signal pathway cross-talk is mediated through TAK1 and SMAD7 in a subset of head and neck cancers.* Oncogene, 2013. **32**(12): p. 1549-59.
97. Chua, H.L., et al., *NF-kappaB represses E-cadherin expression and enhances epithelial to mesenchymal transition of mammary epithelial cells: potential involvement of ZEB-1 and ZEB-2.* Oncogene, 2007. **26**(5): p. 711-24.
98. Barbera, M.J., et al., *Regulation of Snail transcription during epithelial to mesenchymal transition of tumor cells.* Oncogene, 2004. **23**(44): p. 7345-54.
99. Sosic, D. and E.N. Olson, *A new twist on twist--modulation of the NF-kappa B pathway.* Cell Cycle, 2003. **2**(2): p. 76-8.
100. Brown, E.R., et al., *A clinical study assessing the tolerability and biological effects of infliximab, a TNF-alpha inhibitor, in patients with advanced cancer.* Ann Oncol, 2008. **19**(7): p. 1340-6.
101. Wu, C., et al., *Disrupting cytokine signaling in pancreatic cancer: a phase I/II study of etanercept in combination with gemcitabine in patients with advanced disease.* Pancreas, 2013. **42**(5): p. 813-8.
102. Staroslawska, E., et al., *Effect of infliximab on the levels of TNF-alpha and TGF-beta in the whole blood cultures of irradiated patients.* Folia Histochem Cytobiol, 2008. **46**(3): p. 291-7.
103. Timmerman, L.A., et al., *Notch promotes epithelial-mesenchymal transition during cardiac development and oncogenic transformation.* Genes Dev, 2004. **18**(1): p. 99-115.
104. Leong, K.G., et al., *Jagged1-mediated Notch activation induces epithelial-to-mesenchymal transition through Slug-induced repression of E-cadherin.* J Exp Med, 2007. **204**(12): p. 2935-48.
105. Smith, D.C., et al., *A phase I dose escalation and expansion study of the anticancer stem cell agent demcizumab (anti-DLL4) in patients with previously treated solid tumors.* Clin Cancer Res, 2014. **20**(24): p. 6295-303.
106. Cook, N., et al., *A phase I trial of the gamma-secretase inhibitor MK-0752 in combination with gemcitabine in patients with pancreatic ductal adenocarcinoma.* Br J Cancer, 2018. **118**(6): p. 793-801.
107. Chu, E.Y., et al., *Canonical WNT signaling promotes mammary placode development and is essential for initiation of mammary gland morphogenesis.* Development, 2004. **131**(19): p. 4819-29.
108. Bafico, A., et al., *An autocrine mechanism for constitutive Wnt pathway activation in human cancer cells.* Cancer Cell, 2004. **6**(5): p. 497-506.
109. Kemler, R., et al., *Stabilization of beta-catenin in the mouse zygote leads to premature epithelial-mesenchymal transition in the epiblast.* Development, 2004. **131**(23): p. 5817-24.

110. Zhou, B.P., et al., *Dual regulation of Snail by GSK-3beta-mediated phosphorylation in control of epithelial-mesenchymal transition.* Nat Cell Biol, 2004. **6**(10): p. 931-40.
111. Gurney, A., et al., *Wnt pathway inhibition via the targeting of Frizzled receptors results in decreased growth and tumorigenicity of human tumors.* Proc Natl Acad Sci U S A, 2012. **109**(29): p. 11717-22.
112. Jimeno, A., et al., *A First-in-Human Phase I Study of the Anticancer Stem Cell Agent Ipafricept (OMP-54F28), a Decoy Receptor for Wnt Ligands, in Patients with Advanced Solid Tumors.* Clin Cancer Res, 2017. **23**(24): p. 7490-7497.
113. Liu, J., et al., *Targeting Wnt-driven cancer through the inhibition of Porcupine by LGK974.* Proc Natl Acad Sci U S A, 2013. **110**(50): p. 20224-9.
114. Grotegut, S., et al., *Hepatocyte growth factor induces cell scattering through MAPK/Egr-1-mediated upregulation of Snail.* EMBO J, 2006. **25**(15): p. 3534-45.
115. Gotzmann, J., et al., *Hepatocytes convert to a fibroblastoid phenotype through the cooperation of TGF-beta1 and Ha-Ras: steps towards invasiveness.* J Cell Sci, 2002. **115**(Pt 6): p. 1189-202.
116. Janda, E., et al., *Ras and TGF[beta] cooperatively regulate epithelial cell plasticity and metastasis: dissection of Ras signaling pathways.* J Cell Biol, 2002. **156**(2): p. 299-313.
117. Bakin, A.V., et al., *p38 mitogen-activated protein kinase is required for TGFbeta-mediated fibroblastic transdifferentiation and cell migration.* J Cell Sci, 2002. **115**(Pt 15): p. 3193-206.
118. Druker, B.J., et al., *Effects of a selective inhibitor of the Abl tyrosine kinase on the growth of Bcr-Abl positive cells.* Nat Med, 1996. **2**(5): p. 561-6.
119. Presta, L.G., et al., *Humanization of an anti-vascular endothelial growth factor monoclonal antibody for the therapy of solid tumors and other disorders.* Cancer Res, 1997. **57**(20): p. 4593-9.
120. Blumenthal, G.M., et al., *FDA approval summary: sunitinib for the treatment of progressive well-differentiated locally advanced or metastatic pancreatic neuroendocrine tumors.* Oncologist, 2012. **17**(8): p. 1108-13.
121. Martelotto, L.G., et al., *Breast cancer intra-tumor heterogeneity.* Breast Cancer Res, 2014. **16**(3): p. 210.
122. Tlsty, T.D. and L.M. Coussens, *Tumor stroma and regulation of cancer development.* Annu Rev Pathol, 2006. **1**: p. 119-50.
123. Karnoub, A.E., et al., *Mesenchymal stem cells within tumour stroma promote breast cancer metastasis.* Nature, 2007. **449**(7162): p. 557-63.
124. Ren, G., et al., *CCR2-dependent recruitment of macrophages by tumor-educated mesenchymal stromal cells promotes tumor development and is mimicked by TNFalpha.* Cell Stem Cell, 2012. **11**(6): p. 812-24.
125. Brennen, W.N., et al., *Quantification of Mesenchymal Stem Cells (MSCs) at sites of human prostate cancer.* Oncotarget, 2013. **4**(1): p. 106-17.
126. Fox, J.M., et al., *Recent advances into the understanding of mesenchymal stem cell trafficking.* Br J Haematol, 2007. **137**(6): p. 491-502.
127. Nitzsche, F., et al., *Concise Review: MSC Adhesion Cascade-Insights into Homing and Transendothelial Migration.* Stem Cells, 2017. **35**(6): p. 1446-1460.
128. Dominici, M., et al., *Minimal criteria for defining multipotent mesenchymal stromal cells. The International Society for Cellular Therapy position statement.* Cytotherapy, 2006. **8**(4): p. 315-7.
129. Pittenger, M.F., et al., *Multilineage potential of adult human mesenchymal stem cells.* Science, 1999. **284**(5411): p. 143-7.
130. Di Nicola, M., et al., *Human bone marrow stromal cells suppress T-lymphocyte proliferation induced by cellular or nonspecific mitogenic stimuli.* Blood, 2002. **99**(10): p. 3838-43.
131. Corcione, A., et al., *Human mesenchymal stem cells modulate B-cell functions.* Blood, 2006. **107**(1): p. 367-72.

132. Dvorak, H.F., *Tumors: wounds that do not heal. Similarities between tumor stroma generation and wound healing.* N Engl J Med, 1986. **315**(26): p. 1650-9.
133. Uchibori, R., et al., *NF-kappaB activity regulates mesenchymal stem cell accumulation at tumor sites.* Cancer Res, 2013. **73**(1): p. 364-72.
134. Teo, G.S., et al., *Mesenchymal stem cells transmigrate between and directly through tumor necrosis factor-alpha-activated endothelial cells via both leukocyte-like and novel mechanisms.* Stem Cells, 2012. **30**(11): p. 2472-86.
135. Goldstein, R.H., et al., *Human bone marrow-derived MSCs can home to orthotopic breast cancer tumors and promote bone metastasis.* Cancer Res, 2010. **70**(24): p. 10044-50.
136. Gao, H., et al., *Activation of signal transducers and activators of transcription 3 and focal adhesion kinase by stromal cell-derived factor 1 is required for migration of human mesenchymal stem cells in response to tumor cell-conditioned medium.* Stem Cells, 2009. **27**(4): p. 857-65.
137. Ho, I.A., et al., *Matrix metalloproteinase 1 is necessary for the migration of human bone marrow-derived mesenchymal stem cells toward human glioma.* Stem Cells, 2009. **27**(6): p. 1366-75.
138. Hu, Y., et al., *Glioma cells promote the expression of vascular cell adhesion molecule-1 on bone marrow-derived mesenchymal stem cells: a possible mechanism for their tropism toward gliomas.* J Mol Neurosci, 2012. **48**(1): p. 127-35.
139. Paunescu, V., et al., *Tumour-associated fibroblasts and mesenchymal stem cells: more similarities than differences.* J Cell Mol Med, 2011. **15**(3): p. 635-46.
140. Kidd, S., et al., *Origins of the tumor microenvironment: quantitative assessment of adipose-derived and bone marrow-derived stroma.* PLoS One, 2012. **7**(2): p. e30563.
141. Muehlberg, F.L., et al., *Tissue-resident stem cells promote breast cancer growth and metastasis.* Carcinogenesis, 2009. **30**(4): p. 589-97.
142. Shinagawa, K., et al., *Mesenchymal stem cells enhance growth and metastasis of colon cancer.* Int J Cancer, 2010. **127**(10): p. 2323-33.
143. Prockop, D.J., C.A. Gregory, and J.L. Spees, *One strategy for cell and gene therapy: harnessing the power of adult stem cells to repair tissues.* Proc Natl Acad Sci U S A, 2003. **100 Suppl 1**: p. 11917-23.
144. Maishi, N. and K. Hida, *Tumor endothelial cells accelerate tumor metastasis.* Cancer Sci, 2017. **108**(10): p. 1921-1926.
145. Nagy, J.A., et al., *Why are tumour blood vessels abnormal and why is it important to know?* Br J Cancer, 2009. **100**(6): p. 865-9.
146. Trivanovic, D., et al., *The Roles of Mesenchymal Stromal/Stem Cells in Tumor Microenvironment Associated with Inflammation.* Mediators Inflamm, 2016. **2016**: p. 7314016.
147. Brune, J.C., et al., *Mesenchymal stromal cells from primary osteosarcoma are non-malignant and strikingly similar to their bone marrow counterparts.* Int J Cancer, 2011. **129**(2): p. 319-30.
148. Cao, H., et al., *Mesenchymal stem cell-like cells derived from human gastric cancer tissues.* Cancer Lett, 2009. **274**(1): p. 61-71.
149. Lin, J.T., et al., *Colon cancer mesenchymal stem cells modulate the tumorigenicity of colon cancer through interleukin 6.* Exp Cell Res, 2013. **319**(14): p. 2216-29.
150. Xu, X., et al., *Isolation and comparison of mesenchymal stem-like cells from human gastric cancer and adjacent non-cancerous tissues.* J Cancer Res Clin Oncol, 2011. **137**(3): p. 495-504.
151. Hernanda, P.Y., et al., *Tumor promotion through the mesenchymal stem cell compartment in human hepatocellular carcinoma.* Carcinogenesis, 2013. **34**(10): p. 2330-40.
152. Ramasamy, R., et al., *Mesenchymal stem cells inhibit proliferation and apoptosis of tumor cells: impact on in vivo tumor growth.* Leukemia, 2007. **21**(2): p. 304-10.

153. Lu, Y.R., et al., *The growth inhibitory effect of mesenchymal stem cells on tumor cells in vitro and in vivo.* Cancer Biol Ther, 2008. **7**(2): p. 245-51.
154. Sun, B., et al., *Therapeutic potential of mesenchymal stromal cells in a mouse breast cancer metastasis model.* Cytotherapy, 2009. **11**(3): p. 289-98, 1 p following 298.
155. Ho, I.A., et al., *Human bone marrow-derived mesenchymal stem cells suppress human glioma growth through inhibition of angiogenesis.* Stem Cells, 2013. **31**(1): p. 146-55.
156. Corcoran, K.E., et al., *Mesenchymal stem cells in early entry of breast cancer into bone marrow.* PLoS One, 2008. **3**(6): p. e2563.
157. Tsukamoto, S., et al., *Mesenchymal stem cells promote tumor engraftment and metastatic colonization in rat osteosarcoma model.* Int J Oncol, 2012. **40**(1): p. 163-9.
158. Martin, F.T., et al., *Potential role of mesenchymal stem cells (MSCs) in the breast tumour microenvironment: stimulation of epithelial to mesenchymal transition (EMT).* Breast Cancer Res Treat, 2010. **124**(2): p. 317-26.
159. Djouad, F., et al., *Immunosuppressive effect of mesenchymal stem cells favors tumor growth in allogeneic animals.* Blood, 2003. **102**(10): p. 3837-44.
160. Razmkhah, M., et al., *Adipose derived stem cells (ASCs) isolated from breast cancer tissue express IL-4, IL-10 and TGF-beta1 and upregulate expression of regulatory molecules on T cells: do they protect breast cancer cells from the immune response?* Cell Immunol, 2011. **266**(2): p. 116-22.
161. McLean, K., et al., *Human ovarian carcinoma-associated mesenchymal stem cells regulate cancer stem cells and tumorigenesis via altered BMP production.* J Clin Invest, 2011. **121**(8): p. 3206-19.
162. Studeny, M., et al., *Mesenchymal stem cells: potential precursors for tumor stroma and targeted-delivery vehicles for anticancer agents.* J Natl Cancer Inst, 2004. **96**(21): p. 1593-603.
163. Chen, X., et al., *A tumor-selective biotherapy with prolonged impact on established metastases based on cytokine gene-engineered MSCs.* Mol Ther, 2008. **16**(4): p. 749-56.
164. Grisendi, G., et al., *Adipose-derived mesenchymal stem cells as stable source of tumor necrosis factor-related apoptosis-inducing ligand delivery for cancer therapy.* Cancer Res, 2010. **70**(9): p. 3718-29.
165. Yang, B., et al., *Dual-targeted antitumor effects against brainstem glioma by intravenous delivery of tumor necrosis factor-related, apoptosis-inducing, ligand-engineered human mesenchymal stem cells.* Neurosurgery, 2009. **65**(3): p. 610-24; discussion 624.
166. Szegezdi, E., et al., *Stem cells are resistant to TRAIL receptor-mediated apoptosis.* J Cell Mol Med, 2009. **13**(11-12): p. 4409-14.
167. Layek, B., et al., *Nano-engineered mesenchymal stem cells increase therapeutic efficacy of anticancer drug through true active tumor targeting.* Mol Cancer Ther, 2018.
168. Cao, S., et al., *Nano-loaded human umbilical cord mesenchymal stem cells as targeted carriers of doxorubicin for breast cancer therapy.* Artif Cells Nanomed Biotechnol, 2018: p. 1-11.
169. Zhang, X., et al., *Exosomes in cancer: small particle, big player.* J Hematol Oncol, 2015. **8**: p. 83.
170. Yuan, Z., et al., *TRAIL delivery by MSC-derived extracellular vesicles is an effective anticancer therapy.* J Extracell Vesicles, 2017. **6**(1): p. 1265291.
171. Rivoltini, L., et al., *TNF-Related Apoptosis-Inducing Ligand (TRAIL)-Armed Exosomes Deliver Proapoptotic Signals to Tumor Site.* Clin Cancer Res, 2016. **22**(14): p. 3499-512.
172. O'Brien, K.P., et al., *Employing mesenchymal stem cells to support tumor-targeted delivery of extracellular vesicle (EV)-encapsulated microRNA-379.* Oncogene, 2018.
173. Roberts, E.W., et al., *Depletion of stromal cells expressing fibroblast activation protein-alpha from skeletal muscle and bone marrow results in cachexia and anemia.* J Exp Med, 2013. **210**(6): p. 1137-51.

174. Tlsty, T.D., *Stromal cells can contribute oncogenic signals.* Semin Cancer Biol, 2001. **11**(2): p. 97-104.
175. Gascard, P. and T.D. Tlsty, *Carcinoma-associated fibroblasts: orchestrating the composition of malignancy.* Genes Dev, 2016. **30**(9): p. 1002-19.
176. Santi, A., F.G. Kugeratski, and S. Zanivan, *Cancer Associated Fibroblasts: The Architects of Stroma Remodeling.* Proteomics, 2018. **18**(5-6): p. e1700167.
177. Spaeth, E.L., et al., *Mesenchymal stem cell transition to tumor-associated fibroblasts contributes to fibrovascular network expansion and tumor progression.* PLoS One, 2009. **4**(4): p. e4992.
178. Willis, B.C., R.M. duBois, and Z. Borok, *Epithelial origin of myofibroblasts during fibrosis in the lung.* Proc Am Thorac Soc, 2006. **3**(4): p. 377-82.
179. Ringuette Goulet, C., et al., *Exosomes Induce Fibroblast Differentiation into Cancer-Associated Fibroblasts through TGFbeta Signaling.* Mol Cancer Res, 2018. **16**(7): p. 1196-1204.
180. Calon, A., D.V. Tauriello, and E. Batlle, *TGF-beta in CAF-mediated tumor growth and metastasis.* Semin Cancer Biol, 2014. **25**: p. 15-22.
181. Pang, W., et al., *Pancreatic cancer-secreted miR-155 implicates in the conversion from normal fibroblasts to cancer-associated fibroblasts.* Cancer Sci, 2015. **106**(10): p. 1362-9.
182. Bauer, E.A., et al., *Enhanced collagenase production by fibroblasts derived from human basal cell carcinomas.* Cancer Res, 1979. **39**(11): p. 4594-9.
183. Knudson, W., C. Biswas, and B.P. Toole, *Interactions between human tumor cells and fibroblasts stimulate hyaluronate synthesis.* Proc Natl Acad Sci U S A, 1984. **81**(21): p. 6767-71.
184. Sappino, A.P., W. Schurch, and G. Gabbiani, *Differentiation repertoire of fibroblastic cells: expression of cytoskeletal proteins as marker of phenotypic modulations.* Lab Invest, 1990. **63**(2): p. 144-61.
185. van den Hooff, A., *Stromal involvement in malignant growth.* Adv Cancer Res, 1988. **50**: p. 159-96.
186. Dotto, G.P., R.A. Weinberg, and A. Ariza, *Malignant transformation of mouse primary keratinocytes by Harvey sarcoma virus and its modulation by surrounding normal cells.* Proc Natl Acad Sci U S A, 1988. **85**(17): p. 6389-93.
187. Lee, K. and C.M. Nelson, *New insights into the regulation of epithelial-mesenchymal transition and tissue fibrosis.* Int Rev Cell Mol Biol, 2012. **294**: p. 171-221.
188. Orimo, A., et al., *Stromal fibroblasts present in invasive human breast carcinomas promote tumor growth and angiogenesis through elevated SDF-1/CXCL12 secretion.* Cell, 2005. **121**(3): p. 335-48.
189. Wynn, R.F., et al., *A small proportion of mesenchymal stem cells strongly expresses functionally active CXCR4 receptor capable of promoting migration to bone marrow.* Blood, 2004. **104**(9): p. 2643-5.
190. Powell, D.W., et al., *Myofibroblasts. I. Paracrine cells important in health and disease.* Am J Physiol, 1999. **277**(1 Pt 1): p. C1-9.
191. Pinchuk, I.V., et al., *PD-1 ligand expression by human colonic myofibroblasts/fibroblasts regulates CD4+ T-cell activity.* Gastroenterology, 2008. **135**(4): p. 1228-1237, 1237 e1-2.
192. Brunen, D., et al., *TGF-beta: an emerging player in drug resistance.* Cell Cycle, 2013. **12**(18): p. 2960-8.
193. Erkan, M., et al., *The activated stroma index is a novel and independent prognostic marker in pancreatic ductal adenocarcinoma.* Clin Gastroenterol Hepatol, 2008. **6**(10): p. 1155-61.
194. Park, M.S., et al., *Perfusion CT: noninvasive surrogate marker for stratification of pancreatic cancer response to concurrent chemo- and radiation therapy.* Radiology, 2009. **250**(1): p. 110-7.

195. Costa, A., et al., *Fibroblast Heterogeneity and Immunosuppressive Environment in Human Breast Cancer.* Cancer Cell, 2018. **33**(3): p. 463-479 e10.
196. Kraman, M., et al., *Suppression of antitumor immunity by stromal cells expressing fibroblast activation protein-alpha.* Science, 2010. **330**(6005): p. 827-30.
197. Joyce, J.A. and D.T. Fearon, *T cell exclusion, immune privilege, and the tumor microenvironment.* Science, 2015. **348**(6230): p. 74-80.
198. Feig, C., et al., *Targeting CXCL12 from FAP-expressing carcinoma-associated fibroblasts synergizes with anti-PD-L1 immunotherapy in pancreatic cancer.* Proc Natl Acad Sci U S A, 2013. **110**(50): p. 20212-7.
199. Cooke, V.G., et al., *Pericyte depletion results in hypoxia-associated epithelial-to-mesenchymal transition and metastasis mediated by met signaling pathway.* Cancer Cell, 2012. **21**(1): p. 66-81.
200. Alvarez, R., et al., *Stromal disrupting effects of nab-paclitaxel in pancreatic cancer.* Br J Cancer, 2013. **109**(4): p. 926-33.
201. Lee, H.M., et al., *Drug repurposing screening identifies bortezomib and panobinostat as drugs targeting cancer associated fibroblasts (CAFs) by synergistic induction of apoptosis.* Invest New Drugs, 2018.
202. Takai, K., et al., *Targeting the cancer-associated fibroblasts as a treatment in triple-negative breast cancer.* Oncotarget, 2016. **7**(50): p. 82889-82901.
203. Fridman, W.H., et al., *The immune contexture in human tumours: impact on clinical outcome.* Nat Rev Cancer, 2012. **12**(4): p. 298-306.
204. Kaech, S.M. and W. Cui, *Transcriptional control of effector and memory CD8+ T cell differentiation.* Nat Rev Immunol, 2012. **12**(11): p. 749-61.
205. Hsieh, C.S., H.M. Lee, and C.W. Lio, *Selection of regulatory T cells in the thymus.* Nat Rev Immunol, 2012. **12**(3): p. 157-67.
206. Campbell, D.J. and M.A. Koch, *Treg cells: patrolling a dangerous neighborhood.* Nat Med, 2011. **17**(8): p. 929-30.
207. Romano, E., et al., *Ipilimumab-dependent cell-mediated cytotoxicity of regulatory T cells ex vivo by nonclassical monocytes in melanoma patients.* Proc Natl Acad Sci U S A, 2015. **112**(19): p. 6140-5.
208. Hellmann, M.D., et al., *Nivolumab plus Ipilimumab in Lung Cancer with a High Tumor Mutational Burden.* N Engl J Med, 2018. **378**(22): p. 2093-2104.
209. Uyttenhove, C., et al., *Evidence for a tumoral immune resistance mechanism based on tryptophan degradation by indoleamine 2,3-dioxygenase.* Nat Med, 2003. **9**(10): p. 1269-74.
210. Vig, M., et al., *Inducible nitric oxide synthase in T cells regulates T cell death and immune memory.* J Clin Invest, 2004. **113**(12): p. 1734-42.
211. Barnas, J.L., et al., *Reciprocal functional modulation of the activation of T lymphocytes and fibroblasts derived from human solid tumors.* J Immunol, 2010. **185**(5): p. 2681-92.
212. Gill, S. and C.H. June, *Going viral: chimeric antigen receptor T-cell therapy for hematological malignancies.* Immunol Rev, 2015. **263**(1): p. 68-89.
213. Davila, M.L., et al., *Efficacy and toxicity management of 19-28z CAR T cell therapy in B cell acute lymphoblastic leukemia.* Sci Transl Med, 2014. **6**(224): p. 224ra25.
214. Ramos, C.A., H.E. Heslop, and M.K. Brenner, *CAR-T Cell Therapy for Lymphoma.* Annu Rev Med, 2016. **67**: p. 165-83.
215. Yu, S., et al., *Chimeric antigen receptor T cells: a novel therapy for solid tumors.* J Hematol Oncol, 2017. **10**(1): p. 78.
216. Guedan, S., et al., *ICOS-based chimeric antigen receptors program bipolar TH17/TH1 cells.* Blood, 2014. **124**(7): p. 1070-80.
217. Song, D.G., et al., *CD27 costimulation augments the survival and antitumor activity of redirected human T cells in vivo.* Blood, 2012. **119**(3): p. 696-706.

218. Wang, L.C., et al., *Targeting fibroblast activation protein in tumor stroma with chimeric antigen receptor T cells can inhibit tumor growth and augment host immunity without severe toxicity.* Cancer Immunol Res, 2014. **2**(2): p. 154-66.
219. Dudley, M.E., et al., *Generation of tumor-infiltrating lymphocyte cultures for use in adoptive transfer therapy for melanoma patients.* J Immunother, 2003. **26**(4): p. 332-42.
220. Rosenberg, S.A., et al., *Durable complete responses in heavily pretreated patients with metastatic melanoma using T-cell transfer immunotherapy.* Clin Cancer Res, 2011. **17**(13): p. 4550-7.
221. Coronella, J.A., et al., *Evidence for an antigen-driven humoral immune response in medullary ductal breast cancer.* Cancer Res, 2001. **61**(21): p. 7889-99.
222. Mauri, C. and A. Bosma, *Immune regulatory function of B cells.* Annu Rev Immunol, 2012. **30**: p. 221-41.
223. Olkhanud, P.B., et al., *Tumor-evoked regulatory B cells promote breast cancer metastasis by converting resting CD4(+) T cells to T-regulatory cells.* Cancer Res, 2011. **71**(10): p. 3505-15.
224. Horikawa, M., et al., *Regulatory B cell production of IL-10 inhibits lymphoma depletion during CD20 immunotherapy in mice.* J Clin Invest, 2011. **121**(11): p. 4268-80.
225. Schioppa, T., et al., *B regulatory cells and the tumor-promoting actions of TNF-alpha during squamous carcinogenesis.* Proc Natl Acad Sci U S A, 2011. **108**(26): p. 10662-7.
226. Andreu, P., et al., *FcRgamma activation regulates inflammation-associated squamous carcinogenesis.* Cancer Cell, 2010. **17**(2): p. 121-34.
227. Guan, H., et al., *PD-L1 mediated the differentiation of tumor-infiltrating CD19(+) B lymphocytes and T cells in Invasive breast cancer.* Oncoimmunology, 2016. **5**(2): p. e1075112.
228. Franquesa, M., et al., *Immunomodulatory effect of mesenchymal stem cells on B cells.* Front Immunol, 2012. **3**: p. 212.
229. Peng, Y., et al., *Mesenchymal stromal cells infusions improve refractory chronic graft versus host disease through an increase of CD5+ regulatory B cells producing interleukin 10.* Leukemia, 2015. **29**(3): p. 636-46.
230. Voskoboinik, I., M.J. Smyth, and J.A. Trapani, *Perforin-mediated target-cell death and immune homeostasis.* Nat Rev Immunol, 2006. **6**(12): p. 940-52.
231. Tachibana, T., et al., *Increased intratumor Valpha24-positive natural killer T cells: a prognostic factor for primary colorectal carcinomas.* Clin Cancer Res, 2005. **11**(20): p. 7322-7.
232. Selmani, Z., et al., *Human leukocyte antigen-G5 secretion by human mesenchymal stem cells is required to suppress T lymphocyte and natural killer function and to induce CD4+CD25highFOXP3+ regulatory T cells.* Stem Cells, 2008. **26**(1): p. 212-22.
233. Vitale, M., et al., *Effect of tumor cells and tumor microenvironment on NK-cell function.* Eur J Immunol, 2014. **44**(6): p. 1582-92.
234. Krasnova, Y., et al., *Bench to bedside: NK cells and control of metastasis.* Clin Immunol, 2017. **177**: p. 50-59.
235. Curti, A., et al., *Successful transfer of alloreactive haploidentical KIR ligand-mismatched natural killer cells after infusion in elderly high risk acute myeloid leukemia patients.* Blood, 2011. **118**(12): p. 3273-9.
236. Rubnitz, J.E., et al., *NKAML: a pilot study to determine the safety and feasibility of haploidentical natural killer cell transplantation in childhood acute myeloid leukemia.* J Clin Oncol, 2010. **28**(6): p. 955-9.
237. Klingemann, H., *Are natural killer cells superior CAR drivers?* Oncoimmunology, 2014. **3**: p. e28147.
238. Glienke, W., et al., *Advantages and applications of CAR-expressing natural killer cells.* Front Pharmacol, 2015. **6**: p. 21.
239. Bingle, L., N.J. Brown, and C.E. Lewis, *The role of tumour-associated macrophages in tumour progression: implications for new anticancer therapies.* J Pathol, 2002. **196**(3): p. 254-65.

240. Mantovani, A. and P. Allavena, *The interaction of anticancer therapies with tumor-associated macrophages.* J Exp Med, 2015. **212**(4): p. 435-45.
241. Kumar, V., et al., *CD45 Phosphatase Inhibits STAT3 Transcription Factor Activity in Myeloid Cells and Promotes Tumor-Associated Macrophage Differentiation.* Immunity, 2016. **44**(2): p. 303-15.
242. Bronte, V., et al., *Recommendations for myeloid-derived suppressor cell nomenclature and characterization standards.* Nat Commun, 2016. **7**: p. 12150.
243. Noy, R. and J.W. Pollard, *Tumor-associated macrophages: from mechanisms to therapy.* Immunity, 2014. **41**(1): p. 49-61.
244. Pyonteck, S.M., et al., *CSF-1R inhibition alters macrophage polarization and blocks glioma progression.* Nat Med, 2013. **19**(10): p. 1264-72.
245. Henze, A.T. and M. Mazzone, *The impact of hypoxia on tumor-associated macrophages.* J Clin Invest, 2016. **126**(10): p. 3672-3679.
246. Francois, M., et al., *Human MSC suppression correlates with cytokine induction of indoleamine 2,3-dioxygenase and bystander M2 macrophage differentiation.* Mol Ther, 2012. **20**(1): p. 187-95.
247. Kuen, J., et al., *Pancreatic cancer cell/fibroblast co-culture induces M2 like macrophages that influence therapeutic response in a 3D model.* PLoS One, 2017. **12**(7): p. e0182039.
248. Butowski, N., et al., *Orally administered colony stimulating factor 1 receptor inhibitor PLX3397 in recurrent glioblastoma: an Ivy Foundation Early Phase Clinical Trials Consortium phase II study.* Neuro Oncol, 2016. **18**(4): p. 557-64.
249. Cassier, P.A., et al., *CSF1R inhibition with emactuzumab in locally advanced diffuse-type tenosynovial giant cell tumours of the soft tissue: a dose-escalation and dose-expansion phase 1 study.* Lancet Oncol, 2015. **16**(8): p. 949-56.
250. Noman, M.Z., et al., *PD-L1 is a novel direct target of HIF-1alpha, and its blockade under hypoxia enhanced MDSC-mediated T cell activation.* J Exp Med, 2014. **211**(5): p. 781-90.
251. Fridlender, Z.G., et al., *Polarization of tumor-associated neutrophil phenotype by TGF-beta: "N1" versus "N2" TAN.* Cancer Cell, 2009. **16**(3): p. 183-94.
252. Zou, J.M., et al., *IL-35 induces N2 phenotype of neutrophils to promote tumor growth.* Oncotarget, 2017. **8**(20): p. 33501-33514.
253. Spiegel, A., et al., *Neutrophils Suppress Intraluminal NK Cell-Mediated Tumor Cell Clearance and Enhance Extravasation of Disseminated Carcinoma Cells.* Cancer Discov, 2016. **6**(6): p. 630-49.
254. Zhang, J., et al., *Circulating tumor-associated neutrophils (cTAN) contribute to circulating tumor cell survival by suppressing peripheral leukocyte activation.* Tumour Biol, 2016. **37**(4): p. 5397-404.
255. Jamieson, T., et al., *Inhibition of CXCR2 profoundly suppresses inflammation-driven and spontaneous tumorigenesis.* J Clin Invest, 2012. **122**(9): p. 3127-44.
256. Gabrilovich, D.I., S. Ostrand-Rosenberg, and V. Bronte, *Coordinated regulation of myeloid cells by tumours.* Nat Rev Immunol, 2012. **12**(4): p. 253-68.
257. Chomarat, P., et al., *IL-6 switches the differentiation of monocytes from dendritic cells to macrophages.* Nat Immunol, 2000. **1**(6): p. 510-4.
258. Steinman, R.M., D. Hawiger, and M.C. Nussenzweig, *Tolerogenic dendritic cells.* Annu Rev Immunol, 2003. **21**: p. 685-711.
259. Steinbrink, K., et al., *Induction of tolerance by IL-10-treated dendritic cells.* J Immunol, 1997. **159**(10): p. 4772-80.
260. Spaggiari, G.M., et al., *MSCs inhibit monocyte-derived DC maturation and function by selectively interfering with the generation of immature DCs: central role of MSC-derived prostaglandin E2.* Blood, 2009. **113**(26): p. 6576-83.
261. Najar, M., et al., *Mesenchymal stromal cells and immunomodulation: A gathering of regulatory immune cells.* Cytotherapy, 2016. **18**(2): p. 160-71.

262. Carmeliet, P. and R.K. Jain, *Molecular mechanisms and clinical applications of angiogenesis.* Nature, 2011. **473**(7347): p. 298-307.
263. Folkman, J. and D. Hanahan, *Switch to the angiogenic phenotype during tumorigenesis.* Princess Takamatsu Symp, 1991. **22**: p. 339-47.
264. De Wever, O. and M. Mareel, *Role of tissue stroma in cancer cell invasion.* J Pathol, 2003. **200**(4): p. 429-47.
265. Weis, S.M. and D.A. Cheresh, *Pathophysiological consequences of VEGF-induced vascular permeability.* Nature, 2005. **437**(7058): p. 497-504.
266. Hellberg, C., A. Ostman, and C.H. Heldin, *PDGF and vessel maturation.* Recent Results Cancer Res, 2010. **180**: p. 103-14.
267. Chung, A.S., J. Lee, and N. Ferrara, *Targeting the tumour vasculature: insights from physiological angiogenesis.* Nat Rev Cancer, 2010. **10**(7): p. 505-14.
268. Pinto, M.P., et al., *Malignant stroma increases luminal breast cancer cell proliferation and angiogenesis through platelet-derived growth factor signaling.* BMC Cancer, 2014. **14**: p. 735.
269. Naba, A., et al., *The matrisome: in silico definition and in vivo characterization by proteomics of normal and tumor extracellular matrices.* Mol Cell Proteomics, 2012. **11**(4): p. M111 014647.
270. Frantz, C., K.M. Stewart, and V.M. Weaver, *The extracellular matrix at a glance.* J Cell Sci, 2010. **123**(Pt 24): p. 4195-200.
271. Wirtz, D., K. Konstantopoulos, and P.C. Searson, *The physics of cancer: the role of physical interactions and mechanical forces in metastasis.* Nat Rev Cancer, 2011. **11**(7): p. 512-22.
272. Mao, Y., et al., *Stromal cells in tumor microenvironment and breast cancer.* Cancer Metastasis Rev, 2013. **32**(1-2): p. 303-15.
273. van der Rest, M. and R. Garrone, *Collagen family of proteins.* FASEB J, 1991. **5**(13): p. 2814-23.
274. Kauppila, S., et al., *Aberrant type I and type III collagen gene expression in human breast cancer in vivo.* J Pathol, 1998. **186**(3): p. 262-8.
275. Trastour, C., et al., *HIF-1alpha and CA IX staining in invasive breast carcinomas: prognosis and treatment outcome.* Int J Cancer, 2007. **120**(7): p. 1451-8.
276. Halberg, N., et al., *Hypoxia-inducible factor 1alpha induces fibrosis and insulin resistance in white adipose tissue.* Mol Cell Biol, 2009. **29**(16): p. 4467-83.
277. Higgins, D.F., et al., *Hypoxia promotes fibrogenesis in vivo via HIF-1 stimulation of epithelial-to-mesenchymal transition.* J Clin Invest, 2007. **117**(12): p. 3810-20.
278. Gilkes, D.M., et al., *Hypoxia-inducible factor 1 (HIF-1) promotes extracellular matrix remodeling under hypoxic conditions by inducing P4HA1, P4HA2, and PLOD2 expression in fibroblasts.* J Biol Chem, 2013. **288**(15): p. 10819-29.
279. Schietke, R., et al., *The lysyl oxidases LOX and LOXL2 are necessary and sufficient to repress E-cadherin in hypoxia: insights into cellular transformation processes mediated by HIF-1.* J Biol Chem, 2010. **285**(9): p. 6658-69.
280. Wong, C.C., et al., *Hypoxia-inducible factor 1 is a master regulator of breast cancer metastatic niche formation.* Proc Natl Acad Sci U S A, 2011. **108**(39): p. 16369-74.
281. Gilkes, D.M., et al., *Hypoxia-inducible factors mediate coordinated RhoA-ROCK1 expression and signaling in breast cancer cells.* Proc Natl Acad Sci U S A, 2014. **111**(3): p. E384-93.
282. Zhang, H., et al., *HIF-1-dependent expression of angiopoietin-like 4 and L1CAM mediates vascular metastasis of hypoxic breast cancer cells to the lungs.* Oncogene, 2012. **31**(14): p. 1757-70.
283. Couchman, J.R. and C.A. Pataki, *An introduction to proteoglycans and their localization.* J Histochem Cytochem, 2012. **60**(12): p. 885-97.
284. Esko, J.D., K. Kimata, and U. Lindahl, *Proteoglycans and Sulfated Glycosaminoglycans*, in *Essentials of Glycobiology*, nd, et al., Editors. 2009: Cold Spring Harbor (NY).

285. Pomin, V.H. and B. Mulloy, *Glycosaminoglycans and Proteoglycans.* Pharmaceuticals (Basel), 2018. **11**(1).
286. Nugent, M.A., J. Zaia, and J.L. Spencer, *Heparan sulfate-protein binding specificity.* Biochemistry (Mosc), 2013. **78**(7): p. 726-35.
287. Kim, S.H., J. Turnbull, and S. Guimond, *Extracellular matrix and cell signalling: the dynamic cooperation of integrin, proteoglycan and growth factor receptor.* J Endocrinol, 2011. **209**(2): p. 139-51.
288. Lindahl, U. and L. Kjellen, *Pathophysiology of heparan sulphate: many diseases, few drugs.* J Intern Med, 2013. **273**(6): p. 555-71.
289. Raman, K. and B. Kuberan, *Chemical Tumor Biology of Heparan Sulfate Proteoglycans.* Curr Chem Biol, 2010. **4**(1): p. 20-31.
290. Choi, S., et al., *Shed syndecan-2 enhances tumorigenic activities of colon cancer cells.* Oncotarget, 2015. **6**(6): p. 3874-86.
291. Theocharis, A.D. and N.K. Karamanos, *Proteoglycans remodeling in cancer: Underlying molecular mechanisms.* Matrix Biol, 2017.
292. Park, P.W., *Isolation and functional analysis of syndecans.* Methods Cell Biol, 2018. **143**: p. 317-333.
293. Pap, T. and J. Bertrand, *Syndecans in cartilage breakdown and synovial inflammation.* Nat Rev Rheumatol, 2013. **9**(1): p. 43-55.
294. Saunders, S., et al., *Molecular cloning of syndecan, an integral membrane proteoglycan.* J Cell Biol, 1989. **108**(4): p. 1547-56.
295. Kato, M., et al., *Loss of cell surface syndecan-1 causes epithelia to transform into anchorage-independent mesenchyme-like cells.* Mol Biol Cell, 1995. **6**(5): p. 559-76.
296. Sun, D., et al., *Simultaneous loss of expression of syndecan-1 and E-cadherin in the embryonic palate during epithelial-mesenchymal transformation.* Int J Dev Biol, 1998. **42**(5): p. 733-6.
297. Poblete, C.E., et al., *Increased SNAIL expression and low syndecan levels are associated with high Gleason grade in prostate cancer.* Int J Oncol, 2014. **44**(3): p. 647-54.
298. Bayer-Garner, I.B. and B.R. Smoller, *The expression of syndecan-1 is preferentially reduced compared with that of E-cadherin in acantholytic squamous cell carcinoma.* J Cutan Pathol, 2001. **28**(2): p. 83-9.
299. Day, R.M., et al., *Changes in the expression of syndecan-1 in the colorectal adenoma-carcinoma sequence.* Virchows Arch, 1999. **434**(2): p. 121-5.
300. Contreras, H.R., et al., *The expression of syndecan-1 and -2 is associated with Gleason score and epithelial-mesenchymal transition markers, E-cadherin and beta-catenin, in prostate cancer.* Urol Oncol, 2010. **28**(5): p. 534-40.
301. Matsuda, K., et al., *Glypican-1 is overexpressed in human breast cancer and modulates the mitogenic effects of multiple heparin-binding growth factors in breast cancer cells.* Cancer Res, 2001. **61**(14): p. 5562-9.
302. Lendorf, M.E., et al., *Syndecan-1 and syndecan-4 are independent indicators in breast carcinoma.* J Histochem Cytochem, 2011. **59**(6): p. 615-29.
303. Loussouarn, D., et al., *Prognostic impact of syndecan-1 expression in invasive ductal breast carcinomas.* Br J Cancer, 2008. **98**(12): p. 1993-8.
304. Oh, E.S. and J.R. Couchman, *Syndecans-2 and -4; close cousins, but not identical twins.* Mol Cells, 2004. **17**(2): p. 181-7.
305. Roskams, T., et al., *Heparan sulfate proteoglycan expression in normal human liver.* Hepatology, 1995. **21**(4): p. 950-8.
306. David, G., et al., *Spatial and temporal changes in the expression of fibroglycan (syndecan-2) during mouse embryonic development.* Development, 1993. **119**(3): p. 841-54.
307. Mansouri, R., et al., *Role of syndecan-2 in osteoblast biology and pathology.* Bonekey Rep, 2015. **4**: p. 666.

308. Grootjans, J.J., et al., *Syntenin, a PDZ protein that binds syndecan cytoplasmic domains.* Proc Natl Acad Sci U S A, 1997. **94**(25): p. 13683-8.
309. Essner, J.J., E. Chen, and S.C. Ekker, *Syndecan-2.* Int J Biochem Cell Biol, 2006. **38**(2): p. 152-6.
310. Kwon, M.J., et al., *The extracellular domain of syndecan-2 regulates the interaction of HCT116 human colon carcinoma cells with fibronectin.* Biochem Biophys Res Commun, 2013. **431**(3): p. 415-20.
311. Mytilinaiou, M., et al., *Emerging roles of syndecan 2 in epithelial and mesenchymal cancer progression.* IUBMB Life, 2017. **69**(11): p. 824-833.
312. Hu, H.T., et al., *The Involvement of Neuron-Specific Factors in Dendritic Spinogenesis: Molecular Regulation and Association with Neurological Disorders.* Neural Plast, 2016. **2016**: p. 5136286.
313. Do, M.K., et al., *Transmembrane proteoglycans syndecan-2, 4, receptor candidates for the impact of HGF and FGF2 on semaphorin 3A expression in early-differentiated myoblasts.* Physiol Rep, 2015. **3**(9).
314. Chen, L., C. Klass, and A. Woods, *Syndecan-2 regulates transforming growth factor-beta signaling.* J Biol Chem, 2004. **279**(16): p. 15715-8.
315. Cevikbas, F., et al., *Unilateral nephrectomy leads to up-regulation of syndecan-2- and TGF-beta-mediated glomerulosclerosis in syndecan-4 deficient male mice.* Matrix Biol, 2008. **27**(1): p. 42-52.
316. Shi, Y., et al., *Syndecan-2 exerts antifibrotic effects by promoting caveolin-1-mediated transforming growth factor-beta receptor I internalization and inhibiting transforming growth factor-beta1 signaling.* Am J Respir Crit Care Med, 2013. **188**(7): p. 831-41.
317. Mytilinaiou, M., et al., *Syndecan-2 is a key regulator of transforming growth factor beta 2/Smad2-mediated adhesion in fibrosarcoma cells.* IUBMB Life, 2013. **65**(2): p. 134-43.
318. Worapamorn, W., et al., *Cytokine regulation of syndecan-1 and -2 gene expression in human periodontal fibroblasts and osteoblasts.* J Periodontal Res, 2002. **37**(4): p. 273-8.
319. Fears, C.Y., C.L. Gladson, and A. Woods, *Syndecan-2 is expressed in the microvasculature of gliomas and regulates angiogenic processes in microvascular endothelial cells.* J Biol Chem, 2006. **281**(21): p. 14533-6.
320. Granes, F., et al., *Identification of a novel Ezrin-binding site in syndecan-2 cytoplasmic domain.* FEBS Lett, 2003. **547**(1-3): p. 212-6.
321. Yu, H., et al., *The FERM family proteins in cancer invasion and metastasis.* Front Biosci (Landmark Ed), 2011. **16**: p. 1536-50.
322. Granes, F., et al., *Ezrin links syndecan-2 to the cytoskeleton.* J Cell Sci, 2000. **113 (Pt 7)**: p. 1267-76.
323. Granes, F., et al., *Syndecan-2 induces filopodia by active cdc42Hs.* Exp Cell Res, 1999. **248**(2): p. 439-56.
324. Lee, H., et al., *Syndecan-2 cytoplasmic domain regulates colon cancer cell migration via interaction with syntenin-1.* Biochem Biophys Res Commun, 2011. **409**(1): p. 148-53.
325. Whiteford, J.R., et al., *Syndecans promote integrin-mediated adhesion of mesenchymal cells in two distinct pathways.* Exp Cell Res, 2007. **313**(18): p. 3902-13.
326. Noguer, O., et al., *Syndecan-2 downregulation impairs angiogenesis in human microvascular endothelial cells.* Exp Cell Res, 2009. **315**(5): p. 795-808.
327. Lim, H.C. and J.R. Couchman, *Syndecan-2 regulation of morphology in breast carcinoma cells is dependent on RhoGTPases.* Biochim Biophys Acta, 2014. **1840**(8): p. 2482-90.
328. De Oliveira, T., et al., *Syndecan-2 promotes perineural invasion and cooperates with K-ras to induce an invasive pancreatic cancer cell phenotype.* Mol Cancer, 2012. **11**: p. 19.
329. Soares, M.A., et al., *Heparan Sulfate Proteoglycans May Promote or Inhibit Cancer Progression by Interacting with Integrins and Affecting Cell Migration.* Biomed Res Int, 2015. **2015**: p. 453801.

330. Jang, B., et al., *Syndecan-2 enhances E-cadherin shedding and fibroblast-like morphological changes by inducing MMP-7 expression in colon cancer cells.* Biochem Biophys Res Commun, 2016. **477**(1): p. 47-53.
331. Park, H., et al., *Syndecan-2 mediates adhesion and proliferation of colon carcinoma cells.* J Biol Chem, 2002. **277**(33): p. 29730-6.
332. Han, I., H. Park, and E.S. Oh, *New insights into syndecan-2 expression and tumourigenic activity in colon carcinoma cells.* J Mol Histol, 2004. **35**(3): p. 319-26.
333. Kousidou, O., et al., *Estradiol-estrogen receptor: a key interplay of the expression of syndecan-2 and metalloproteinase-9 in breast cancer cells.* Mol Oncol, 2008. **2**(3): p. 223-32.
334. Choi, S., et al., *Syndecan-2 overexpression regulates adhesion and migration through cooperation with integrin alpha2.* Biochem Biophys Res Commun, 2009. **384**(2): p. 231-5.
335. Ryu, H.Y., et al., *Syndecan-2 functions as a docking receptor for pro-matrix metalloproteinase-7 in human colon cancer cells.* J Biol Chem, 2009. **284**(51): p. 35692-701.
336. Choi, S., et al., *The matrix metalloproteinase-7 regulates the extracellular shedding of syndecan-2 from colon cancer cells.* Biochem Biophys Res Commun, 2012. **417**(4): p. 1260-4.
337. Lim, H.C., H.A. Multhaupt, and J.R. Couchman, *Cell surface heparan sulfate proteoglycans control adhesion and invasion of breast carcinoma cells.* Mol Cancer, 2015. **14**: p. 15.
338. Sun, M., et al., *RKIP and HMGA2 regulate breast tumor survival and metastasis through lysyl oxidase and syndecan-2.* Oncogene, 2014. **33**(27): p. 3528-37.
339. Park, H., et al., *Focal adhesion kinase regulates syndecan-2-mediated tumorigenic activity of HT1080 fibrosarcoma cells.* Cancer Res, 2005. **65**(21): p. 9899-905.
340. Peterfia, B., et al., *Syndecan-1 enhances proliferation, migration and metastasis of HT-1080 cells in cooperation with syndecan-2.* PLoS One, 2012. **7**(6): p. e39474.
341. Yoon, S. and R. Seger, *The extracellular signal-regulated kinase: multiple substrates regulate diverse cellular functions.* Growth Factors, 2006. **24**(1): p. 21-44.
342. Lemma, S., et al., *Identification and Validation of Housekeeping Genes for Gene Expression Analysis of Cancer Stem Cells.* PLoS One, 2016. **11**(2): p. e0149481.
343. Tsaur, I., et al., *Reliable housekeeping gene combination for quantitative PCR of lymph nodes in patients with prostate cancer.* Anticancer Res, 2013. **33**(12): p. 5243-8.
344. Yan, Z., et al., *Quantitative Evaluation and Selection of Reference Genes for Quantitative RT-PCR in Mouse Acute Pancreatitis.* Biomed Res Int, 2016. **2016**: p. 8367063.
345. Arendt, L.M., et al., *Stroma in breast development and disease.* Semin Cell Dev Biol, 2010. **21**(1): p. 11-8.
346. Fearon, D.T., *The carcinoma-associated fibroblast expressing fibroblast activation protein and escape from immune surveillance.* Cancer Immunol Res, 2014. **2**(3): p. 187-93.
347. Liu, L., et al., *ZEB1 Upregulates VEGF Expression and Stimulates Angiogenesis in Breast Cancer.* PLoS One, 2016. **11**(2): p. e0148774.
348. Zhao, X.P., et al., *Transforming growth factor-beta1 upregulates the expression of CXC chemokine receptor 4 (CXCR4) in human breast cancer MCF-7 cells.* Acta Pharmacol Sin, 2010. **31**(3): p. 347-54.
349. Hocevar, B.A., T.L. Brown, and P.H. Howe, *TGF-beta induces fibronectin synthesis through a c-Jun N-terminal kinase-dependent, Smad4-independent pathway.* EMBO J, 1999. **18**(5): p. 1345-56.
350. Joseph, J.V., et al., *TGF-beta is an inducer of ZEB1-dependent mesenchymal transdifferentiation in glioblastoma that is associated with tumor invasion.* Cell Death Dis, 2014. **5**: p. e1443.
351. DaCosta Byfield, S., et al., *SB-505124 is a selective inhibitor of transforming growth factor-beta type I receptors ALK4, ALK5, and ALK7.* Mol Pharmacol, 2004. **65**(3): p. 744-52.
352. Li, C.L., et al., *Fibronectin induces epithelial-mesenchymal transition in human breast cancer MCF-7 cells via activation of calpain.* Oncol Lett, 2017. **13**(5): p. 3889-3895.

353. Masterson, C., et al., *Syndecan-2-positive, Bone Marrow-derived Human Mesenchymal Stromal Cells Attenuate Bacterial-induced Acute Lung Injury and Enhance Resolution of Ventilator-induced Lung Injury in Rats.* Anesthesiology, 2018. **129**(3): p. 502-516.
354. Mi, Z., et al., *Osteopontin promotes CCL5-mesenchymal stromal cell-mediated breast cancer metastasis.* Carcinogenesis, 2011. **32**(4): p. 477-87.
355. Arora, P., et al., *Persistent transactivation of EGFR and ErbB2/HER2 by protease-activated receptor-1 promotes breast carcinoma cell invasion.* Oncogene, 2008. **27**(32): p. 4434-45.
356. Kucerova, L., et al., *Adipose tissue-derived human mesenchymal stem cells mediated prodrug cancer gene therapy.* Cancer Res, 2007. **67**(13): p. 6304-13.
357. Kucerova, L., et al., *Tumor cell behaviour modulation by mesenchymal stromal cells.* Mol Cancer, 2010. **9**: p. 129.
358. Hamon, M., et al., *A syndecan-4/CXCR4 complex expressed on human primary lymphocytes and macrophages and HeLa cell line binds the CXC chemokine stromal cell-derived factor-1 (SDF-1).* Glycobiology, 2004. **14**(4): p. 311-23.
359. Connell, B.J., et al., *Heparan sulfate differentially controls CXCL12alpha- and CXCL12gamma-mediated cell migration through differential presentation to their receptor CXCR4.* Sci Signal, 2016. **9**(452): p. ra107.
360. Brule, S., et al., *The shedding of syndecan-4 and syndecan-1 from HeLa cells and human primary macrophages is accelerated by SDF-1/CXCL12 and mediated by the matrix metalloproteinase-9.* Glycobiology, 2006. **16**(6): p. 488-501.
361. Sadir, R., et al., *Heparan sulfate/heparin oligosaccharides protect stromal cell-derived factor-1 (SDF-1)/CXCL12 against proteolysis induced by CD26/dipeptidyl peptidase IV.* J Biol Chem, 2004. **279**(42): p. 43854-60.
362. Agajanian, M., et al., *PEAK1 Acts as a Molecular Switch to Regulate Context-Dependent TGFbeta Responses in Breast Cancer.* PLoS One, 2015. **10**(8): p. e0135748.
363. Agajanian, M., F. Runa, and J.A. Kelber, *Identification of a PEAK1/ZEB1 signaling axis during TGFbeta/fibronectin-induced EMT in breast cancer.* Biochem Biophys Res Commun, 2015. **465**(3): p. 606-12.
364. Zhu, X., et al., *Epithelial derived CTGF promotes breast tumor progression via inducing EMT and collagen I fibers deposition.* Oncotarget, 2015. **6**(28): p. 25320-38.
365. Xu, J., et al., *Epithelial-mesenchymal transition induced PAI-1 is associated with prognosis of triple-negative breast cancer patients.* Gene, 2018. **670**: p. 7-14.
366. Rovira-Clave, X., et al., *Syndecan-2 can promote clearance of T-cell receptor/CD3 from the cell surface.* Immunology, 2012. **137**(3): p. 214-25.
367. Drews, J., *Genomic sciences and the medicine of tomorrow.* Nat Biotechnol, 1996. **14**(11): p. 1516-8.
368. Thundimadathil, J., *Cancer treatment using peptides: current therapies and future prospects.* J Amino Acids, 2012. **2012**: p. 967347.
369. Pearce, T.R., K. Shroff, and E. Kokkoli, *Peptide targeted lipid nanoparticles for anticancer drug delivery.* Adv Mater, 2012. **24**(28): p. 3803-22, 3710.
370. Hruby, V.J., *Designing peptide receptor agonists and antagonists.* Nat Rev Drug Discov, 2002. **1**(11): p. 847-58.
371. Aina, O.H., et al., *From combinatorial chemistry to cancer-targeting peptides.* Mol Pharm, 2007. **4**(5): p. 631-51.
372. Harding, T.C., et al., *Blockade of nonhormonal fibroblast growth factors by FP-1039 inhibits growth of multiple types of cancer.* Sci Transl Med, 2013. **5**(178): p. 178ra39.
373. Lau, J.L. and M.K. Dunn, *Therapeutic peptides: Historical perspectives, current development trends, and future directions.* Bioorg Med Chem, 2018. **26**(10): p. 2700-2707.
374. *Peptide Therapeutics Market by Route of Administration (Parenteral, Oral, and Others), by Type (Innovative and Generic), by Type of Manufacturers (In-house and Outsourced), by Type of Molecule (Vasopressin, Somatostatin, Calcitonin, Immunopeptide, Natriuretic, and*

Others), by Technology (Liquid Phase, Solid Phase, and Hybrid Phase), and by Application (Cancer, Cardiovascular Disease, Metabolic Disease, Respiratory Disease, Infectious Disease, and Others): Global Industry Perspective, Comprehensive Analysis and Forecast, 2017 – 2024. 2018.

375. Beauvais, D.M., et al., *Syndecan-1 regulates alphavbeta3 and alphavbeta5 integrin activation during angiogenesis and is blocked by synstatin, a novel peptide inhibitor.* J Exp Med, 2009. **206**(3): p. 691-705.
376. De Rossi, G., et al., *Shed syndecan-2 inhibits angiogenesis.* J Cell Sci, 2014. **127**(Pt 21): p. 4788-99.
377. De Rossi, G. and J.R. Whiteford, *A novel role for syndecan-3 in angiogenesis.* F1000Res, 2013. **2**: p. 270.
378. Zhou, K.X., et al., *CXCR4 antagonist AMD3100 enhances the response of MDA-MB-231 triple-negative breast cancer cells to ionizing radiation.* Cancer Lett, 2018. **418**: p. 196-203.
379. Lee, C.H., et al., *CTGF directs fibroblast differentiation from human mesenchymal stem/stromal cells and defines connective tissue healing in a rodent injury model.* J Clin Invest, 2010. **120**(9): p. 3340-9.
380. Petrylak, D.P., et al., *Atezolizumab (MPDL3280A) Monotherapy for Patients With Metastatic Urothelial Cancer: Long-term Outcomes From a Phase 1 Study.* JAMA Oncol, 2018. **4**(4): p. 537-544.
381. Santa-Maria, C.A., et al., *A pilot study of durvalumab and tremelimumab and immunogenomic dynamics in metastatic breast cancer.* Oncotarget, 2018. **9**(27): p. 18985-18996.
382. Bachman, K.E. and B.H. Park, *Duel nature of TGF-beta signaling: tumor suppressor vs. tumor promoter.* Curr Opin Oncol, 2005. **17**(1): p. 49-54.
383. Inman, G.J., *Switching TGFbeta from a tumor suppressor to a tumor promoter.* Curr Opin Genet Dev, 2011. **21**(1): p. 93-9.
384. Ajona, D., et al., *A Combined PD-1/C5a Blockade Synergistically Protects against Lung Cancer Growth and Metastasis.* Cancer Discov, 2017. **7**(7): p. 694-703.
385. McDermott, J. and A. Jimeno, *Pembrolizumab: PD-1 inhibition as a therapeutic strategy in cancer.* Drugs Today (Barc), 2015. **51**(1): p. 7-20.
386. Zhang, F., et al., *CXCR4-Targeted and Redox Responsive Dextrin Nanogel for Metastatic Breast Cancer Therapy.* Biomacromolecules, 2017. **18**(6): p. 1793-1802.
387. Tamamura, H. and N. Fujii, *The therapeutic potential of CXCR4 antagonists in the treatment of HIV infection, cancer metastasis and rheumatoid arthritis.* Expert Opin Ther Targets, 2005. **9**(6): p. 1267-82.
388. Platt, D., et al., *Violacein inhibits matrix metalloproteinase mediated CXCR4 expression: potential anti-tumor effect in cancer invasion and metastasis.* Biochem Biophys Res Commun, 2014. **455**(1-2): p. 107-12.
389. Liang, Z., et al., *Inhibition of breast cancer metastasis by selective synthetic polypeptide against CXCR4.* Cancer Res, 2004. **64**(12): p. 4302-8.
390. Zhang, F., et al., *Naringenin prevents TGF-beta1 secretion from breast cancer and suppresses pulmonary metastasis by inhibiting PKC activation.* Breast Cancer Res, 2016. **18**(1): p. 38.
391. Li, Q., et al., *Chamaejasmenin B, a novel candidate, inhibits breast tumor metastasis by rebalancing TGF-beta paradox.* Oncotarget, 2016. **7**(30): p. 48180-48192.
392. Park, C.Y., et al., *An novel inhibitor of TGF-beta type I receptor, IN-1130, blocks breast cancer lung metastasis through inhibition of epithelial-mesenchymal transition.* Cancer Lett, 2014. **351**(1): p. 72-80.
393. He, X., et al., *Mechanism of action and efficacy of LY2109761, a TGF-beta receptor inhibitor, targeting tumor microenvironment in liver cancer after TACE.* Oncotarget, 2018. **9**(1): p. 1130-1142.

394. Bouquet, F., et al., *TGFbeta1 inhibition increases the radiosensitivity of breast cancer cells in vitro and promotes tumor control by radiation in vivo.* Clin Cancer Res, 2011. **17**(21): p. 6754-65.
395. Chen, E., S. Hermanson, and S.C. Ekker, *Syndecan-2 is essential for angiogenic sprouting during zebrafish development.* Blood, 2004. **103**(5): p. 1710-9.
396. Kramer, K.L. and H.J. Yost, *Ectodermal syndecan-2 mediates left-right axis formation in migrating mesoderm as a cell-nonautonomous Vg1 cofactor.* Dev Cell, 2002. **2**(1): p. 115-24.
397. Arrington, C.B. and H.J. Yost, *Extra-embryonic syndecan 2 regulates organ primordia migration and fibrillogenesis throughout the zebrafish embryo.* Development, 2009. **136**(18): p. 3143-52.
398. Poulain, F.E. and H.J. Yost, *Heparan sulfate proteoglycans: a sugar code for vertebrate development?* Development, 2015. **142**(20): p. 3456-67.
399. Boddu, P., et al., *Initial Report of a Phase I Study of LY2510924, Idarubicin, and Cytarabine in Relapsed/Refractory Acute Myeloid Leukemia.* Front Oncol, 2018. **8**: p. 369.